



HAL
open science

Synthesis of electroactive macrocycles and rotaxanes

Luca Pesciottani

► **To cite this version:**

Luca Pesciottani. Synthesis of electroactive macrocycles and rotaxanes. Organic chemistry. Université de Bordeaux, 2018. English. NNT : 2018BORD0270 . tel-02426196

HAL Id: tel-02426196

<https://theses.hal.science/tel-02426196>

Submitted on 2 Jan 2020

HAL is a multi-disciplinary open access archive for the deposit and dissemination of scientific research documents, whether they are published or not. The documents may come from teaching and research institutions in France or abroad, or from public or private research centers.

L'archive ouverte pluridisciplinaire **HAL**, est destinée au dépôt et à la diffusion de documents scientifiques de niveau recherche, publiés ou non, émanant des établissements d'enseignement et de recherche français ou étrangers, des laboratoires publics ou privés.

THÈSE PRÉSENTÉE

POUR OBTENIR LE GRADE DE

DOCTEUR

DE

L'UNIVERSITÉ DE BORDEAUX

ÉCOLE DOCTORALE DES SCIENCES CHIMIQUES

SPÉCIALITÉ : CHIMIE ORGANIQUE

Par Luca PISCIOTTANI

Synthèse de macrocycles et rotaxanes électroactifs

Sous la direction de Dr. Nathan D. McClenaghan

Soutenue le 11 décembre 2018

Membres du jury :

M.me RODRIGUEZ RAURELL, Laura , Associate professor, Univ. of Barcelona	Rapporteur
M. VIVES, Guillaume , Maître de Conférences, Sorbonne University	Rapporteur
M.me FREIXA, Zoraida , Ikerbasque research professor, Univ. of the Basque Country	Président
M. McCLENAGHAN, Nathan D. , Directeur de recherche au CNRS, Univ. of Bordeaux	Directeur de thèse

THESIS PRESENTED
TO OBTAIN THE DEGREE OF
DOCTOR
AT
UNIVERSITY OF BORDEAUX

DOCTORAL SCHOOL OF CHEICAL SCIENCES

SPECIALTY : ORGANIC CHEMISTRY

By Luca PISCIOTTANI

Synthesis of electroactive macrocycles and rotaxanes

under the supervision of Dr. Nathan D. McClenaghan

Defend on December 11th 2018

In front of a jury composed of:

M.me RODRIGUEZ RAURELL, Laura , Associate professor, Univ. of Barcelona	Reporter
M. VIVES, Guillaume , Maître de Conférences, Sorbonne University	Reporter
M.me FREIXA, Zoraida , Ikerbasque research professor, Univ. of the Basque Country	President
M. McCLENAGHAN, Nathan D. , Directeur de recherche au CNRS, Univ. of Bordeaux	Thesis director

Acknowledgements

Firstly I would like to thank my supervisor, Dr. Nathan D. McClenaghan, for gave me the opportunity to undertake this project.

I would like to thank Mykhaylo for all the precious teachings and Maxime for his help in the lab, as well as Sergey, Shilin, Marcello, Kars, Philip, Alex and Leire for all the good moments. Thanks also to Pascale, Clotilde and Damien and all the members of the NEO group.

The CESAMO group, who helped me with NMR samples and mass spectroscopy, is highly acknowledged. Dr. Brice Kauffmann in IECB is also greatly appreciated, for his help in X-ray crystallography.

My gratitude goes in particular to the Université de Bordeaux & Minisitry of Research and Education for a doctoral grant and the Agence Nationale de la Recherche (ANR) program for financing this research project (grant number ANR-16-CE29-0011).

General introduction.....	1
1. Introduction.....	5
1.1. Supramolecular chemistry	5
1.1.1. Brief history of supramolecular chemistry.....	6
1.1.2. Intermolecular Forces	9
1.2. Mechanically Interlocked Molecules	21
1.2.1. Definition	21
1.2.2. Catenanes	22
1.2.3. Rotaxanes	25
1.2.4. Characteristics and effect	28
1.2.5. Applications	31
1.3. Click chemistry.....	37
2. Electroactive macrocycles	45
2.1 Introduction	45
2.2 Development of ferrocene-containing macrocycles.....	51
2.2.1 Introduction.....	51
2.2.2 Synthesis	54
2.2.3 Characterization	57
2.2.3.1 NMR studies.....	57
2.2.3.2 Binding study with macrocyclic hosts.....	59
2.2.3.3 Electrochemistry.....	62
2.2.3.4 Single crystal X-ray diffraction structure determination.....	64
2.3 Development of a triarylamine containing macrocycle	67
2.3.1 Introduction.....	67
2.3.2 Synthesis	74
2.3.3 Characterization	81
2.3.3.1 NMR studies.....	81
2.3.3.2 Binding study with the TAA macrocycle.....	83
2.3.3.3 Electrochemistry studies.....	85
2.3.3.4 Single crystal X-ray diffraction structural determination.....	86
2.4 Conclusion and Perspectives	88
3. Photoactive components and stoppers	89
3.1 Introduction	89
3.1.1 Boron dypyrromethene dyes	89

3.1.2	Aza-dipyrromethenes: synthesis and applications	91
3.2	Design of methoxypropargyloxy BF ₂ -chelate azadipyrromethene	100
3.2.1	Synthesis	100
3.3	Design of <i>tert</i> Bu-carboxypropargyloxy BF ₂ -chelate azadipyrromethene.....	105
3.3.1	Synthesis	105
3.3.2	Characterization	106
3.4	Silicon-rhodamine	107
3.4.1	Introduction.....	107
3.4.2	Synthesis	108
3.5	Alkyne- and azide-stoppers	112
3.5.1	Introduction.....	112
3.5.2	Synthesis	113
3.6	Design of barbiturate-containing BF ₂ -chelate azadipyrromethene thread	118
3.6.1	Synthesis	118
3.6.2	Characterization	121
3.7	Conclusion and perspectives	122
4.	Assembly of functional [2]rotaxanes	123
4.1	Introduction	123
4.1.1	Capping approach	124
4.1.2	Clipping approach	126
4.1.3	Slipping approach	127
4.1.4	Active metal-template approach	128
4.1.5	Miscellaneous methods	129
4.2	Development of functional [2]rotaxane by an active metal-template approach	131
4.2.1	Synthesis	131
4.2.2	Characterization	133
4.3	Development of functional [2]rotaxanes by a clipping approach	134
4.3.1	Synthesis	134
4.3.2	Characterization	139
4.3.2.1	NMR studies and mass spectrometry	139
4.3.2.2	Electrochemistry studies.....	141
4.3.2.3	X-ray structural determination	142
4.4	Conclusion and perspectives	146
5.	General conclusion and perspectives	147

6. Experimental part.....	151
6.1 Solvents	151
6.2 Thin layer chromatography and column chromatography	151
6.3 Nuclear magnetic resonance spectroscopy (NMR)	151
6.4 Mass spectrometry.....	152
6.5 Electrochemistry.....	152
6.6 Titrations	153
6.7 UV-Vis and Fluorescence	154
6.8 Single X-ray crystallographic information.....	154
6.9 Synthesis.....	154
7. Annexes.....	207

General introduction

Supramolecular chemistry has become a central topic in chemistry. This type of chemistry is based on harnessing intermolecular forces, or non-covalent bonds, which were found to play a fundamental role in biological processes, like DNA replication, protein folding, neural communication, molecular recognition and membrane and cell formation. Organic chemists can take inspiration from Nature to develop artificial biomimetic systems which are based on the same intermolecular interactions.

Over the years, supramolecular architectures have become more and more sophisticated and efficient synthetic tools are required. For this reason the construction of mechanically interlocked molecules is closely related to “click chemistry”. This topic was conceptually introduced for the first time by Sharpless in 2002 and refers to a field of organic synthesis which has as main goal the study and the development of straightforward and efficient chemical reactions, that generally have to be high yielding and highly selective and the reaction conditions have to be as mild as possible in order to be performed in the presence of a wide range of functional groups. Different reactions have those requirements and belong to this family, like thiol-ene reaction, Diels-Alder reaction, [4+1] cycloaddition between isonitriles and tetrazines, nucleophilic substitution of small rings and 1,3-dipolar azide-alkyne Huisgen cycloaddition. The last reaction is the most famous member of this class of reactions and its copper(I)-catalyzed version is ubiquitous in chemistry.

In the past three decades, development of supramolecular architectures and mechanically interlocked molecules have continuously raised a huge interest inside the scientific community. The 1987 Nobel Prize in Chemistry was awarded for the development of artificial biomimetic receptors and the topic of 2016 Nobel Prize in Chemistry was the development of artificial molecular machines. These structures include ring-on-thread rotaxane structures, formed by a rod-like molecule (the thread) which is threaded through a macrocyclic molecule. The unthreading of the

two components is prevented by the presence of bulky groups at the ends of the thread that are larger than the cavity of the ring. The rupture of a covalent bond is required to dissociate the thread from the ring.

Over the years, lot of different rotaxane-based architectures have been developed but only a little percentage of them comprises functional groups. Photoactive mechanically interlocked molecules are present in literature but only few classes of UV-vis chromophore have been exploited and most of them showed low photostability. Near-infrared (NIR) chromophores are a class of chromophores which are photoactive in the near infrared region (from 650 to 1350 nm). The interest about the NIR chromophore raised in the last years, especially for their biological and medical application, in fact, in this region of the electromagnetic spectrum, biological tissue are transparent and no damages to biological processes occur upon irradiation.

Moreover, thanks to their extreme photostability and their easy functionalization, azadipyrrromethene BF_2 -chelates have been also applied in the development of photoactive chemosensors, polymers and materials, but have not yet been exploited as novel NIR chromophore-bearing building blocks in order to develop photoactive mechanically-interlocked molecules.

The goal of this thesis is the design, the synthesis and the characterization of electroactive and photoactive components for the development of novel functional mechanically interlocked molecules.

Chapter 1 gives a general introduction to supramolecular chemistry, in particular on the mechanical bond and mechanically-interlocked molecular architectures. Basic introductions about non-covalent interactions and their application in supramolecular systems and click chemistry are also given.

Chapter 2 provides a brief overview of several hydrogen bonding-based supramolecular systems, alongside concise introductions to triarylamine-based systems and ferrocene. The main topic of this

chapter is the design and development of different macrocyclic structures, which have both a bis(2,6-diamidopyridine) motif for barbiturate motif and an electroactive moiety.

X-ray crystal structures of electroactive macrocycles are also shown.

Chapter 3 concerns near-infrared (NIR) chromophores, in particular BF_2 -chelate of tetraaryl azadipyrrromethene derivate and synthesis of multi-functional NIR building blocks for future incorporation in mechanically-interlocked molecules are reported. Improved synthesis of trityl-based stoppers and their alkyne and azide derivatives are also described.

Chapter 4 provides an introduction to the main synthetic approaches for the synthesis of rotaxanes and reports the synthesis and the full characterization of the functional [2]rotaxanes which were obtained with the components described in the other chapters. X-ray crystal structures of [2]rotaxanes are also shown.

Chapter 5 gives a general conclusion of the thesis and perspectives, while chapter 6 reports the detailed experimental procedures of the new compounds discussed in the previous chapters, alongside the modified and improved procedures of known compounds that have been adapted from the literature. Chemical structures, purification details, reaction yields and characterizations (^1H -, ^{13}C -NMR and mass spectrometry data) are also reported.

1. Introduction

1.1. Supramolecular chemistry

Supramolecular chemistry is a wide and multidisciplinary domain of chemistry, which studies chemical systems formed by a discrete number of assembled molecules or subcomponents.

According to Nobel laureate J.-M. Lehn, supramolecular chemistry is the “chemistry beyond the molecule”, which means that it cannot be related to the classical concept of covalent chemical bonds, but rather it focuses on weak and reversible non-covalent interactions between molecules, such as hydrogen bonding, metal coordination, hydrophobic forces, van der Waals forces, π - π interactions and electrostatic effect.¹

In the past three decades, supramolecular chemistry played a key role for the development of concepts like molecular self-assembly, folding, molecular recognition, host-guest chemistry, mechanically-interlocked molecular architectures and dynamic covalent chemistry. Moreover, supramolecular chemistry and biological systems have a long and symbiotic relationship: on one hand, since their discovery, the study of non-covalent interactions has been crucial for the understanding of many biological process, on the other hand the Nature is an endless source of inspiration for the supramolecular chemists.

¹ a) H.-J. Schneider, *Angew. Chem. Int. Ed.* **2009**, *48*, 3924.

b) J.-M. Lehn, *Supramolecular Chemistry - Scope and Perspective Molecules, Supramolecules and Molecular Devices*, *Angew. Chem. Int. Ed.* **1988**, *27*, 89.

c) F. Biedermann and H.-J. Schneider, *Chem. Rev.*, **2016**, *116*, 5216.

1.1.1. Brief history of supramolecular chemistry

The first main contribution to the conceptual development of the supramolecular chemistry came in 1894, when Nobel laureate Herman Emil Fischer suggested that enzyme-substrate interactions are similar to a "lock and key" system, which is the fundamental principle of molecular recognition.

In 1953, J. Watson and F. Crick published one of the most important scientific discoveries of the past century: the structure of DNA was found to be a double helix composed by two separate strands of nucleotides held together with complementary hydrogen bonds (Figure 1.1).²

The role of reversible and non-covalent interactions is essential for life because replication can occur only if the two strands are allowed to be separated and used to template new double stranded DNA.

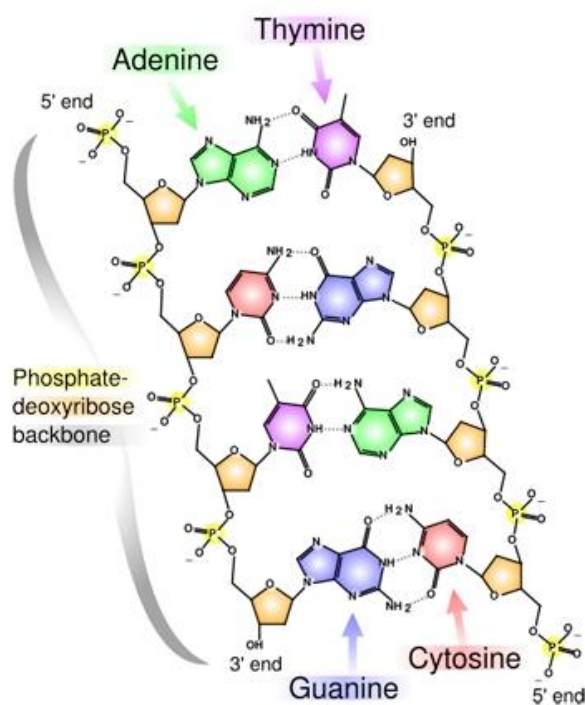


Figure 1.1 – Representation of hydrogen bonding interactions between double helical structures of DNA.

² J.D Watson and F.H. Crick, *Nature*, **1953**, 171, 737.

In the 1960s, even if the concept of intermolecular interactions was widely known in biology and many biological processes were understood and studied, there were not yet examples of a pure synthetic supramolecular system. The breakthrough arrived in 1967, thanks to the pioneering work of C. J. Pedersen, an industrial chemist working for DuPont. During his attempt to synthesize a multidentate ligand for copper and vanadium, the bis[2-(o-hydroxy-phenoxy)ethyl]ether **I-4**, Pedersen accidentally synthesized the first example of a new class of compounds that can be considered as the beginning of purely synthetic supramolecular chemistry: the crown-ethers, having a crown-like shape (Figure 1.2).³

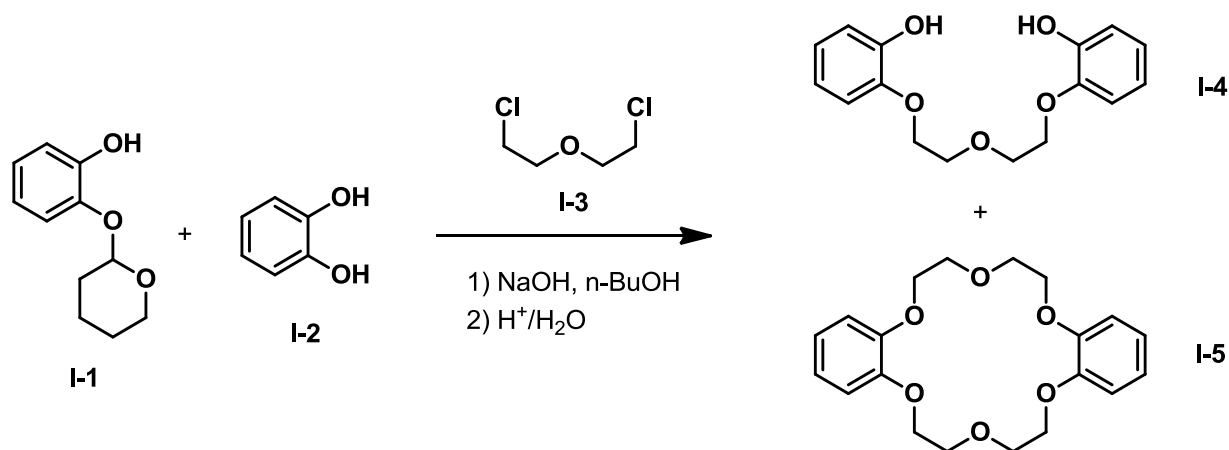


Figure 1.2 - Synthetic procedure of the intended product, bis[2-(o-hydroxy-phenoxy)ethyl]ether **I-4**, and obtained side-product, dibenzo[18]crown-6 **I-5**.

The importance of supramolecular chemistry was finally established by the 1987, being the topic of the Nobel Prize for Chemistry.

The strong interest for this young discipline lies in the possibility of implementing new functionalities and building artificial molecular biomimetic machines, as well as understanding natural architectures with, for example, kinesin and ATP Synthase.

³ C. J. Pedersen, *J. Am. Chem. Soc.*, **1967**, 89, 2495.

Molecular machines are ubiquitous in nature, that abounds in biological processes induced by natural machines. Those assemblies have been sources of inspiration for chemists, which imitated the natural machines by transposing their functions into artificial supramolecular machines and to be able to generate a specific movement in artificial systems. Unidirectional movement within molecular machines, for example, has given rise to artificial molecular motors. The importance of this area was reflected in the conceptual breadth of which it has made and continues to show for many years.

Over the years, sophisticated supramolecular architectures have been designed and synthesized, especially in the field of mechanically interlocked molecules and molecular machines. The main contributors of this new branch of supramolecular chemistry have been J. F. Stoddart, J.-P. Sauvage and B.L. Feringa, which, in 2016, jointly won the Nobel Prize “*for the design and synthesis of molecular machines*”.⁴

⁴ a) W.R. Browne and B.L. Feringa, *Nature Nanotechnology*, **2006**, *1*, 25.

b) J.F. Stoddart, *Chem. Soc. Rev.*, **2009**, *38*, 1802.

c) A. Coskun, M. Banaszak, R.D. Astumian, J.F. Stoddart and B.A. Grzybowski, *Chem. Soc. Rev.*, **2012**, *41*, 19.

d) F. Duroola, V. Heitz, F. Reviriego, C. Roche, J.-P. Sauvage, A. Sour and Y. Trolez, *Accounts of Chemical Research*, **2014**, *47*, 633.

1.1.2. Intermolecular Forces

Supramolecular chemistry can be considered as the “chemistry of non-covalent interactions”: a non-covalent interaction does not involve the sharing of electrons but involves more dispersed variations of electromagnetic interactions between molecules. For this reason, they are often indicated as intermolecular forces (Table 1.1).⁵

Generally, the bond energy of a typical covalent bond is around 350 kJmol⁻¹, rising up to 942 kJmol⁻¹ for the triple bond in molecular nitrogen; the strengths of many non-covalent interactions are generally much weaker, ranging from 2 kJmol⁻¹, through to 20 kJmol⁻¹ for a hydrogen bond to 250 kJmol⁻¹ for an ion-ion interaction.⁶

Table 1.1 - Strength of intermolecular interactions.

Bond type	Dissociation energy (kJmol ⁻¹)
Hydrophobic effect	< 8
$\pi - \pi$ Stacking	0 - 50
π -Cation Interaction	4 - 80
Halogen bond	4 - 60
Hydrogen bond	4 - 125
Dipole-dipole interaction	4 - 50
Dipole ion interaction	50 - 200
Ionic interaction	200 - 290

⁵ E.V. Anslyn and D.A. Dougherty, *Modern Physical Organic Chemistry*, Sausalito, CA, University Science, **2004**.

⁶ J.W. Steed and J.L. Atwood, *Supramolecular Chemistry*, John Wiley & Sons, **2009**.

The synergic use of geometric complementarity and combination of different intermolecular interactions has allowed to synthesize an extremely wide variety of artificial supramolecular architectures, like anion, cation or neutral receptors, chemosensors, self-assembly systems, biomimetic catalysts (Figure 1.3).⁷

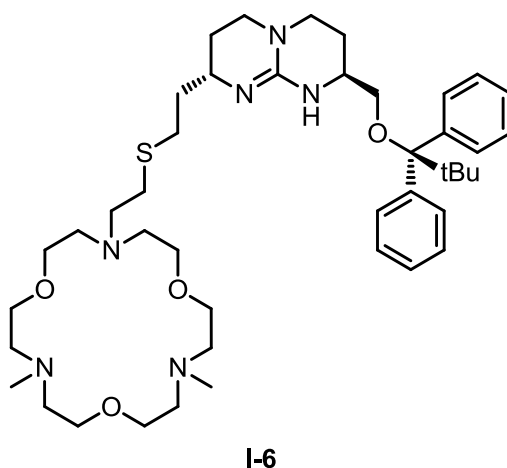


Figure 1.3- Artificial amino acid receptor **I-6**.

- ⁷ a) A. Metzger, K. Gloe, H. Stephan and F. P. Schmidtchen, *J. Org. Chem.*, **1996**, *61*, 2051.
b) A. Galan, D. Andreu, A.M. Echavarren, P. Prados and J. De Mendoza, *J. Am. Chem. Soc.*, **1992**, *114*, 1511.
c) J. Rebek Jr., B. Askew, D. Nemeth and K. Parris, *J. Am. Chem. Soc.*, **1987**, *109*, 2432.
d) J. Sunamoto, K. Iwamoto, Y. Mokri and T. Kominato, *J. Am. Chem. Soc.*, **1982**, *104*, 5502.
e) I. Willner and S. Marx-Tibbon, *J. Chem. Soc., Chem. Commun.*, **1994**, 1261.
f) K. Maruyama, H. Tsukube and T. Araki, *J. Am. Chem. Soc.*, **1982**, *104*, 5197.
g) M.T. Reetz, J.R. Huff, K. Tollner, A. Deege and R. Goddard, *J. Am. Chem. Soc.*, **1994**, *116*, 11588.
h) L.K. Mohler and A.W. Czarnik, *J. Am. Chem. Soc.*, **1993**, *115*, 7037.
i) L.A. Cabell, M.K. Monahan and E.V. Anslyn, *Tetrahedron Lett.*, **1999**, *40*, 7753.
j) Z. Zhong and E.V. Anslyn, *J. Am. Chem. Soc.*, **2002**, *124*, 9014.
k) Z. Murtaza, L. Tolosa, P. Harms and J. R. Lakowicz, *J. Fluorescence*, **2002**, *12*, 187.
l) J.T. Suri, D.B. Cordes, F.E. Cappuccio, R.A. Wessling and B. Singaram, *Langmuir*, **2003**, *19*, 5145.
m) V. Král, J.L. Sessler, R.S. Zimmerman, D. Seidel, V. Lynch and B. Andrioletti, *Angew. Chem., Int. Ed.*, **2000**, *39*, 1055.
n) J.L. Sessler, W.-S. Cho, S.P. Dudek, L. Hicks, V. M. Lynch and M. T. Huggins, *J. Porphyrins Phthalocyanines*, **2003**, *7*, 97.
o) T.W. Bell and V.J. Santora, *J. Am. Chem. Soc.*, **1992**, *114*, 8300.
p) C. Bucher, D. Seidel, V. Lynch, V. Král and J.L. Sessler, *Org. Lett.*, **2000**, *2*, 3103.
q) A. Kraft and A. Reichert, *Tetrahedron*, **1999**, *55*, 3923.
r) A.P. Davis and L.J. Lawless, *Chem. Commun.*, **1999**, *0*, 9.
s) J.N. Camara, J.T. Suri, F.E. Cappuccio, R.A. Wessling and B. Singaram, *Tetrahedron Lett.*, **2002**, *43*, 113.
t) A. Kraft, L. Peters and H.R. Powell, *Tetrahedron*, **2002**, *58*, 3499.

Electrostatic interactions are based on the Coulombic attraction between species that show formal or partial opposite charges and they include ion-ion, ion-dipole (50-200 kJmol⁻¹) and dipole-dipole interactions (5-50 kJmol⁻¹).

In 1986, Cram studied different crown ether, half-spherand and spherand based systems and first introduced the principle of “preorganization”, which states that “*the more highly hosts and guests are organized for binding and low solvation prior to their complexation, the more stable will be their complexes*” (Figure 1.4).⁸

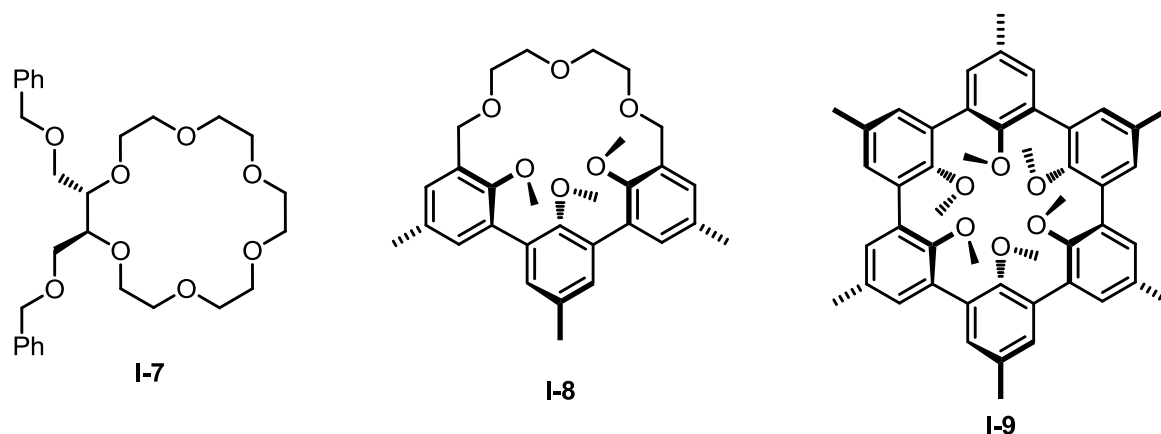


Figure 1.4 - Chemical structures of crown ether **I-7**, half-spherand **I-8** and spherand **I-9**.

The pioneering work in supramolecular chemistry and molecular recognition of Lehn, Cram and Pedersen was recognized in 1987, when they were jointly awarded with the Nobel Prize for “*their development and use of molecules with structure-specific interactions of high selectivity*”.⁹

⁸ D.J. Cram, *Angew. Chem. Int. Ed.*, **1986**, 25, 1039.

⁹ a) C. J. Pedersen, *J. Am. Chem. Soc.*, **1967**, 89, 7017.

b) J. Yoon; C.B. Knobler, E.F. Maverick and D.J. Cram, *Chem. Commun.*, **1997**, 14, 1303.

c) R. Alberto, K. Ortner, N. Wheatley, R. Schibli and A.P. Schubiger, *J. Am. Chem. Soc.*, **2001**, 121 3135.

d) A. Von Zelewsky, *Stereochemistry of Coordination Compounds*. Chichester: John Wiley, **1995**.

e) J. M. Lehn, *Supramolecular Chemistry: Concepts and Perspectives*. Weinheim: VCH., **1995**.

f) J. Kim, A.S. Ichimura, R.H. Huang, M. Redko, R.C. Phillips, J.E. Jackson and J.L. Dye, *J. Am. Chem. Soc.*, **1999**, 121, 10666

g) G.W.Gokel, *Comprehensive Supramolecular Chemistry 1*, Oxford: Elsevier, **1996**.

h) D. Landini, A. Maia, F. Montanari and P. Tundo, *J. Am. Chem. Soc.*, **1979**, 101, 2526.

In 1981 Manabe and coworkers developed a photoresponsive molecular tweezer **I-10**, comprising two 15-crown-5-ether moieties connected by an azobenzene bridge, which was able to perform a “butterfly-like” movement (Figure 1.5).

In the “*trans*” state, the tweezer showed high affinity towards sodium cations, while the “*cis*” state, obtained by photoisomerization upon irradiation at UV light, showed high affinity for larger ions, like potassium, cesium or rubidium cations. Moreover, they noticed that the rate of thermal isomerization (from *cis* to *trans*) was drastically slowed upon addition of alkali metal cations and the order of inhibitory effect was $\text{Rb}^+ > \text{Cs}^+ > \text{K}^+ > \text{Na}^+$.

This system was applied as efficient and highly selective photo-regulated extractor of alkali metal cations.¹⁰

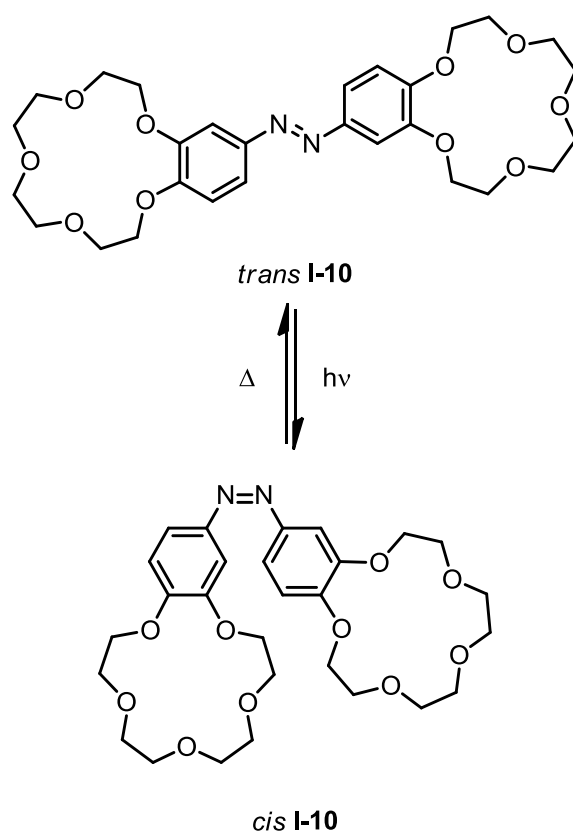


Figure 1.5 - Photoisomerization of crown ether-based molecular tweezer **I-10**.

¹⁰ a) S. Shinkai, T. Nakaji, T. Ogawa, K. Shigematsu and O. Manabe *J. Am. Chem. Soc.*, **1981**, *103*, 11.

b) S. Shinkai, T. Nakaji, Y. Nishida, T. Ogawa and Osamu Manabe, *J. Am. Chem. Soc.*, **1980**, *102*, 5860.

In 1993 de Silva and coworkers developed photoionic AND logic gate **I-11** in which the fluorescence was quenched, unless complexation of a sodium cation by the 15-crown-5-ether moiety and protonation of morpholine unit occurred (Figure 1.6).¹¹

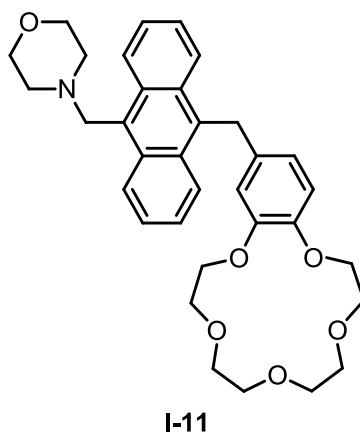


Figure 1.6 - Crown ether-containing logic gate **I-11**.

In 1997, Shinkai and coworkers reported the synthesis of an azacrown ether-based “molecular syringe” **I-12**. The change of pH induced the translocation of the silver ion (Figure 1.7).¹²

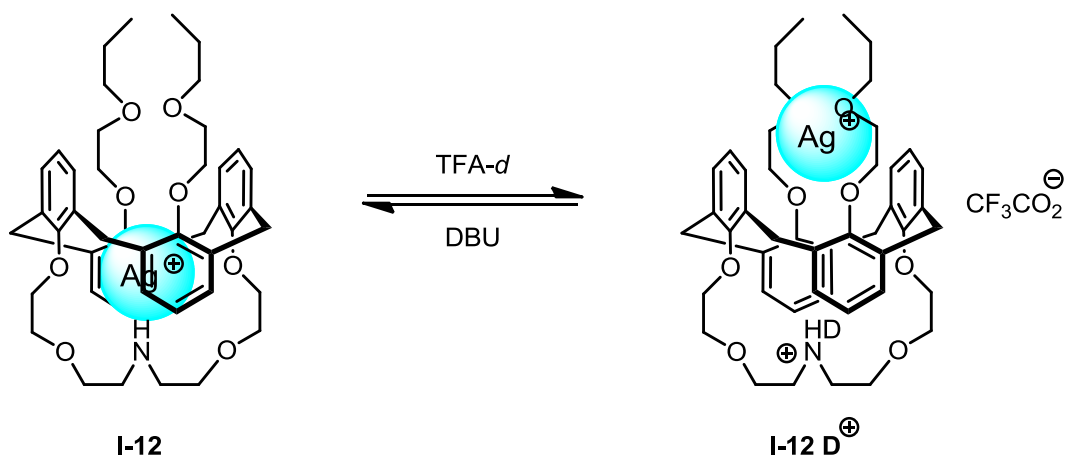


Figure 1.7 - Molecular syringe **I-12**.

¹¹ a) A.P. de Silva, H.Q.N. Gunaratne and C.P. McCoy, *Nature*, **1993**, 364, 42.

b) C. R. Cooper and T. D. James, *J. Chem. Soc. Perkin Trans. 2*, **2000**, 963.

c) A.P. de Silva, H.Q.N. Gunaratne and C.P. McCoy, *J. Am. Chem. Soc.*, **1997**, 119, 7891.

¹² A. Ikeda, T. Tsudera and S. Shinkai, *J. Org. Chem.*, **1997**, 62, 568.

Crown ether-based macrocycles are widely used in mechanically interlocked molecules, so straightforward methods to obtain them are required.

In 2015, Gibson and coworkers reported an efficient and high yielding synthetic route which allowed synthesis of dibenzo-30-crown-10-ether (DB30C10) **I-13** and dibenzo-24-crown-8-ether (DB24C8) **I-14** in three steps, on gram-scale with yields higher than 80% (Figure 1.8). The efficiency of this methodology relied on the use of potassium hexafluorophosphate as a templating agent in the macrocyclization step.^{13, 14}

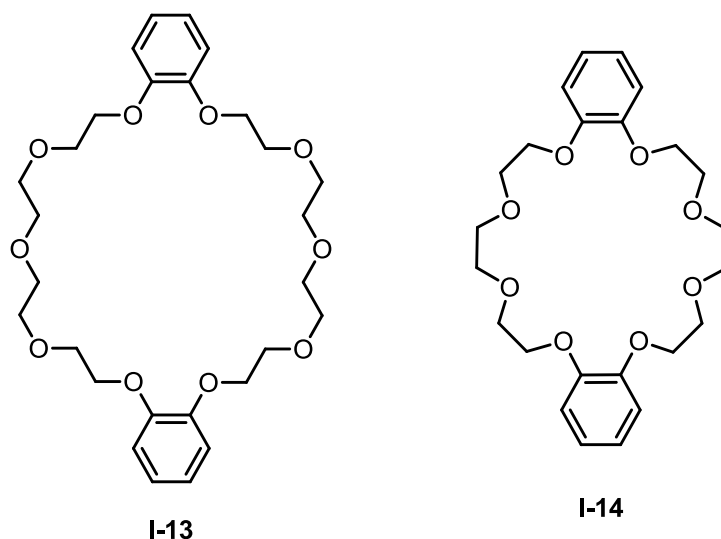


Figure 1.8 - Chemical structures of dibenzo-30-crown-10-ether (DB30C10) **I-13** and dibenzo-24-crown-8-ether (DB24C8) **I-14**.

¹³ a) P.R. Ashton, M.C.T. Fyfe, C. Schiavo, J.F. Stoddart, A.J.P. White and D.J. Williams, *Tetrahedron Lett.*, **1998**, 39, 5455.

b) K. Zhu, ; V.N. Vukotiic, N. Noujeim and S.J. Loeb, *Chem. Sci.*, **2012**, 3, 3265.

c) Y.-L. Zhao, L. Liu, W. Zhang, C.-H. Sue, Q. Li, O.S. Miljanic, O.M. Yaghi and J.F. Stoddart, *Chem. Eur. J.*, **2009**, 15, 13356.

d) Z. Niu and H.W. Gibson, *Chem. Rev.*, **2009**, 109, 6024.

¹⁴ H.R. Wessels and H.W. Gibson, *Tetrahedron*, **2016**, 72, 396.

Hydrogen bonding interactions ($4\text{-}120\text{ kJmol}^{-1}$) may be considered as a specific type of dipole-dipole interaction or, more precisely, it is “an attractive interaction between a hydrogen atom from a molecule or a molecular fragment $X\text{-H}$ in which X is more electronegative than H , and an atom or a group of atoms in the same or a different molecule, in which there is evidence of bond formation”.¹⁵

Being characterized by a high level of directionality and the absence of a formal charge, hydrogen bonding interactions (or H-bonding) and their modulation have been extensively studied and exploited to develop a wide range of supramolecular systems.¹⁶

In 2012, Ungaro and coworkers reported the synthesis of an artificial tetraguanidinocalix[4]arene - based phosphodiesterase **I-15**: the hydrogen bonds had the key role to bind and activate the substrate (Figure 1.9).¹⁷

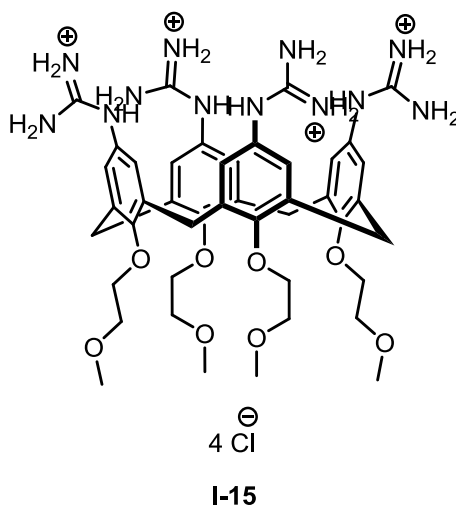


Figure 1.9 - Artificial calix[4]arene -based phosphodiesterase **I-15**.

¹⁵ E. Arunan, G.R. Desiraju, R.A. Klein, J. Sadlej, S. Scheiner, I. Alkorta, D.C. Clary, R.H. Crabtree, J.J. Dannenberg, P. Hobza, H.G. Kjaergaard, A.C. Legon, B. Mennucci and D.J. Nesbitt, *Pure Appl. Chem.*, **2011**, 83, 1637.

¹⁶ a) C.S. Wilcox, E. Kim, D. Romano, L.H. Kuo, A.L. Burt, and D.P. Curran, *Tetrahedron*, 1995, 51, 621.

b) C.-T. Chen and J.S. Siegel, *J. Am. Chem. Soc.*, **1994**, 116, 5959.

c) R. Deans, A. Cuello, T.H. Galow, M. Obera and V.M. Rotello, *J. Chem. Soc., Perkin Trans. 2*, **2000**, 0, 1309.

d) V. Berl, M. J. Krische, I. Huc, J.-M. Lehn and M. Schmutz, *Chem. Eur. J.* **2000**, 6, 1938.

¹⁷ R. Salvio, A. Casnati, L. Mandolini, F. Sansone and R. Ungaro, *Org. Biomol. Chem.*, **2012**, 10, 8941.

Carbohydrate recognition by artificial receptors is one of the most fascinating and challenging goals of molecular recognition, as proved by the large amount of literature about this topic, and hydrogen bonding interactions are a key aspect of these biomimetic supramolecular systems.¹⁸

Fucose is a rare naturally occurring saccharide characterized by the lack of an hydroxyl group in 6-position and its L-configuration. Recently, many studies highlighted the importance of fucose and fucose-containing oligosaccharides in anticancer therapies and antibodies-related biological processes.^{19, 20, 21}

In 2018, Roelens and coworkers developed a carbazole-based hydrogen-bonding biomimetic artificial receptor **I-16** for fucose (Figure 1.10).²²

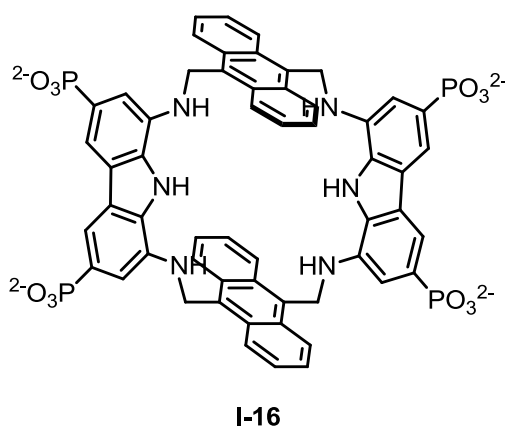


Figure 1.10 - Carbazole-based biomimetic receptor **I-16** .

¹⁸ a) Y. Ferrand, M.P. Crump and A.P. Davis, *Science*, **2007**, *318*, 619.

b) S. Kubik, *Angew. Chem. Int. Ed.*, **2009**, *48*, 1722.

c) A.P. Davis, *Org. Biomol. Chem.*, **2009**, *7*, 3629.

d) C. Nativi, O. Francesconi, G. Gabrielli, I. De Simone, B. Turchetti, T. Mello, L. Di Cesare Mannelli, C. Ghelardini, P. Buzzini and S. Roelens, *Chem. Eur. J.*, **2012**, *18*, 5064.

e) O. Francesconi, C. Nativi, G. Gabrielli, I. De Simone, S. Noppen, J. Balzarini, S. Liekens and S. Roelens, *Chem. Eur. J.*, **2015**, *21*, 10089.

f) S.-H. Park, Y. P. Choi, J. Park, A. Share, O. Francesconi, C. Nativi, W. Namkung, J. L. Sessler, S. Roelens and I. Shin, *Chem. Sci.*, **2015**, *6*, 7284.

g) A.P. Davis and R.S. Wareham, *Angew. Chem. Int. Ed.*, **1999**, *38*, 2978.

¹⁹ C. Chemani, A. Imberty, S. de Bentzmann, M. Pierre, M. Wimmerová, B.P. Guevry and K. Faure, *Infect. Immun.*, **2009**, *77*, 2065.

²⁰ S. Pinho, C.A. Reis, *Nat. Rev. Cancer*, **2015**, *15*, 540.

²¹ A. Breiman, M.D.L. Robles, S. de Carné Trécesson, K. Echasserieau, K. Bernardeau, K. Drickamer, A. Imberty, S. Barillé-Nion, F. Altare and J. Le Pendu, *Oncotarget*, **2016**, *7*, 14064.

²² O. Francesconi, M. Martinucci, L. Badii, C. Nativi and S. Roelens, *Chem. Eur. J.*, **2018**, *24*, 6828.

Halogen bonding interaction ($4 - 60 \text{ kJmol}^{-1}$) is a “net attractive interaction between an electrophilic region associated with a halogen atom in a molecular entity and a nucleophilic region in another, or the same, molecular entity”.²³

The halogen bond has been widely studied and applied in of assembly of supramolecular systems, crystal engineering, conductive materials and medicinal chemistry.²⁴

This interaction has a prominent role in supramolecular chemistry and, in 2017, it was visualize for the first time at atomic level by Rissanen and coworkers that reported the X-ray crystal structure of the dimeric halogen-bonded supramolecular cage **I-17** in which three $[\text{N}\cdots\text{I}^+\cdots\text{N}]$ halogen bond interactions were present (Figure 1.11).²⁵

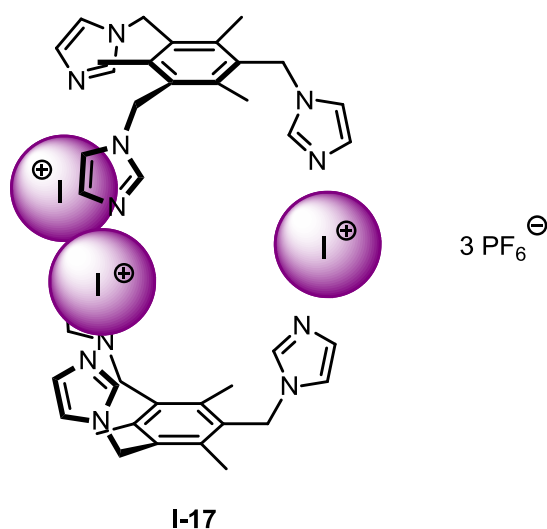


Figure 1.11 - Dimeric halogen-bonded supramolecular cage **I-17**.

²³ G.R. Desijaru, P.S. Ho, L. Kloo, A.C. Legon, R. Marquardt, P. Metrangolo, P. Politzer, G. Resnati and K. Rissanen, *Pure Appl. Chem.*, **2013**, 85, 1711.

²⁴ a) A.C.C. Carlsson, J. Gräfenstein, A. Budnjo, J.L. Laurila, J. Bergquist, A. Karim, R. Kleinmaier, U. Brath and M. Erdelyi, *J. Am. Chem. Soc.*, **2012**, 134, 5706.

b) S. B. Hakkert, M. Erdélyi, *J. Phys. Org. Chem.*, **2015**, 28, 226.

c) A.C.C. Carlsson, M. Uhrbom, A. Karim, U. Brath, J. Gräfenstein and M. Erdélyi, *CrystEngComm*, **2013**, 15, 3087.

d) A.C.C. Carlsson, K. Mehmeti, M. Uhrbom, A. Karim, M. Bedin, R. Puttreddy, R. Kleinmaier, A.A. Neverov, B. Nekoueishahraki, J. Gräfenstein, K. Rissanen and M. Erdélyi, *J. Am. Chem. Soc.*, **2016**, 138, 9853.

e) L. Turunen, U. Warzok, R. Puttreddy, N.K. Beyeh, C. A. Schalley and K. Rissanen, *Angew. Chem. Int. Ed.*, **2016**, 55, 14033.

f) G. Cavallo, P. Metrangolo, R. Milani, T. Pilati, A. Priimagi, G. Resnati and G. Terraneo, *Chem. Rev.*, **2016**, 116, 2478.

g) L.C. Gilday, S.W. Robinson, T.A. Barendt, M.J. Langton, B.R. Mullaney and P.D. Beer, *Chem. Rev.*, **2015**, 115, 7118.

²⁵ L. Turunen, A. Peuronen, S. Forsblom, E. Kalenius, M. Lahtinen and K. Rissanen, *Chem. Eur. J.*, **2017**, 23, 11714.

π - π stacking (0 - 50 kJmol⁻¹) is an attractive, non-covalent interaction between aromatic rings, since they contain π -bonds. The benzene dimer was used as model to study this type of interaction and the bond has been found to have an experimental energy of 8 - 12 kJmol⁻¹.²⁶

π - systems are very important for biological macromolecules, like in nucleobase stacking in DNA, and are widely incorporated in artificial supramolecular assemblies because of their versatility and the wide range of functionalization of the aromatic rings.²⁷

In 2018 Colquhoun and coworkers reported the synthesis and the X-ray crystal structure of the supramolecular 1:1 complex, which was based on the mutual complexation between a π -electron rich pyrene-based molecular tweezer **I-18** and π -electron deficient bisdiimide-bearing molecular tweezer **I-19**. They observed an association constant of $1200 \pm 90 \text{ M}^{-1}$ (Figure 1.12).²⁸

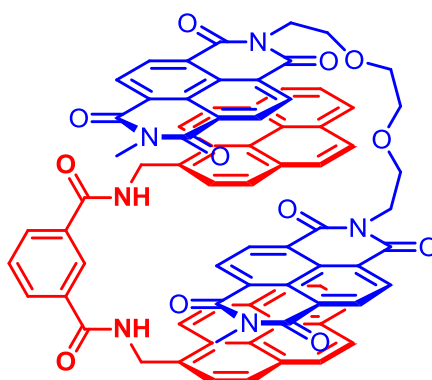


Figure 1.12 - “Tweezer -tweezer” complex **I-18:I-19**.

Olmstead and coworkers exploited the strength of this interaction to design a molecular tweezer, which was able to bind a fullerene (C₆₀) molecule.²⁹

²⁶ M. Sinnokrot, E.F. Valeev and C.D. Sherrill, *J. Am. Chem. Soc.*, **2002**, *124*, 10887.

²⁷ R.E. Babine and S.L. Bender, *Chem. Rev.*, **1997**, *97*, 1359.

²⁸ M.P. Parker, C.A. Murray, L.R. Hart, B.W. Greenland, W. Hayes, C.J. Cardin, H.M. Colquhoun, *Cryst. Growth Des.*, **2018**, *18*, 386.

²⁹ A. Sygula, F.R. Fronczek, R. Sygula, P.W. Rabideau and M.M. Olmstead, *J. Am. Chem. Soc.*, **2007**, *129*, 3842.

Cation - π interactions (4 - 80 kJmol⁻¹) arise between an electron-rich π - system and an electron-poor moiety (cations or positively charged molecule). These interactions play a fundamental role in nature, as in the nicotinic acetylcholine receptor, as well as in synthetic systems.³⁰

Dougherty and coworkers reported several studies about this type of interaction and, in 1992 they developed cyclophane macrocycles **I-20** and **I-21** which were able to catalyse the quaternarization of quinolone structures (Figure 1.13).^{31,32}

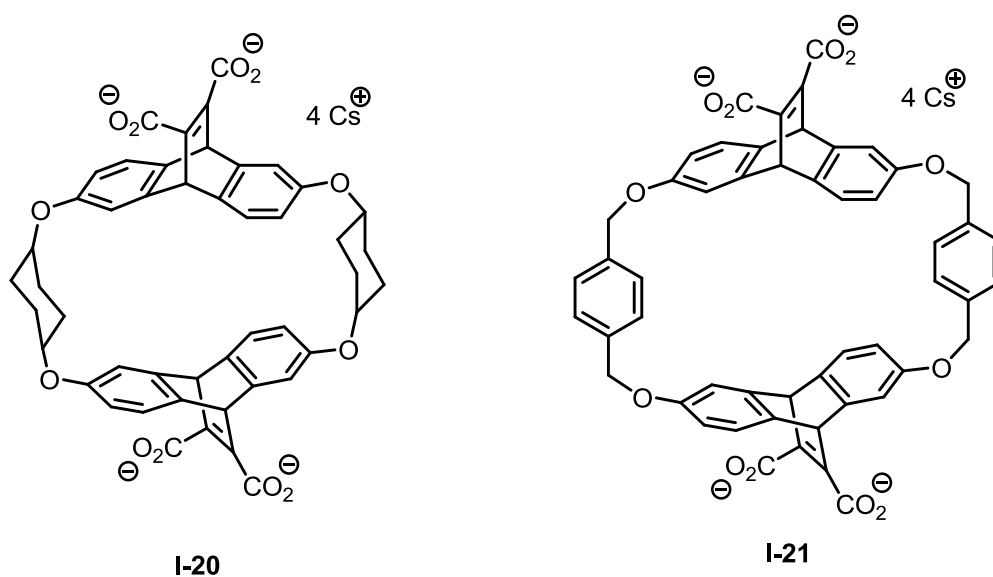


Figure 1.13 - Biomimetic cyclophane-based catalysts **I-20** and **I-21**.

The catalytic ability of macrocyclic receptors were based on the stabilization of the positive charge of the product by cation - π interactions.

³⁰ X. Xiu, N.L. Puskar, J.A.P. Shanata, H.A. Lester and D.A. Dougherty, *Nature*, **2009**, 458, 534.

³¹ a) T.J. Shepodd, M.A. Petti and D.A. Dougherty, *J. Am. Chem. Soc.*, **1986**, 108, 6085.

b) T.J. Shepodd, M.A. Petti and D.A. Dougherty, *J. Am. Chem. Soc.*, **1988**, 110, 1983.

c) M.A. Petti, T.J. Shepodd, R.E. Barrans Jr. and D.A. Dougherty, *J. Am. Chem. Soc.*, **1988**, 110, 6825.

d) D.A. Stauffer and D.A. Dougherty, *Tetrahedron Lett.*, **1988**, 29, 6039.

e) D.A. Stauffer, R.E. Barrans Jr. and D.A. Dougherty, *J. Org. Chem.*, **1990**, 55, 2762.

³² A. McCurdy, L. Jimenez, D.A. Stauffer and D.A. Dougherty, *J. Am. Chem. Soc.*, **1992**, 114, 10314.

Hydrophobic effect is not a non-covalent interaction, it can be defined as the “*tendency of hydrocarbons (or of lipophilic hydrocarbon-like groups in solutes) to form intermolecular aggregates in an aqueous medium, and analogous intramolecular interactions*”.^{33, 34}

This interaction is fundamental for life, being the key of phenomena like cell membrane formation, protein folding and protein-small molecules association.^{35, 36, 37, 38}

In 1980, Koga and coworkers reported the first X-ray crystal structure of the inclusion complex between 1,2,4,5-tetramethylbenzene (durene) and a synthetic water-soluble paracyclophane receptor **I-22** in acidic aqueous environment: this was the first time the hydrophobic effect was observed directly (Figure 1.14).³⁹

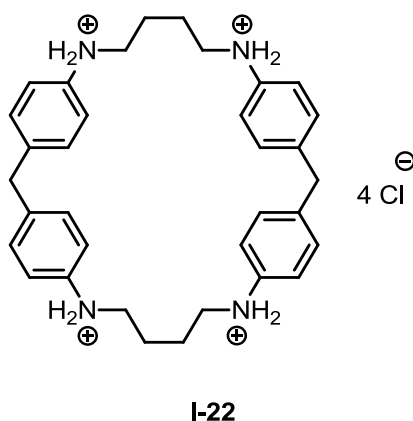


Figure 1.14- Water soluble paracyclophane-based durene receptor **I-22**.

In 1990, Schneider and coworkers synthesized several paracyclophanes with different size to study the correlation between size cavity and selectivity.⁴⁰

³³ D. Chandler, *Nature*, **2005**, 437, 640.

³⁴ C. Tanford, "*The hydrophobic effect: formation of micelles and biological membranes*". New York, Wiley, **1973**.

³⁵ W. Kauzmann, *Advances in Protein Chemistry*, **1959**, 14, 1.

³⁶ M. Charton and B. Charton, *Journal of Theoretical Biology*, **1982**, 99, 629.

³⁷ M.R. Lockett, H. Lange, B. Breiten, A. Heroux, W. Sherman, D. Rappoport, P.O. Yau, O.W. Snyder and G.M. Whitesides, *Angew. Chem. Int. Ed. Engl.*, **2013**, 52, 7714.

³⁸ B. Breiten, M.R. Lockett, W. Sherman, S. Fujita S, M. Al-Sayah M, H. Lange, C.M. Bowers, A. Heroux, G. Krilov and G.M. Whitesides, *J. Am. Chem. Soc.*, **2013**, 135, 15579.

³⁹ K. Odashima, A. Itai, Y. Iitaka, and K. Koga, *J. Am. Chem. Soc.*, **1980**, 102, 2504.

⁴⁰ H.-J. Schneider, T. Blatter and P. Zimmermann, *Angew. Chem. Int. Ed. Engl.*, **1990**, 29, 1161.

1.2. Mechanically Interlocked Molecules

1.2.1. Definition

The term mechanically interlocked molecules (or MIM) indicates a class of supramolecular assemblies composed by molecular subunits, which are electronically independent of each other, and the breaking of a covalent bond is a necessary condition for the disassembly of those architectures.

This type of structure is closely related to the concept of molecular topology, a topic which has raised a great interest in supramolecular chemistry in the past thirty years and concerns the study of molecules with a non-trivial topology, which means molecules that cannot be represented in two dimensions without an intersection.^{41, 42}

Catenanes, rotaxanes, molecular knots and molecular Borromean rings are the most famous examples of mechanically interlocked molecular architectures.⁴³

⁴¹ J.-P. Sauvage and C. Dietrich-Buchecker, *Molecular Catenanes, Rotaxanes and Knots : A journey through the World of Molecular Topology*, Eds. ; Wiley-VCM : Weinheim, Germany **1999**.

⁴² G.A. Breault, C.A. Hunter and P.C. Mayers, *Tetrahedron*, **1999**, 55, 5265.

⁴³ a) P.R. Ashton, C.L. Brown, E.J.T. Chrystal, T.T. Goodnow, A.E. Kaifer, K.P. Parry, D. Philp, A.M.Z. Slawin, N. Spencer, J.F. Stoddart and D.J. Williams, *Journal of the Chemical Society, Chem. Commun.*, **1991**, 9, 634.

b) J.A. Bravo, F.M. Raymo, J.F. Stoddart, A.J.P. White and D. J. Williams, *Eur. J. Org. Chem.*, **1998**, 11, 2565.

c) J. Guo, P.C. Mayers, G.A. Breault and C.A. Hunter, *Nat. Chem.*, **2010**, 2, 218.

d) J.J. Danon, A. Krüger, D.A. Leigh, J.-F. Lemonnier, A.J. Stephens. I. J. Vitorica-Yrezabal and S.L. Woltering, *Science*, **2017**, 355, 159.

e) K.S. Chichak, S.J. Cantrill, A.R. Pease, S.-H. Chiu, G.W.V. Cave, J.L. Atwood and J.F. Stoddart, *Science*, **2005**, 304, 1308.

1.2.2. Catenanes

A *catenane* (from latin *catena*, chain) is a structure composed by two or more interlocked rings that cannot be separated without breaking a covalent bond.⁴⁴

The systematic nomenclature is [n]catenane, where $n \geq 2$ indicates the number of subunits that form the complete structure: as shown in Figure 1.15, [2]catenane is the simplest member of this class of mechanically interlocked molecular architectures.

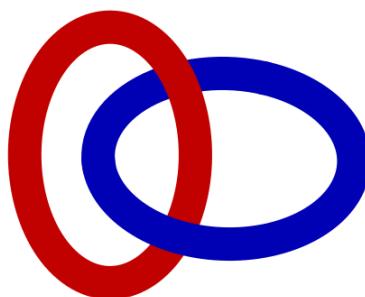


Figure 1.15 - Representation of a [2]catenane.

This type of molecular geometry is present in biological systems and it is a possible topological isomer of DNA, as observed by Vinograd and coworkers using atomic force microscopy.⁴⁵

The first artificial [2]catenane was obtained by Wasserman and coworkers in 1960, but the first directed synthesis was developed by Schill and coworkers in 1964 using a statistical approach, that consisted in the synthesis of two macrocycles connected by a covalent bond and rupture of this bond in the final steps.^{46, 47}

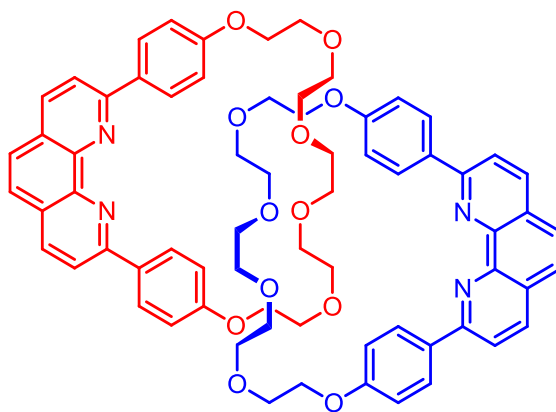
⁴⁴ IUPAC Compendium of Chemical Terminology **1995**, 67, 1327.

⁴⁵ B. Hudson and J. Vinograd, *Nature*, **1967**, 216, 647.

⁴⁶ H.L. Frisch and E. Wasserman, *J. Am. Chem. Soc.*, **1961**, 83, 3789.

⁴⁷ G. Schill and A. Lüttringhaus, *Angew. Chem. Int. Ed.* **1964**, 3, 546.

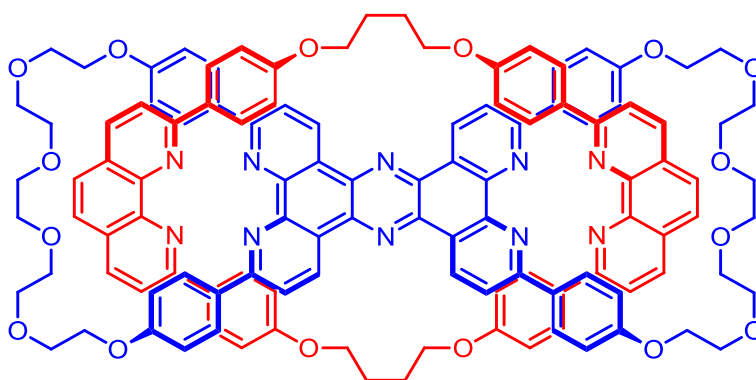
The breakthrough in the synthesis of catenanes was made by Sauvage and coworkers in 1983 when a copper(I)-template assisted method allowed to synthesize the [2]catenane **I-23** in one step synthesis in 27% yield (Figure 1.16).⁴⁸



I-23

Figure 1.16- 1,10-phenanthroline-based [2]catenane **I-23**.

A strong example of the huge efficacy of the template effect provided by copper(I) was the synthesis of a handcuff-shaped [2]catenane **I-24**, achieved by Sauvage and coworkers in 2005 (Figure 1.17).⁴⁹



I-24

Figure 1.17- Handcuff-shaped [2]catenane **I-24**.

⁴⁸ C.O. Dietrich-Buchecker, J.P. Sauvage and J.P. Kintzinger, *Tetrahedron Lett.*, **1983**, 24, 5095.

⁴⁹ J. Frey, T. Kraus, V. Heitz and J.-P. Sauvage, *Chem. Commun.*, **2005**, 42, 5310.

In 1989, Stoddart and coworkers synthesized a [2]catenane **I-26** exploiting the strong interactions between an π -electron rich bisparaphenylene-34-crown-10 and an positively charged electron-poor pyridinium unit **I-25** (Figure 1.18).⁵⁰

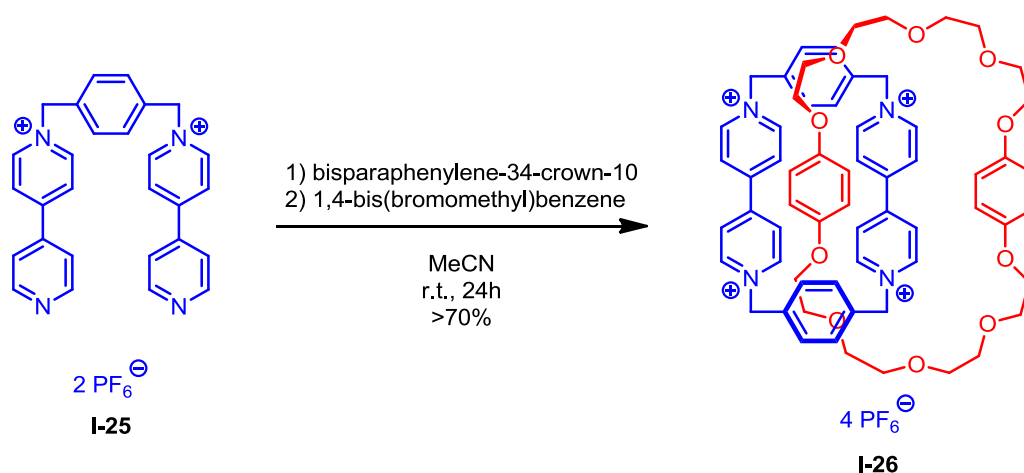


Figure 1.18 - π - π Stacking-based synthesis of [2]catenane **I-26**.

The strong interactions between rings allowed development of a straightforward methodology, which allowed to obtain several catenane-based supramolecular assemblies.^{51, 52}

In the past two decades, Sanders and coworkers contributed enormously to this field, developing a huge number of catenane-based supramolecular architectures.⁵³

⁵⁰ P.R. Ashton, T.T. Goodnow, A.E. Kaifer, M. V.Reddington, A.M.Z.Slawin, N. Spencer, J.F. Stoddart, C. Vicent and D.J. Williams, *Angew. Chem. Int. Ed.*, **1989**, 28, 1396.

⁵¹ D.B. Amabilino, P.R. Ashton, A.S. Reder, N. Spencer and J.F. Stoddart, *Angew. Chem. Int. Ed. Engl.*, **1994**, 33, 1286.

⁵² D.B. Amabilino, P.R. Ashton, C.L. Brown, E. Cordova, L.A. Godinez, L.A. Goodnow, T.T. Goodnow, A.E. Kaifer, S.P. Newton, M. Pietraszkiewicz, D. Phiip, F.M. Raymo, A.S. Reder, M.T.Rutland, A.M.Z. Slawin, ; N. Spencer, ; J.F. Stoddart and D.J. Williams, *J. Am. Chem. Soc.*, **1995**, 117, 1271.

⁵³ a) F.B.L. Cougnon, H.Y. Au-Yeung, G.D. Pantos, and J.K.M. Sanders, *J. Am. Chem. Soc.*, **2011**, 133, 3198.

b) H.Y. Au-Yeung, G.D. Pantos and J.K.M. Sanders, *J. Org. Chem.*, **2011**, 76, 1257.

c) H.Y. Au-Yeung, G.D. Pantos and J.K.M. Sanders, *Angew. Chem. Int. Ed.*, **2010**, 49, 5331.

d) H.Y. Au-Yeung, G.D. Pantos and J.K.M. Sanders, *J. Am. Chem.Soc.*, **2009**, 131, 16030.

e) R.T.S. Lam, A. Belenguer, S.L. Roberts, C.Naumann, T. Jarrosson, S. Otto and J.K.M. Sanders, *Science*, **2005**, 308, 667.

f) D.G. Hamilton, J.E. Davies, L. Prodi and J.K.M. Sanders, *Chem. Eur. J.*, **1998**, 4, 608.

g) F.B.L. Cougnon, N.A. Jenkins, G.D. Pantos and J.K.M. Sanders, *Angew. Chem. Int. Ed.*, **2012**, 51, 1443.

1.2.3. Rotaxanes

A rotaxane (from latin *rota*, wheel and *axis*, axle) is a “molecule in which a ring encloses another, rod-like molecule having end groups too large to pass through the ring opening, and thus holds the rod-like molecule in position without covalent bonding”.⁵⁴

A rotaxane is composed of one dumbbell-like component or thread (blue), one ring component (red) and bulky groups or stoppers (yellow), which prevent the dethreading of the ring (Figure 1.19). As in the case of catenanes, the systematic nomenclature is [n]rotaxane, where $n \geq 2$ indicates the number of subunits that form the complete structure

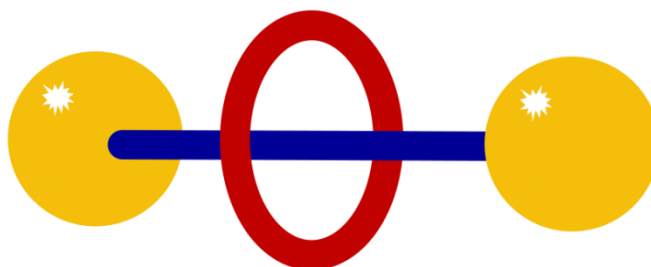


Figure 1.19 – Cartoon representation of a [2]rotaxane.

The first synthesis of a rotaxane was reported in 1967 by Harrison and coworkers. This first attempt to synthesize a rotaxane (or “hooplane”, as the authors suggested in the work) was based on statistics: reacting 1,10-decanediol and (triphenyl)methyl chloride in presence of a resin-supported 30-members acyloin macrocycle, a certain number of reactions should take place inside the cavity of the ring-shaped molecule **I-27**, affording the mechanically interlocked molecule.

The first rotaxane **I-28** was obtained in 6% yield after 70 “threading” treatments (Figure 1.20).⁵⁵

⁵⁴ IUPAC, *Compendium of Chemical Terminology*, 2nd ed., **1997**

⁵⁵ I.A. Harrison and S. Harrison, *J. Am. Chem. Soc.*, **1967**, 89, 5723.

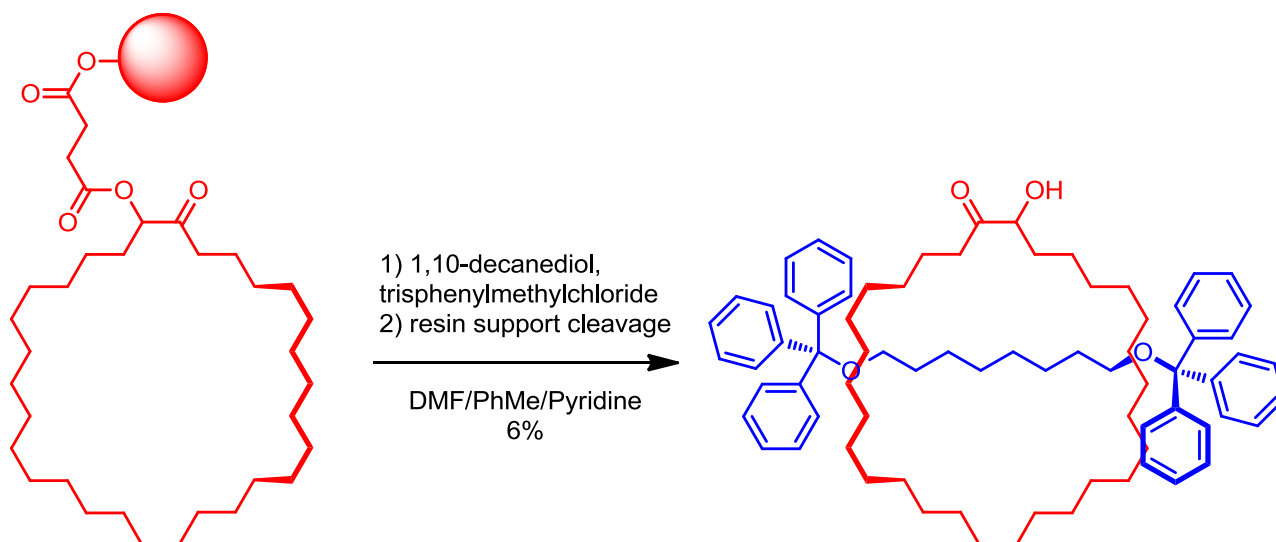


Figure 1.20 - Synthetic scheme of first [2]rotaxane **I-28**.

During the past three decades, the synthetic methods to obtain [2]rotaxanes have been hugely improved and four main synthetic strategies have been developed:

- *Capping approach*
- *Slipping approach*
- *Clipping approach*
- *Active metal-template approach*

The details of each approach will be discussed in Chapter 4.

These strategies allowed the synthesis of a wide range of rotaxanes and rotaxane-based supramolecular assemblies, namely Janus [2]rotaxane, multi-threaded rotaxanes, quasi[1]rotaxane, polyrotaxanes (Figure 1.21).⁵⁶

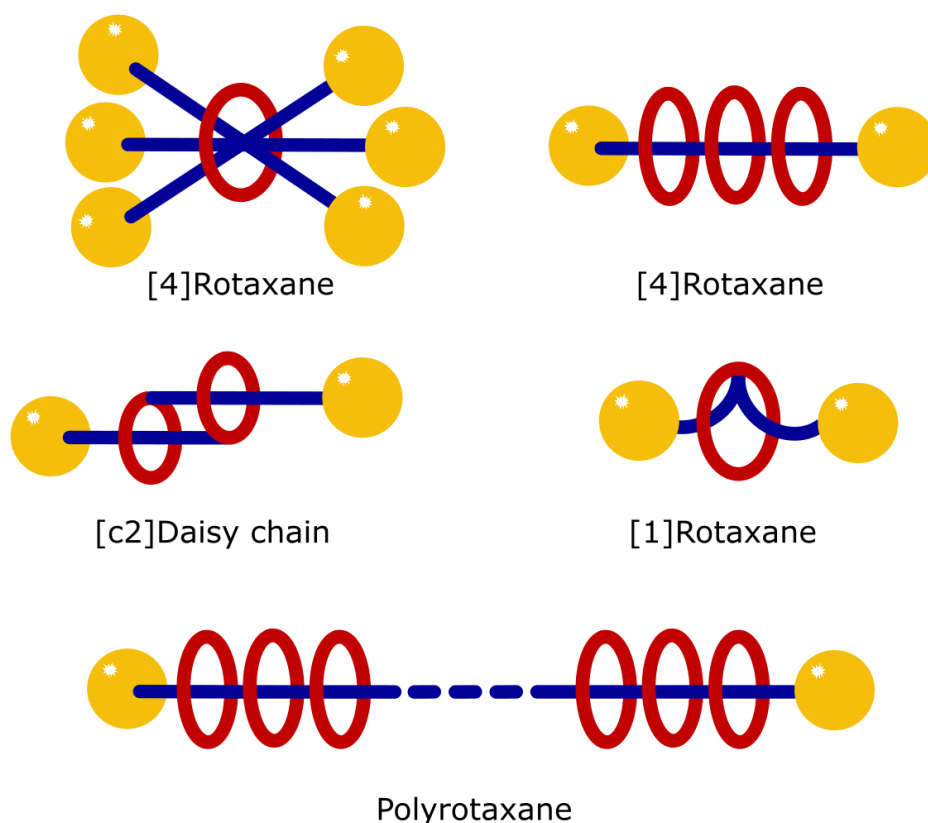


Figure 1.21 - Rotaxane-based supramolecular assemblies.

⁵⁶ a) D.R. Kohn, L.D. Movsisyan, A.L. Thompson and H.L. Anderson, *Org. Lett.*, **2017**, *19*, 348.

b) L.D. Movsisyan, M. Franz, F. Hampel, A.L. Thompson, R.R. Tykwinski and H.L. Anderson, *J. Am. Chem. Soc.*, **2016**, *138*, 1366.

c) M. Franz, J.A. Januszewski, D. Wendinger, C. Neiss, L.D. Movsisyan, F. Hampel, H.L. Anderson, A. Görling, R.R. Tykwinski, *Angew. Chem. Int. Ed.*, **2015**, *54*, 6645.

d) N.H. Evans and P.D. Beer, *Chem. Eur. J.*, **2011**, *17*, 10542.

e) S. Brovelli, G. Latini, M.J. Frampton, S.O. McDonnell, F.E. Oddy, O. Fenwick, H.L. Anderson and F. Cacialli, *Nano Lett.*, **2008**, *8*, 4546.

f) D.A. Leigh, V. Marcos, T. Nalbantoglu, I.J. Vitorica-Yrezabal, F.T. Yasar and X. Zhu, *J. Am. Chem. Soc.*, **2017**, *139*, 7104.

g) J.J. Danon, D.A. Leigh, P.R. McGonigal, J.W. Ward and J. Wu, *J. Am. Chem. Soc.*, **2016**, *138*, 12643.

h) L. Steemers, M.J. Wanner, M. Lutz, H. Hiemstra and J.H. van Maarseveen, *Nat. Commun.*, **2017**, *8*, 15392.

i) A. Harada, J. Li and M. Kamachi, *Nature*, **1992**, *356*, 325.

j) J.E.M. Lewis, J. Winn, L. Cera, S.M. Goldup, *J. Am. Chem. Soc.*, **2016**, *138*, 16329.

1.2.4. Characteristics and effect

The presence of a mechanical bond influences the chemistry of the components that form the mechanically interlocked molecular architecture.⁵⁷

In the first place, the mechanical bond increases the strength of the non-covalent interaction on which the supramolecular architecture is based: in 1985 Sauvage and coworkers noticed that harsher conditions were required to remove the copper(I) ion from a [2]catenane if compared to the usual demetalation conditions for the copper(I):1,10-phenantroline complex. Even if the structural motif was the same, the presence of mechanical bond reduced the degree of freedom of the components, leading to an increase of the interaction. This effect was called “catenand effect”.⁵⁸

In 2006, Takata and coworkers noticed a similar feature in secondary ammonium:crown ether-based supramolecular architectures: in this case, the pK_a of the mechanically bonded ammonium component was higher than the free component.⁵⁹

In 2011, Goldup and coworkers studied the correlation between the loss of degree of freedom of the components in a mechanically interlocked molecule and the increase of the non-covalent interaction strength: by ¹H-NMR studies, they noticed that the strength of the hydrogen bond between the triazole proton on the thread and the nitrogen of a bipyridine unit on the ring increased if smaller macrocycles were involved. The same correlation was observed when smaller threads were used as well.⁶⁰

⁵⁷ E.A. Neal and S.M. Goldup, *Chem. Comm.*, **2014**, 50, 5128.

⁵⁸ A.M. Albrecht-Gary, Z. Saad, C.O. Dietrich-Buchecker and J.P. Sauvage, *J. Am. Chem. Soc.*, **1985**, 107, 3205.

⁵⁹ Y. Tachibana, H. Kawasaki, N. Kihara and T. Takata, *J. Org. Chem.*, **2006**, 71, 5093.

⁶⁰ H. Lahlali, K. Jobe, M. Watkinson and S.M. Goldup, *Angew. Chem., Int. Ed.*, **2011**, 50, 4151.

A second important consequence of the presence of a mechanical bond on the chemistry of the component is the alteration of the chemical reactivity: in mechanically interlocked molecules, the components are close one to another, which means a dramatic increase of the steric hindrance.

In 1999 Vögtle and coworkers observed a strong resistance of the alkene moiety of fumaramide-containing [2]rotaxane **I-29** towards hydrogenation: only 6% yield of hydrogenated rotaxane was obtained after 18 hours under hydrogenation conditions (H_2 in presence of Pd/C), while 91% yield was obtained for the free thread. The presence of mechanical bond was the cause of this decrease of reactivity (Figure 1.22).⁶¹

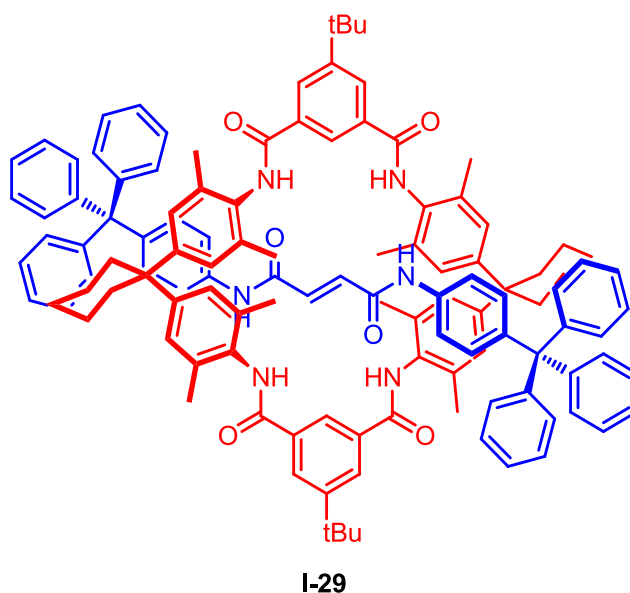


Figure 1.22 - Fumaramide-containing rotaxane **I-29**.

A similar feature was also observed by Leigh and coworkers in 2004: during the study of reversible covalent chemistry-induced molecular shuttling, a decrease in reactivity of a fumaramide unit towards Diels-Alder cycloaddition with cyclopentadiene was observed. They ascribed this phenomenon to the presence of the macrocycle around the fumaramide moiety.⁶²

⁶¹ A.H. Parham, B. Windisch and F. Vögtle, *Eur. J. Org. Chem.*, **1999**, 5, 1233.

⁶² D.A. Leigh and E.M. Perez, *Chem. Commun.*, **2004**, 2262.

Damping the chemical reactivity is not always something to avoid, especially in the case of elusive or highly reactive molecules.

In 2003, Takata and coworkers were able to synthesize and fully characterize a reactive thiophosphonium salt in a “rotaxanated form” **I-30**. All the attempts to synthesize the free thiophosphonium thread were unsuccessful. The presence of the macrocycle was necessary to stabilize the reactive salt and the hexamethylphosphonium group was bulky enough to prevent the dethreading. X-ray crystallography proved the interlocked nature of the assembly (Figure 1.23).⁶³

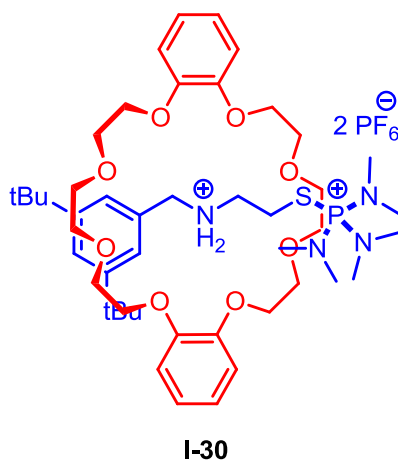


Figure 1.23 - Thiophosphonium salt-bearing [2]rotaxane **I-30**.

In 2013, Goldup and coworkers reported the synthesis of an air- and moisture-stable copper(I)-triazolide rotaxane. Copper(I)-carbon is an organometallic bond known to be highly reactive and most of the organocopper compounds are air- and moisture-sensitive, but the mechanical bond allowed to synthesize in aqueous condition an air-stable complex in high yield, which was stable enough to be characterized by X-ray crystallography.^{64, 65}

⁶³ T. Oku, Y. Furusho and T. Takata, *Org. Lett.*, **2003**, *5*, 12384.

⁶⁴ R.C. Böttger, *Annalen.*, **1859**, *109*, 351.

⁶⁵ J. Winn, A. Pinczewska and S.M. Goldup, *J. Am. Chem. Soc.*, **2013**, *135*, 13318.

1.2.5. Applications

The alteration of chemical reactivity of the components, due to presence of mechanical bond, has been exploited and applied in different ways.

In 2005, Smith and coworkers showed how the rotaxane-based architecture was able to enhance the chemical stability of a squaraine-containing thread and avoid aggregation between the dyes (Figure 1.24).⁶⁶

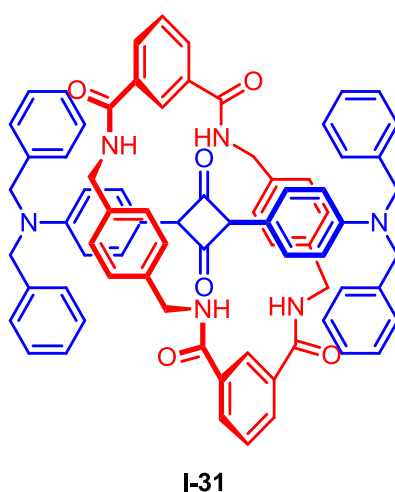


Figure 1.24 - Squaraine-based [2]rotaxane **I-31**.

The squaraine motif has been largely used in the construction of rotaxane-based dyes, probes and dendrimers.⁶⁷

Several studies about enhancement of stability of different dyes in polyrotaxane-derived structures were reported by Anderson and coworkers.⁶⁸

⁶⁶ E. Arunkumar, C.C. Forbes, B.C. Noll and B.D. Smith, *J. Am. Chem. Soc.*, **2005**, *127*, 3288.

⁶⁷ a) J.J. Gassensmith, L. Barr, J.M. Baumes, A. Paek, A. Nguyen and B.D. Smith, *Org. Lett.*, **2008**, *10*, 3343.

b) T.S. Jarvis, C.G. Collins, J.M. Dempsey, A.G. Oliver and B.D. Smith, *J. Org. Chem.*, **2017**, *82*, 5819.

c) C.G. Collins, J.M. Lee, A.G. Oliver, O. Wiest and B.D. Smith, *J. Org. Chem.*, **2014**, *79*, 1120.

d) A.G. White, N. Fu, W. Matthew Leevy, J.-J. Lee, M.A. Blasco and B.D. Smith, *Bioconjugate Chem.*, **2010**, *21*, 1297.

⁶⁸ a) F. Cacialli, J.S. Wilson, J.J. Michels, C. Daniel, C. Silva, R.H. Friend, N. Severin, P. Samori, J.P. Rabe, M. O'Connell, P.N. Taylor and H.L. Anderson, *Nat. Mater.*, **2002**, *1*, 160.

b) J.E.H. Buston, J.R. Young and H.L. Anderson, *Chem. Commun.*, **2000**, 905.

c) S. Anderson, T. D. W. Claridge and H. L. Anderson, *Angew. Chem., Int. Ed.*, **1997**, *36*, 1310.

d) M.J. Frampton and H.L. Anderson, *Angew. Chem., Int. Ed.*, **2007**, *46*, 1028.

e) R. Eelkema, K. Maeda, B. Odell and H.L. Anderson, *J. Am. Chem. Soc.*, **2007**, *129*, 12384.

In mechanically interlocked molecules, the components can move one respect to the other. If the movement is induced and/or controlled in some manner, the supramolecular assembly can be considered as a molecular machine. To be classify as machine, “a molecular assembly should produce mechanical motion (output) like macroscopic machines, in response to some appropriate external stimulus (input)”.⁶⁹

A wide variety of molecular machines have been synthetize and, even if some of them are based on single molecules, most of them are mechanically interlocked molecular architectures, namely molecular shuttle, molecular switches, molecular assemblers.⁷⁰

From literature, different types of energy have been used to induce motion in mechanically interlocked molecular assemblies:

- chemical energy⁷¹
- electrochemical energy⁷²
- photochemical energy⁷³
- other type of energy like entropy change or solvent change^{74, 75}

⁶⁹ R. Ballardini, V. Balzani, A. Credi, M.T. Gandolfi and M. Venturi, *Acc. Chem. Res.*, **2001**, *34*, 445.

⁷⁰ a) U.G.E. Perera, F.Ample, H. Kersell, Y. Zhang, G. Vives, J. Echeverria, M. Grisolia, G. Rapenne and C. Joachim, *Nature Nanotechnology*, 2013, *8*, 46.

b) M. Schliwa and G. Woehlke, *Nature*, **2003**, *422*, 759.

c) A.I. Day, R.J. Blanch, A.P. Arnold, S. Lorenzo, G.R. Lewis and I. Dance, *Angew. Chem. Int. Ed.*, **2002**, *41*, 275.

d) B. Lewandowski, G. De Bo, J.W. Ward, M. Pappmeyer, S. Kuschel, M.J. Aldegunde, P.M.E. Gramlich, D. Heckmann, S.M. Goldup, D.M. D’Souza, A.E. Fernandes, D.A. Leigh, *Science*, **2013**, *339*, 189.

e) G. De Bo, S. Kuschel, D.A. Leigh, B. Lewandowski, M. Pappmeyer, J.W. Ward, *J. Am. Chem. Soc.*, **2014**, *136*, 5811.

f) G. De Bo, Gall, A.Y.M. Gall, M.O. Kitching, S. Kuschel, D.A. Leigh, D.J. Tetlow and J.W. Ward, *J. Am. Chem. Soc.*, **2017**, *139*, 10875.

g) S. Kassem, Salma; Lee, Alan T. L.; D.A. Leigh.; Marcos, Vanesa; Palmer, I. Leoni I.; S. Pisano, *Nature*, **2017**, *549*, 374.

h) G. De Bo, A.Y.M. Gall, S. Kuschel, J.De Winter, P. Gerbaux and D.A Leigh, *Nature Nanotechnology*, **2018**, *13*, 381.

⁷¹ Y. Jiang , J. B. Guo and C. F. Chen, *Org. Lett.*, **2010**, *12*, 4248.

⁷² J.C. Olsen ,A. C.Fahrenbach, A. Trabolsi , D.C.Friedman, S.K. Dey , C.M. Gothard, A.K.Shveyd, T.B.Gasa , J. M.Spruell , M. A. Olson , C. Wang , H.P. Jacquot de Rouville , Y.Y.Botros and J. F. Stoddart, *Org. Biomol. Chem.*, **2011**, *9*, 7126.

⁷³ Balzani V., Clemente-León M., Credi A., Ferrer B., Venturi M., A.H. Flood, J.F. Stoddart, *Proc. Natl. Acad. Sci. U.S.A.*, **2006**, *103*, 1178.

⁷⁴ A. Mateo-Alonso , C. Ehli , D.M. Guldi and M. Prato, *Org. Lett.*, **2013**, *15*, 84.

⁷⁵ T. Umehara, H. Kawai, K. Fujiwara, T. Suzuki, *J. Am. Chem. Soc.*, **2008**, *130*, 13981.

In 2004, Leigh and coworkers reported the synthesis of the first pH-dependent [2]rotaxane-based molecular shuttle **I-32**, comprising a NH \cdots anion hydrogen bonding interaction between ring and succinamide station (Figure 1.25).⁷⁶

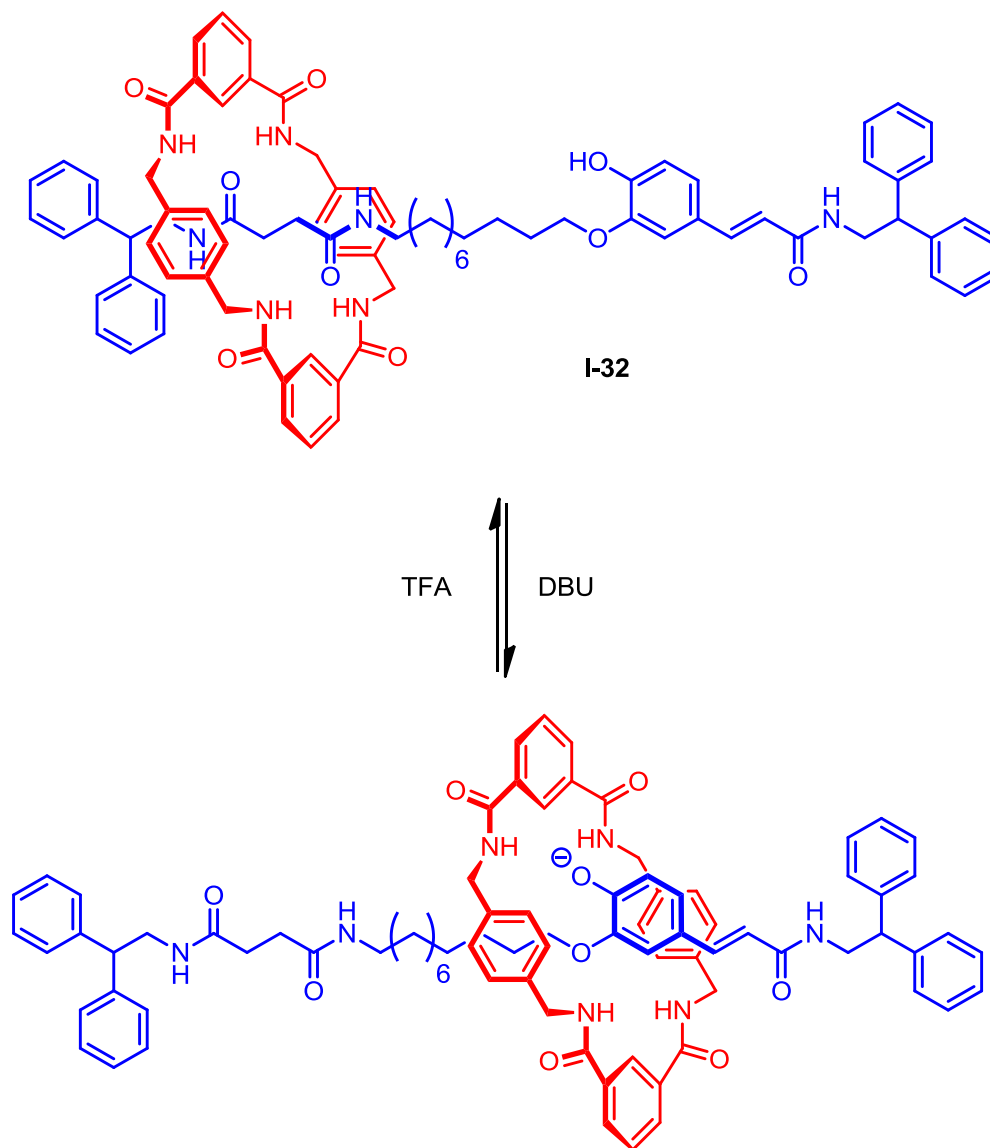


Figure 1.25 - pH-dependent molecular shuttle **I-32**.

⁷⁶ C.M. Keaveney and D.A. Leigh, *Angew. Chem. Int. Ed.*, **2004**, *43*, 1222.

In 1994, Sauvage and coworkers developed an electrochemical-controlled [2]catenane-based heterocircuit **I-33** (Figure 1.26). The movement was induced by the change of oxidation state of the copper ion and consequent change of the geometry in the coordination sphere: copper(I) ion coordinates the two 1,10-phenanthroline moieties of the rings in a tetrahedral arrangement. Upon oxidation, copper (I) is converted in copper(II), which is preferentially bonded by a tert-pyridine moiety and a 1,0-phenanthroline moiety in a 5-coordinated geometry.⁷⁷

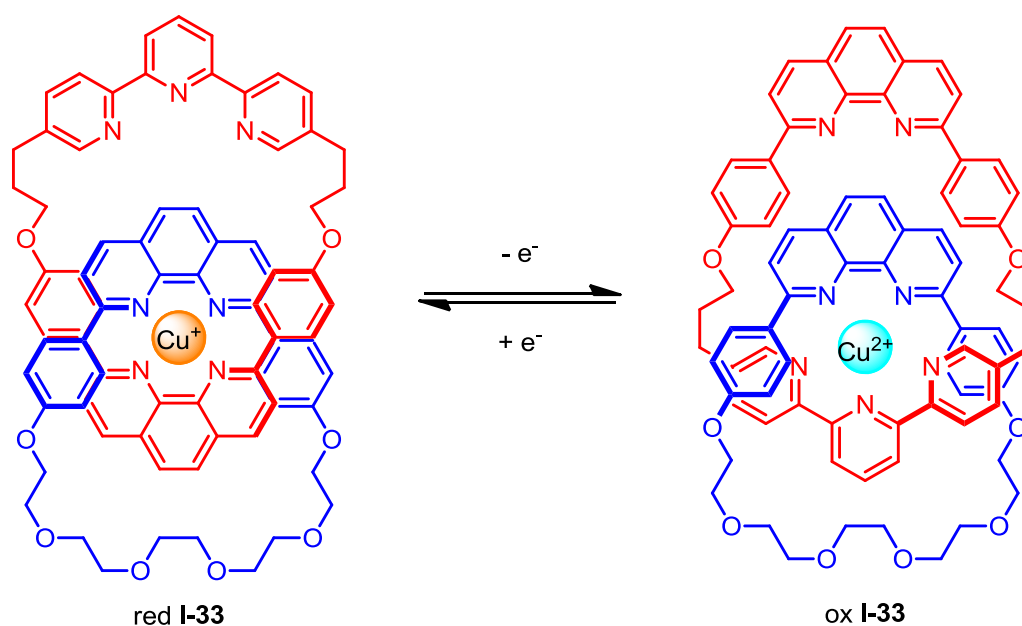


Figure 1.26 - Electrochemical-controlled [2]catenane **I-33**.

Several [2]catenane-based electrochemically switched molecular homo- and heterocircuit have been developed.⁷⁸

⁷⁷ A. Livoreil, C.O. Dietrich-Buchecker and J.-P. Sauvage, *J. Am. Chem. Soc.*, **1994**, *116*, 9399.

⁷⁸ a) F. Baumann, A. Livoreil, W. Kaim, J.-P. Sauvage, *Chem. Commun.*, **1997**, 35.

b) A. Livoreil, J.-P. Sauvage, N. Armaroli, V. Balzani, L. Flamigni and B. Ventura, *J. Am. Chem. Soc.*, **1997**, *119*, 12114.

In 2004, Leigh and coworkers developed a photochemical-switched bistable fluorescent molecular shuttle **I-34** (Figure 1.27). Upon irradiation at 312 nm, the double bond of fumaramide was photoisomerized and the ring was shuttled from the so-formed maleamide station to the peptide station: the pyridinium-containing macrocycle was close enough to quench the fluorescence. ⁷⁹

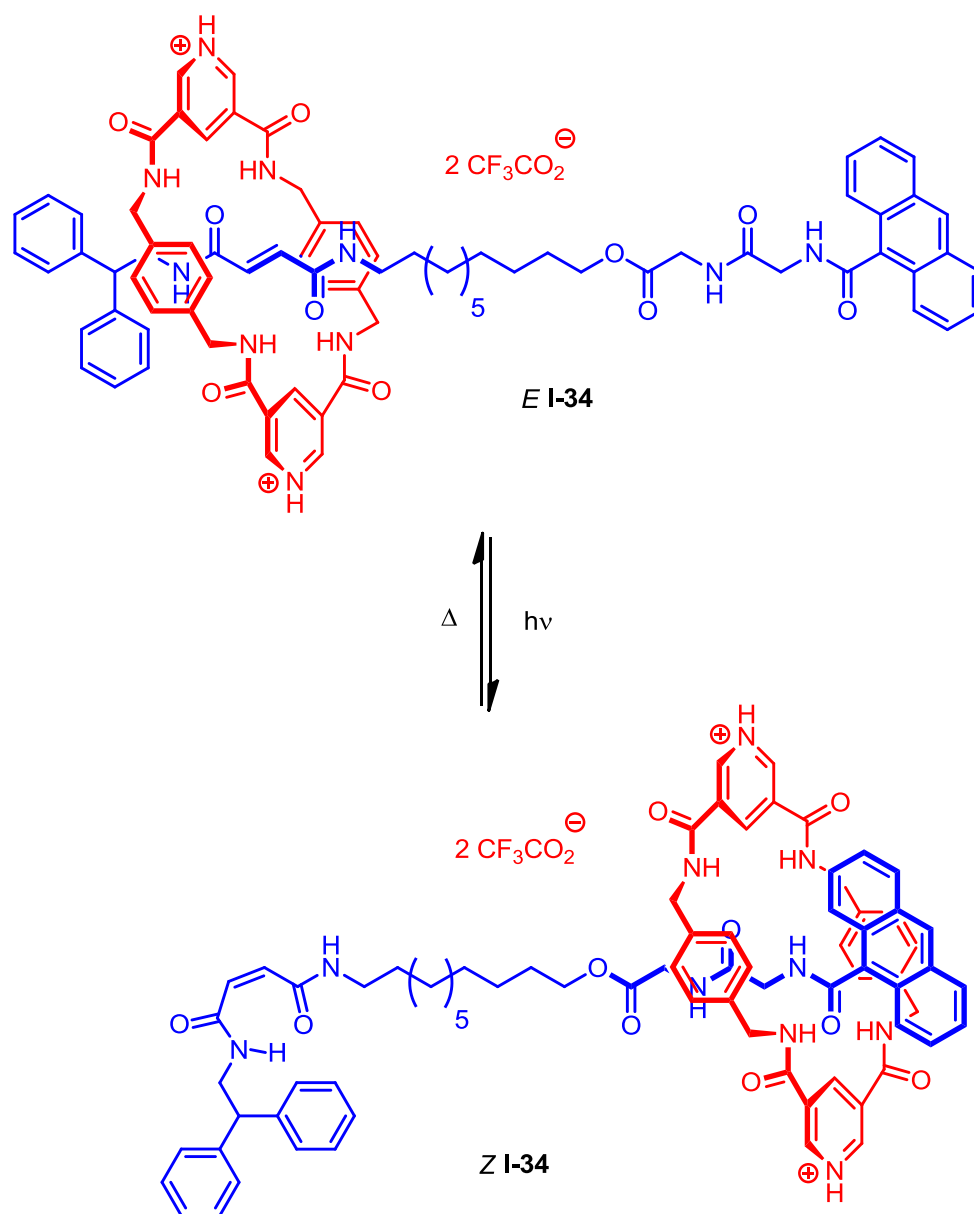


Figure 1.27 - Light-dependent molecular shuttle **I-34**.

⁷⁹ E.M. Pérez, D.T.F. Dryden, D.A. Leigh, G. Teobaldi and F. Zerbetto, *J. Am. Chem. Soc.*, **2004**, *126*, 12210.

In 2003, Turco and coworkers developed a solvent-dependent [2]rotaxane-based molecular shuttle **I-35**. In nonpolar solvents, like DCM, macrocycle and peptide station were bonded by hydrogen-bonding interactions, while in polar solvents, like DMSO, the hydrogen bonds were broken by the competing solvent and the macrocycle shuttled to the alkyl chain (Figure 1.28).⁸⁰

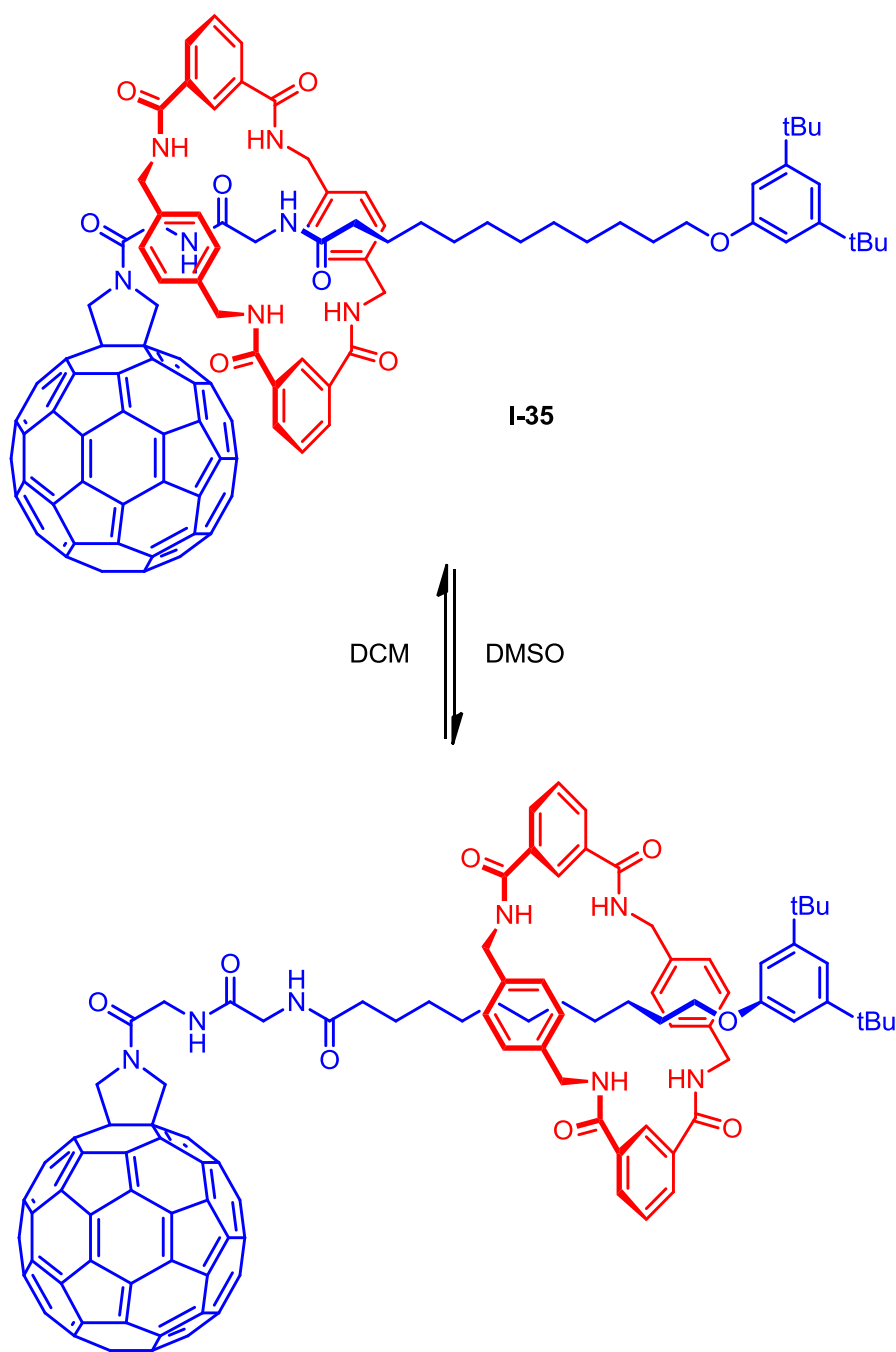


Figure 1.28 - Solvent-dependent molecular shuttle **I-35**.

⁸⁰ T. Da Ros, D.M. Guldi, A. Farran Morales, D.A. Leigh, M. Prato and R. Turco, *Org. Lett.*, **2003**, 5, 689.

1.3. Click chemistry

The structural complexity of molecular interlocked molecules is reflected by the multi-step and difficult syntheses which are required to obtain them, moreover the presence of a wide number of different functional groups limit the type of reactions that can be involved.

For all these reasons, straightforward, highly selective and high yield reactions are necessary and the “click” reactions are one of the most appealing class of reactions for the construction of supramolecular architectures.

The “click chemistry” concept was introduced by Sharpless and coworkers in 2001 and, since its discovery, this topic has been ubiquitous in scientific literature.^{81, 82, 83}

To be defined as “click”, a reaction has to have some requirements:

- high yields
- high tolerance towards other functional groups
- high selectivity
- high stereospecificity
- high thermodynamic driving force ($> \text{kJmol}^{-1}$)
- equimolarity

In addition, also reaction conditions and purification step should satisfy some conditions:

- no chromatographic techniques, preferably recrystallization, precipitation or distillation
- involvement of readily accessible starting materials
- elevated mildness in reaction condition
- high atomic economy

⁸¹ H.C. Kolb, M.G. Finn and K.B. Sharpless, *Angew. Chem. Int. Ed.*, **2001**, *40*, 2004.

⁸² J.E. Moses and A.D. Moorhouse, *Chem. Soc. Rev.*, **2007**, *36*, 1249.

⁸³ V.V. Rostovtsev, L.G. Green, V.V. Fokin and B.K. Sharpless, *Angew. Chem., Int. Ed.*, **2002**, *41*, 2596.

Even if the requirements narrow the number of possible candidates, some reactions have found to be defined as “click” reactions:

- thiol-ene reaction^{84, 85}
- Diels-Alder reactions^{86, 87}
- [4+1] cycloaddition between isocyanides and tetrazines⁸⁸
- nucleophilic substitution on small strained rings⁸⁹

The most famous member of the “click” reactions is the 1,3-dipolar azide-alkyne Huisgen cycloaddition, named after Huisgen who first developed and reported this reaction in 1963.^{90, 91}

This reaction can be catalyzed by metals like silver or ruthenium, but the most popular version is the copper(I)-catalyzed 1,3-dipolar azide-alkyne cycloaddition, or CuAAC.^{92, 93, 94}

The reaction is usually performed using commercially available sources of copper(I), like copper(I) bromide, copper(I) iodide, tetrakisacetonitrile copper(I) hexafluorophosphate, but better results were obtained using a mixture of a copper(II) salt, like copper(II) sulfate or copper acetate, and a reducing agent, sodium ascorbate or copper powder, to produce the copper (I) species in situ. Due to the instability of copper (I) compounds towards air and moisture, stabilizing ligands have been developed and synthesized in order to improve the reaction outcome.⁹⁵

⁸⁴ C.E. Hoyle and C.N. Bowman, *Angew. Chem. Int. Ed.*, **2010**, *49*, 1540.

⁸⁵ A.B. Lowe, *Polymer Chemistry*, **2010**, *1*, 17.

⁸⁶ M.L. Blackman, M. Royzen and J.M. Fox, *J. Am. Chem. Soc.*, **2008**, *130*, 13518.

⁸⁷ N.K. Devaraj, R. Weissleder and S.A. Hilderbrand, *Bioconjugate Chem.*, **2008**, *19*, 2297.

⁸⁸ H. Stöckmann, A. Neves, S. Stairs, K. Brindle and F. Leeper, *Org. Biom. Chem.*, **2011**, *9*, 7303.

⁸⁹ B.A. Kashemirov, J.L.F. Bala, X. Chen, F.H. Ebetino, Z. Xia, R.G.G. Russell, F.P. Coxon, A.J. Roelofs, M.J. Rogers and C.E. McKenna, *Bioconjugate Chem.*, **2008**, *19*, 2308.

⁹⁰ R. Huisgen, *Angew. Chem. Int. Ed.*, **1963**, *2*, 633.

⁹¹ R. Huisgen, *Angew. Chem. Int. Ed.*, **1963**, *2*, 565.

⁹² C.W. Tornøe, C. Christensen and M. Meldal, *J. Org. Chem.*, **2002**, *67*, 3057.

⁹³ L. Zhang, X. Chen, P. Xue, H.H.Y. Sun, I.D. Williams, K.B. Sharpless, V.V. Fokin and G. Jia, *J. Am. Chem. Soc.*, **2005**, *127*, 15998.

⁹⁴ J. McNulty, K. Keskar and R. Vemula, *Chem. Eur. J.*, **2011**, *17*, 14727.

⁹⁵ J.M. Spruell, W.R. Dichtel, J.R. Heath and J.F. Stoddart, *Chem. Eur. J.*, **2008**, *14*, 4168.

Polytriazole-containing compounds have found to be very efficient stabilizing ligands for copper(I) species (Figure 1.29).^{96,97}

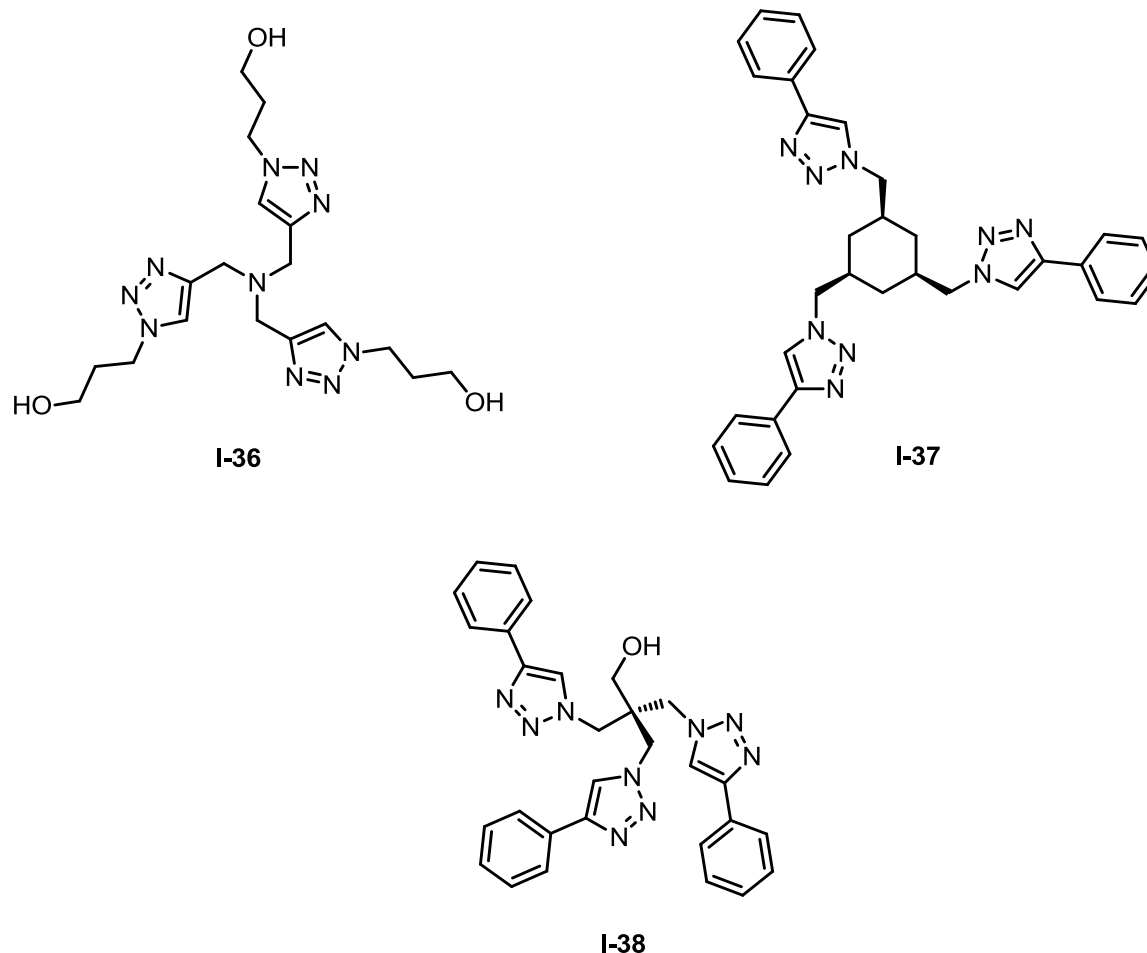


Figure 1.29 - Chemical structures of polytriazole-based ligands **I-36**, **I-37** and **I-38**.

Lot of different solvents have been used to perform this reaction, alongside mixtures of water with a variety of partially miscible organic solvents including alcohols, dimethyl sulfoxide, dimethylformamide, tetrahydrofuran and acetone. The reaction can be performed also in biphasic systems.⁹⁸

⁹⁶ T.R. Chan, R. Hilgraf, K.B. Sharpless and V.V. Fokin, *Org. Lett.*, **2004**, *6*, 2853.

⁹⁷ P.S. Donnelly, S.D. Zanatta, S.C. Zammit, J.M. White and S.J. Williams, *Chem. Commun.*, **2008**, *21*, 2459.

⁹⁸ A. Ravi, A.S. Oshchepkov, K.E. German, G.A. Kirakosyan, A.V. Safonov, V.N. Khrustalev and E.A. Kataev, *Chem. Commun.*, **2018**, *54*, 4826.

This reaction has been largely used for the construction of mechanically interlocked molecules, but it also found applications in materials chemistry, surface science and biochemistry.⁹⁹

Copper-catalyzed alkyne-azide cycloaddition was proved to be also an efficient polymerization reaction: in 2005 Reek and coworkers exploited this click reaction to develop novel fluorene-based conjugate polymers (Figure 1.30).¹⁰⁰

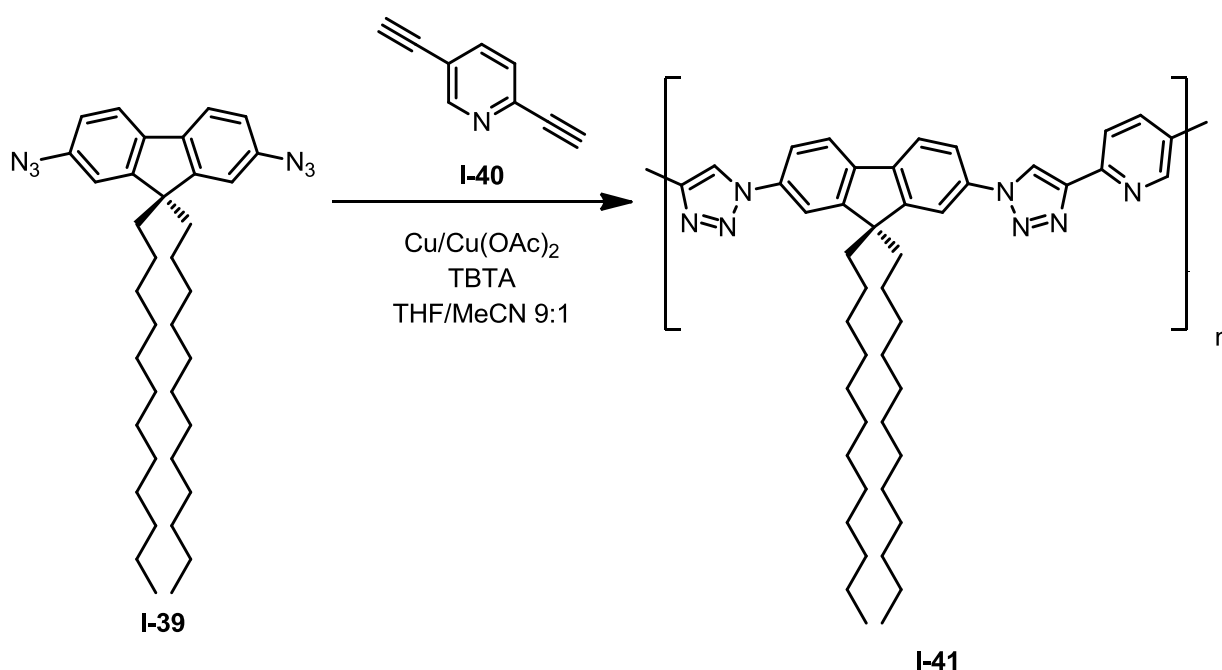


Figure 1.30 - Synthetic scheme of fluorene-based “click” polymer **I-41**.

⁹⁹ a) R. Kumar, A. El-Sagheer, J. Tumpane, P. Lincoln, L. M. Wilhelmsson and T. Brown, *J. Am. Chem. Soc.*, **2007**, *129*, 6859.

b) J.D. Megiatto Jr. and D.I. Schuster, *J. Am. Chem. Soc.*, **2008**, *130*, 12872.

c) J.D. Megiatto Jr. and D.I. Schuster, *Chem. Eur. J.*, **2009**, *15*, 5444.

d) S.M. Goldup, D.A. Leigh, T. Long, P.R. McGonigal, M.D. Symes and J. Wu, *J. Am. Chem. Soc.*, **2009**, *131*, 15924.

e) J.D. Megiatto Jr., D.I. Schuster, *New J. Chem.*, **2010**, *34*, 276.

f) Y. Zhao, Y. Li, Y. Li, H. Zheng, X. Yin and H. Liu, *Chem. Commun.*, **2010**, *46*, 5698.

g) W. Yang, Y. Li, J. Zhang, N. Chen, S. Chen, H. Liu and Y. Li, *J. Org. Chem.*, **2011**, *76*, 7750.

h) A.I. Prikhod'ko, F. Durola and J.-P. Sauvage, *J. Am. Chem. Soc.*, **2008**, *130*, 448.

i) A.I. Prikhod'ko and J.-P. Sauvage, *J. Am. Chem. Soc.*, **2009**, *131*, 6794.

¹⁰⁰ D.J.V.C. van Steenis, O.R.P. David, G.P.F. van Strijdonck, J.H. van Maarseveen and J.N.H. Reek, *Chem. Commun.*, **2005**, *34*, 4333.

In 1996, Williams and coworkers reported the synthesis of triazole-containing [2]- and [3]rotaxanes **I-42** and **I-43**. All the mechanically interlocked molecules were based on secondary alkylammonium salts and dibenzo-24-crown-8-ether **I-14** and they were obtained by a capping approach on the self-assembled [2]- and [3]pseudorotaxanes using an uncatalyzed thermal Huisgen 1,3-cycloaddition between azide-containing thread and di-*tert*-butyl acetylenedicarboxylate (Figure 1.31).¹⁰¹

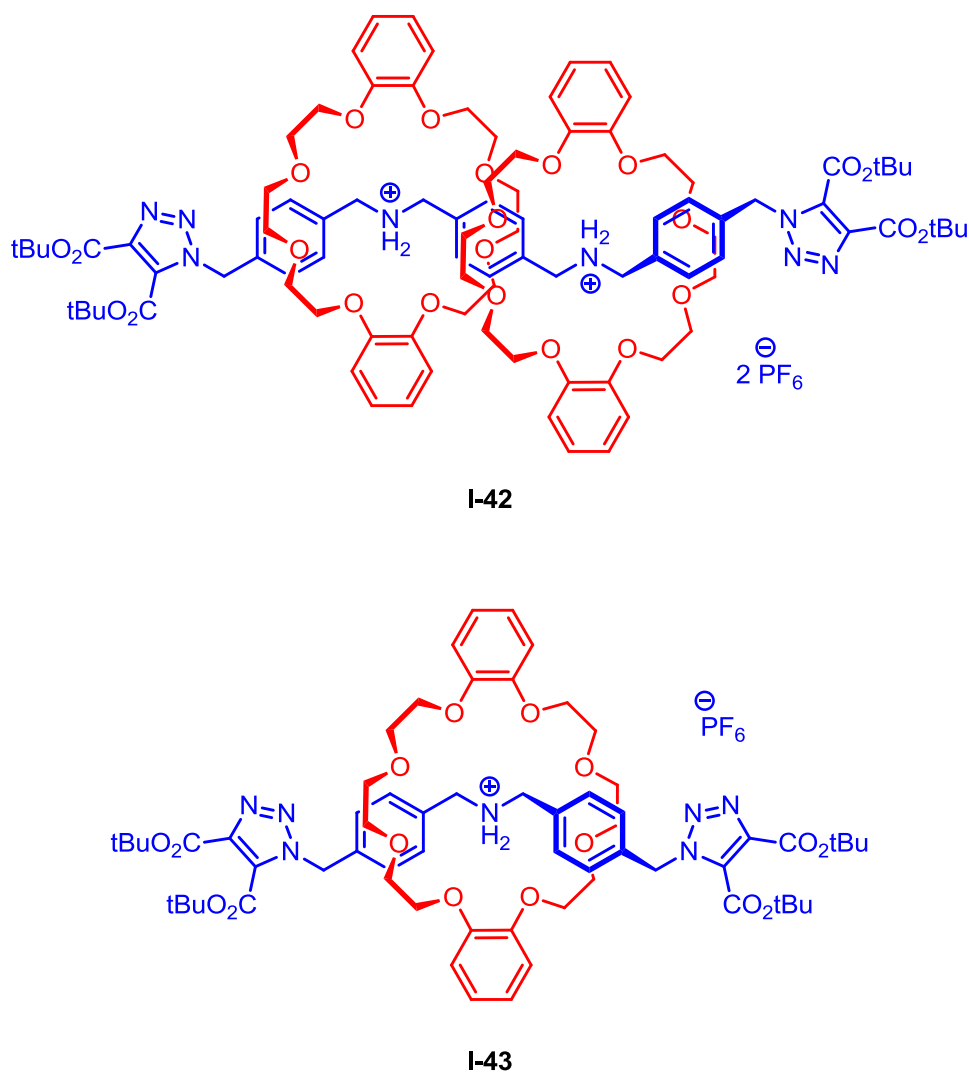


Figure 1.31- Triazole-containing [2]- and [3]rotaxanes **I-42** and **I-43**.

¹⁰¹ P.R. Ashton, P.T. Glink, J.F. Stoddart, P.A. Tasker, A.J.P. White and D.J. Williams, *Chem. Eur. J.*, **1996**, 2, 729.

In 2010, Takata and coworkers reported the synthesis of several alkylammonium-crown ether - based [2]rotaxanes via a capping approach, exploiting a new class of “click” reactions: the C-C bond forming 1,3-dipolar cycloaddition between N-nitrile oxide and unsaturated bonds (Figure 1.32).¹⁰²

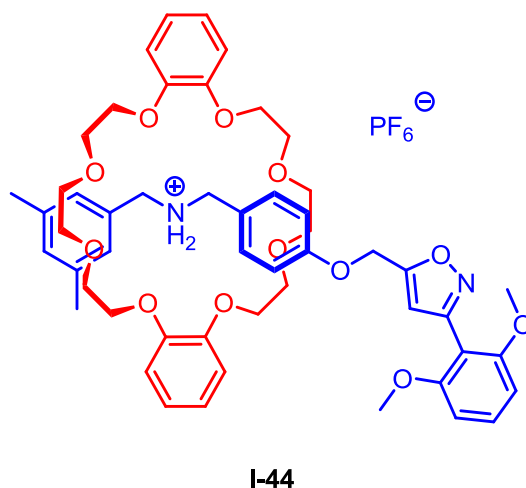


Figure 1.32 - [2]Rotaxane **I-44** by N-nitrile oxide cycloaddition-based capping approach.

The reaction was proved to be a new and interesting tool for the construction of mechanically interlocked molecules, in fact all the reactions led to stable heteroaromatic linkages, proceeded fast in extremely mild catalyst-free conditions (DCM at room temperature for 2 hours) and high yields were obtained, especially when allylic- and propargylic-bearing threads were involved (98% yield in both the cases).

Takata's group reported several other works about the synthesis of mechanically interlocked molecules, including polyrotaxanes, in which this new click reaction has been exploited.¹⁰³

¹⁰² T. Matsumura, F. Ishiwari, Y. Koyama and T. Takata, *Org. Lett.*, **2010**, *12*, 3828.

¹⁰³ a) K. Jang, K. Miura, Y. Koyama and T. Takata, *Org. Lett.*, **2012**, *14*, 3088.

b) H. Iguchi, S. Uchida, Y. Koyama and T. Takata, *ACS Macro Lett.*, **2013**, *2*, 527.

c) T. Yuki, Y. Koyama, T. Matsumura and T. Takata, *Org Lett.*, **2013**, *15*, 4438.

Since its discovery in the past century, the supramolecular chemistry influenced deeply the science and its most recent branch, the artificial molecular machines, is and will continue to be an important research topic thanks to its wide range of potential multidisciplinary applications, from smart materials to biomedical tools. For this reason the development of functionalized components for the construction of novel mechanically interlocked molecular assemblies is of fundamental importance.

Major goals of this thesis are the synthesis and characterization of macrocycles which comprise an electroactive group, namely a ferrocene or a triarylamine, and a bis(2,6-diamidopyridine) moiety and propargyl-containing NIR photoactive components which are bulky enough to act as stoppers. Due to its versatility, propargyl moiety is one of the best linkage functional group because it can be exploited in a wide range of reactions, like click reactions (1,3-dipolar azide-alkyne Huisgen cycloadditions, thiol-yne reactions or 1,3-dipolar N-nitrile oxide-alkyne cycloaddition) or metal-catalyzed reactions (Glaser reaction or Cadiot-Chodkiewicz reaction).

2. Electroactive macrocycles

2.1 Introduction

The assembly of supramolecular architectures is intimately related to the concepts of spatial organization and non-covalent intermolecular interactions. Among them, hydrogen bonding (H-bonding) interactions occupy a prominent place in supramolecular chemistry due to their directionality and specificity: thanks to these properties, this interaction has been deeply exploited in the domain of molecular recognition.^{104, 105, 106}

Moreover, the rational combination of H-bond acceptor (A) and donor (D) groups in a functional unit can dramatically enhance the specificity of hydrogen bonding interactions, leading to a huge increase in the association constant between components. In 2011, Leigh and Hunter developed an quadruple hydrogen-bond complex with a AAAA-DDDD⁺ pattern. The complex presented only attractive interactions, both primary and secondary, which led to an exceptional complex stability, having an association constant higher than 10^{12} M^{-1} (Figure 2.1).¹⁰⁷

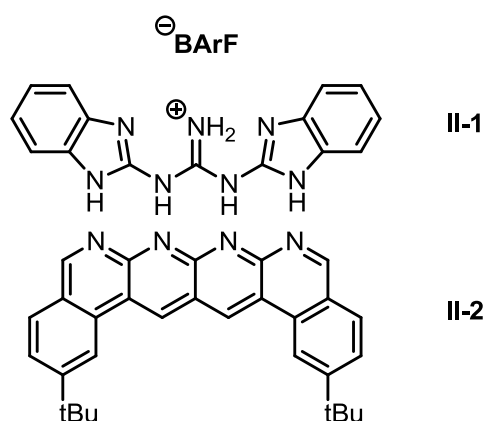


Figure 2.1 - AAAA-DDDD⁺ quadruple hydrogen-bond array.

¹⁰⁴ L. Brunsveld, B.J.B. Folmer, E.W. Meijer and R.P. Sijbesma, *Chem. Rev.*, **2001**, *101*, 4071.

¹⁰⁵ C.A. Hunter, *Angew. Chem. Int. Ed.* **2004**, *43*, 5310.

¹⁰⁶ J. Emsley, *Chem. Soc. Rev.* **1980**, *9*, 91.

¹⁰⁷ B.A. Blight, C.A. Hunter, D.A. Leigh, H. McNab and P.I.T. Thomson, *Nat. Chem.*, **2011**, *3*, 244.

One of the finest examples of hydrogen bonded neutral artificial receptors is the diaminopyridine - substituted isophthalamide receptor **II-3** for barbital (5,5'-diethylbarbituric acid) **II-4**, named the Hamilton receptor, after the publication of the first synthesis achieved by A. D. Hamilton and coworkers in 1988 (Figure 2.2).^{108, 109}

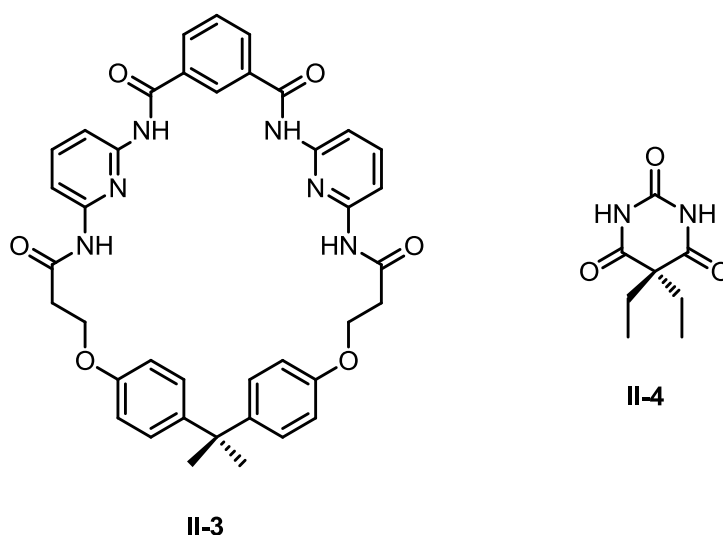


Figure 2.2 - Chemical structures of Hamilton receptor **II-3** and barbital **II-4**.

The macrocyclic receptor was obtained in a two steps synthesis from commercially available starting materials in a 9% overall yield. In the work, Hamilton's group reported an association constant with barbital higher than 10^6 M^{-1} in non-protic solvents: the reason of this extremely strong interaction relies on six complementary donor (D) - acceptor (A) hydrogen bond interactions, according to the pattern ADAADA and DADDAD for barbiturate and receptor, respectively.

¹⁰⁸ S. K. Chang and A.D. Hamilton, *J. Am. Chem. Soc.*, **1988**, 110, 1318.

¹⁰⁹ S.-K.Chang, D.Van Engen, E. Fan and A.D. Hamilton, *J. Am. Chem. Soc.*, **1991**, 113, 7640.

In 2014, Pluth and McGrath studied the influence of parameters like preorganization, rigidity and steric hindrance on the binding affinity between different Hamilton-type receptors **II-3**, **II-5** and **II-6** as hosts and barbitol **II-4** or 3-methyl-7-propylxanthine **II-7** as guests.¹¹⁰ They synthesized a series of Hamilton-type receptors with different linkage units between the 2,6-diamidopyridine moieties in order to have different levels of flexibility in the binding site (Figure 2.3).

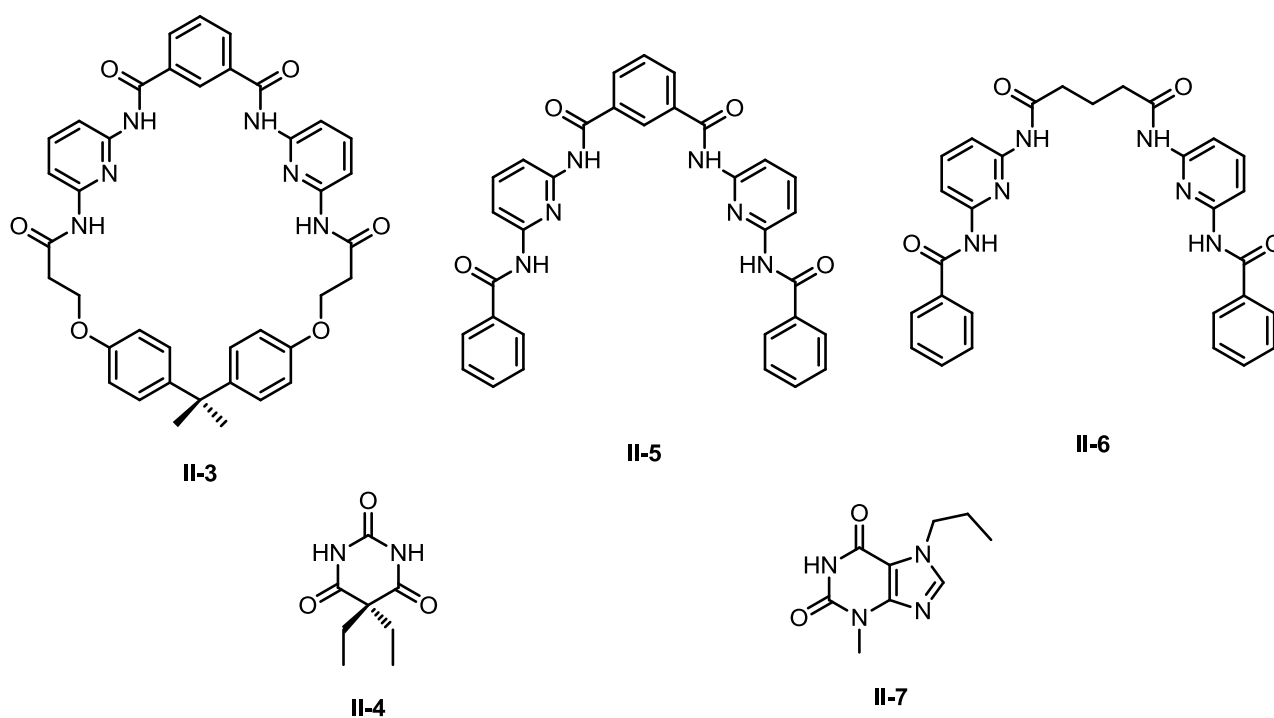


Figure 2.3 - Hamilton-type receptors **II-3**, **II-5** and **II-6**, barbitol **II-4** and 3-methyl-7-propylxanthine **II-7**.

This study was based on both ¹H-NMR titrations and DFT calculations and proved the existence of a relation between preorganization, given by the rigidity of the bridge unit which links the 2,6-diamidopyridine moieties, and the formation of the necessary interactions for the self-assembly of the systems.

¹¹⁰ J.M. McGrath and M.D. Pluth, *J. Org. Chem.* **2014**, 79, 711.

In 2002, Lehn and coworkers developed Hamilton receptor-based supramolecular polymers in order to obtain adaptive and dynamic combinatorial materials. In this work, the self-assembly of the polymers is induced by the molecular recognition between the two homoditopic monomer, which present a cyanuric acid unit **II-8** and a diamidopyridine -substituted isophthalamide unit **II-9**¹¹¹ (Figure 2.4).

Based on this work, several such supramolecular polymeric systems have been developed.^{112, 113}

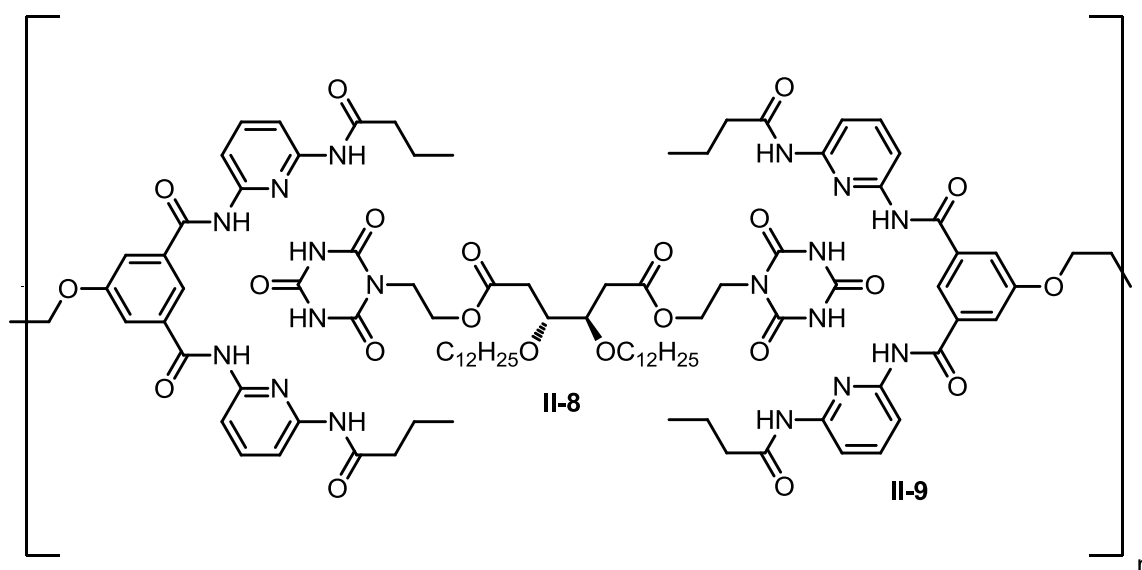


Figure 2.4 - Chemical structure of Hamilton receptor-based linear supramolecular polymer.

Other multi-Hamilton receptor supramolecular systems have been developed including foldamers, gelators and dendrimers.¹¹⁴

¹¹¹ V. Berl, M. Schmutz, M. J. Krische, R. G. Khoury, J.M. Lehn, *Chem. Eur. J.* **2002**, *8*, 1227.

¹¹² E. Kolomiets and J.-M. Lehn, *Chem. Commun.* **2005**, 1519.

¹¹³ E. Kolomiets, E. Buhler, S. J. Candau and J.-M. Lehn, *Macromolecules* **2006**, *39*, 1173.

¹¹⁴ a) V. Berl, M. J. Krische, I. Huc, J.-M. Lehn and M. Schmutz, *Chem. Eur. J.* **2000**, *6*, 1938.

b) K. Inoue, Y. Ono, Y. Kanekiyo, T. Ishii, K. Yoshihara and S. Shinkai, *J. Org. Chem.* **1999**, *64*, 2933.

c) T. Rossow, S. Hackelbusch, P. van Assenbergh and S. Seiffert, *Polymer Chem.* **2013**, *4*, 2515.

d) K. P. Nair, V. Breedveld and M. Weck, *Macromolecules* **2011**, *44*, 3346.

e) K. P. Nair, V. Breedveld and M. Weck, *Macromolecules* **2008**, *41*, 3429.

f) A. Dirksen, U. Hahn, F. Schwanke, M. Nieger, J.N.H. Reek, F. Vögtle and L. De Cola, *Chem. Eur. J.* **2004**, *10*, 2036.

g) A. Franz, W. Bauer and A. Hirsch, *Angew. Chem. Int. Ed.* **2005**, *44*, 1564.

h) K. Hager, A. Franz and A. Hirsch, *Chem. Eur. J.* **2006**, *12*, 2663.

i) K. Maurer, K. Hager and A. Hirsch, *Eur. J. Org. Chem.* **2006**, 3338.

j) K. Hager, U. Hartnagel and A. Hirsch, *Eur. J. Org. Chem.* **2007**, 1942.

In 2004, Branda and coworkers developed a bipyridine-containing Hamilton receptor **II-10** in which the affinity between the receptor and the barbiturate can be modulated by an allosteric effect.¹¹⁵

Allosteric effects are positive when the induced conformational changes increase the binding efficacy and negative when there is a decrease in the binding efficacy.^{116, 117}

The affinity between the barbital and the bipyridine containing receptor has been measured by ¹H NMR in CD₂Cl₂/CD₃CN 9:1, v/v and the resulting binding constant was 2.8 × 10³ M⁻¹. Upon addition of zinc triflate, the bipyridines bind the Zn²⁺ and negative allosteric effects induce conformational change which results in the ejection of the barbital **II-4** (Figure 2.5).

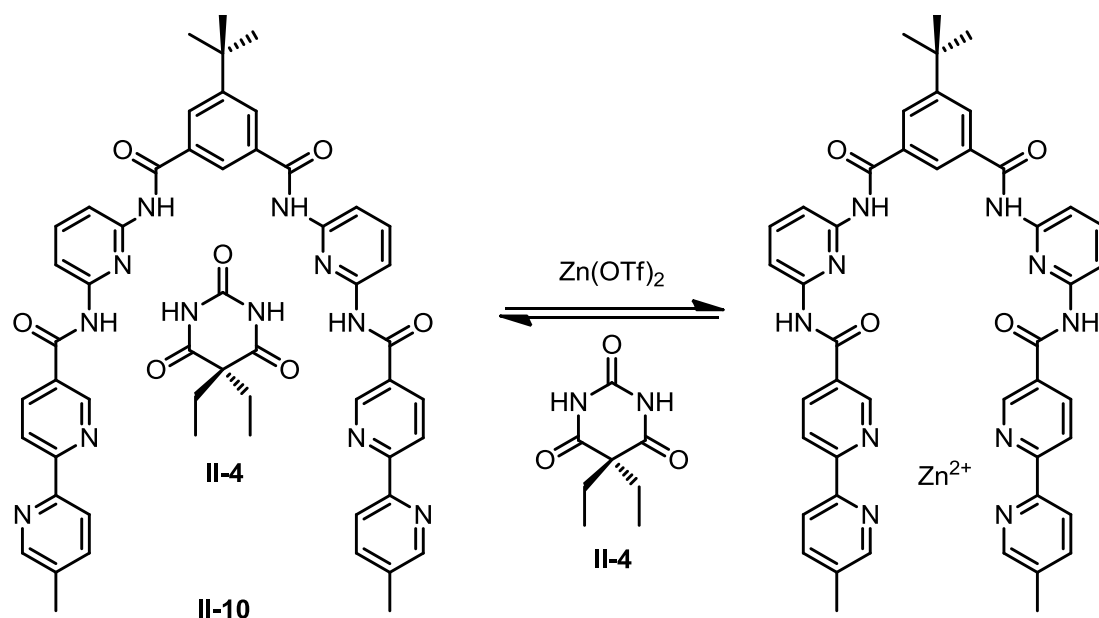


Figure 2.5 - Hamilton receptor -based allosteric ditopic host:guest system sensitive to barbiturate and Zn²⁺.

¹¹⁵ M.H. Al-Sayah, R. McDonald and N.R. Branda, *Eur. J. Org. Chem.* **2004**, 173.

¹¹⁶ A. Levitzki, *Quantitative Aspects of Allosteric Mechanisms*, Springer-Verlag, Heidelberg, **1978**.

¹¹⁷ K.G. Scrimgeour, *Chemistry and Control of Enzyme Reactions*, Academic Press Inc., New York, **1977**.

The orthogonality between the barbiturate substituents in 5-position and the plane of a cyclic Hamilton receptor can be exploited for the construction of rotaxanes.

In 2014 a mechanically interlocked molecule was synthesized comprising a cyclic Hamilton-type receptor **II-11**. Mixing the H-bonding macrocycle with a barbiturate bearing short azide-terminated arms **II-12** gave a pseudorotaxane **II-11:II-12**. This intermediate was subsequently converted in the corresponding [2] rotaxane **II-13** by a Cu-catalyzed alkyne-azide 1,3-cycloaddition “click” reaction with alkyne-bearing trityl stoppers **II-14** and TBTA **II-15** as Cu(I)-stabiligand (Figure 2.6).¹¹⁸

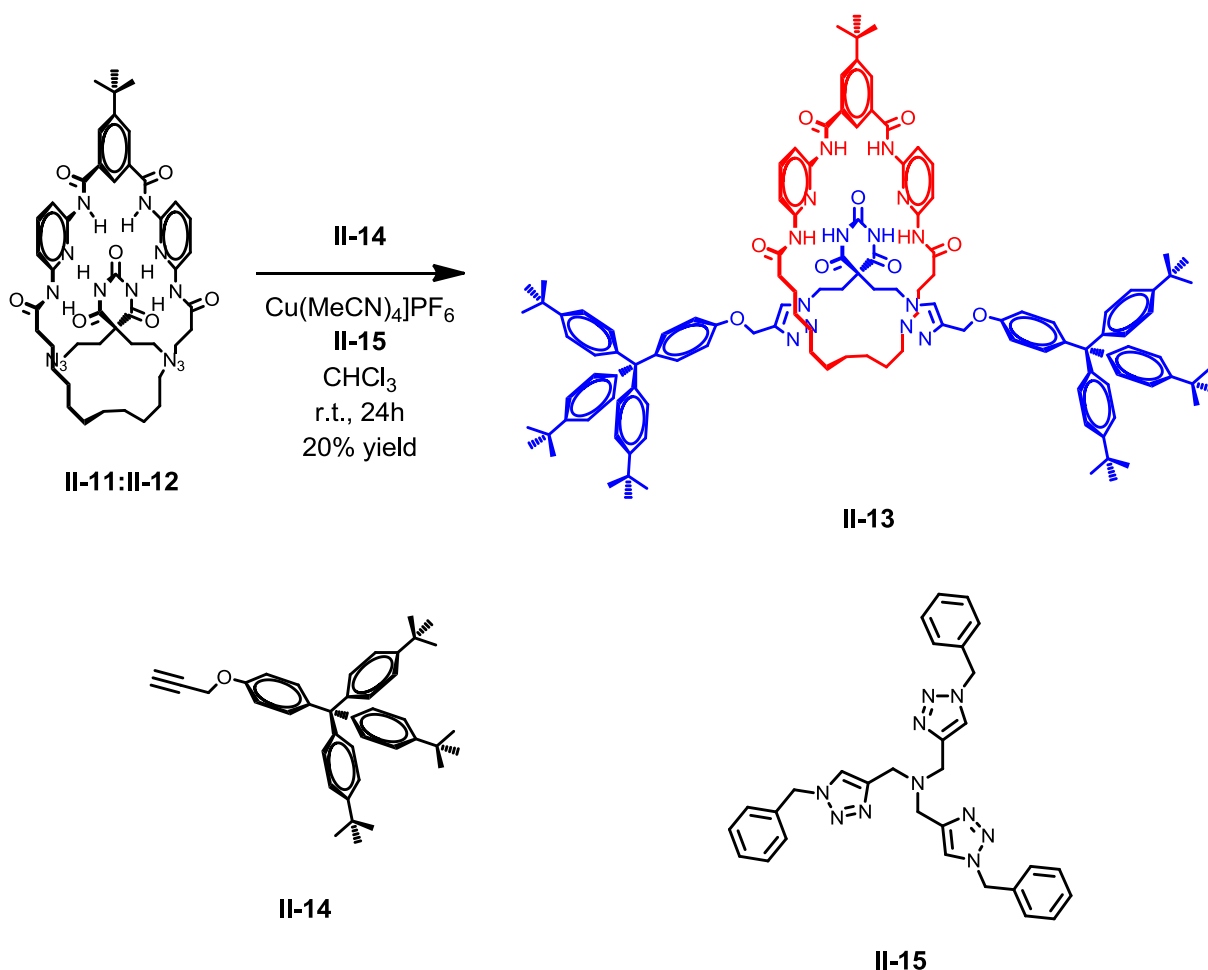


Figure 2.6 - Hydrogen-bonded barbiturate [2]-rotaxane.

¹¹⁸ A. Tron, P. J. Thornton, M. Rocher, H.-P. Jacquot de Rouville, J.-P. Desvergne, B. Kauffmann, T. Buffeteau, D. Cavagnat, J. H. R. Tucker and N. D. McClenaghan, *Org. Lett.*, **2014**, *16*, 1358.

2.2 Development of ferrocene-containing macrocycles

2.2.1 Introduction

Ferrocene was first prepared unintentionally in 1951. Pauson and Kealy reported the reaction of cyclopentadienyl magnesium bromide and ferric chloride in an attempt to prepare fulvalene by oxidative coupling. Instead, they obtained a light orange powder of "remarkable stability".¹¹⁹

The stability of the new organometallic compound was related to the aromatic character of the negatively charged cyclopentadienyls, but the η^5 (pentahapto) sandwich structure **II-17** was recognized by Woodward and Wilkinson, which deduced the structure based on its reactivity (Figure 2.7).¹²⁰

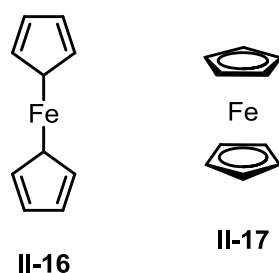


Figure 2.7 - Pauson-Kealy's incorrect structure of ferrocene **II-16** and Woodward- Wilkinson's correct one **II-17**.

In 1952 Fischer supposed a "sandwich" structure for the ferrocene and started to synthesize similar compounds, obtaining nickelocene and cobaltocene.¹²¹

The sandwich structure for the ferrocene was proved by NMR and X-ray crystallography studies¹²²,¹²³ and the discovery of its idiosyncratic properties aroused a huge interest in the scientific community, being the subject of the 1973 Nobel Prize in Chemistry which was awarded to Fischer

¹¹⁹ T.J. Kealy, P.L. Pauson, *Nature*, **1951**, 168, 1039.

¹²⁰ G. Wilkinson, M. Rosenblum, M. C. Whiting, R. B. Woodward, *J. Am. Chem. Soc.*, **1952**, 74, 2125.

¹²¹ E.O. Fischer and W. Pfab, *Zeitschrift für Naturforschung B.*, **1952**, 7, 377.

¹²² J.D. Dunitz and L.E. Orgel, *Nature*, **1953**, 171, 121.

¹²³ P.F. Eiland and R. Pepinsky, *J. Am. Chem. Soc.*, **1952**, 74, 4971.

and Wilkinson “for their pioneering work performed independently on the chemistry of the organometallic, so called sandwich compounds”.

Ferrocene undergoes many characteristic reactions of aromatic compounds, enabling the preparation of substituted derivatives.¹²⁴

One of the most useful and exploited reactions is the lithiation of ferrocene: 1,1'-dilithioferrocene. This versatile nucleophile can be obtained by treating ferrocene with n-butyllithium, while tert-butyllithium produces monolithioferrocene in almost quantitative yields.¹²⁵

Ferrocene compounds are well-known for their substituent-dependent electrochemical properties: in 2016 Seppelt and coworkers reported that decamethylferrocene is much more easily oxidised than ferrocene and can even be oxidised to the corresponding dication, finding applications as an internal standard in non-aqueous electrochemistry.¹²⁶

Ferrocene has also been used as building block in the synthesis of chiral ligands in transition metal-catalyzed reactions or in the development on novel drugs, like 1N-ferrocenylmethyl thymine **II-18**, an anticancer, and ferroquine **II-19**, and antimalarial (Figure 2.8).^{127, 128, 129, 130}

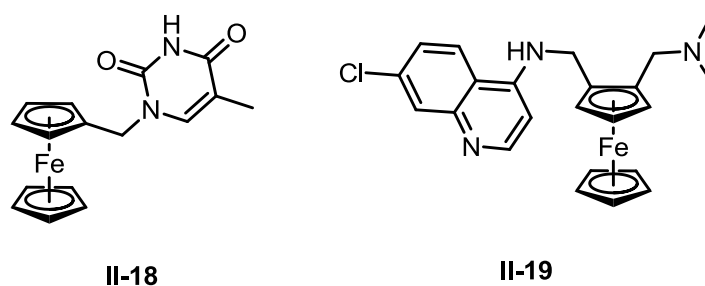


Figure 2.8 - Chemical structure of 1N-ferrocenylmethyl thymine **II-18**, an anticancer, and ferroquine **II-19**, and antimalarial.

¹²⁴ M.D. Rausch, E.O. Fischer and H. Grubert, *J. Am. Chem. Soc.*, **1960**, 82, 76.

¹²⁵ F. Rebiere, O. Samuel and H.B. Kagan, *Tetrahedron Lett.*, **1990**, 31, 3121.

¹²⁶ M. Malischewski, M. Adelhardt, J. Sutter, K. Meyer and K. Seppelt, *Science*, **2016**, 353, 678.

¹²⁷ P. Stepnicka, *Ferrocenes: Ligands, Materials and Biomolecules*, Hoboken, NJ, J. Wiley, **2008**

¹²⁸ C. Biot, F. Nosten, L. Fraisse, D. Ter-Minassian, J. Khalife and D. Dive, *Parasite*, **2011**, 18, 207.

¹²⁹ C. Ornelas, *New J. Chem.*, **2011**, 35, 1973

¹³⁰ S. Top, A. Vessières, G. Leclercq, J. Quivy, J. Tang, J. Vaissermann, M. Huché and G. Jaouen, *Chem. Eur. J.*, **2003**, 9, 5223.

Ferrocene derivatives have also been used in materials chemistry, in particular for the synthesis of iron nanoparticles and electroactive polymers.^{131, 132}

Ferrocene-containing Hamilton receptor structural analogues have also been developed: in 2001 Tucker and coworkers synthesized a barbiturate receptor where the isophthalamide linkage has been replaced by 1,3-ferrocenedicarboxylic acid, in order to obtain an electroactive chemosensor **II-21** (Figure 2.9).¹³³

¹H-NMR studies and X-ray crystal structure proved a 1:1 stoichiometry in the complex between barbital **II-4** and receptor **II-21** and an association constant with barbital of 2150 M⁻¹. The chemosensor **II-21** gave a quasi-reversible oxidation relative to the ferrocene/ferrocenium pair. Electrochemical data also indicated that the strength of barbital binding may be modulated by a redox process occurring on the ferrocene moiety.^{134, 135}

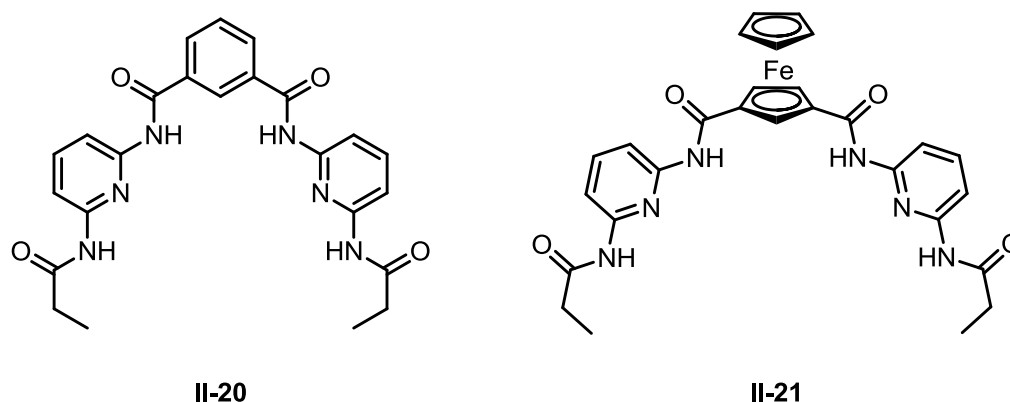


Figure 2.9 - Classical Hamilton receptor **II-20** and ferrocene bearing structure analogue **II-21**.

¹³¹ D. Conroya, A. Moialab, S. Cardoso, A. Windleb and J. Davidson, *Chem. Eng. Sci.*, **2010**, 65, 2965.

¹³² R. Pietschnig, *Chem. Soc. Rev.*, **2016**, 45, 5216.

¹³³ S. R. Collinson, T. Gelbrich, M. B. Hursthouse and J. H. R. Tucker, *Chem. Commun.* **2001**, 555.

¹³⁴ J. H. R. Tucker and S. R. Collinson, *Chem. Soc. Rev.* **2002**, 31, 147.

¹³⁵ J. Westwood, S. J. Coles, S. R. Collinson, G. Gasser, S. J. Green, M. B. Hursthouse, M. E. Light, J. H. R. Tucker, *Organometallics*, **2004**, 23, 946.

2.2.2 Synthesis

In order to obtain functional mechanically interlocked molecules, an electroactive Hamilton-type macrocycle has been designed. The requirements we needed were an electroactive group, a bis(2,6-diamidopyridine) moiety as binding site for barbiturates and a long chain in order to have a ring-shaped structure (Figure 2.10).

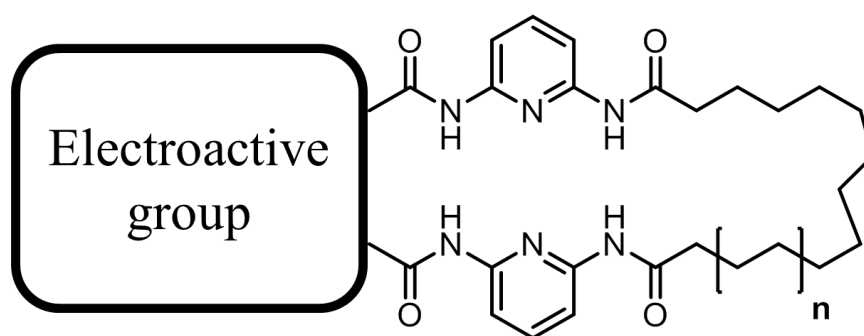


Figure 2.10 - Schematic representation for the design of an electroactive hydrogen-bonded macrocycle.

The synthetic scheme for the functionalization of ferrocene and formation of macrocyclic receptors is shown in Figure 2.11.

Commercially available ferrocene **II-17** was first reacted under Friedel-Crafts conditions, using three equivalent of freshly distilled acetyl chloride in presence of a stoichiometric amount of anhydrous aluminum chloride in dry dichloromethane to afford the crude 1,1'-diacetylferrocene **II-22**, which was purified by recrystallization in cyclohexane. The diketone was subsequently oxidized to the corresponding dicarboxylic acid by a haloform reaction, treating the substrate with a sodium hypochlorite solution in the dark for five hours. Then the 1,1'-ferrocenedicarboxylic acid **II-23** was refluxed overnight in dry chloroform in presence of three equivalent of oxalyl chloride and a catalytic amount of pyridine. The 1,1'-ferrocenedicarboxy chloride **II-24** was reacted at room temperature overnight with three equivalents of 2,6-diaminopyridine in presence of an excess of

triethylamine in dry tetrahydrofuran. It is noteworthy that a black insoluble tar was always formed as by product in all the steps reported above. Even if this degradation product was formed in minimal amount and no change in the ^1H - NMR spectra or additional spots other than products on TLC were observed, the presence of these impurities seemed to drastically lower the yields. So it was noted in passing that higher quality intermediates, namely the 2,6-diaminopyridine, the 1,1'-ferrocene dicarboxylic acid **II-23** and the corresponding acid chloride **II-24**, could be obtained by recrystallization in chloroform, acetic acid and heptane, respectively.

The macrocyclic receptors **II-28** and **II-29** were obtained in the last steps in moderate yields through a one-pot double condensation between both terminal $-\text{NH}_2$ groups of the acyclic receptor **II-25** with the freshly prepared 1,16-hexadecanedioyl dichloride **II-26** and 1,20 - eicosanedioyl dichloride **II-27**, respectively, which were simultaneously added dropwise during 4 hours to a stirring solution of an excess of triethylamine in dry tetrahydrofuran under high dilution conditions at room temperature for 4 days.

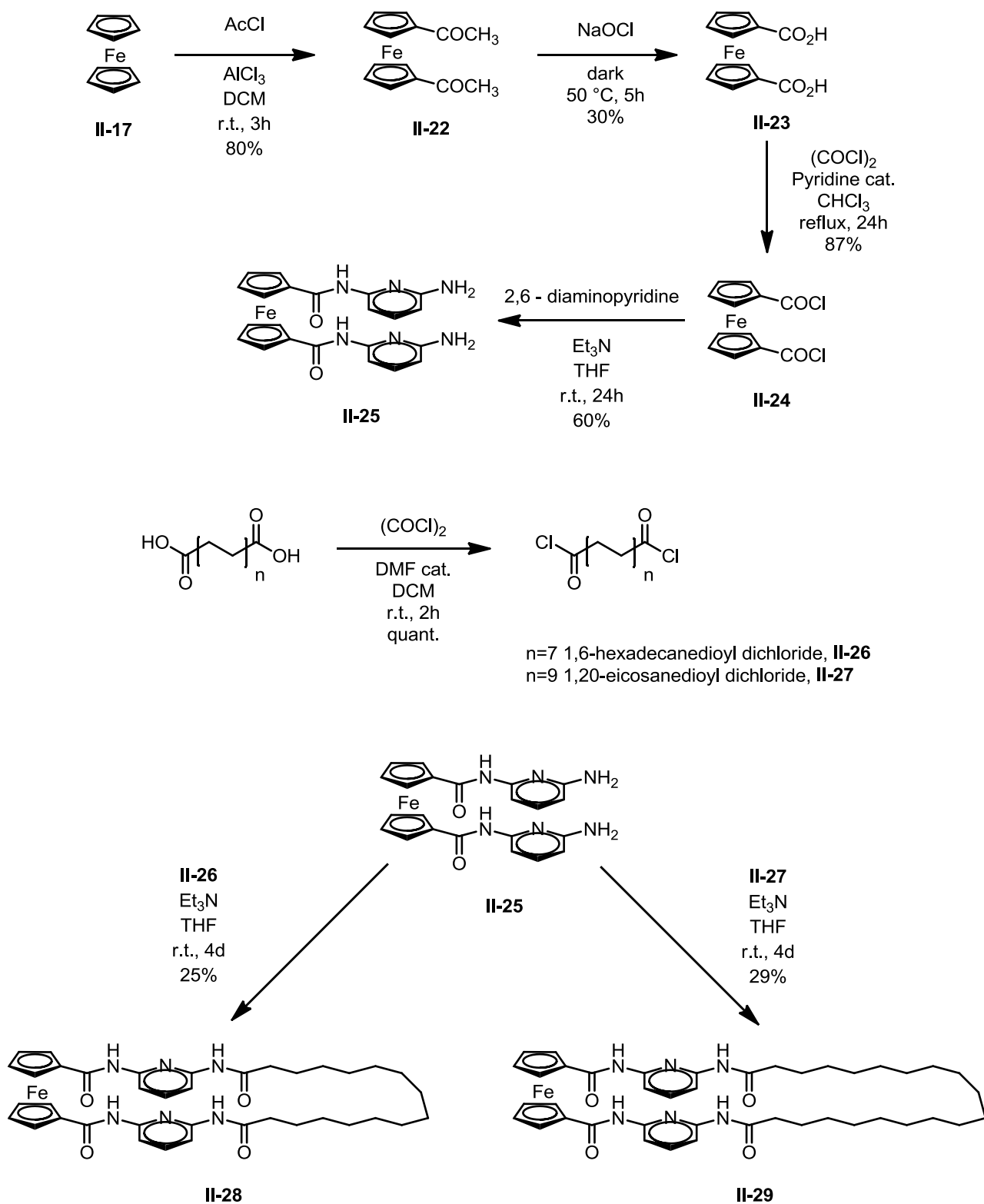


Figure 2.11 - Synthetic scheme of cyclic ferrocene Hamilton-type receptors **II-28** and **II-29**.

2.2.3 Characterization

2.2.3.1 NMR studies

Ferrocene Hamilton-type macrocycles **II-28** and **II-29** were fully characterized by ^1H -, ^{13}C -NMR and mass spectrometry. Both macrocycles showed poor solubility in most of the common deuterated solvents, with the exception of deuterated DMSO and AcOH. The last one was the solvent of choice because fast degradation of samples occurred when dimethylsulfoxide was used, while deuterated acetic acid solutions of samples showed a very good stability. High quality NMR spectra were recorded for both macrocycles with no sign of degradation even a few days after the preparation of the samples (Figure 2.12 and 2.13).

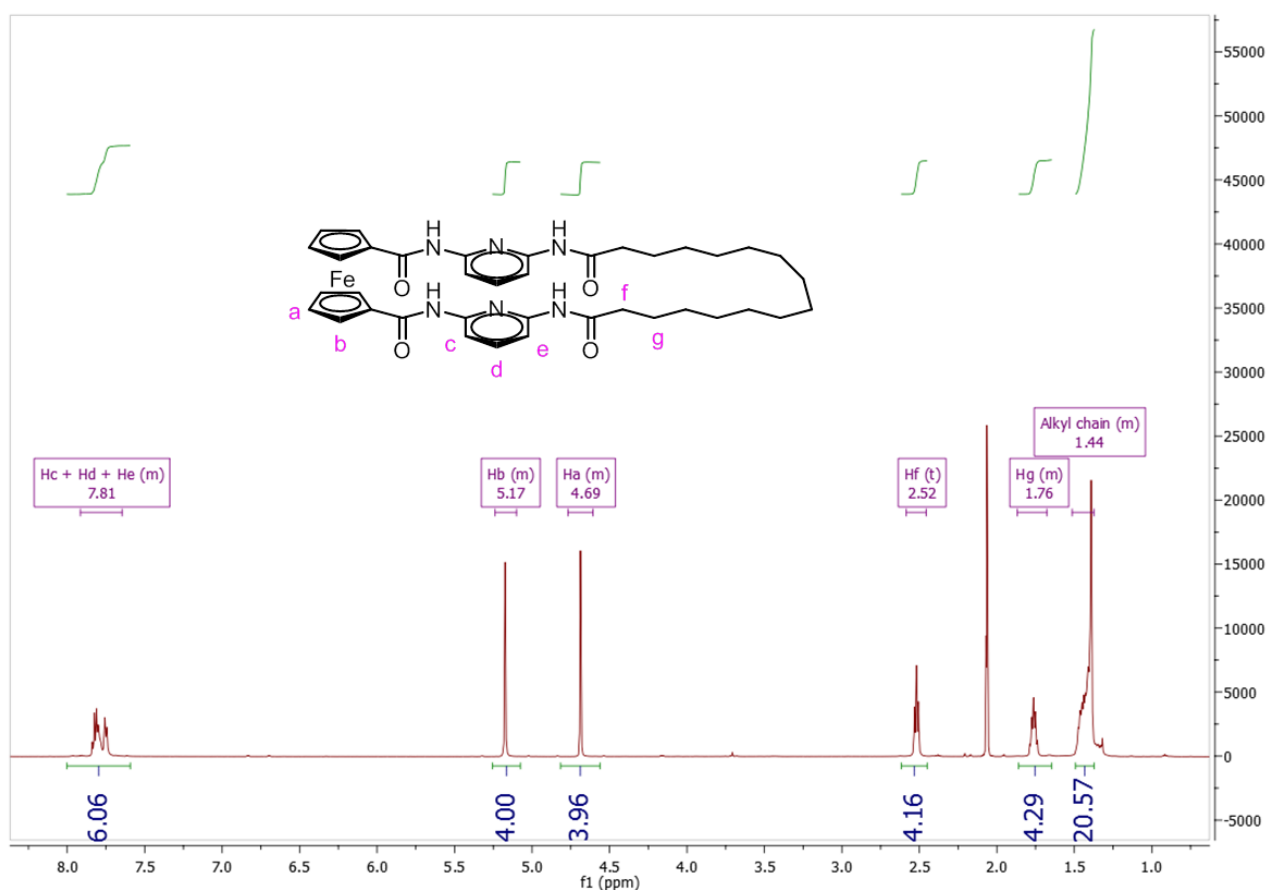


Figure 2.12 - ^1H - NMR of ferrocene Hamilton-type macrocycle **II-28** (600 MHz in AcOH- d_4).

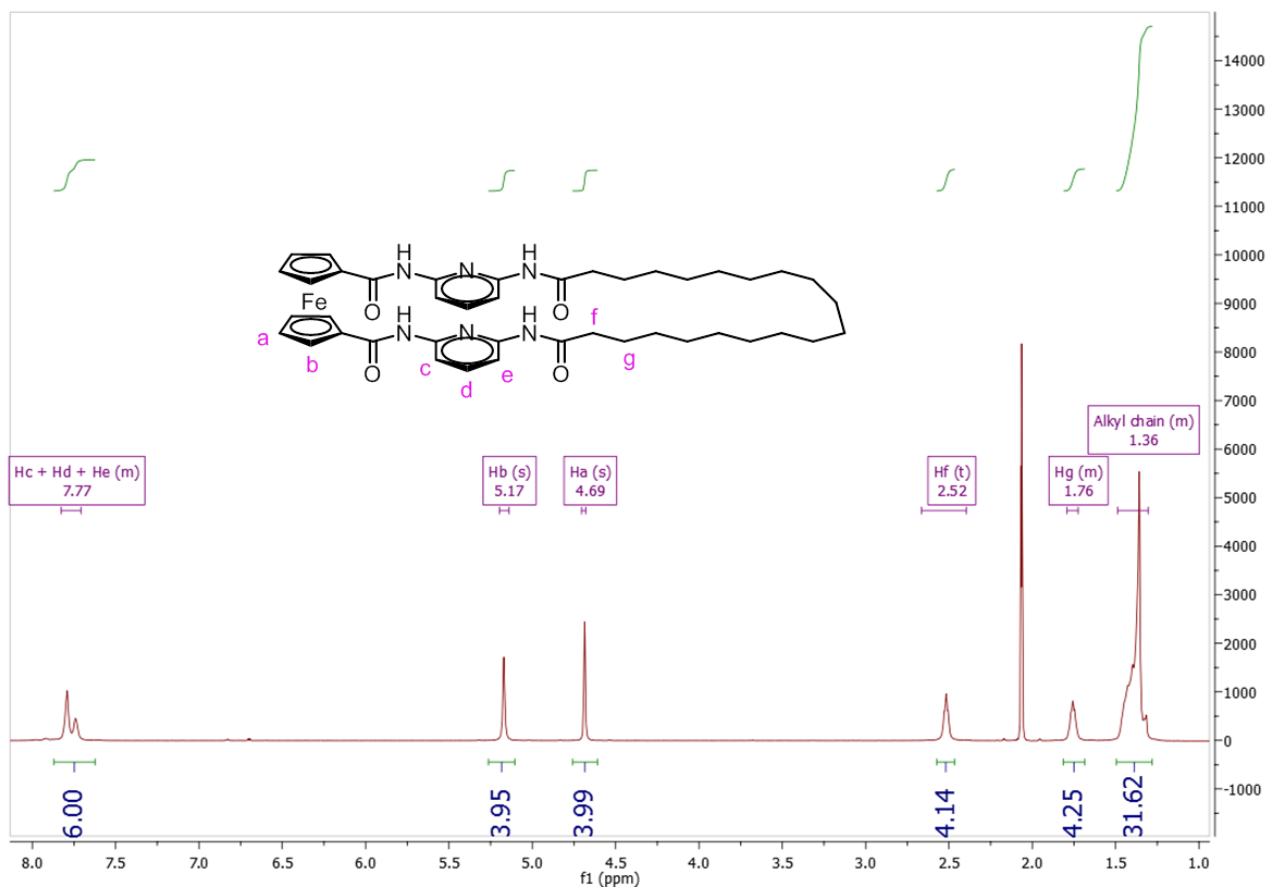


Figure 2.13 - ¹H - NMR of ferrocene Hamilton-type macrocycle **II-29** (600 MHz in AcOH-d₄).

In Figure 2.12, peaks at δ 2.52 (t, $J = 7.5$ Hz, 4H) and δ 1.76 (m, 4H) are the methylene groups of alkyl chain in α - and β -position to the carbonyl groups, respectively. The 1:1 ratio of those peaks with the peaks of the ferrocene core, which are at δ 5.17 (s, 4H) and δ 4.69 (s, 4H), proved the formation of the macrocyclic receptor **II-28**. In Figure 2.13, same observations can be done, which are consistent with the formation of macrocyclic receptor **II-29**.

2.2.3.2 Binding study with macrocyclic hosts

The interactions between the cyclic ferrocene Hamilton-type receptor **II-28** and **II-29** with barbitol **II-4** as guest were studied by electronic absorption and $^1\text{H-NMR}$ spectroscopies. (Figure 2.14)

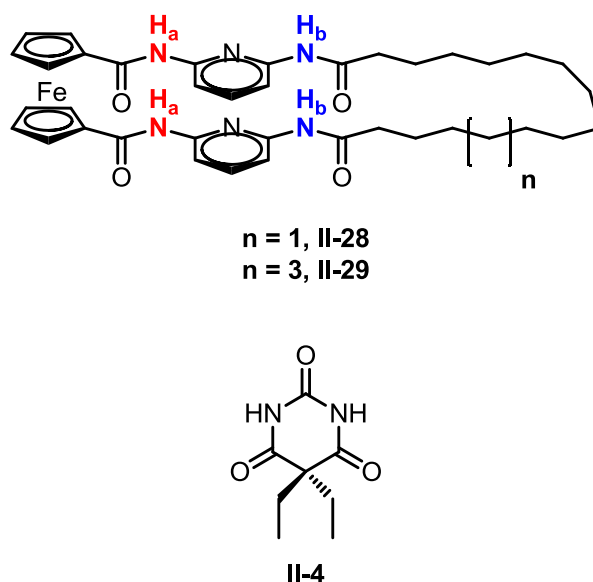


Figure 2.14 - Structural formulae of macrocyclic receptors **II-28** and **II-29** and barbitol. H_a and H_b denote protons used to follow guest binding in NMR studies.

The titrations monitored by electronic absorption spectroscopy showed a small bathochromic shift of some nanometers in the pyridine absorption band upon addition of barbitol. The analysis of data provided 1:1 association constants (K_{ass}) with barbitol of $727 \pm 1 \text{ M}^{-1}$ for **II-28** and $1032 \pm 1 \text{ M}^{-1}$ for **II-29** in dichloromethane (Figure 2.15). The macrocycle **II-29** proved to be a better receptor for barbitol than macrocycle **II-28**, probably due to the bigger cavity for the guest.

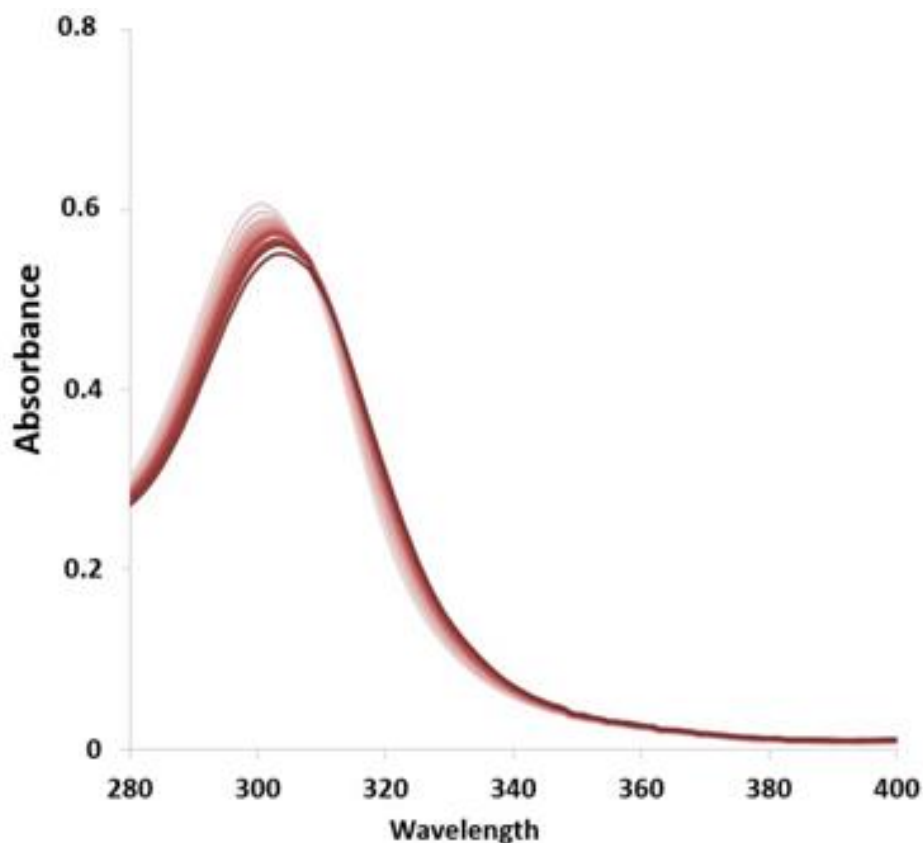


Figure 2.15 - Titration of **II-28** in the presence of barbital **II-4** monitored by electronic absorption spectroscopy in dichloromethane ($[\text{II-28}] = 25 \mu\text{M}$).

The titrations monitored by ^1H NMR in deuterated chloroform showed that the signals for both NH groups of the different amide groups in macrocycles **II-28** and **II-29** are shifted downfield upon addition of barbital. This observation is consistent with the expected formation of hydrogen bonds between host and guest. The analysis of the data provided binding constants of *ca.* 10^3 M^{-1} : $742 \pm 10 \text{ M}^{-1}$ for **II-28** and $1011 \pm 8 \text{ M}^{-1}$ for **II-29**, respectively (Figure 2.16).

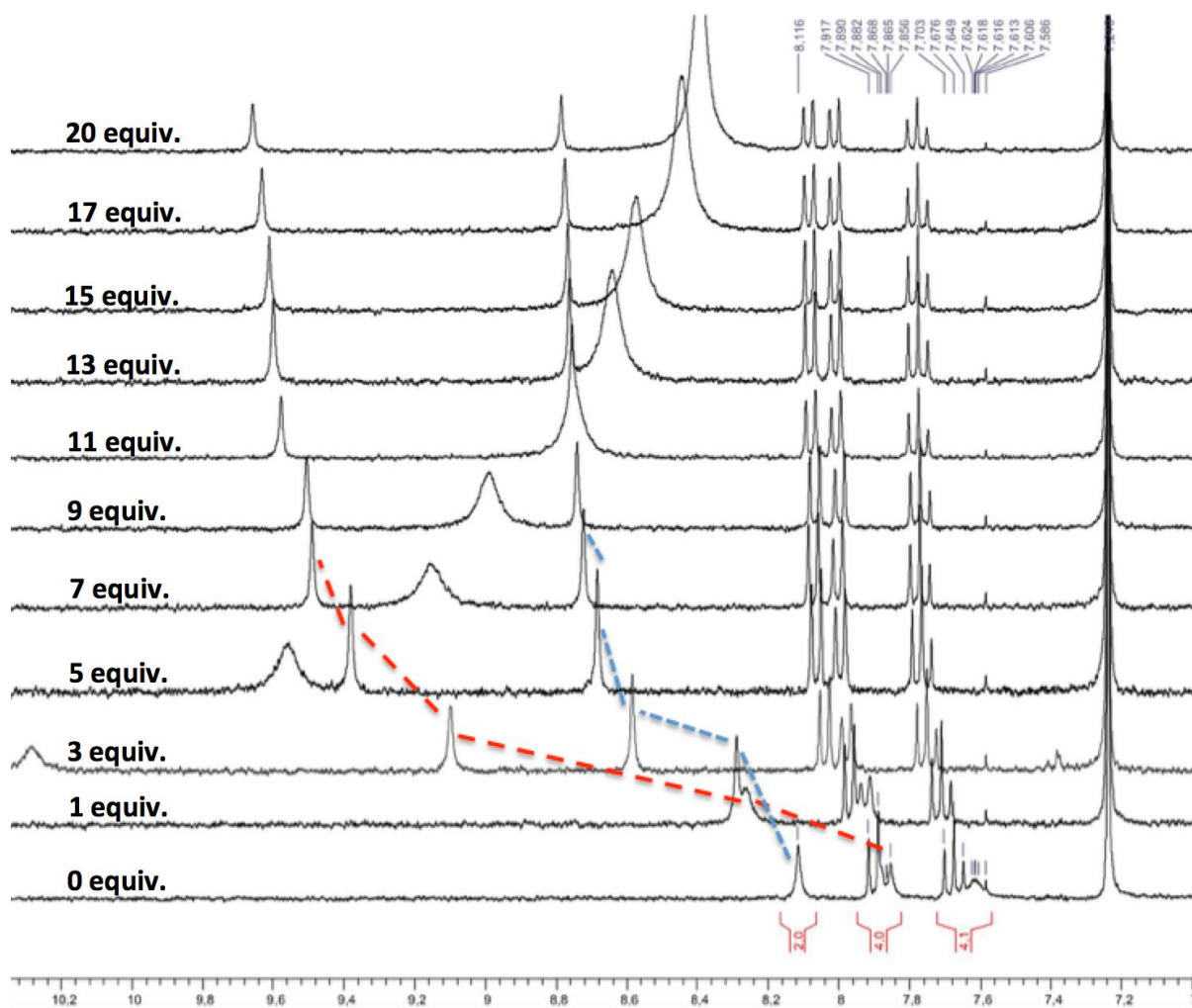


Figure 2.16 - Titration of ferrocene-containing macrocycle **II-28** in the presence of barbital **II-4** monitored by ^1H NMR using the chemical shifts of the host amide protons (1 mM in *d*-chloroform).

Red squares = N-H_A protons; blue diamonds = N-H_B protons

Thus binding constants of the ferrocene-containing macrocycles with barbital **II-4** determined by both UV-visible and NMR monitoring proved to be consistent.

2.2.3.3 Electrochemistry

Cyclic ferrocene-containing Hamilton-type receptor **II-29** was studied by cyclic voltammetry (CV) using a three electrode cell, with a glassy carbon working electrode, silver wire counter electrode and silver/silver chloride reference electrode (Figure 2.17).

The samples was dissolved in dry tetrahydrofuran at a concentration of 1 mg/mL, degassed for 5 minutes then diluted in the same solvent, tetrabutylammonium hexafluorophosphate (TBAPF₆) was used as supporting electrolyte and decamethylferrocene (DCMF) as an internal reference.

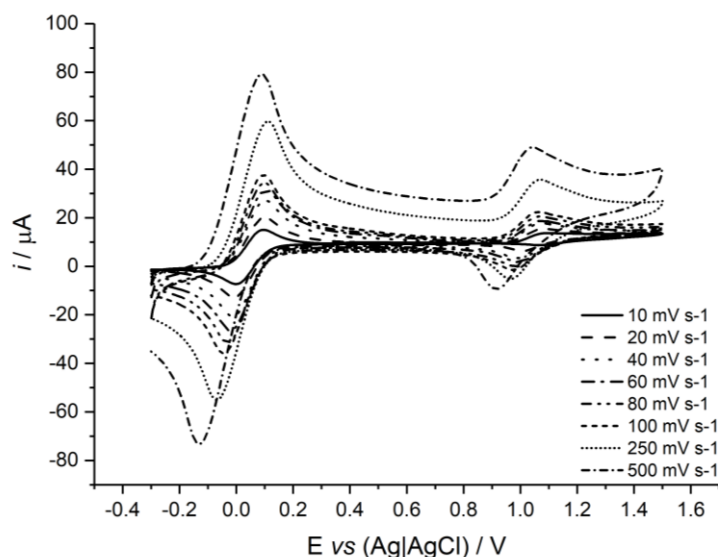


Figure 2.17 - Cyclic voltammogram of 1:1 DCMF and macrocycle **II-29**, in a solution of 10^{-1} M TBAPF₆ in dry degassed dichloromethane at different scan rates.

From electrochemical experiments, macrocycle **II-29** was seen to undergo a redox transition (Fc/Fc^+) at $E_{1/2} = 1 (\pm 0.005)$ V vs. decamethyl ferrocene as internal standard, where $E_{1/2} = (E_p^a + E_p^c) / 2$.

The interactions between the cyclic ferrocene Hamilton-type receptor **II-29** with barbital **II-4** as guest were also studied (Figure 2.18).

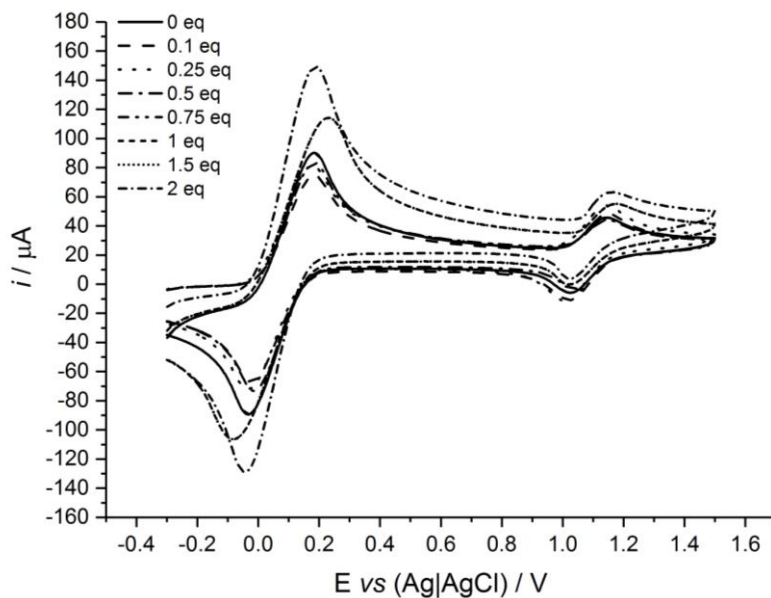


Figure 2.18 - CVs recorded of DCMF and macrocycle **II-29** on addition of 0.1-2 molar equivalents of barbital **II-4**. Scan rate = 500 mV s^{-1} , in $10^{-1} \text{ M TBAPF}_6$ in in dry degassed dichloromethane.

The titrations monitored by cyclic voltammetry showed no significant changes in the electrochemical properties of the cyclic ferrocene Hamilton-type receptor **II-29** upon complexation with barbital **II-4**.

2.2.3.4 Single crystal X-ray diffraction structure determination

Single crystals of suitable quality for X-ray diffraction structural determination were obtained for **II-29** (Figure 2.19).

Crystals were grown by vapor diffusion of diethyl ether into a concentrated acetic acid solution of **II-29** at room temperature.

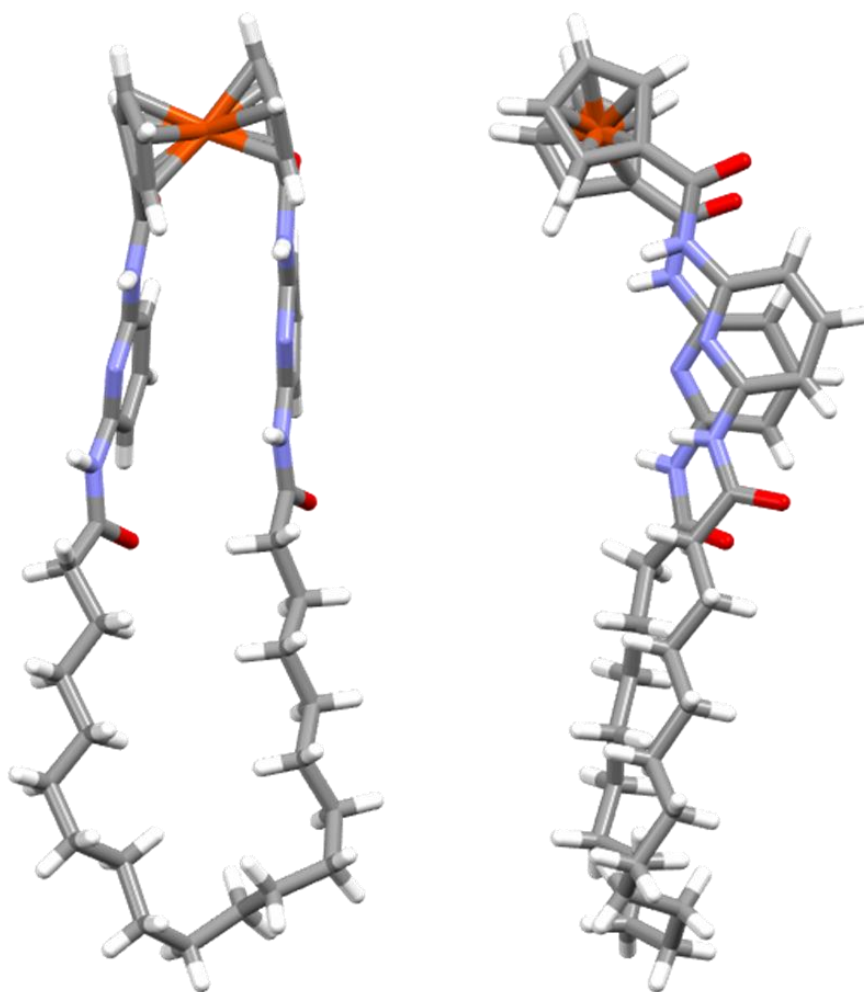


Figure 2.19 - Crystal structure of ferrocene Hamilton-type macrocycle **II-29**, front view (left) and side view (right).

The crystal structure of **II-29** verifies the macrocyclic structure of the product.

Comparing the crystal structures of **II-29** and **II-11**, a significant difference between the binding sites can be seen. The lack of rigidity between the bis(2,6-diamidopyridine) moieties attached to the cyclopentadienyl rings of the ferrocene group allows the adoption of a crescent-like conformation for the macrocyclic receptor **II-29**, while the isophthalic linkage in the Hamilton-type macrocycle **II-11** lock the 2,6-diamidopyridine moieties one in front of the other, providing a rigid and well-defined binding site (Figure 2.20).

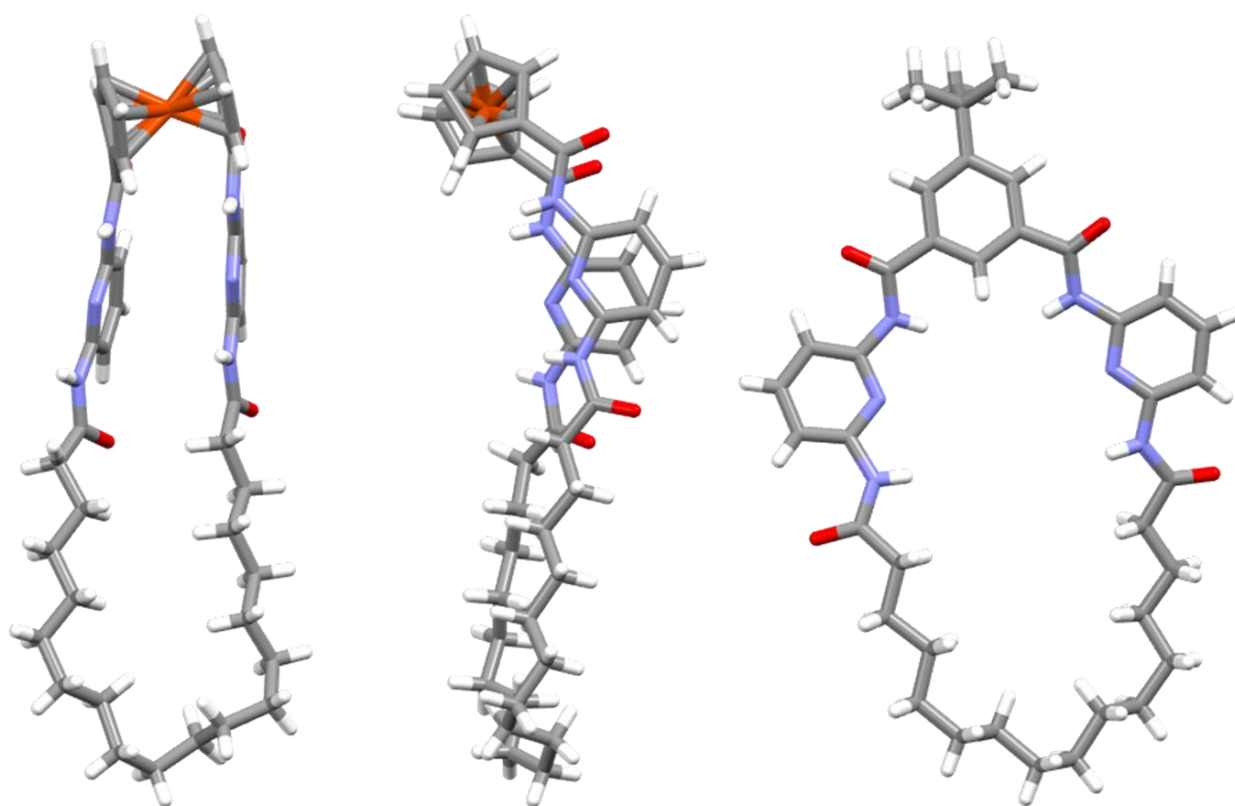


Figure 2.20 - Crystal structure of ferrocene-containing Hamilton-type macrocycle **II-29**, front view (left) and side view (centre), and Hamilton-type macrocycle **II-11**.¹³⁶

A not-defined binding site for barbiturates inside the cavity of the macrocycle made the receptor **II-29** unable to provide mechanically interlocked molecules.

¹³⁶ L. Pisciotanni, M. Douarre, B. Bibal, C. Davies, H. Roberts, B. Kauffmann, S.L. Horswell, J.H.R. Tucker and N.D. McClenaghan, *Supramol. Chem.*, **2018**, *30*, 869.

Table 2.1 - Crystal data of **II-29**.

Compound	II-29
Empirical formula	C ₄₂ H ₅₄ FeN ₆ O ₄
Formula weight	762.26
Temperature/K	293(2)
Radiation type	CuK α
Crystal system	Monoclinic
Space group	P2 ₁ /c
a/Å	40.430(11)
b/Å	8.605(3)
c/Å	10.8201(12)
α /deg	90
β /deg	91.440(15)
γ /deg	90
V/Å ³	3762.9(16)
Z	4
Abs. coeff. (mm ⁻¹)	3.621
F(000)	1624
Resolution (Å)	0.811
Index ranges	-34 \leq h \leq 36, -7 \leq k \leq 7, -9 \leq l \leq 8
No. of collected reflections	7356
Data/restraints/parameters	2932/479/0

2.3 Development of a triarylamine containing macrocycle

2.3.1 Introduction

A new electroactive hydrogen-bonded macrocyclic receptor was designed for having a defined cavity and a binding site which was coplanar with the macrocycle. An isophthalic linkage was proven to be necessary in order to ensure the rigidity of the binding site, moreover the electroactive group was put on periphery so as not to influence the binding site (Figure 2.21).

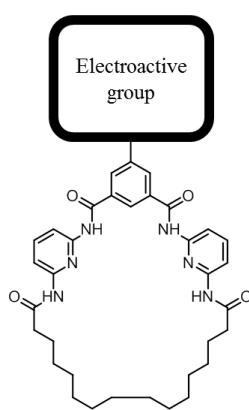
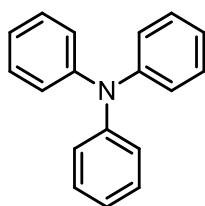


Figure 2.21 - Schematic representation for the design of an electroactive hydrogen-bonded macrocycle comprising an isophthalic group.

A different electron-donating group was considered and the triarylamine was the group of choice.

Triarylamine (TAA) is a class of amine substituted by three aryl groups and triphenylamine (TPA)

II-30 is the simplest member (Figure 2.22).



II-30

Figure 2.22 - Chemical structure of triphenylamine (TPA).

Taking the triphenylamine (TPA) **II-30** as the example, the central nitrogen atom is bounded with three carbon atoms via sp^2 -hybridization with a C-N bond length of 1.42 Å and a C-N-C bond angle of 120° , and the three phenyl groups assume a propeller-like structure with a torsion angle of 41.7° relative to the plane defined by the three C-N bonds which provides a framework to develop materials with different aggregation states (Figure 2.23).^{137, 138}

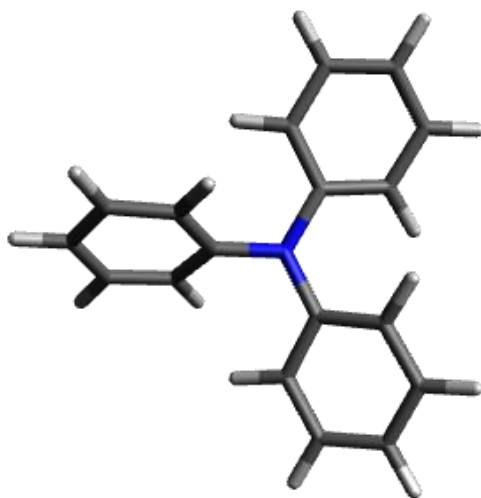


Figure 2.23 - Molecular model of triphenylamine **II-30**.

Triphenylamine **II-30** also possesses a strong electron-donating capability, with an ionization potential of 6.80 eV, is lower than many inorganic and organic materials: this property allows to adjust optical and electronic properties of a material.¹³⁹

Due to these properties, in the past decade triarylamines and related materials have been widely applied in the development of new generation solar cells, such as organic solar cells (OSCs),¹⁴⁰ dye-sensitized solar cells (DSSCs)¹⁴¹ and perovskite solar cells (PSCs).¹⁴²

¹³⁷ A. N. Sobolev, V. K. Belsky, I. P. Romm, N. Y. Chernikova and E. N. Guryanova, *Acta Crystallogr., Sect. C: Cryst. Struct. Commun.*, **1985**, *41*, 967.

¹³⁸ M. Malagoli and J.L. Brédas, *Chem. Phys. Lett.*, **2000**, *327*, 13.

¹³⁹ C. -G. Zhan, J.A. Nichols and D.A. Dixon, *J. Phys. Chem. A*, **2003**, *107*, 4184.

¹⁴⁰ S. Günes, H. Neugebauer and N.S. Sariciftci, *Chem. Rev.*, **2007**, *107*, 1324.

¹⁴¹ A. Mishra, M. K. R. Fischer and P. Bäuerle, *Angew. Chem., Int. Ed.*, **2009**, *48*, 2474.

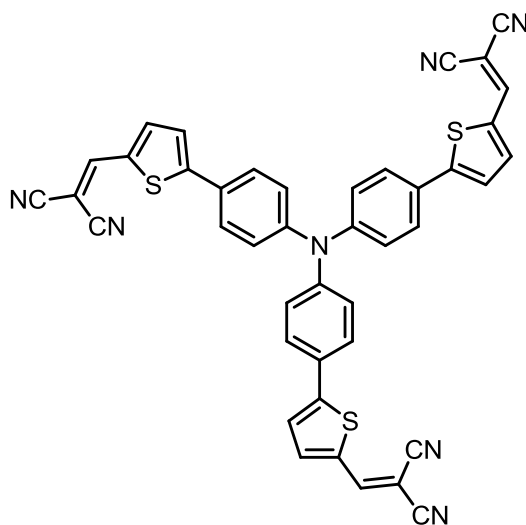
¹⁴² M. A. Green, A. Ho-Baillie and H. J. Snaith, *Nat. Photonics*, **2014**, *8*, 506.

Organic solar cells (OSCs) possess some advantages, such as lightweight, low cost fabrication and flexibility.^{143, 144, 145}

The two main architectures of OSCs are bilayer heterojunction and bulk heterojunction, whose mechanism is the following: 1) incident light forms excitons, 2) which diffuse to the interface, 3) at this point excitons dissociate into holes and electrons and 4) then they migrate to the corresponding counter electrode to generate current.

Roncali and coworkers pioneered the application of triarylamine-based materials in the development of organic solar cells.

In 2006 they synthesized a star-shaped small molecule, having a triphenylamine core and a thienylenevinyl arm as electron donating groups and a dicyanovinyl end as electron withdrawing group (Figure 2.24).¹⁴⁶



II-31

Figure 2.24 - Triarylamine-containing star-shaped molecule **II-31**.

¹⁴³ B. C. Thompson and J. M. J. Fréchet, *Angew. Chem., Int. Ed.*, **2008**, *47*, 58.

¹⁴⁴ G. Li, R. Zhu and Y. Yang, *Nat. Photonics*, **2012**, *6*, 153.

¹⁴⁵ Y. Lin, Y. Li and X. Zhan, *Chem. Soc. Rev.*, **2012**, *41*, 4245.

¹⁴⁶ S. Roquet, A. Cravino, P. Leriche, O. Alévêque, P. Frère and J. Roncali, *J. Am. Chem. Soc.*, **2006**, *128*, 3459.

Since the pioneering work of Grätzel and O'Regan, dye-sensitized solar cells (DSSCs) have raised a wide interest due to their simple fabrication and high performance.^{147, 148, 149}

Compared with other solar cells, DSSCs possess a peculiar aspect in that the light absorption and the charge transport are separated, which allows optimization of each process separately.

In 2013, Han and coworkers developed a triarylamine-containing dye **II-32**, which present the classical donor - π -spacer - acceptor structure in a unique [1]rotaxane-based topology (Figure 2.25).

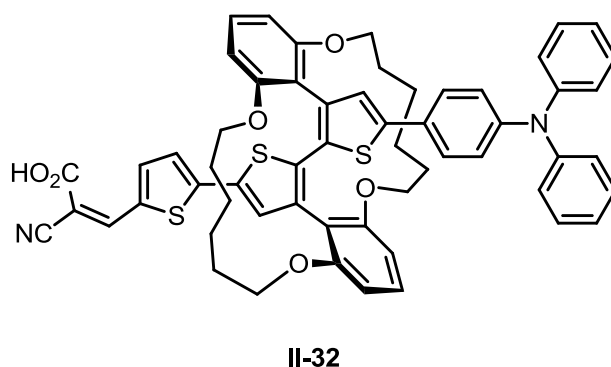


Figure 2.25 - Triarylamine-containing [1]rotaxane dye **II-32**.

The triarylamine core was introduced by a Suzuki coupling between a brominated thiophene and a triphenylamine-bearing boronic acid.

The constraint geometry is proven to play a central role in this molecule: the circular chain fixes the planar π -conjugation and limits the intermolecular π - π interactions, leading to a significant improvement of the photocurrent and photoefficiency.¹⁵⁰

¹⁴⁷ B. O'Regan and M. Grätzel, *Nature*, **1991**, 353,737.

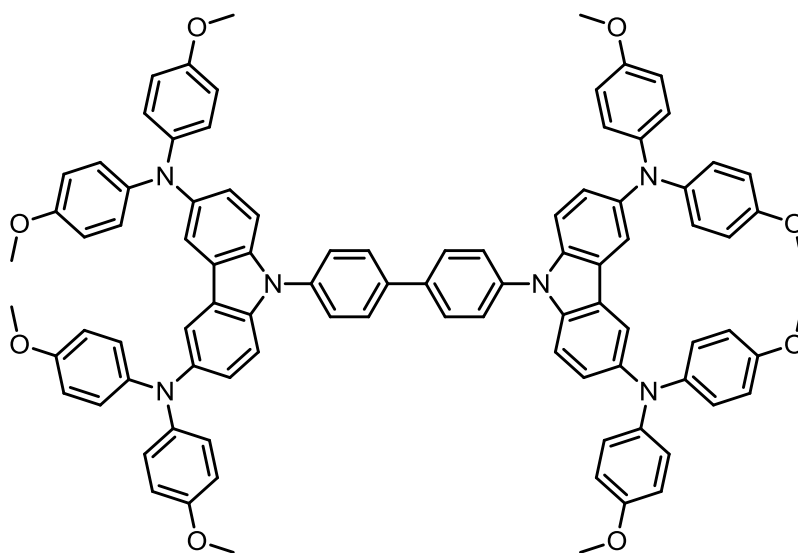
¹⁴⁸ M. Grätzel, *Acc. Chem. Res.*, **2009**, 42, 1788.

¹⁴⁹ A. Hagfeldt, G. Boschloo, L. Sun, L. Kloo and H. Pettersson, *Chem. Rev.*, **2010**, 110, 6595.

¹⁵⁰ J. Liu, Y. Numata, C. Qin, A. Islam, X. Yang and L. Han, *Chem. Commun.*, **2013**, 49, 7587.

Perovskite solar cells (PSCs) differ from the other solar cells because they have a nonexcitonic mechanism: the incident light generates holes, which are extracted by hole transporting materials (HTMs) to the counter electrode. The absence of exciton dissociation and migration provides an efficiency increase in photocurrent generation.^{151, 152}

In 2014 Sun and coworkers synthesized a carbazole-based hole transporting material **II-30**: carbazole is a cheap and commercially available molecule, it has good charge-transport properties and a fine substituent-dependent tuning of optical and electrical properties (Figure 2.26).



II-33

Figure 2.26 - Four-armed carbazole-based hole transporting material **II-33**.

The hole transporting material **II-33** was synthesized in 5 steps starting from commercially available carbazole and the triarylamine cores were obtained by a copper-catalyzed Ullman reaction and a palladium-catalyzed Buchwald-Hartwig reaction.¹⁵³

¹⁵¹ S. Kazim, M. K. Nazeeruddin, M. Grätzel and S. Ahmad, *Angew. Chem., Int. Ed.*, **2014**, 53, 2812.

¹⁵² Z. Yu and L. Sun, *Adv. Energy Mater.*, **2015**, 5, 1500213.

¹⁵³ B. Xu, E. Sheibani, P. Liu, J. Zhang, H. Tian, N. Vlachopoulos, G. Boschloo, L. Kloo, A. Hagfeldt and L. Sun, *Adv. Mater.*, **2014**, 26, 6629.

The simplest triarylamine, the triphenylamine (TPA) **II-30**, was first synthesized by Merz and Weith in 1873 with aniline or diphenylamine, metallic potassium, and bromobenzene.¹⁵⁴

In 1907, Goldberg and Nimerovsky synthesized triphenylamine **II-30** by an Ullmann-type copper-catalyzed aromatic amination reaction between diphenylamine and iodobenzene to obtain TPA in a nearly quantitative yield.¹⁵⁵

During the last century, the rising interest in organic electronics, like electroluminescent devices, integrated polymeric electro-optic switches and modulator, demanded ever more straightforward and efficient ways to obtain functionalized triarylamines.¹⁵⁶

New efficient reactions have been discovered and published and they can be divided in two main categories. In 1998 Goodbrand and Hu reported modified versions of Ullmann and Goldberg reactions, which involves copper(I)-catalyzed reactions, having the robustness and the easy-availability of cheap catalysts as advantages (Figure 2.27).

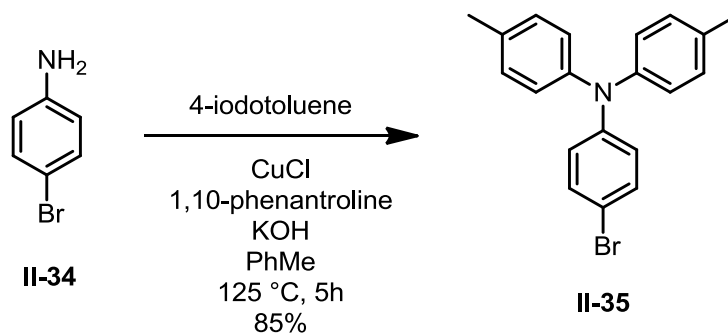


Figure 2.27 - Copper-catalyzed synthesis of functionalized triarylamine **II-35**.

In the same study, they also noticed the dependence of the reaction rate from the nature of the ligand and the fact that copper(II) acetate could be used as alternative of the corrosive copper(I) chloride without any loss of efficiency.¹⁵⁷

¹⁵⁴ V. Merz, W. Weith, *Vermischte Mittheilungen. Ber. Dtsch. Chem. Ges.*, **1873**, 6, 1511.

¹⁵⁵ I. Goldberg and M. Nimerovsky, *Ber. Dtsch. Chem. Ges.*, **1907**, 40, 2448.

¹⁵⁶ R. D. Miller, V. Y. Lee, R. J. Twieg, *J. Chem. Soc., Chem. Commun.*, **1995**, 245.

¹⁵⁷ H. B. Goodbrand, N. X. Hu, *J. Org. Chem.*, **1999**, 64, 2, 670-674.

One of the most important breakthrough in the C-N bond forming reaction occurred in 1995 with the works of Buchwald and Hartwig. The main advantage of this novel palladium catalyzed C-N bond forming methodology was the mildness of the reaction conditions: as long harsh conditions, like Goldberg reaction of aromatic nucleophilic substitution, were no longer required, the facile synthesis of aryl amines was possible and this new methodology was applied in the synthesis of natural products and industrial scale preparation of pharmaceuticals.^{158, 159, 160}

In 1997, Buchwald and coworkers proved the efficiency and the mildness of this new synthetic methodology, synthesizing the amine **II-38** in 72% yield with no racemization or removal of protecting group (Figure 2.28).¹⁶¹

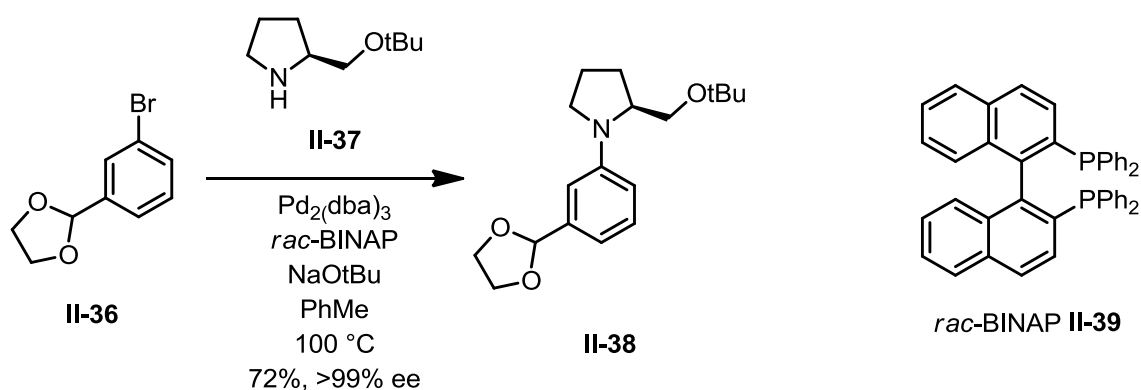


Figure 2.28 - Bidentate ligand-assisted Buchwald-Hartwig amination.

In 1998, Chan and Lam reported a new method for C-N bond formation: the Chan-Lam coupling, which consists in the cross coupling between an aryl boronic acid and a secondary aryl amine. The main advantages of this reaction are the use of inexpensive copper(II) catalysts and the possibility to perform the reaction in air at room temperature.¹⁶²

¹⁵⁸ J. F. Hartwig, *Angew. Chem., Int. Ed.*, **1998**, 37, 2046.

¹⁵⁹ J.P. Wolfe, S. Wagaw, J.-F. Marcoux and S.L. Buchwald, *Acc. Chem. Res.*, **1998**, 31, 805.

¹⁶⁰ J. F. Hartwig, *Acc. Chem. Res.*, **1998**, 31, 852.

¹⁶¹ S. Wagaw, R.A. Rennels and S.L. Buchwald, *J. Am. Chem. Soc.*, **1997**, 119, 8451.

¹⁶² P.Y.S. Lam, C.G. Clark, S. Saubern, J. Adams, M.P. Winters, D.M.T. Chan and A. Combs, *Tetrahedron Lett.*, **1998**, 39, 2941.

2.3.2 Synthesis

The first step to obtain the rigid electroactive macrocycle was the synthesis of a dimethyl 5-[bis(4-methoxyphenyl)amino]-isophthalate **II-43**. Being a keystone molecule of the entire synthesis, a solid, straightforward and easy-reproducible procedure that can provide the electroactive diester in gram-scale and in high yield was necessary.

A metal-catalyzed carbon-nitrogen bond forming reaction between an aryl iodide and commercially available 4,4'-dimethoxydiphenylamine **II-42** was the approach of choice.

The required iodide substrate was the dimethyl 5-iodoisophthalate **II-41**, which was obtained in one-step synthesis from dimethyl 5-aminosophthalate **II-40** in 88% yield (Figure 2.29).

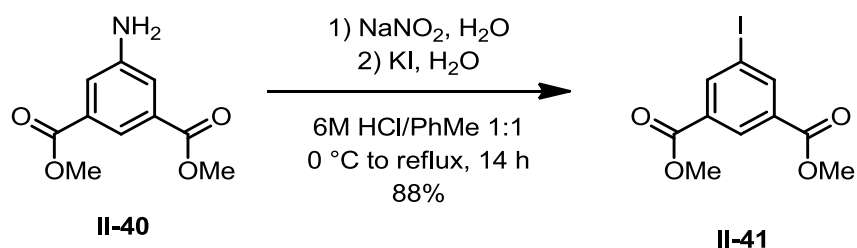


Figure 2.29 - Synthetic scheme of dimethyl 5-iodoisophthalate **II-9**.

We supposed that the main causes of these moderate yields were the heterogeneous nature of the reaction mixture, that hamper the reaction, and the formation of a thick emulsion during the work-up, that prevent the total recover of the product.

Based on this hypothesis, we sought to use a biphasic solvent system. The modified procedure we adopted ¹⁶³ is the following: the dimethyl 5-aminosophthalate **II-40** was suspended in 6M hydrochloric acid solution and cooled to 0 °C in an ice bath. Subsequently an aqueous solution of sodium nitrite was added dropwise at the same temperature, the dissolution of the suspension and the appearance of a yellow coloration confirmed the formation of the diazonium salt. After stirring for 15 minutes at 0 °C, an aqueous solution of potassium iodide was added, causing an immediate

¹⁶³ W. Boomgaarden, F. Vögtle, M. Nieger and Heike Hupfer, *Chem. Eur. J.*, **1999**, *5*, 345.

appearance of a deep red coloration and the formation of a foam. The reaction mixture was soon diluted with an equal volume of toluene and then the biphasic solution was vigorously stirred first for 12 hours at room temperature and then at reflux for 2 hours. The presence of an organic solvent in the reaction mixture and the subsequent heating allowed us to obtain the desired product in very good yield for the following reasons:

- the presence of a high boiling point organic solvent in the reaction mixture allows the dissolution of the product as soon it forms, preventing the formation of a foam that hinders stirring
- the refluxing of the biphasic mixture allows the “breaking” of the emulsion before the work-up, providing two well-defined and easy-separable layers.

The desired product was obtained as pale yellow microcrystalline powder after recrystallization in hot methanol.

Once the desired iodide substrate **II-41** was obtained, different conditions for the C-N bond forming reaction were tested. A screening of different reaction conditions was performed, varying solvent, base, presence of additive and nature of catalyst. (Figure 2.30 and Table 2.2)

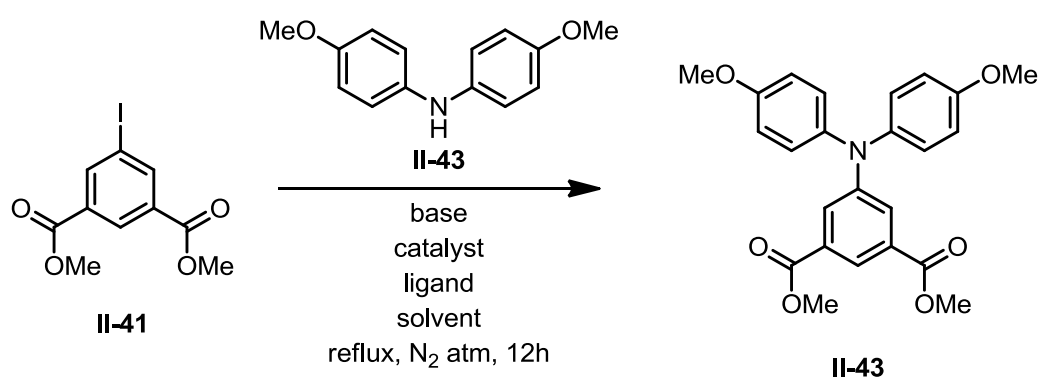


Figure 2.30 - Attempted synthesis of dimethyl 5-[bis(4-methoxyphenyl)amino]-isophthalate **II-43**

Table 2.2 - Reaction conditions screening for the formation of triarylamine isophthalate **II-43**

Entry	Solvent	Base (3 equiv.)	Catalyst (10% mol)	Additive (20% mol)	Yield of II-43
1	PhMe	Cs ₂ CO ₃	CuI	-	-
2	PhMe	Cs ₂ CO ₃	CuI	Phenanthroline	-
3	PhMe	Cs ₂ CO ₃	Cu powder	-	-
4	PhMe	KOtBu	Pd(OAc) ₂	P(tBu) ₃	-
5	PhMe	KOtBu	Pd(PPh ₃) ₄	-	-
6	oDCB	Cs ₂ CO ₃	CuI	-	-
7	oDCB	Cs ₂ CO ₃	CuI	Phenanthroline	-
8	oDCB	Cs ₂ CO ₃	Cu powder	-	-
9	oDCB	KOtBu	Pd(OAc) ₂	P(tBu) ₃	-
10	oDCB	KOtBu	Pd(PPh ₃) ₄	-	-
11	1,4-dioxane	Cs ₂ CO ₃	CuI	-	-
12	1,4-dioxane	Cs ₂ CO ₃	CuI	Phenanthroline	-
13	1,4-dioxane	Cs ₂ CO ₃	Cu powder	-	-
14	1,4-dioxane	KOtBu	Pd(OAc) ₂	P(tBu) ₃	-
15	1,4-dioxane	KOtBu	Pd(PPh ₃) ₄	-	-
16	DMF	Cs ₂ CO ₃	CuI	-	-
17	DMF	Cs ₂ CO ₃	CuI	Phenanthroline	-
18	DMF	Cs ₂ CO ₃	Cu powder	-	-
19	DMF	KOtBu	Pd(OAc) ₂	P(tBu) ₃	-
20	DMF	KOtBu	Pd(PPh ₃) ₄	-	-

All the reactions were performed according to the following conditions: aryl halide (1.2 equiv.), catalyst (10% mol), aryl amine (1 equiv.) and base (3 equiv.) in commercially available organic solvents (oDCB = ortho-dichlorobenzene, DMF = dimethylformamide) were deaerated and purged with nitrogen, and then stirred at 145 °C (heating plate) overnight. The progress of the reaction was followed by thin layer chromatography. Unfortunately, in our hands, none of the tested procedures afforded the desired triarylamine isophthalate **II-43**.

An alternative of the aryl iodinate substrate was synthesized: the dimethyl 5-[(trifluoromethylsulfonyl)oxy]isophthalate **II-46** was obtained in excellent yield in two-step synthesis starting from commercially available 5-hydroxyisophthalic acid **II-44** (Figure 2.31). Unfortunately, no significant improvements were observed.

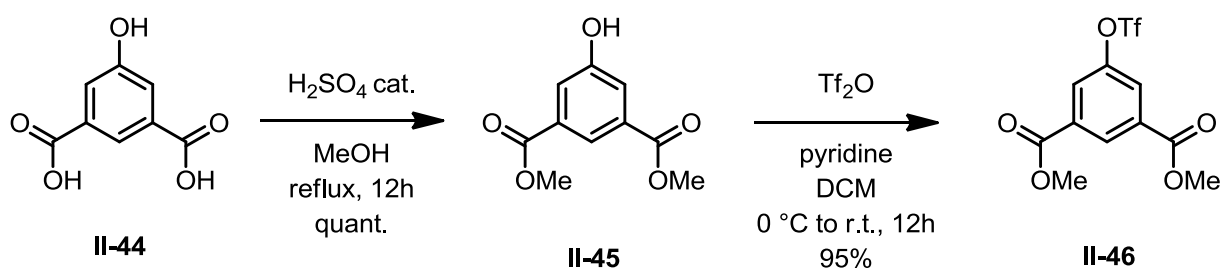


Figure 2.31 - Synthetic scheme of dimethyl 5-[(trifluoromethylsulfonyl)oxy]isophthalate **II-46**.

Based on these data, it was surmised that the causes of those failures were the easy oxidation of the metal catalysts, especially when palladium complexes were used, the hydrolysis of the ester groups in presence of the base and the thermal degradation of the solvent, especially in the case of dimethylformamide.

The desired triarylamine isophthalate **II-43** was obtained in good yield by a Goldberg-like reaction using tetraethyl orthosilicate as solvent (Figure 2.32).

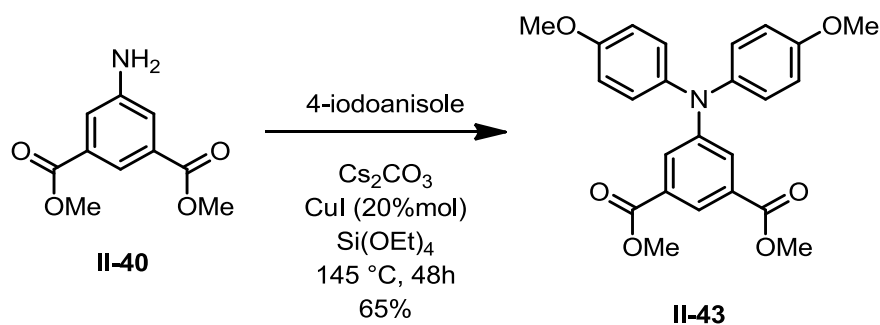


Figure 2.32 - Synthetic scheme of dimethyl 5-[bis(4-methoxyphenyl)amino]-isophthalate **II-43**.

The reaction conditions are quite mild and degradation products were not observed.

It was thought that the use of TEOS (tetraethyl orthosilicate) as solvent was the key to the success of this coupling reaction for two main reasons:

- being a desiccant, TEOS reacts with water, removing it from the reaction mixture and preventing the basic hydrolysis of the ester groups.
- the boiling point is higher than the reaction temperature, this avoids the degradation of the solvent and the formation of by-product which are difficult to remove, as in the case of DMF.

The work-up is straightforward: firstly the reaction mixture was cooled and treated with an aqueous ammonium fluoride solution in order to hydrolyse the solvent into silicon dioxide and ethanol, then the crude is recovered by addition of ethyl acetate and filtration. Finally the product was isolated by column chromatography on silica gel (Pentane/AcOEt 9:1, v/v or pure chloroform) followed by recrystallization in EtOH. Another significant aspect of this reaction is the fact that it involves cheap and commercially available reactants and it can be easily performed on the gram-scale.

Once the triarylamine-bearing isophthalate was obtained, the synthesis of the macrocycle was straightforward.

The triarylamine diester **II-43** was hydrolysed by refluxing overnight in a 1:1 methanol/2M sodium hydroxide aqueous solution and then the triarylamine-bearing isophthalic acid was recovered by acidification, filtration and subsequent recrystallization in EtOH.

Then the triarylamine dicarboxylic acid **II-47** was stirred in dry DCM in the presence of three equivalents of oxalyl chloride and a catalytic amount of DMF. The full conversion of the substrate into the corresponding dichloride **II-48** was obtained after 2 hours when a bright clear red solution was obtained. This intermediate was recovered by solvent removal, redissolved in a minimal amount of dry tetrahydrofuran and added dropwise to a stirring tetrahydrofuran solution of three equivalents of 2,6-diaminopyridine in presence of an excess of triethylamine. The reaction was allowed to stir overnight at room temperature and then the acyclic triarylamine-bearing Hamilton receptor **II-49** was isolated by column chromatography on silica gel (Pentane/AcOEt 4:1). The macrocyclic triarylamine-bearing Hamilton receptor **II-50** was obtained in the last step in moderate yields through a one-pot double condensation between both terminal -NH_2 groups of the acyclic receptor with the freshly prepared 1,16-hexadecanedioyl dichloride **II-26**, which were simultaneously added dropwise during 4 hours to a stirring solution of an excess of trimethylamine in dry tetrahydrofuran under high dilution conditions at room temperature overnight (Figure 2.33).

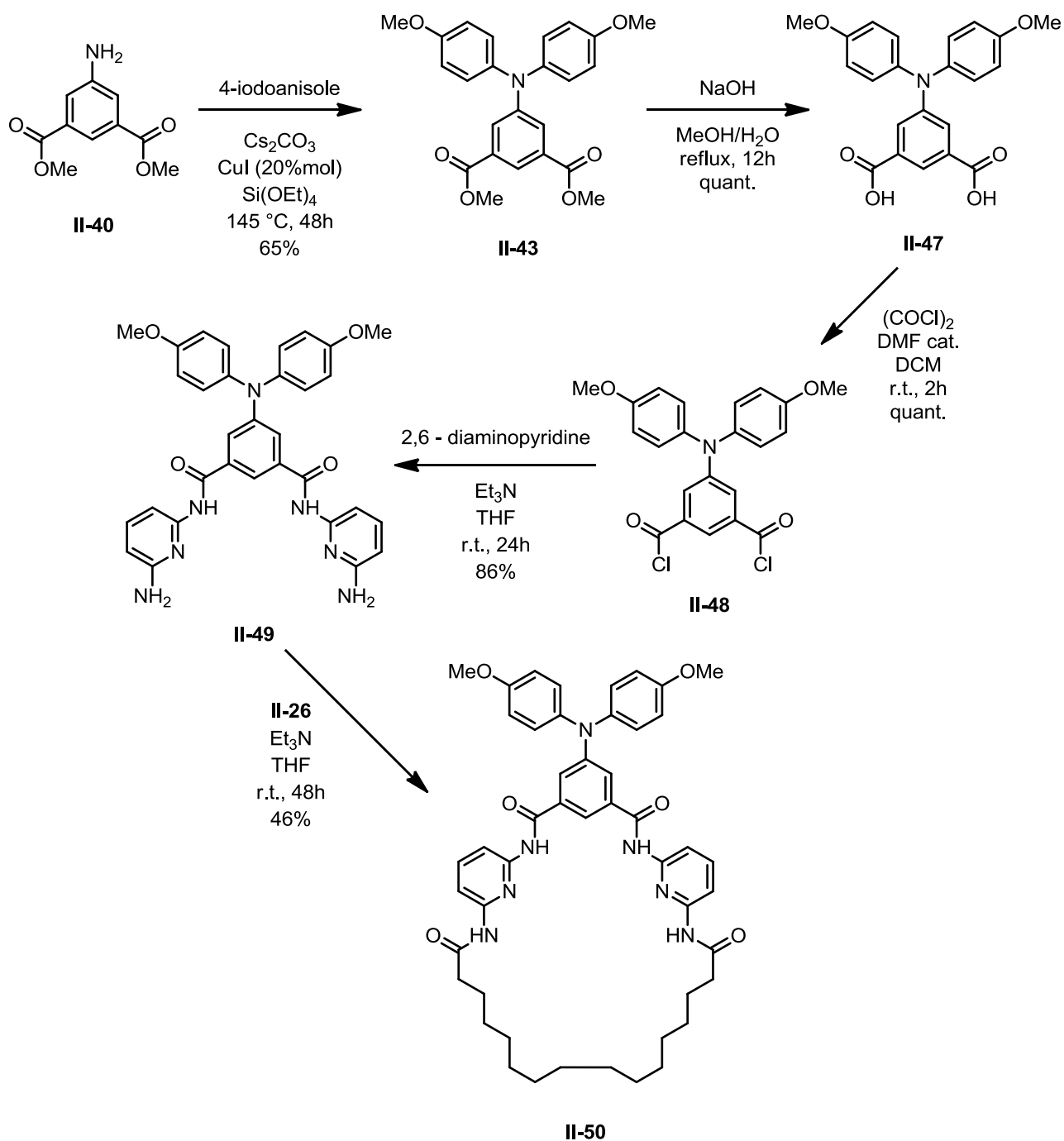


Figure 2.33 - Synthetic scheme of macrocyclic triarylamine-bearing receptor **II-50**.

2.3.3 Characterization

2.3.3.1 NMR studies

The cyclic triarylamine Hamilton receptor **II-50** and his acyclic precursor **II-49** were fully characterized by ^1H -, ^{13}C - NMR and mass spectrometry (Figure 2.34 and 2.35).

Both of them show high solubility in most of the common deuterated solvents. High quality NMR spectra can be recorded even after few days from the preparation of the samples.

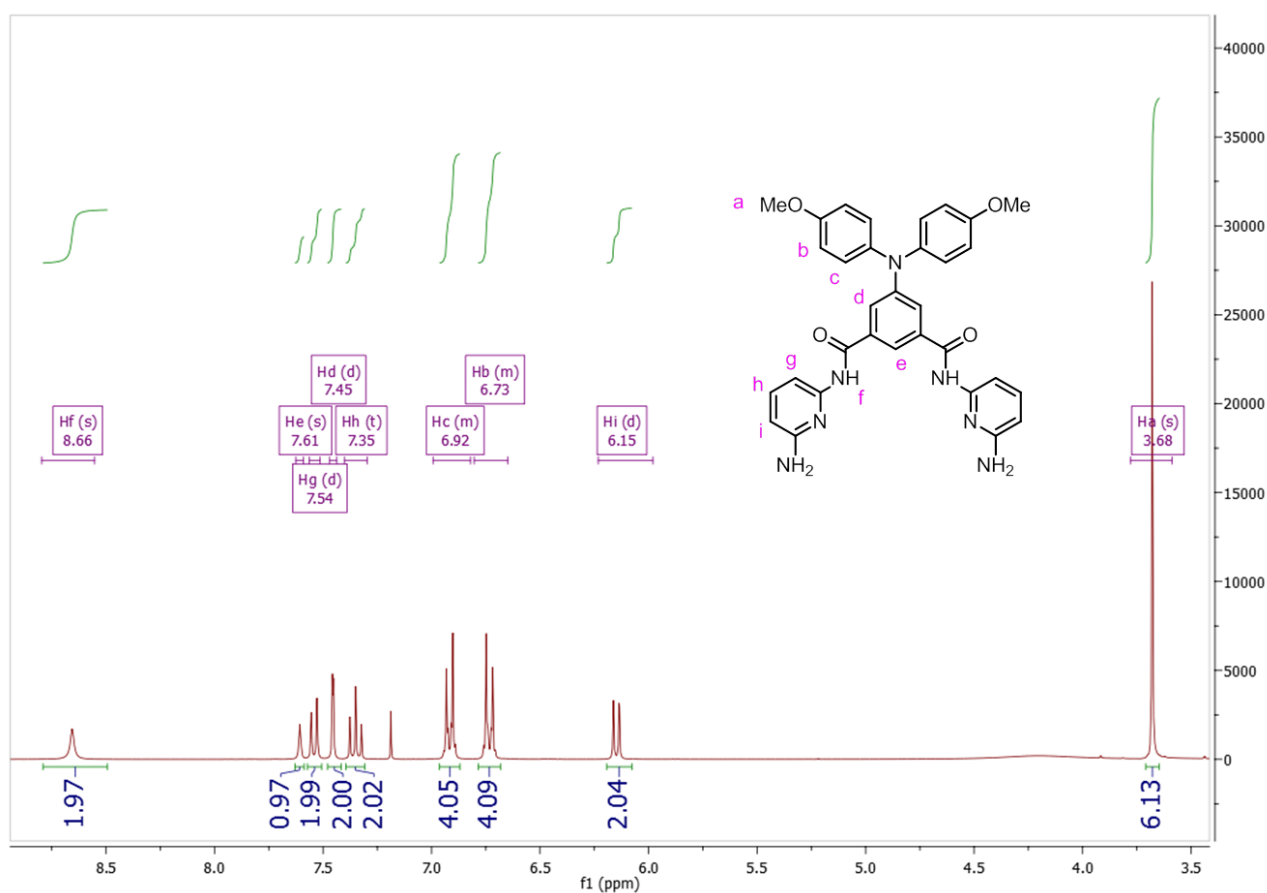


Figure 2.34 - ^1H -NMR of acyclic triarylamine Hamilton-type receptor **II-49** (600 MHz in CDCl_3).

In Figure 2.33, peaks at δ 6.92 (m, 4H) and δ 6.73 (m, 4H) are the aromatic proton of the triarylamine core. The 2:1 ratio of those peaks with the aromatic peaks of the pyridine core, which are at δ 7.54 (d, 2H), δ 7.35 (t, 2H) and δ 6.15 (d, 4H), proved the formation of the acyclic receptor **II-49**.

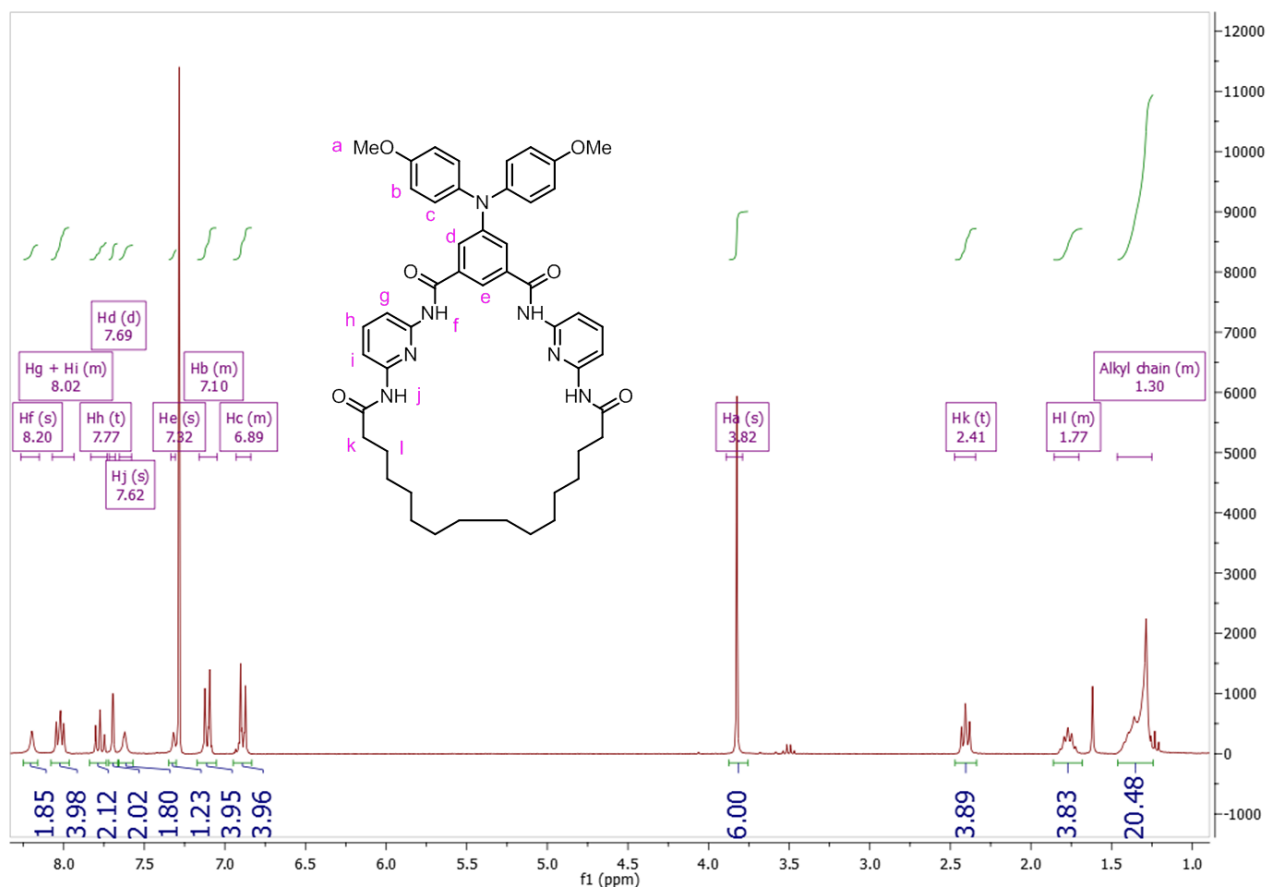


Figure 2.35 - ¹H NMR of cyclic triarylamine Hamilton-type receptor **II-50** (600 MHz in CDCl₃).

In Figure 2.34, peaks at δ 2.41 (t, $J = 7.5$ Hz, 4H) and δ 1.77 (m, 4H) are the methylene groups of alkyl chain in α - and β -position to the carbonyl groups, respectively. The 1:1 ratio of those peaks with the aromatic peaks of the triarylamine core, which are at δ 7.10 (m, 4H) and δ 6.89 (m, 4H), proved the formation of the macrocyclic receptor **II-50**.

2.3.3.2 Binding study with the TAA macrocycle

The formation of the complex between the cyclic triarylamine Hamilton-type receptor **II-50** and barbital **II-4** was studied by UV-vis spectroscopic titration (Figure 2.36).

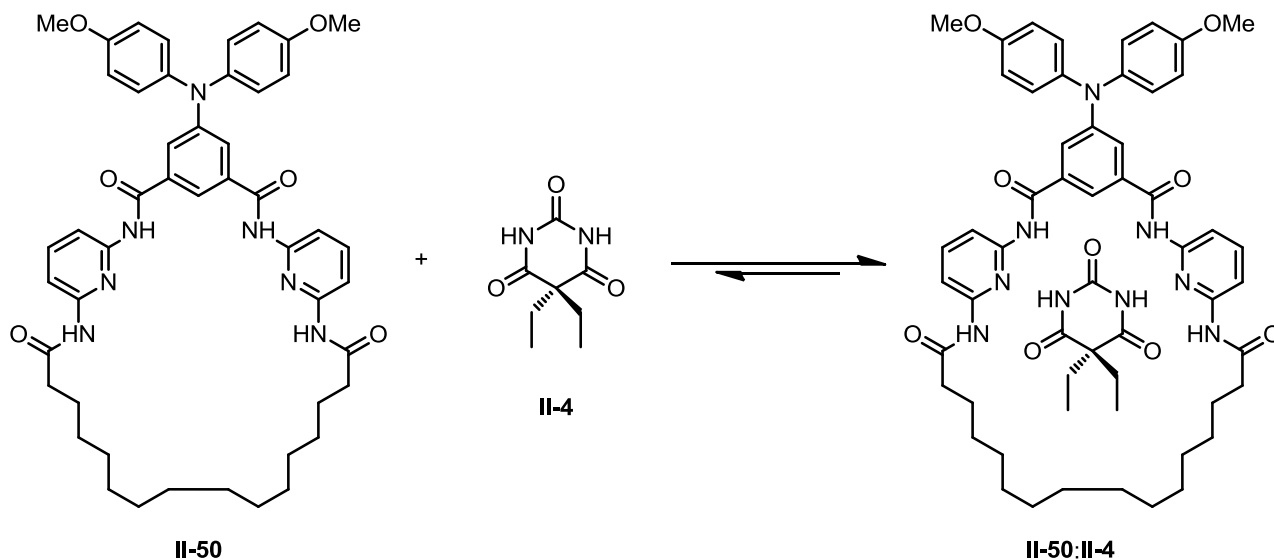


Figure 2.36 - 1:1 complex formation between cyclic triarylamine Hamilton-type receptor **II-50** and barbital **II-4**.

Upon the addition of a first equivalent of barbital **II-4**, a bathochromic shift in the absorption band of the pyridine was observed. The macrocycle **II-50** showed a molar attenuation coefficient (ϵ) of $46160 \text{ M}^{-1}\text{cm}^{-1}$ at 304 nm in dichloromethane and an association constant (K_{ass}) with barbital of 62750 M^{-1} (Figure 2.37).

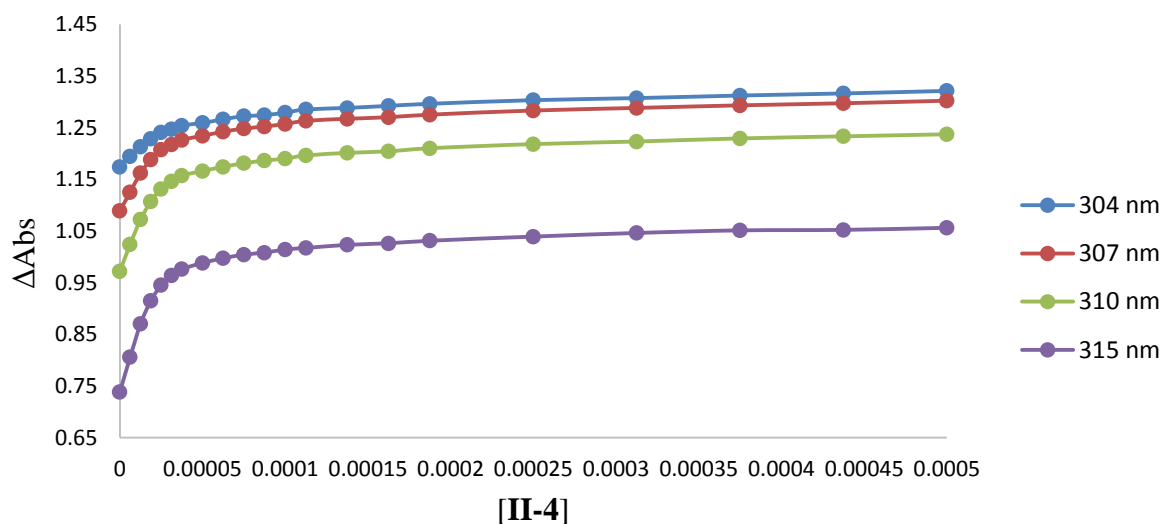


Figure 2.37 - Titration of **II-50** in the presence of barbital **II-4** monitored by electronic absorption spectroscopy in dichloromethane ($[\text{II-50}] = 25 \mu\text{M}$).

The complex between the macrocycle **II-50** and barbital **II-4** showed a 1:1 stoichiometry, as confirmed by the Job plot and in accordance with literature data for Hamilton-type receptors (Figure 2.38).

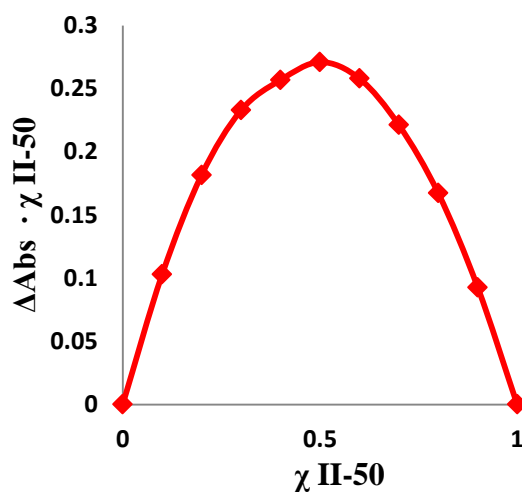


Figure 2.38 - Job plot for the change of absorption of macrocycle **II-50** at 304 nm in dichloromethane in presence of barbital **II-4** ($[\text{II-50}] = 25 \mu\text{M}$).

2.3.3.3 Electrochemistry studies

Cyclic triarylamine Hamilton-type receptor **II-50** was studied by cyclic voltammetry (CV) using a three electrode cell, with a glassy carbon working electrode, silver wire counter electrode and silver/silver chloride reference electrode (Figure 2.39).

The samples was dissolved in the minimal amount of dry tetrahydrofuran, degassed for 5 minutes then diluted in the same solvent, tetrabutylammonium hexafluorophosphate (TBAPF₆) was used as supporting electrolyte.

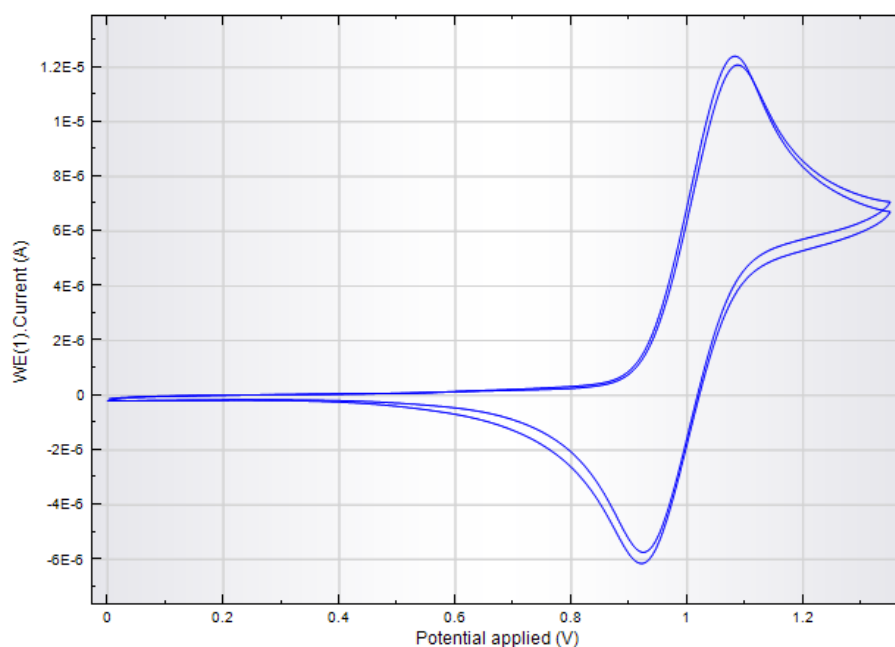


Figure 2.39 - Cyclic voltammogram of **II-50**, in a solution of 10^{-2} M TBAPF₆ in dry degassed tetrahydrofuran at scan rate = 100 mVs^{-1} .

From data analysis, macrocycle **II-50** was seen to undergo a redox transition at $E_{1/2} = 1.001 \text{ V}$, where $E_{1/2} = (E_p^a + E_p^c) / 2$.

2.3.3.4 Single crystal X-ray diffraction structural determination

Single crystals of suitable quality for X-ray structural determination were obtained for cyclic triarylamine Hamilton-type receptor **II-50** (Figure 2.40). Crystals were grown by slow cooling of a hot ethanolic solution of **II-50**.

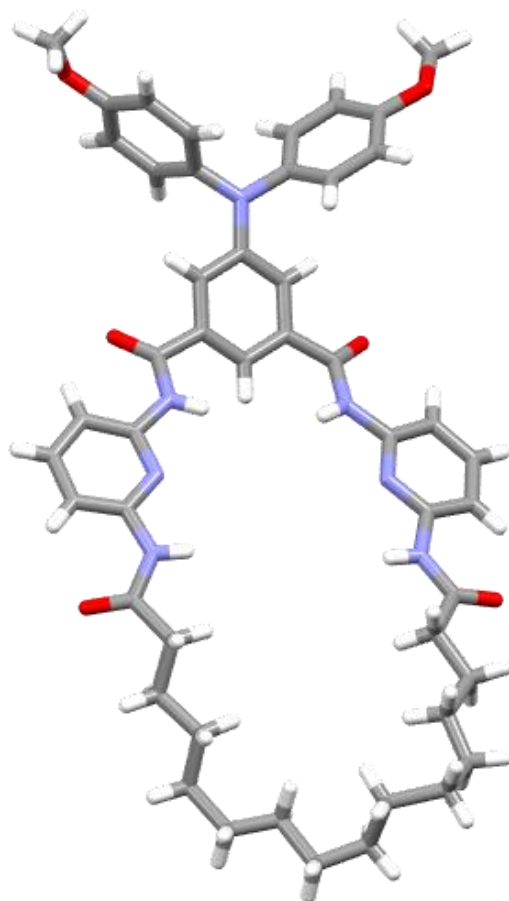


Figure 2.40 - Crystal structure of cyclic triarylamine Hamilton-type receptor **II-50**.

The macrocycle **II-50** presents the characteristic DADDAD hydrogen-bonding pattern, which was observed to be on the same plane of the binding cavity.

The triarylamine core presents C-N bonds length of 1.407, 1.428 and 1.433 Å and C-N-C angles of 122.05°, 116.81° and 120.96°.

Table 2.3 - Crystal data of cyclic triarylamine Hamilton-type receptor **II-50**

Compound	II-50
Empirical formula	C ₉₆ H ₁₁₄ N ₁₄ O ₁₂
Formula weight	1656.01
Temperature/K	293(2)
Radiation type	CuK α
Crystal system	Monoclinic
Space group	P2 ₁ /c
a/Å	25.694(5)
b/Å	9.9780(15)
c/Å	17.466(3)
α /deg	90
β /deg	105.721(6)
γ /deg	90
V/Å ³	4310.3(13)
Abs. coeff. (mm ⁻¹)	0.686
F(000)	1768
Resolution (Å)	0.811
Index ranges	-28 ≤ h ≤ 29, -11 ≤ k ≤ 10, -19 ≤ l ≤ 18
No. of collected reflections	26289
Data/restraints/parameters	6474/553/42

2.4 Conclusion and Perspectives

Three new macrocyclic versions of a Hamilton-like receptor incorporating a central ferrocene (**II-28** and **II-29**) and a triarylamine (**II-50**) have been successfully synthesized and fully characterized. High resolution crystal structures have been also obtained which were fundamental for the elucidation of the structures and a better comprehension of their roles in the future construction of interpenetrating molecular architectures.

- **Ferrocene - bearing macrocycles:** Crystallographic structural analysis of **II-29** showed a crescent-shaped structure and twisting of H-bonding groups out of the plane of the binding cavity, making the receptor site ill-adapted to accommodate a barbiturate guest through six strong H-bonds, thereby off-setting the advantage imparted by the macrocyclic nature of the receptor. The determined binding constants ($K_{\text{ass}} = 742 \text{ M}^{-1}$ for **II-28** and $K_{\text{ass}} = 1011 \text{ M}^{-1}$ for **II-29** in *d*-chloroform, respectively) were found to be higher than the previously reported acyclic version ($K_{\text{ass}} = 575 \text{ M}^{-1}$ in *d*-chloroform).
- **Triarylamine - bearing macrocycle:** a very well-defined cavity was observed with all the H-bonding groups in the plane of the binding cavity, the determined binding constant ($K_{\text{ass}} = 70000 \text{ M}^{-1}$ *d*₂-dichloromethane) is much higher than the structural analogue where a central tert-butyl phenyl is surrogate for the triarylamine moiety ($K_{\text{ass}} = 23500 \text{ M}^{-1}$ in *d*-chloroform) and a reversible oxidation was observed by cyclic voltammetry. All those properties make the cyclic triarylamine Hamilton-type receptor **II-50** an excellent candidate for the construction of interpenetrating molecular architectures.

3. Photoactive components and stoppers

3.1 Introduction

3.1.1 Boron dipyrrromethene dyes

The 4,4-difluoro-4-bora-3a,4a-diaza-*s*-indacene (boron dipyrrromethene or BODIPY) dyes are a class of fluorophores that are formed by BF₂ complexation of dipyrrromethene ligand (Figure 3.1).¹⁶⁴ They are characterized by intense absorption, high fluorescence quantum yields and substituent tuneable emission in the visible/NIR, alongside an excellent thermal and photochemical stability.

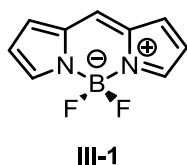


Figure 3.1 - Molecular structure of BODIPY core **III-1**.

They were first synthesized in 1968 by German chemists Treibs and Kreuzer and they have been widely applied in solar cells, bio-labelling, fluorescent probes and selective and sensitive chemosensors.^{165, 166, 167, 168, 169, 170, 171}

BODIPY core modification affects the optical properties of the molecule: the addition of the bulky phenyl groups enhances the rigidity of the molecule and increases the electron density, consequently causing a 60 nm red shift in the absorption wavelength.¹⁷²

¹⁶⁴ A. Loudet and K. Burgess, *Chem. Rev.*, **2007**, *11*, 4891.

¹⁶⁵ A. Treibs and F.H. Kreuzer, *Annalen Der Chemie-Justus Liebig*, **1968**, *718*, 208.

¹⁶⁶ S. Kolemen, Y. Cakmak, T. Ozdemir, S. Erten-Ela, M. Buyuktemiz, Y. Dede and E. U. Akkaya, *Tetrahedron*, **2014**, *70*, 6229

¹⁶⁷ D. Wang, J. Fan, X. Gao, B. Wang, S. Sun and X. Peng, *J. Org. Chem.*, **2009**, *74*, 7675.

¹⁶⁸ Z. Li, E. Mintzer and R. Bittman, *J. Org. Chem.*, **2006**, *71*, 1718.

¹⁶⁹ B.W. Michel, A.R. Lippert and C.J. Chang, *J. Am. Chem. Soc.*, **2012**, *134*, 15668.

¹⁷⁰ F. Sozmen, S. Kolemen, H.O. Kumada, M. Ono, H. Saji and E.U. Akkaya, *RSC Advances*, **2014**, *4*, 51032.

¹⁷¹ X. Qi, E. J. Jun, L. Xu, S.-J. Kim, J.S.J. Hong, Y.J. Yoon and J. Yoon, *J. Org. Chem.*, **2006**, *71*, 2881.

Moreover, the substitution of a carbon atom with a more electron-donating nitrogen causes a 83 nm red shift in absorption wavelength: these new generation fluorophores are called aza-dipyrromethene boron difluoride (Figure 3.2).¹⁷³

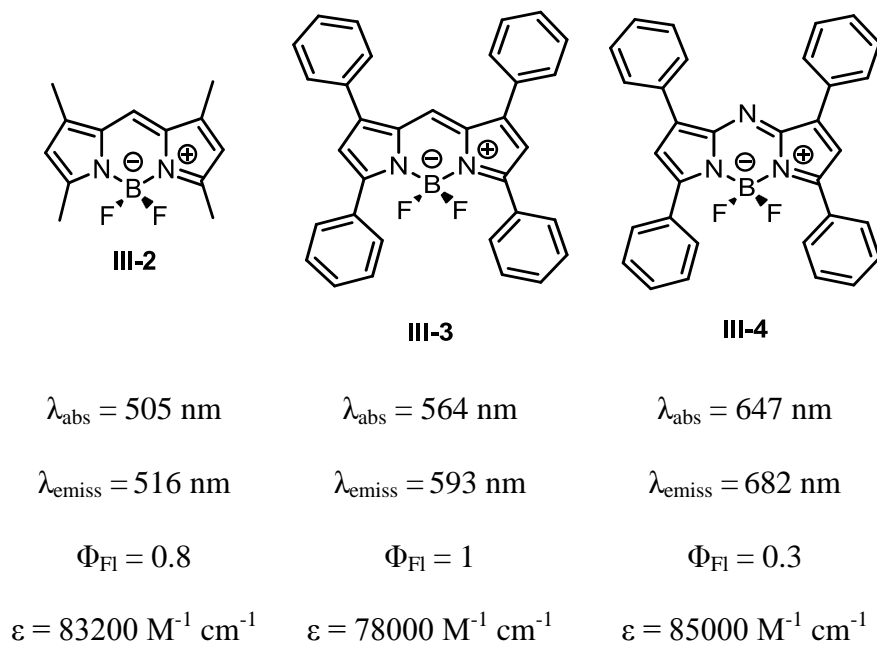


Figure 3.2 - Molecular structure and optical properties of BF₂-chelates of dipyrromethenes and aza-dipyrromethenes (solvent = DCM).

Despite the aforementioned useful optical properties, the limited wavelength range of absorption restricts their application in cell imaging and in photodynamic therapy (PDT) as a photosensitizer. However, the absorption of the aza-dipyrromethene fluorophores can be shifted above 740 nm by core or side group modification, which offers the possibility of working in the NIR region and so the possibility to apply this class of chromophores in biology and medicine.¹⁷⁴

¹⁷² L. Wu, and K. Burgess, *Chem. Comm.*, **2008**, 4933.

¹⁷³ A. B. Nepomnyashchii, M. Bröring, J. Ahrens and A.J. Bard, *J. Am. Chem. Soc.*, **2011**, 133, 8633.

¹⁷⁴ W. Zhao and E. M. Carreira, *Angew. Chem. Int. Ed.* **2005**, 44, 1677.

3.1.2 Boron aza-dipyrromethene dyes: synthesis and applications

Despite the fact that BF_2 complexes of the aza-dipyrromethene ligand started to be explored in the last two decades, the ligand itself was first synthesized in 1943 by Rogers and coworkers.^{175, 176}

It was used as an efficient blue colouring dye. Derivatives of aza-dipyrromethene ligand were synthesized in two ways: the first was a one-pot condensation reaction of two molecules of 4-nitro-1,3-diphenylbutan-1-one at elevated temperature in the presence of an excess of ammonium formate in solvent-free conditions. The second way was a one-pot condensation between a molecule of 5-nitroso-2,4-diphenylpyrrole and 2-phenyl-4-anisylpyrrole at elevated temperature in acetic acid. The reported yields were moderate in both cases (30 - 40%) (Figure 3.3).

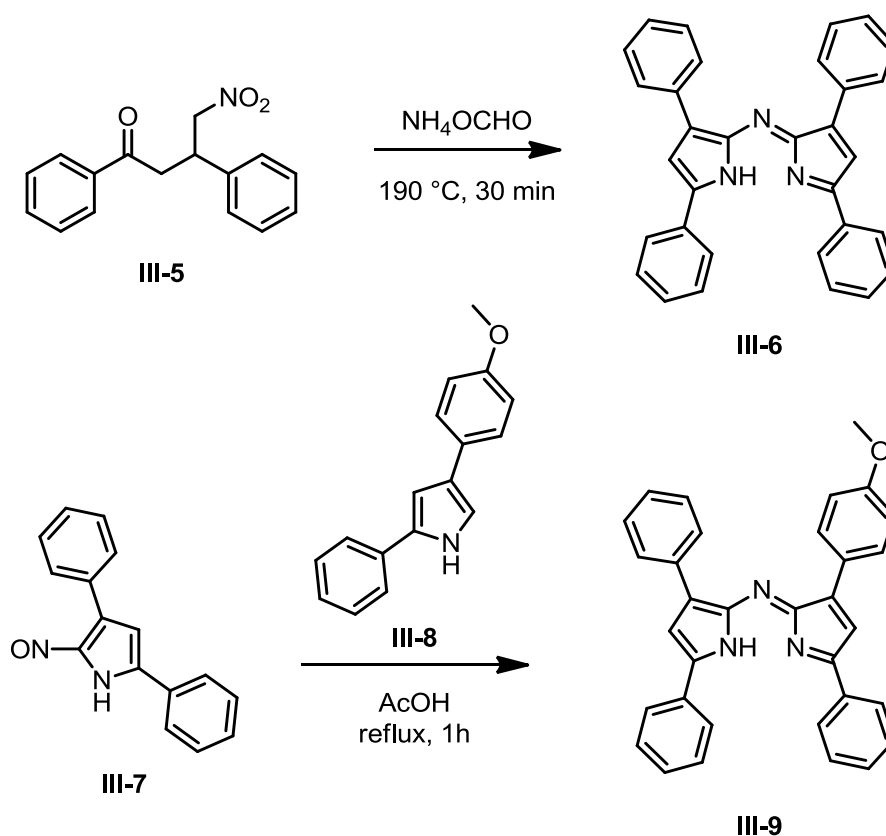


Figure 3.3 - Aza-dipyrromethene ligand syntheses.

¹⁷⁵ M.A.T. Rogers, *J. Chem. Soc.*, **1943**, 590.

¹⁷⁶ W.H. Davies and M.A.T. Rogers, *J. Chem. Soc.*, **1944**, 126.

The synthesis of BF₂-chelate of the 1,3,5,7-tetraphenyl-8-aza-dipyrromethene was first reported in 1990s as a laser dye by Govindarao and coworkers: the molecule was obtained by the complexation of the boron trifluoride with the tetraphenyl substituted ligand in 12% yield (Figure 3.4).

The reported optical properties were the following: $\lambda_{\text{abs}} = 650 \text{ nm}$, $\lambda_{\text{em}} = 680 \text{ nm}$ and $\Phi_{\text{F}} = 0.77$ in *o*-xylene.^{177, 178}

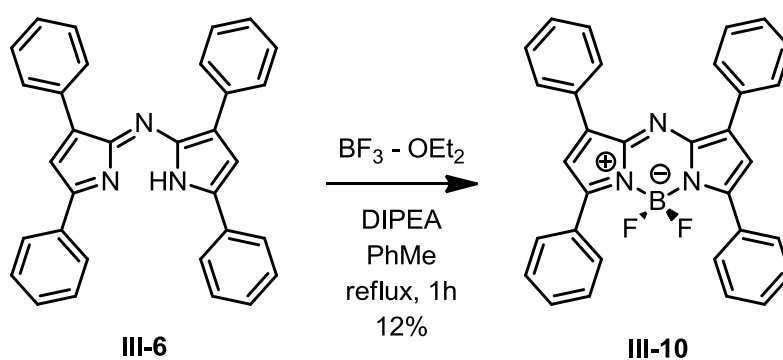


Figure 3.4 - Synthesis of BF₂-chelate of the 1,3,5,7-tetraphenyl-8-aza-dipyrromethene **III-10**.

In 2002 there has been a resurgence of interest in the BF₂-chelate aza-dipyrromethene as new tools in cancer treatment. Photodynamic therapy (PDT) is a non-invasive technique for the treatment of tumors by the combined use of visible or near-visible light with a photosensitizing drug.¹⁷⁹ The therapeutic strategy is the following: a photosensitizer is introduced into the body, which accumulates preferentially within the tumor. The tumor is then irradiated with low energy light of a wavelength that can pass through the body (650–800 nm, beyond the absorbance of body tissue) resulting in excitation of the photosensitizer. The light-activated photosensitizer then transfers its excited state energy to surrounding biological tissue through singlet oxygen, resulting in oxidative cellular damage, leading to cell death *via* apoptosis and/or necrosis.¹⁸⁰

¹⁷⁷ S. Govindarao, M. L. Soong, T.W. Ross and J.H. Boyer, *Heteroat. Chem.*, **1993**, 4, 603.

¹⁷⁸ H.A. Toomas, S. Govindarao and H.B. Joseph, *Proc. SPIE-Int. Soc. Opt. Eng.*, **1994**, 2115, 9.

¹⁷⁹ a) R. Bonnett, *Chem. Soc. Rev.*, **1995**, 24, 19.

b) T. J. Dougherty, C. J. Gomer, B. W. Henderson, G. Jori, D. Kessel, M. Korbelik, J. Moan and Q. Peng, *J. Natl. Cancer Inst.*, **1998**, 90, 889.

¹⁸⁰ N.L. Oleinick, R.L. Morris and I. Belichenko, *Photochem. Photobiol. Sci.*, **2002**, 1, 1

O'Shea and coworkers first reported the syntheses and photophysical investigation of a novel class of photodynamic therapeutic agents based on different substituted BF₂-chelatetaza-dipyrromethenes (Figure 3.5).¹⁸¹

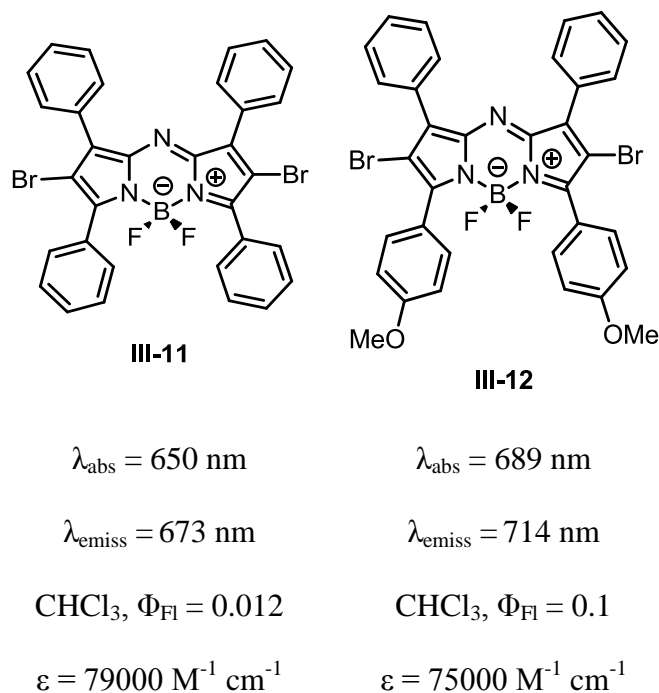


Figure 3.5 - Molecular structures and optical properties of aza-dipyrromethene-based PDT agents **III-11** and **III-12**.

The most important contribution of O'Shea's group to this field was the significant improvement of the aza-dipyrromethene ligands synthesis conditions: the ligand skeletons are still prepared from nitromethane adducts to the corresponding substituted 1,3-diphenylbutan-1-one (or chalcone), but ammonium acetate, instead of the corresponding formate, as ammonia source in refluxing butanol, rather than methanol or solvent-free conditions, was the best system to obtain the ligand. The syntheses were completed by adding boron trifluoride diethyl etherate in presence of base at room temperature in dichloromethane.

¹⁸¹ J. Killoran, L. Allen, J. Gallagher, W. Gallagher and D.F. O'Shea, *Chem. Commun.* **2002**, 0, 1862.

This improved procedure allowed the synthesis of a series of differently substituted BF₂ chelate of tetraaryl-8-aza-dipyrromethene and a consequent detailed investigation of the substitution effects on the optical properties (Figure 3.6).^{182,183}

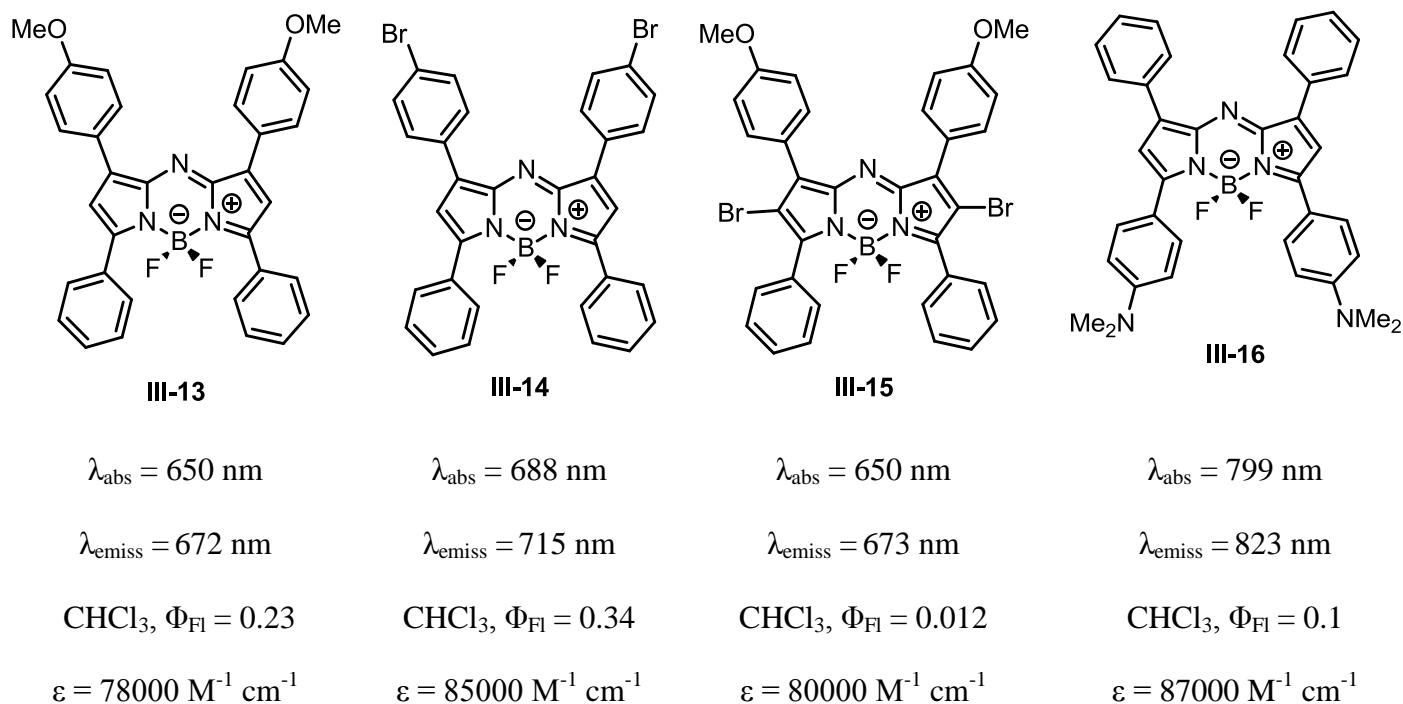


Figure 3.6 - Molecular structures and optical properties of differently substituted BF₂-chelates of tetraaryl-8-aza-dipyrromethenes.

Absorption band maxima of the tetraaryl-8-azadipyrromethene BF₂-chelates strongly depend on the aryl substituents. The introduction of a strong electron donating groups in the para-position, such as the dimethylamino group, on the 5-aryl substituents gives increased extinction coefficients and red shifts of 152 nm in the λ_{abs} . Substitution with an electron donating group on the 3-aryl ring has less impact, but still gives a bathochromic shift. Moreover, the extinction coefficients of BF₂-aza-dipyrromethenes range from 75000 to 85000 M⁻¹ cm⁻¹, almost 20 times greater than substituted porphyrins (from 3000 to 5000 M⁻¹ cm⁻¹), which is the class of photosensitizer currently used in

¹⁸² A. Gorman, J. Killoran, C. O'Shea, T. Kenna, W. M. Gallagher and D.F. O'Shea, *J. Am. Chem. Soc.* **2004**, *126*, 10619.

¹⁸³ S.O. McDonnell and D.F. O'Shea, *Org. Lett.* **2006**, *8*, 3493.

photodynamic therapy. This strong absorption is one of the factors that facilitate efficient singlet-oxygen generation.

Another important aspect of this class of NIR chromophores is their excellent photostability. The photodegradation of brominated and non-brominated BF_2 -azadipyrromethenes compared to fluorescein isocyanate, a widely used label in microscopy experiments and fluorescence imaging is shown below (Figure 3.7).¹⁸⁴

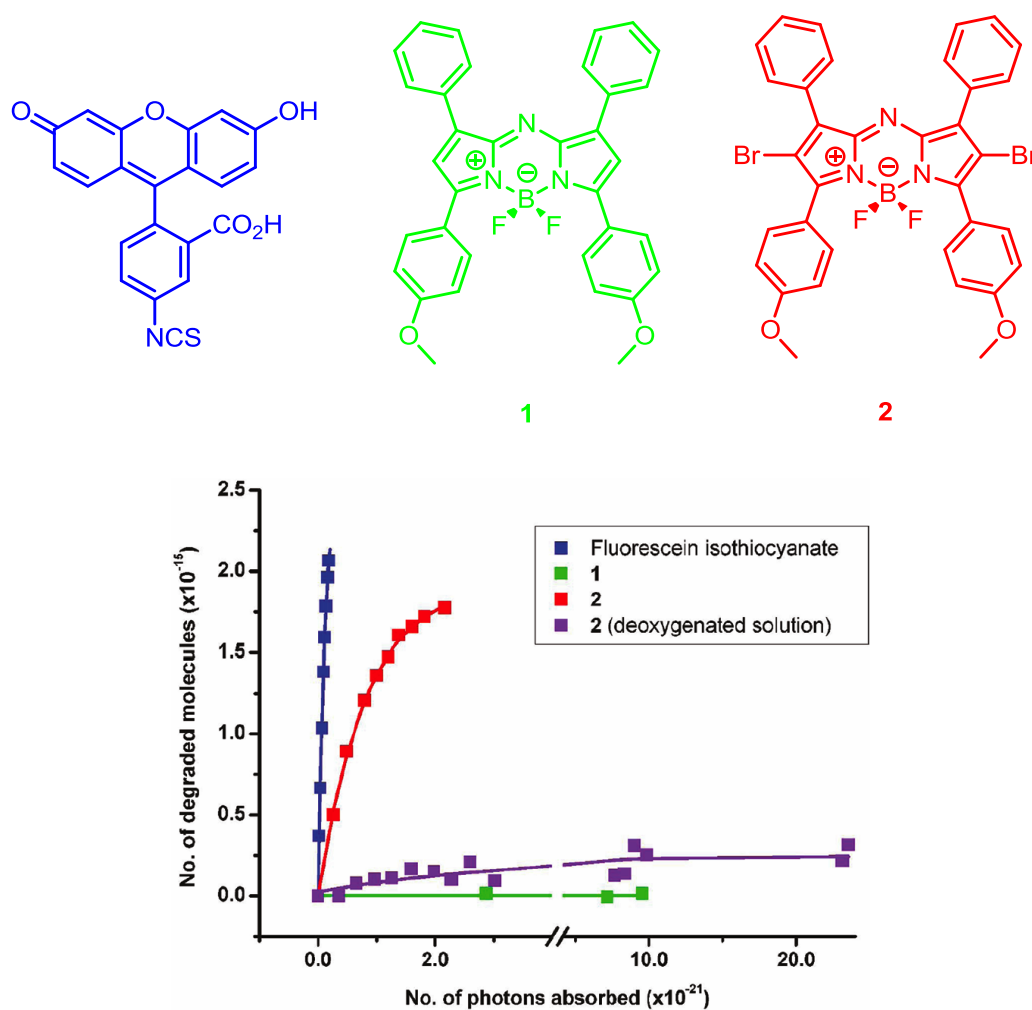


Figure 3.7 - Molecular structures of fluorescein isocyanate, brominated and non-brominated BF_2 -azadipyrromethenes (top) and advancement of photodegradation in exciting dilute solutions (bottom).

¹⁸⁴ P. Batat, M. Cantuel, G. Jonusauskas, L. Scarpantonio, A. Palma, D.F. O'Shea and N.D. McClenaghan, *J. Phys. Chem. A*, **2011**, *115*, 14034.

Different functionalizations of the boron centre have also been reported: the replacement of the fluorine groups with aryl units induces a 29 nm blue shifting in absorption and remarkable decrease in fluorescence quantum yield compared to BF₂ complex of the same ligand.¹⁸⁵

The opposite phenomenon was observed when a B-O ring extended azadipyrromethenes was synthesized by forming benzi(1,3,2)oxozaborinine rings (Figure 3.8).

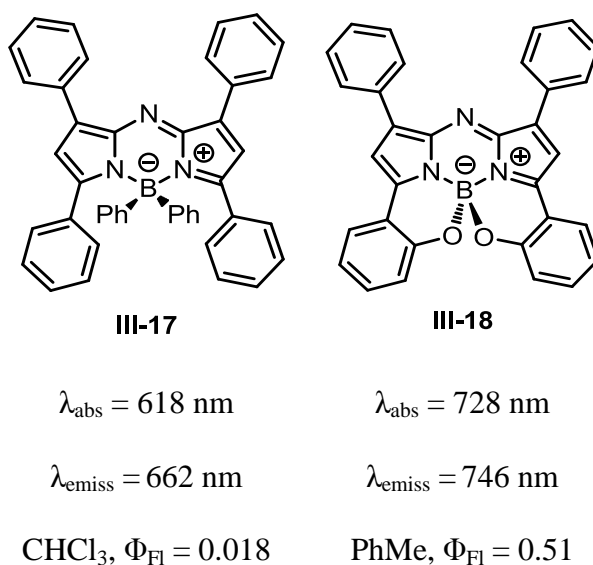


Figure 3.8 - Molecular structures and optical properties of differently boron-functionalized azadipyrromethenes.

The presence of two B-O bonds gives a geometric restriction to the molecule, which causes a 81 nm red shifting in absorption and an increase in fluorescence quantum yield were observed compared to the conventional BF₂-azadipyrromethene.¹⁸⁶

¹⁸⁵ X. -D. Jiang, Y. Fu, T. Zhang and W. Zhao, *Tetrahedron Letters* **2012**, 53, 5703.

¹⁸⁶ A. Loudet, R. Bandichhor, K. Burgess, A. Palma, S.O. McDonnell, M.J. Hall and D.F. O'Shea, *Org Lett*, **2008**, 10, 4771.

BF₂-chelate aza-dipyrromethene dyes mostly have been discussed in the context of agents for photodynamic therapy, but chemosensors have also been developed from these compounds.

In 2007, Akkaya and coworkers developed a BF₂-azadipyrromethene-based sensor, which is highly selective for mercuric ions that can be chelated between the pyridyl groups.

Mercuric ion complexation red-shifts both the absorption and fluorescence emission maxima. The dissociation constant was determined to be 5.4×10^{-6} M, with a 1:1 binding stoichiometry (Figure 3.9).¹⁸⁷

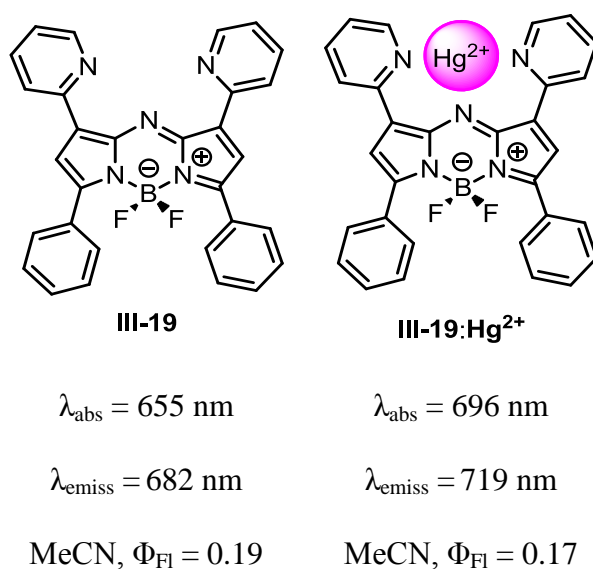


Figure 3.9 - Chemical structures and optical properties of BF₂-azadipyrromethene chemosensor **III-19** and its 1:1 mercuric ion complex **III-19:Hg²⁺**.

¹⁸⁷ A. Coskun, M..D Yilmaz and E.U. Akkaya, *Org. Lett.*, **2007**, *9*, 607.

In 2007, Pharr and coworkers developed a photoinduced electron transfer (PET) crown ether chemosensor featuring BF₂-azadipyromethene chromophore; it is used as visible sensor ($\lambda_{\text{abs}} = 650$ nm and $\lambda_{\text{emiss}} = 680$ nm) for the paralytic shellfish toxin Saxitoxin. This toxin contains guanidine groups, and it is these functional groups that interact with the crown ether moiety of the sensor. In the absence of Saxitoxin, PET from the crown ether to the fluorophore quenches the fluorescence. Upon complexation of the toxin, PET can no longer take place and fluorescence is turned on. At 1:1 toxin/crown stoichiometry, the fluorescence enhancement was over 100% and the average binding constant, $6.2 \times 10^5 \text{ M}^{-1}$, was among the highest observed for any chemosensor of that toxin (Figure 3.10).¹⁸⁸

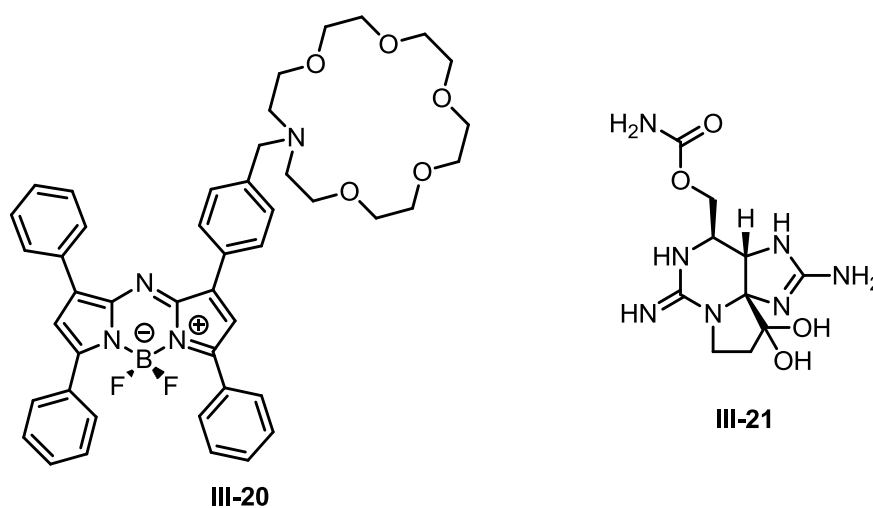
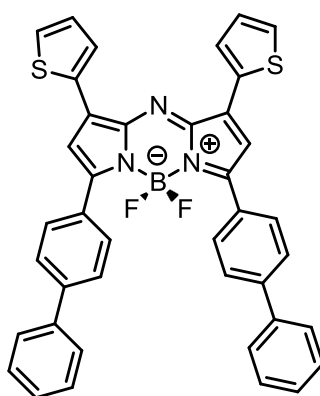


Figure 3.10 - Chemical structures of BF₂-azadipyromethene-based chemosensors **III-20** and Saxitoxin **III-21**.

¹⁸⁸ R.E. Gawley, H. Mao, M.M. Haque, J.B. Thorne and J.S.J. Pharr, *J. Org. Chem.* **2007**, *72*, 2187.

Besides desirable photophysical properties, BF₂-azadipyrromethenes were shown to possess interesting electrochemical properties, which makes them good candidates for organic solar cell applications. Indeed, in 2014 Agarwal and coworkers reported a new BF₂-azadipyrromethene derivative with low band gaps and high electron affinity for solar cell applications (Figure 3.11).

Due to the long π -conjugated skeleton, this BF₂-azadipyrromethene derivative exhibits longer absorption and fluorescence wavelengths and has a lower optical band gap energy (1.28 eV).¹⁸⁹



III-22

$$\lambda_{\text{abs}} = 708 \text{ nm}$$

$$\lambda_{\text{emiss}} = 738 \text{ nm}$$

$$\text{CHCl}_3, \Phi_{\text{Fl}} = 0.27$$

$$\epsilon = 47000 \text{ M}^{-1} \text{ cm}^{-1}$$

Figure 3.11 - Chemical structures and optical properties of BF₂-azadipyrromethene.

Due to their photostability, biocompatibility and a wide range of functionalizations, BF₂-chelate aza-dipyrromethene dyes are interesting candidates for the development of NIR chromophore-containing building block for functional mechanically interlocked molecules.

¹⁸⁹ T. K. Khan, P. Sheokand and N. Agarwal, *Eur. J. Org. Chem.*, **2014**, 2014, 1416.

3.2 Design of methoxypropargyloxy BF₂-chelate azadipyrromethene

3.2.1 Synthesis

The synthesis of both non-symmetrical NIR components was based on the previously mentioned procedure of dihydroxy-azadipyrromethene BF₂-chelate **III-27**.¹⁹⁰

As shown in Figure 3-12, commercially available 4'-hydroxyacetophenone **III-23** was first reacted with an equimolar amount of benzaldehyde in ethanol in presence of an aqueous solution of sodium hydroxide. We noticed that the product does not precipitate during the reaction, as mentioned in literature, but it is soluble in the basic medium. The detailed work-up we used for the isolation of the crude product is the following: the reaction mixture was first diluted in 10-fold distilled water then the solution was acidified with concentrated hydrochloric acid until pH=0, where precipitation of a pale fluffy solid was observed. The heterogeneous mixture was stirred for 1 hour to assure the complete precipitation of the product **III-24**, which was recovered by filtration on a fritted funnel, washed with distilled water and the purified by recrystallization in ethanol. The presence of only *E*-isomer was confirmed by ¹H NMR.

The 4'-hydroxychalcone **III-24** was then reacted with 5 equivalents of diethylamine and 10 equivalents of nitromethane. We note in passing that an easier separation, which leads to a higher yield, is possible if the reaction mixture is carefully concentrated under reduced pressure in order to remove the ethanol before the quenching by addition of an acidic aqueous solution: in this way an orange oil is obtained, which is fully soluble even in a small amount of ethyl acetate, instead a sticky solid that is partially soluble in the aqueous phase due to the presence of ethanol.

The crude product was a thick oil that can be purified by stirring it at 0 °C in a 9:1, v/v cyclohexane/diethyl ether mixture for 1h, providing a white powder. Some batches showed darker colorations, from beige to pale brown: the reason was the presence of unreacted chalcone, which

¹⁹⁰ J. Murtagh, D.O. Frimannsson and D.F. O'Shea, *Org. Lett.*, **2009**, *11*, 5386.

never affected the yields in the following steps, being these impurities negligible as showed by proton NMR.

The dipyrromethene ligand was obtained reacting the Michael addition product **III-25** with a 35-fold excess of ammonium acetate in ethanol at reflux for 2 days. The formation of the ligand can be easily visualized by the dramatic color change of the reaction mixture, from orange to dark blue.

The product **III-26** crystallized in shiny gold powder directly in the flask if the reaction mixture is allowed to cool slowly at room temperature over 1 day, then the product is isolated by simple filtration and washing with cold distilled water. It is noteworthy that the purity of the ligand is strongly dependent on the state of the ammonium acetate: if highly hydrated ammonium acetate is used, the product is obtained as a pasty blue solid and a remarkable quantity of ammonium acetate is included in the solid. We observed that the presence of this salt decreases significantly the yield of the complexation reaction.

The complexation reaction is performed by treating the ligand **III-26** with an excess of boron trifluoride - diethyl ether complex in presence of diisopropylethylamine in dry dichloromethane. Also in this case, we noticed that the removal of the reaction solvent before the quenching leads to an easier work-up because the product is not very soluble in dichloromethane and adding ethyl acetate without removing the halogenated solvent can compromise the phase separation during the extraction. The product **III-27** was obtained as a red metallic solid in good yields after purification by column chromatography.

The monopropargylation of the dihydroxy azadipyrromethene BF₂-chelate **III-27** was not trivial and most of the procedures found in the literature leads to low yields in our hands.

Being a key intermediate for the development of clickable NIR components, a straightforward and highly reproducible protocol for the monopropargylation step was sought. Different procedures from the literature were adapted, but that reported by O'Shea and coworkers proved most efficient,

where cesium fluoride was used as base, DMSO as solvent and *tert*-butyl bromoacetate as alkylating agent: the monoalkylated product was obtained in 75% yield.¹⁹¹

We adapted this procedure and were able to obtain the desired monopropargylated azadipyrromethene BF₂-chelate **III-28** in 85% yield. After only 30 minutes the TLC showed the full conversion of the starting material into the desired product, alongside traces of dipropargylated side-product. The dryness of both solvent and base is a key factor for the success of this reaction.

Also the purification was straightforward: the small amount of dipropargylated product was eluted first with pure DCM, then the monopropargylated product **III-28** was isolated by eluting the column with a 9:1, v/v DCM/ethyl acetate mixture (Figure 3.12).

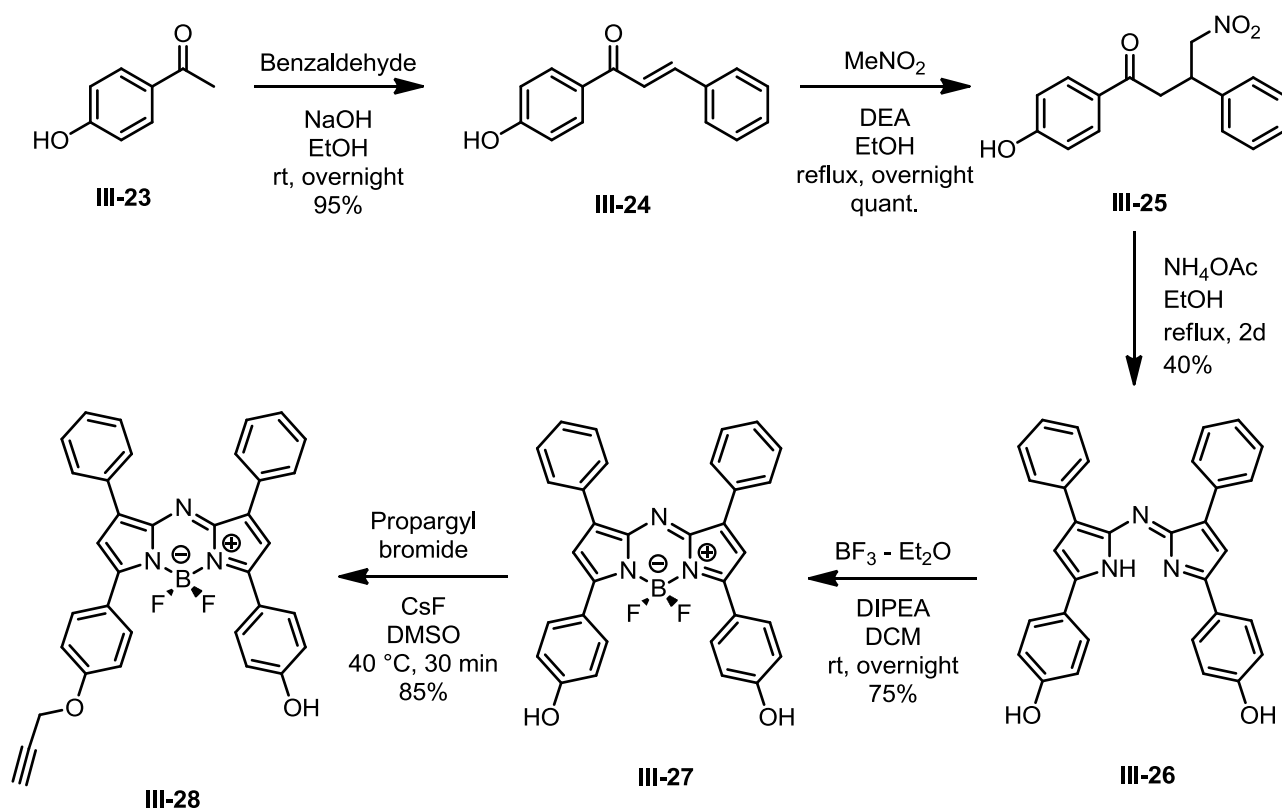


Figure 3.12 - Synthetic scheme of hydroxypropargyloxy BF₂ - azadipyrromethene **III-28**.

¹⁹¹ D. Wu, S. Cheung, R. Daly, H. Burke, E.M. Scanlan and D.F. O'Shea, *Eur. J. Org. Chem.*, **2014**, 6841.

The methoxypropargyloxy BF₂ - azadipyrromethene **III-29** was obtained in the last step by treating the hydroxypropargyloxy precursor **III-28** with a 20-fold excess of methyl iodide in presence of potassium carbonate in refluxing acetone. The product was isolated by column chromatography using pure DCM as eluent and obtained as a red metallic solid in good yield (Figure 3.13).

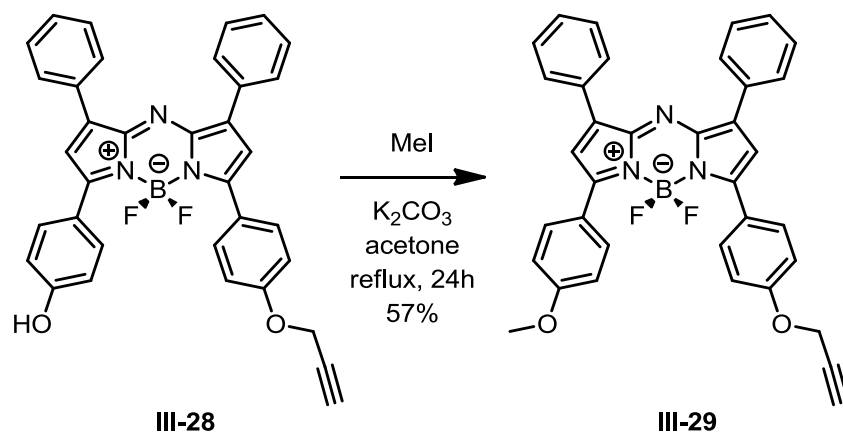


Figure 3.13 - Synthetic scheme of methoxypropargyloxy BF₂ - azadipyrromethene **III-29**.

It is noteworthy that the success of the alkylation reaction is strongly dependent on the state of the potassium carbonate: if hydrated potassium carbonate is used, the product is obtained in yield lower than 40%, even if the reaction is stirred at reflux for more than 72 hours.

Moreover the use of hydrate potassium carbonate can lead to the displacement of BF₂ center: we think that this can be explained by the formation of hydroxide anions in the reaction mixture.

3.2.2 Characterization

Methoxypropargyloxy BF₂-chelate azadipyrromethene **III-29** was characterized by ¹H- and ¹³C-NMR and mass spectrometry. The chromophore showed a very high solubility in common deuterated halogenated solvents (Figure 3.14).

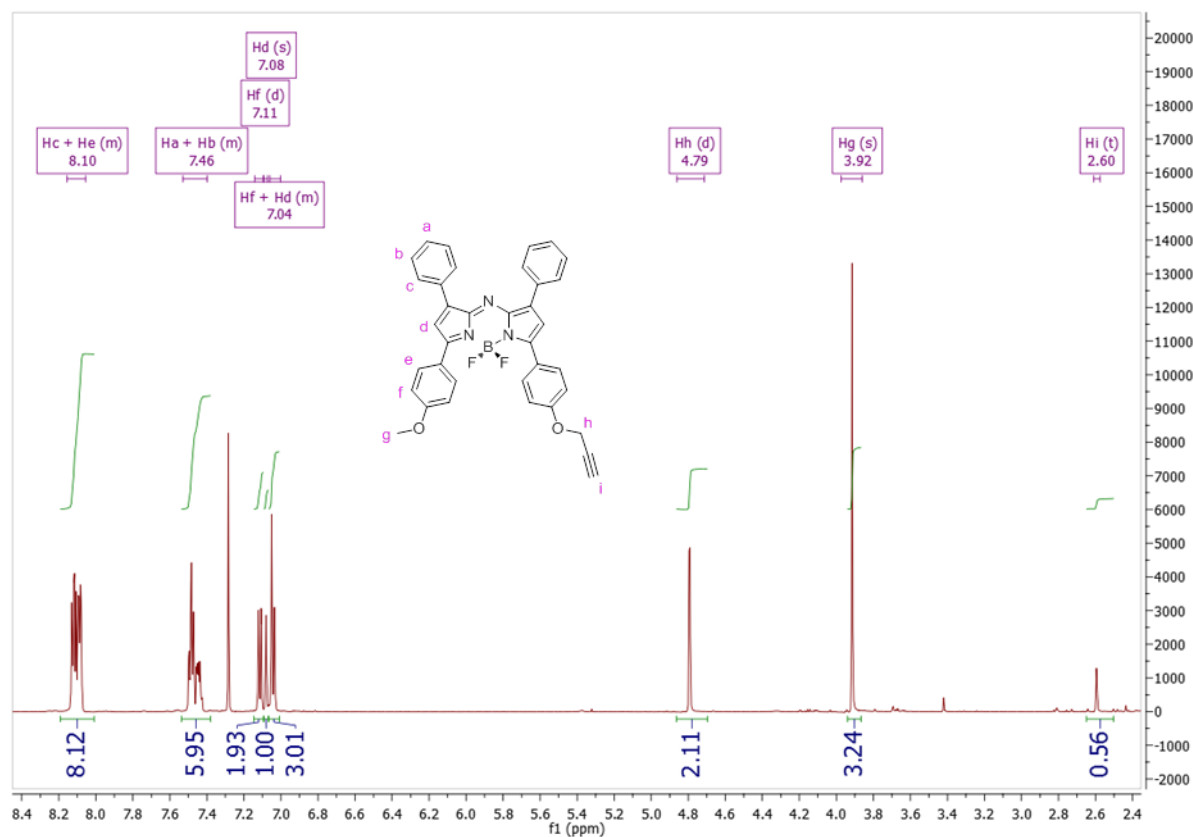


Figure 3.14 - ¹H NMR of methoxypropargyloxy BF₂ - azadipyrromethene **III-29** (600 MHz in CDCl₃).

Peaks at δ 4.79 (d, $J = 2.3$ Hz, 2H) and δ 3.92 (s, 2H), which are the methylene group of propargyl chain and methyl chain of the methoxy group, prove the unsymmetrical functionalization of the tetraaryl BF₂-azadipyrromethene core.

Peak at δ 2.60 (t, $J = 2.3$ Hz, 1H) is the terminal proton of the alkyne chain: even if the integral value is less than 1, the coupling constant and the multiplicity confirmed the fact that it belongs to the propargyl chain.

3.3 Design of *tert*Bu-carboxypropargyloxy BF₂-chelate azadipyrromethene

3.3.1 Synthesis

The *tert*-butyl-carboxypropargyloxy BF₂-azadipyrromethene **III-30** was obtained by alkylation with *tert*-butylbromoacetate of the hydroxypropargyloxy precursor **III-28** in the presence of potassium carbonate as base in refluxing acetone. The product was isolated by column chromatography using pure DCM as eluent and obtained as a red metallic solid in 70% yield (Figure 3.15).

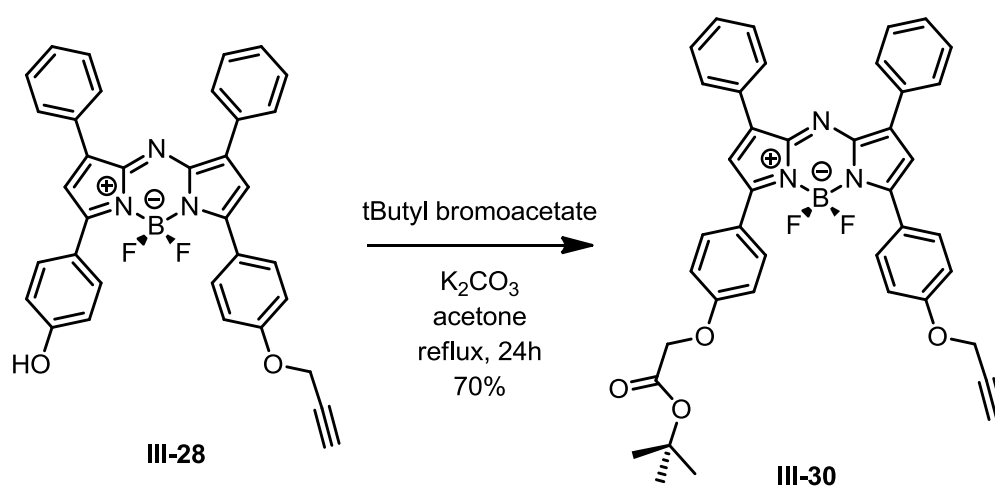


Figure 3.15 - Synthetic scheme of *tert*-butyl-carboxypropargyloxy BF₂ - azadipyrromethene **III-30**.

It is noteworthy that the success of the alkylation reaction is strongly dependent on the state of the potassium carbonate: if hydrated potassium carbonate is used, the product is obtained in yield lower than 40%, even if the reaction is stirred at reflux for more than 72 hours.

Moreover the use of hydrate potassium carbonate can lead to the displacement of BF₂ center: this may be explained by the formation of hydroxide anions in the reaction mixture.

3.3.2 Characterization

tert-Butyl-carboxypropargyloxy BF₂ - azadipyrromethene **III-30** was fully characterized by ¹H-, ¹³C-NMR and mass spectrometry. The chromophore showed a very good solubility in common deuterated halogenated solvents (Figure 3.16).

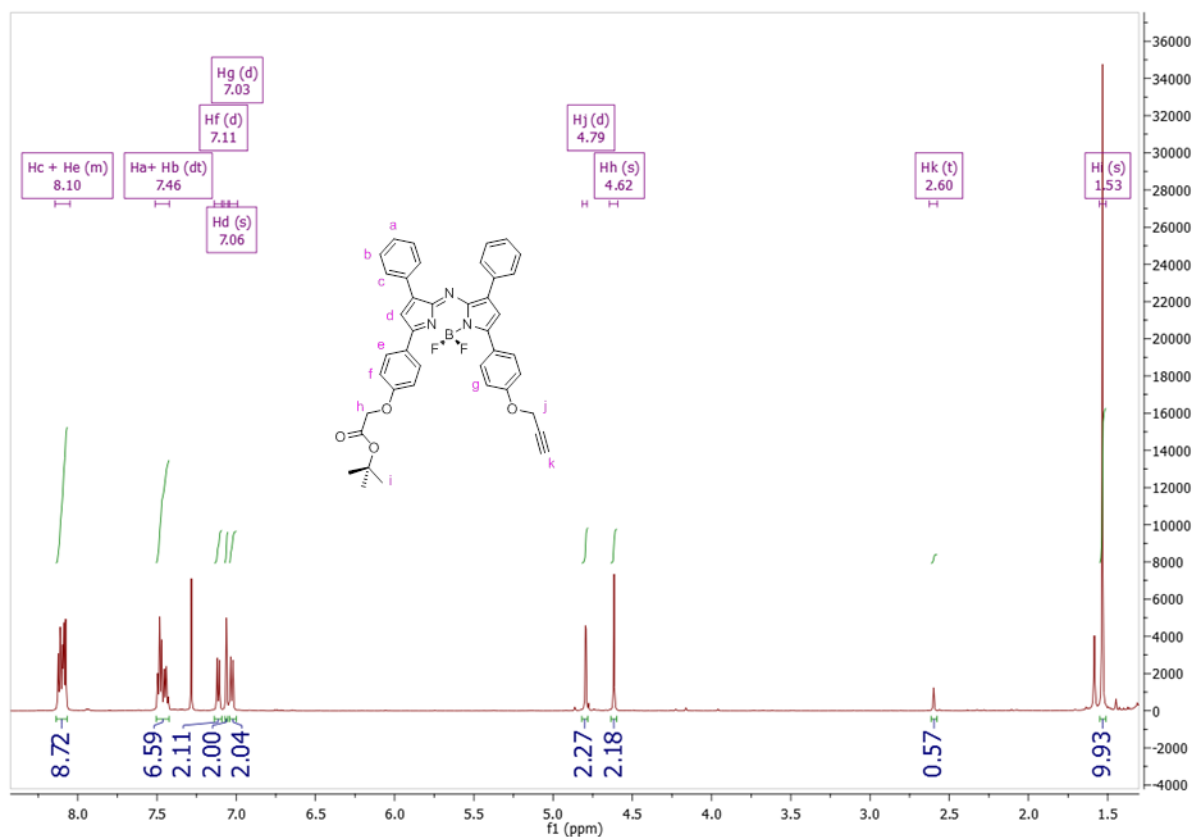


Figure 3.16 - ¹H NMR of *tert*-butyl-carboxypropargyloxy BF₂ - azadipyrromethene **III-30** (600 MHz in CDCl₃).

Peaks at δ 4.79 (d, $J = 2.3$ Hz, 2H) and δ 4.62 (s, 2H), which are the methylene groups of propargyl chain and *tert*-butylacetate chain, respectively, prove the unsymmetrical functionalization of the tetraaryl BF₂-azadipyrromethene core. Peak at δ 2.60 (t, $J = 2.3$ Hz, 1H) is the terminal proton of the alkyne chain, the integral value is less than 1 but it is consistent with the previous observation on **III-29**.

3.4 Silicon-rhodamine

3.4.1 Introduction

Silicon-rhodamines (SiR) are a novel class of fluorophores that gained huge attention recently due to their high photostability, PET-regulated far-red to NIR fluorescence, high quantum efficiency and biocompatibility. They have been applied in development of metal ion chemsensors **III-33**, optical voltage-sensitive probes for transmembrane potentials **III-31** and fluorescent probes for cancer-associated aminopeptidases **III-32** (Figure 3.17).^{192, 193, 194}

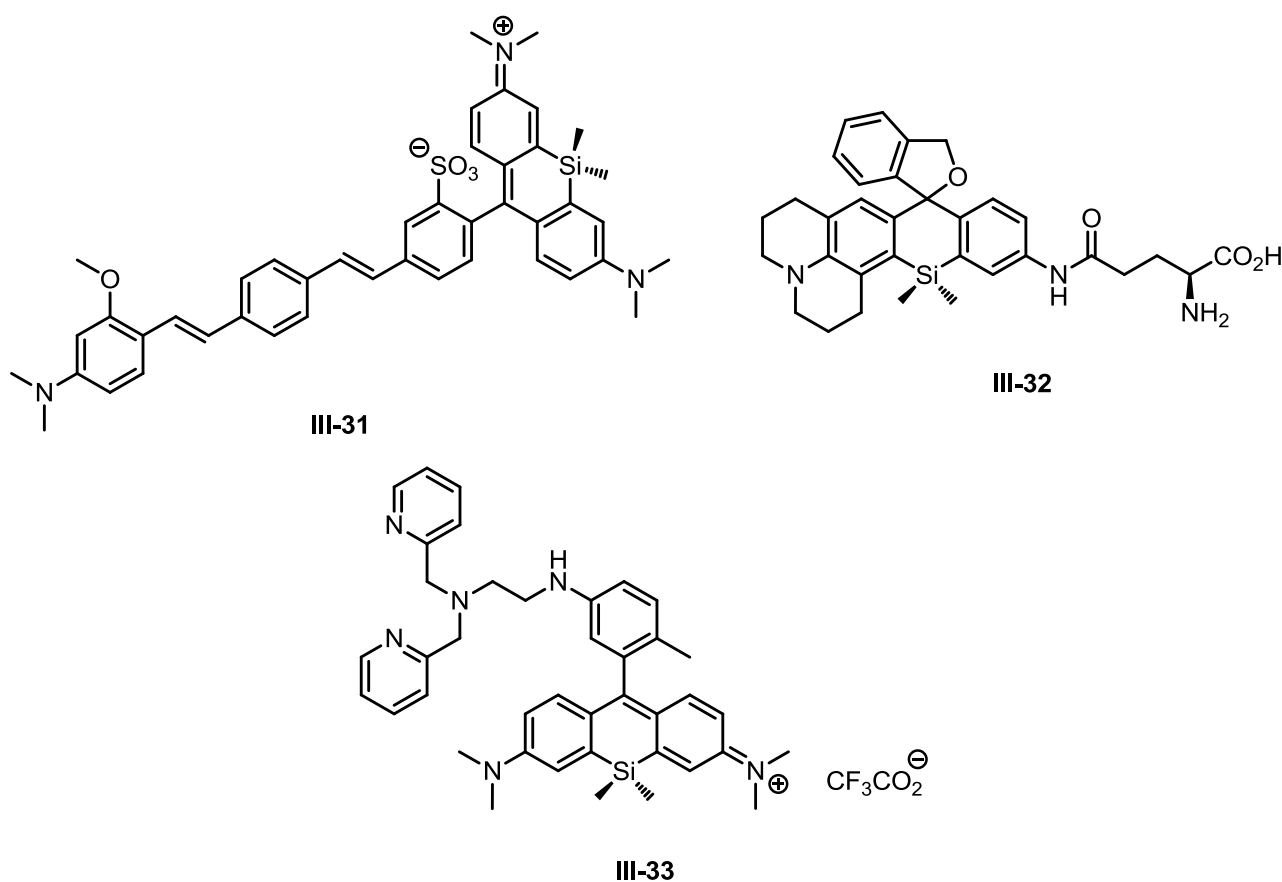


Figure 3.17 - Silicon rhodamine-based NIR fluorescent probes

An optimized and detailed procedure of the SiR we synthesized is outlined in the following section.

¹⁹² Y. Koide, Y. Urano, K. Hanaoka, T. Terai and T. Nagano, *ACS Chem. Biol.*, **2011**, *6*, 600.

¹⁹³ Y.-L. Huang, A. S. Walker and E. W. Miller, *J. Am. Chem. Soc.*, **2015**, *137*, 10767.

¹⁹⁴ R. J. Iwatate, M. Kamiya, K. Umezawa, H. Kashima, M. Nakadate, R. Kojima and Y. Urano, *Bioconjugate Chem.*, **2018**, *29*, 241.

3.4.2 Synthesis

The carboxyl-methyl silicon rhodamine **III-34** was first synthesized by Johnsson's group in 2013 (Figure 3.18).¹⁹⁵

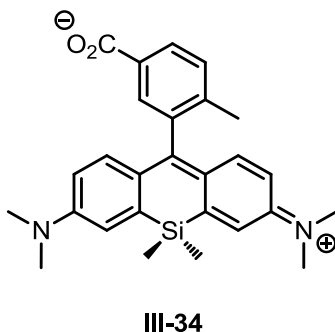


Figure 3.18 - Molecular structure of carboxyl-methyl silicon rhodamine **III-34**.

The published procedure proved practically not straightforward in our hands, especially in the reported purification steps, so we adapted some reactions from a paper of Klan,¹⁹⁶ and the detailed convergent procedure we used to synthesize the carboxyl-methyl silicon rhodamine is described below.

Commercially available 3-bromo-N,N-dimethylaniline **III-35** was first reacted under Friedel-Crafts conditions using a 5-fold excess of 37% formaldehyde aqueous solution in acetic acid for 1 hour at 90 °C. The crude product was isolated upon quenching with saturated sodium bicarbonate solution and purified by column chromatography using a 19:1, v/v n-hexane/ethyl acetate mixture in order to remove the by-products then the polarity was increased (9:1 v/v n-hexane/ethyl acetate) in order to recover the desired product **III-36**, which was obtained as a pale pink crystalline powder in 88% yield.

The 4,4'-methylenebis(3-bromo-N,N-dimethylaniline) **III-36** was then treated with 2.6 equivalent of *sec*-BuLi at -80 °C in tetrahydrofuran in strictly anhydrous conditions. The reaction mixture was

¹⁹⁵ G. Lukinavicius, K. Umezawa, N. Olivier, A. Honigmann, G. Yang, T. Plass, V. Mueller, L. Reymond, I. R. Correa Jr, Z.-G. Luo, C. Schultz, E. A. Lemke, P. Heppenstall, C. Eggeling, S. Manley and K. Johnsson, *Nat. Chem.*, **2013**, *5*, 132.

¹⁹⁶ T. Pastierik, P. Šebej, J. Medalová, P. Štacko and P. Klán, *J. Org. Chem.*, **2014**, *79*, 3374.

left stirring for 15 minutes at the same temperature to assure the complete conversion of the starting material in the dilithiated analogue. Dichlorodimethylsilane was then added to the organolithium reagent and the reaction mixture was stirred overnight, allowing it to warm at room temperature.

We note in passing that shorter reaction time for the formation of the organolithium reagent and longer reaction time for the formation of two Si-C bonds increase dramatically the overall yield, from traces to 50% over two steps.

After 12 hours, no starting material is present on the TLC and an intense red spot can be detected at $\lambda = 365$ nm. The reaction was quenched upon addition of dilute hydrochloric acid solution and the deep blue oil obtained has to be used immediately in the next step without further purification, due to its extreme sensitivity to oxygen.

The crude 2,7-bis(dimethylamino)-9,10-dihydro-9,9-dimethyl-9-silaanthracene **III-37** was dissolved in degassed acetone and converted into the corresponding air-stable ketone by oxidation with an excess of potassium permanganate. Purification by column chromatography on silica using 3:1, v/v petroleum ether/ethyl acetate, followed by reprecipitation in n-hexane afforded the pure 2,7-bis(dimethylamino)-9,9-dimethyl-9-silaanthracen-10(9H)-one **III-38** as a yellow crystalline powder (Figure 3.19).

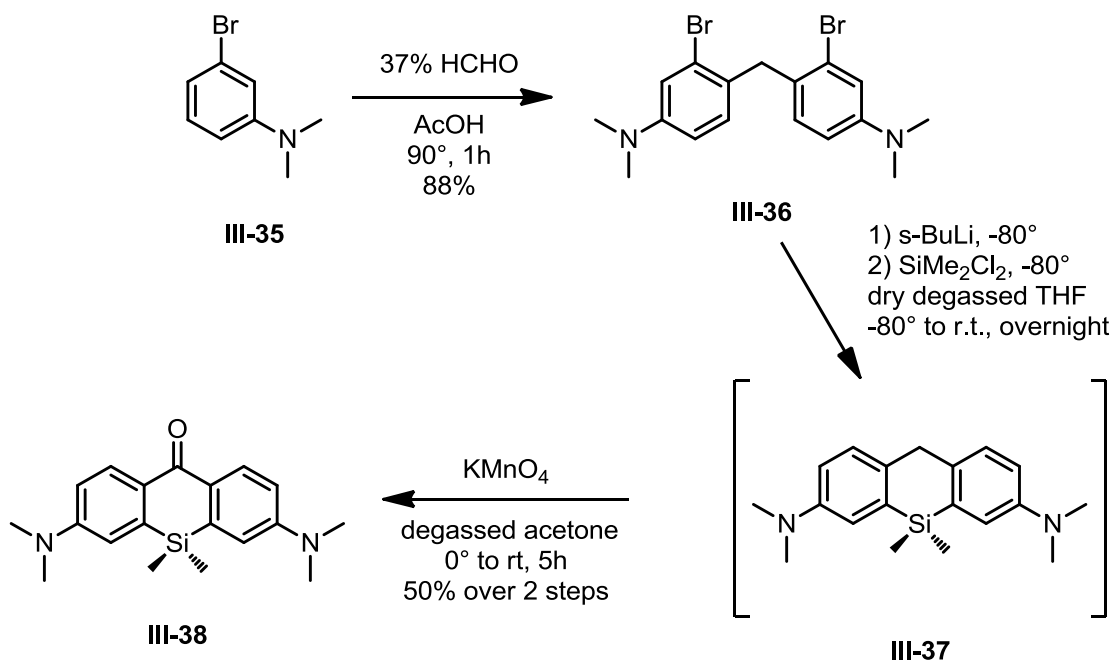


Figure 3.19 - Synthetic scheme of 2,7-bis(dimethylamino)-9,9-dimethyl-9-silaanthracen-10(9H)-one **III-38**.

The upper ring of the silicon rhodamine was synthesized in one step by Boc-protection of commercially available 3-bromo-4-methylbenzoic acid **III-39**. The product **III-40** was obtained as a colorless oil in nearly quantitative yield. (Figure 3.20)

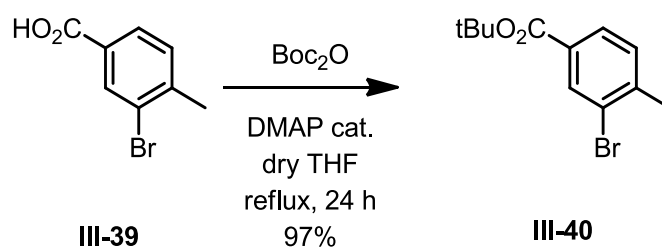


Figure 3.20 - Synthetic scheme of *tert*-butyl 3-bromo-4-methylbenzoate **III-40**.

The final step was the coupling between the two aromatic parts of the molecule: the protected brominated benzoic acid **III-40** was converted in the corresponding organolithium reagent, treating it with 2 equivalent of *tert*-BuLi and letting it stir for 15 minutes at -80 °C; a solution of silylanthracenone **III-38** in dry degassed tetrahydrofuran was then slowly added and the mixture was stirred and allowed to warm at room temperature. The complete conversion of the ketone **III-38** was observed by TLC after 12 hours. The crude intermediate **III-41** was then dissolved in acetonitrile and treated with 6M hydrochloric acid solution. The carboxyl-methyl silicon rhodamine **III-34** was purified by column chromatography and obtained as shiny dark blue powder in good overall yield (Figure 3.21).

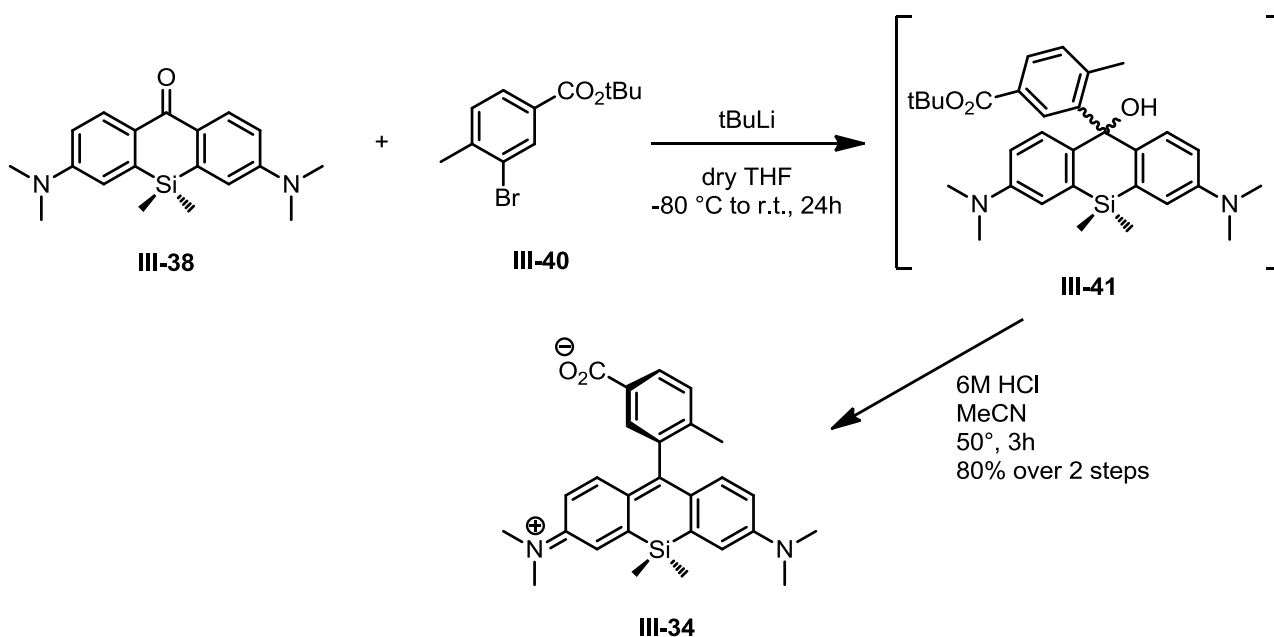
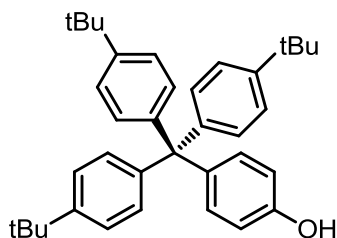


Figure 3.21 - Final steps of carboxyl-methyl silicon rhodamine **III-34** synthesis.

3.5 Alkyne- and azide-stoppers

3.5.1 Introduction

The 4-(tris(4-(tert-butyl)phenyl)methyl)phenol **III-42** is an extremely hindered *p*-substituted phenol and is a popular “stopper” (or blocking group) used in the construction of interlocked molecules (Figure 3.22).



III-42

Figure 3.22 - Molecular structure of 4-(tris(4-(tert-butyl)phenyl)methyl)phenol **III-42**.

Its synthesis was first reported by Stoddart and coworkers in 1992, then in 1993, due to the rising interest in the mechanically interlocked molecules, Bheda and coworkers published a detailed and improved synthesis of a series of triarylmethyl derivatives.^{197, 198}

From these structures, a huge number of derivatives have been synthesized in the last three decades making this structural motif ubiquitous in the field of molecular machines.^{199, 200, 201}

Following the literature procedures, the synthesis proceeded readily and the bulky phenol was synthesized in multigram-scale, high purity intermediate and high yielding reaction steps.

¹⁹⁷ P.R. Ashton, D. Philp, N. Spencer and J.F. Stoddart, *J. Chem. Soc., Chem. Commun.*, **1992**, 0, 1124.

¹⁹⁸ H. W. Gibson, S. H. Lee, P.T. Engen, P. Lecavallier, J. Sze, Y.X. Shen and M. Bheda, *J. Org. Chem.*, **1993**, 58, 3748.

¹⁹⁹ P.R. Ashton, R. Ballardini, V. Balzani, M. Bělohradský, M. T. Gandolfi, D. Philp, L. Prodi, F. M. Raymo, M. V. Reddington, N. Spencer, J. F. Stoddart, M. Venturi, and D.J. Williams *J. Am. Chem. Soc.*, **1996**, 118, 4931.

²⁰⁰ B. Lewandowski, G. De Bo, J. W. Wardl, M. Pappmeyer, S. Kuschel, M. J. Aldegunde, P. M. E. Gramlich, D. Heckmann, S.M. Goldup, D.M. D'Souza, A. E. Fernandes and D. A. Leigh, *Science*, **2013**, 339, 189.

²⁰¹ L.D. Movsisyan, M. Franz, F. Hampel, A.L. Thompson, R.R. Tykwinski and H.L. Anderson, *J. Am. Chem. Soc.*, **2016**, 138, 1366.

3.5.2 Synthesis

Commercially available 4-tert-butylbromobenzene **III-43** was first converted into the corresponding Grignard reagent, treating it with freshly cut magnesium in presence of a catalytic amount of crystalline iodine in dry tetrahydrofuran under gentle heating. The color change of the reaction mixture (from deep purple to colorless) indicates the formation of the organomagnesium reagent. The mixture is stirred for a further 1 hour, then diethyl carbonate was added and the reaction stirred overnight at reflux. The reaction is then quenched upon addition of a saturated solution of ammonium chloride in the way to hydrolyze the magnesium salt and removing the excess of metallic magnesium. According to the literature, the purification of crude tris(4-(tert-butyl)phenyl)methanol **III-44** can be performed in a different way but, in the present work, the recrystallization in n-hexane gave the best result in terms of yield and purity.

The desired bulky phenol can be prepared in two different way, by a one step reaction in which the bulky carbinol is reacted directly with an excess of phenol in presence of a catalytic amount of hydrochloric acid at elevated temperature in solvent-free conditions or by a two step reaction which consists first in the conversion of the hindered methanol in the corresponding chloride and then the condensation of the chloride with an equimolar quantity of phenol at elevated temperature in solvent-free conditions.

We note in passing that simple boiling in n-hexane of the crude bulky phenol is sufficient to obtain the desired product in high purity when freshly recrystallized phenol is used, while column chromatography is necessary when commercial phenol is used, moreover the second way, which involves the chloride intermediate, gives higher purity products, due to the possibility to recrystallize and isolate the chloride, that can be stored at room temperature for weeks, without any loss of purity and/or reactivity.

Treatment of tris(4-(tert-butyl)phenyl)methanol **III-44** with an excess of acetyl chloride in refluxing dry toluene (benzene was used in the original procedure but less toxic toluene can be used as

alternative solvent without any loss of yield). The 4-(tris(4-(tert-butyl)phenyl)methyl)chloride **III-45** was crystallized directly from the reaction mixture upon addition of an excess of n-hexane, a drop of thionyl chloride and cooling at 0 °C overnight.

The final step was a Friedel-Crafts alkylation of phenol with the hindered chloride, performed at elevated temperature in solvent-free conditions without addition of Lewis acids.

The immediate color change of the reaction mixture (from colorless to blood red) indicates the formation of the carbocation. The reaction was then quenched upon cooling and addition of toluene and 2M sodium hydroxide solution. The 4-(tris(4-(tert-butyl)phenyl)methyl)phenol **III-42** was finally obtained as a fine off-white powder by boiling its crude in n-hexane for 30 minutes (Figure 3.23).

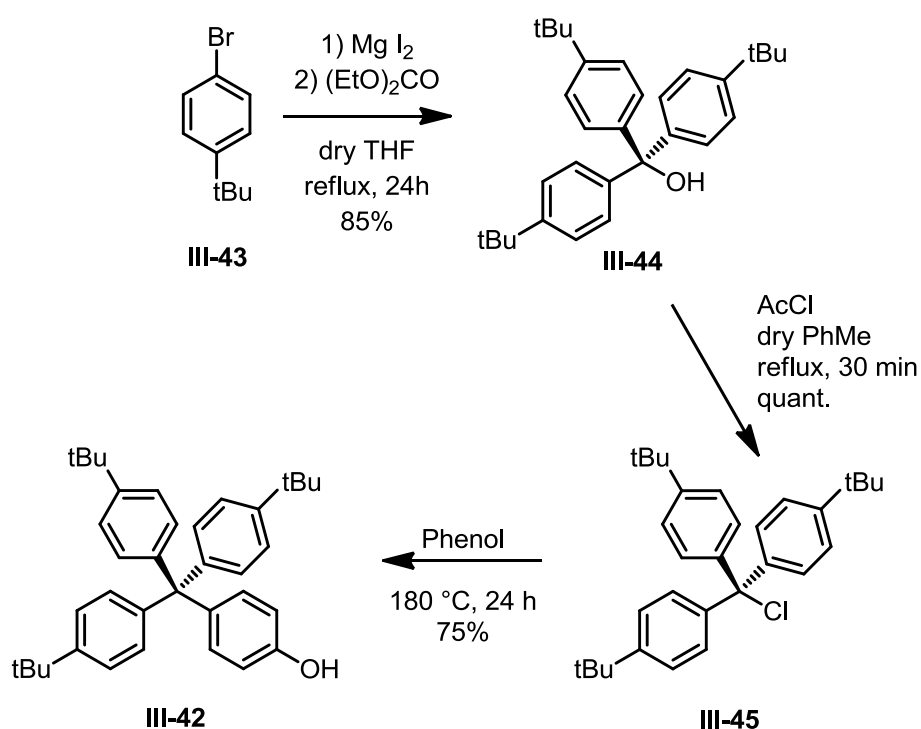


Figure 3.23 - Synthetic scheme of 4-(tris(4-(tert-butyl)phenyl)methyl)phenol **III-42**.

Depending on the specific application, the free OH of the bulky phenol can now be functionalized with a wide range of reacting groups under Williamson etherification conditions as outlined in the following sections.

The azide trityl stopper **III-50** was obtained by treatment of the bulky phenol with 3-azido-1-iodopropane **III-49** in presence of potassium carbonate in refluxing acetone. The azide-containing alkylating agent was synthesized in 3 steps (nucleophilic substitution, tosylation and Finkelstein reaction) in high overall yield. (Figure 3.24)

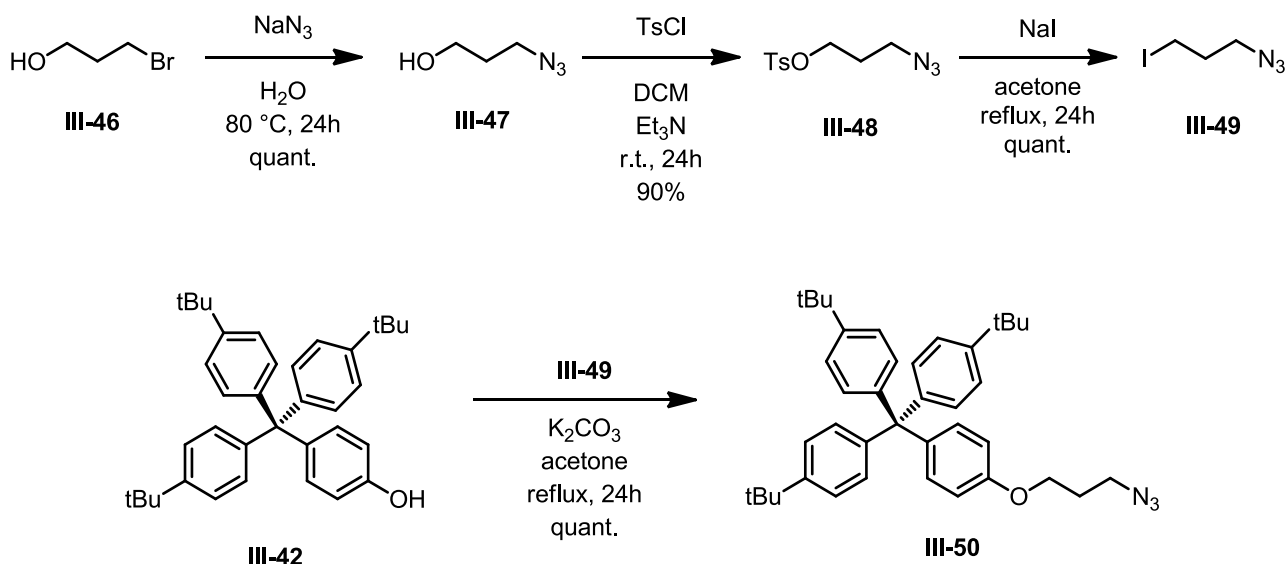


Figure 3.24 - Synthetic schemes of azide-containing alkylating agent **III-49** and azide trityl stopper **III-50**.

The alkyne trityl stopper **II-14** was obtained by treatment of the bulky phenol with propargyl bromide in presence of potassium carbonate in refluxing acetone. The alkyne stopper was isolated by column chromatography and obtained in 90% yield (Figure 3.25).

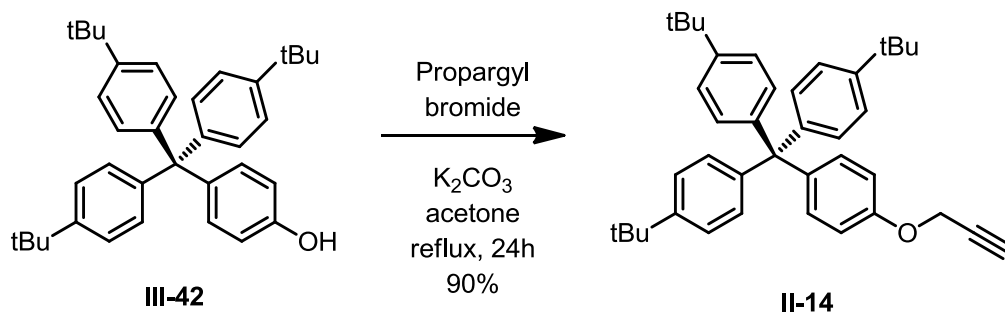


Figure 3.25 - Synthetic scheme of alkyne trityl stopper **II-14**.

Translational motion of the ring along the thread is an important feature in rotaxane-based architectures. The gliding rate of the macrocycle between two station on the thread or between the two stoppers is influenced by different factors, depending on the nature of the intermolecular force which is present on the mechanically interlocked molecule. In the case of hydrogen bonding-based supramolecular systems, the presence of water influenced dramatically the motion of the ring along the thread.²⁰² Pyridine units and triazole moieties are ubiquitous in mechanically interlocked architectures and, in 2011, Goldup and coworkers proved the presence of a hydrogen bonding interaction between these units.²⁰³

In order to study the gliding of the ring along the thread and understand the role of the pyridine - triazole hydrogen bonding interaction in the translation motion, a ²D-labeled terminal alkyne trityl stopper **III-51** was synthesized.

²⁰² M.R. Panman, B.H. Bakker, D. den Uyl, E.R. Kay ER, D.A. Leigh, W.J. Buma, A.M. Brouwer, J.A. Geenevasen and S. Woutersen, *Nat. Chem.*, **2013**, 5, 929.

²⁰³ H. Lahlali, K. Jobe, M. Watkinson and S.M. Goldup, *Angew. Chem., Int. Ed.*, **2011**, 50, 4151.

The propargylic proton of the alkyne stopper was removed by sodium hydride in dry tetrahydrofuran, the reaction mixture was stirred for 1 hour then deuterated methanol was added. The product **III-51** was obtained in quantitative yield (Figure 3.26).

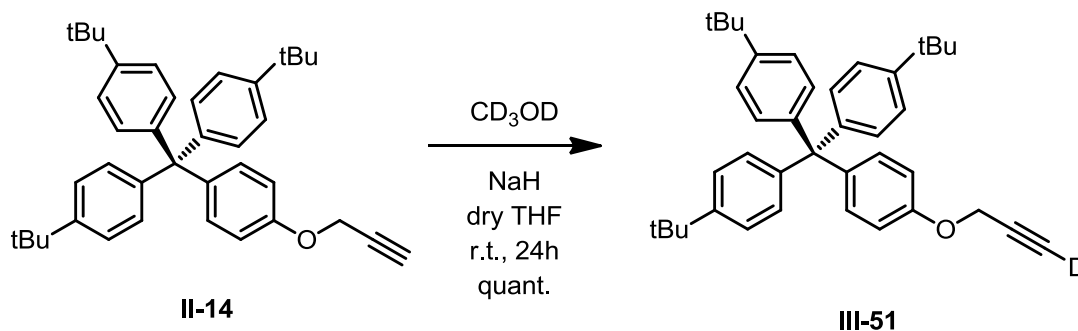


Figure 3.26 - Synthetic scheme of deuterated alkyne trityl stopper **III-51**.

The formation of C-D bond was proven by ¹H NMR and HRMS. The replacement of the propargylic proton with a deuterium atom dramatically changes the nature of the alkyne chain: the CH signal disappears and the CH₂ signal changes from a doublet to a singlet (Figure 3.27).

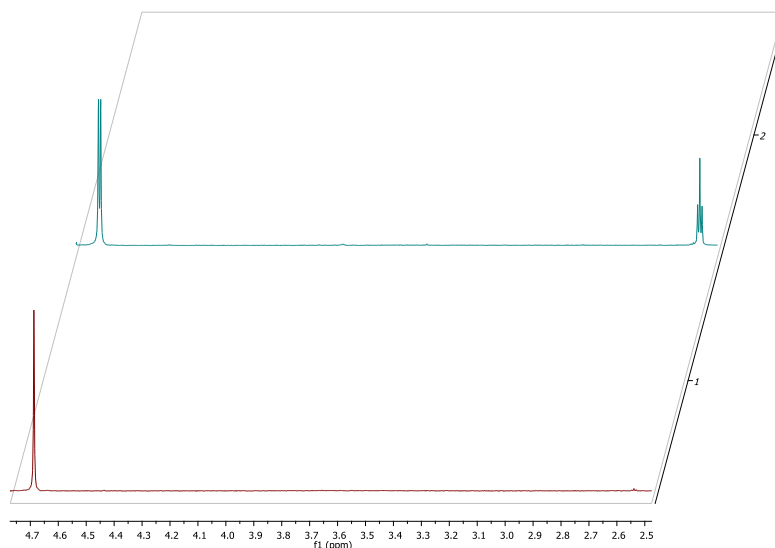


Figure 3.27 - ¹H NMR of alkyne stopper **II-14** (top) compared to deuterated alkyne stopper **III-51** (bottom) (300 MHz in CDCl₃).

3.6 Design of barbiturate-containing BF₂-chelate azadipyrromethene thread

3.6.1 Synthesis

A barbiturate-containing BF₂-chelate azadipyrromethene thread **III-52** has been designed and synthesized in order to test the possibility to build functional mechanically interlocked molecules via a slipping approach (Figure 3.28).

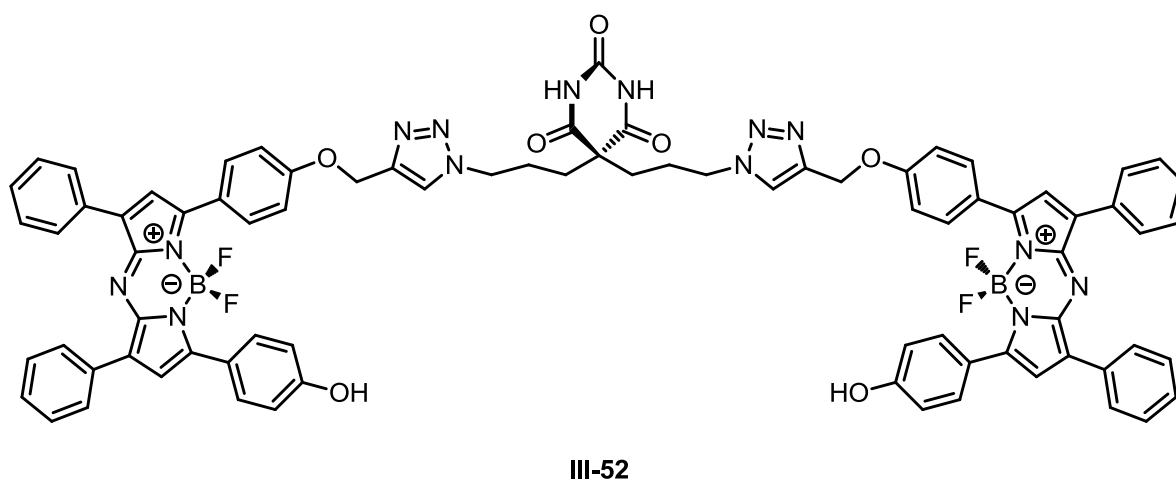


Figure 3.28 - Molecular structure of barbiturate-containing BF₂-chelate azadipyrromethene thread **III-52**.

The thread **III-52** comprises a barbiturate motif, which is complementary to the hydrogen bond pattern present in the triarylamine-containing Hamilton-type macrocycle **II-50**, and BF₂-chelate azadipyrromethene moieties.

The starting point of the synthesis is the barbiturate bearing short azide-terminated arms **II-12**, which was synthesized following the procedure previously reported in literature (Figure 3.34).²⁰⁴

Commercially available diethyl malonate **III-53** was first reacted with 3 equivalents of sodium hydride in dry tetrahydrofuran. Azidopropane **III-49** was then added and the reaction was stirred at reflux overnight. The crude product was isolated upon quenching with saturated ammonium

²⁰⁴ A. Tron, P.J. Thornton, M. Rocher, H.-P. Jacquot de Rouville, J.-P. Desvergne, B. Kauffmann, T. Buffeteau, D. Cavagnat, J.H.R. Tucker and N.D. McClenaghan, *Org. Lett.*, **2014**, *16*, 1358.

chloride solution and purified by column chromatography using a 4:1 petroleum ether/ethyl acetate, v/v mixture in order to recover the desired product **III-54**, which was obtained as a colorless oil in 85% yield.

The diethyl 5,5-dialkylated malonate **III-54** was then reacted with 5 equivalent of urea and 10 equivalent of sodium hydride in dry dimethyl sulfoxide. The reaction mixture was stirred at room temperature for 5 hours before cooling and quenching by slow addition of saturated ammonium chloride solution. Purification by column chromatography using 1:1, v/v petroleum ether/ethyl acetate, followed by reprecipitation in n-hexane afforded the pure azide-bearing barbiturate **II-12** as white crystalline powder in 50% yield (Figure 3.29).

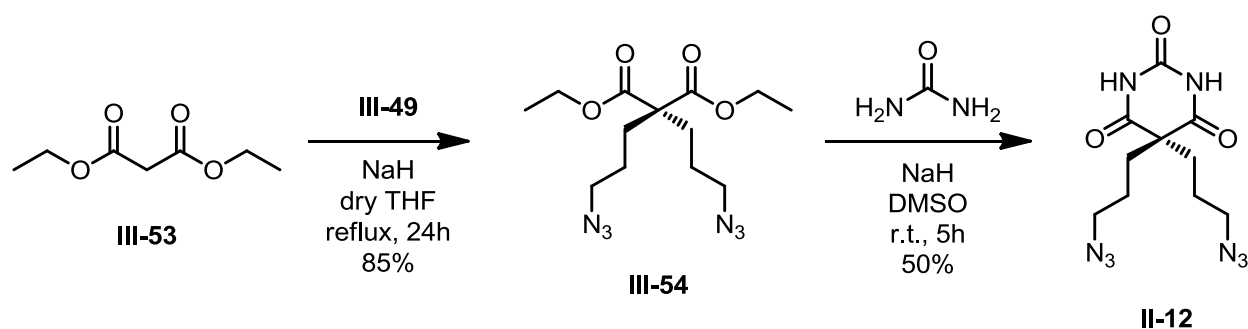


Figure 3.29 - Synthetic scheme of azide-bearing barbiturate **II-12**.

The barbiturate-containing BF₂-chelate azadipyrromethene thread **III-52** was obtained in the last step by a copper(I)-catalyzed alkyne-azide cycloaddition. Due to the high sensitivity to the oxygen, tetrakis(acetonitrile)copper(I) hexafluorophosphate was freshly prepared in high yield, following a previously reported procedure in literature.²⁰⁵

Barbiturate **II-12** and monopropargylated azadipyrromethene BF₂-chelate **III-28** were dissolved in a dry degassed 1:1, v/v, chloroform/methanol mixture and stirred at room temperature for 1 hour. Tetrakis(acetonitrile)copper(I) hexafluorophosphate was then added and the reaction mixture was stirred at 50 °C for 1 week. The crude was isolated upon addition of 1M aqueous potassium cyanide

²⁰⁵ G.J. Kubas, *Inorganic Syntheses*, **1979**, 19, 90.

solution and extraction with ethyl acetate. The barbiturate-containing BF_2 -chelate azadipyrromethene thread **III-52** was purified by column chromatography and obtained as dark green solid in 60% yield (Figure 3.30).

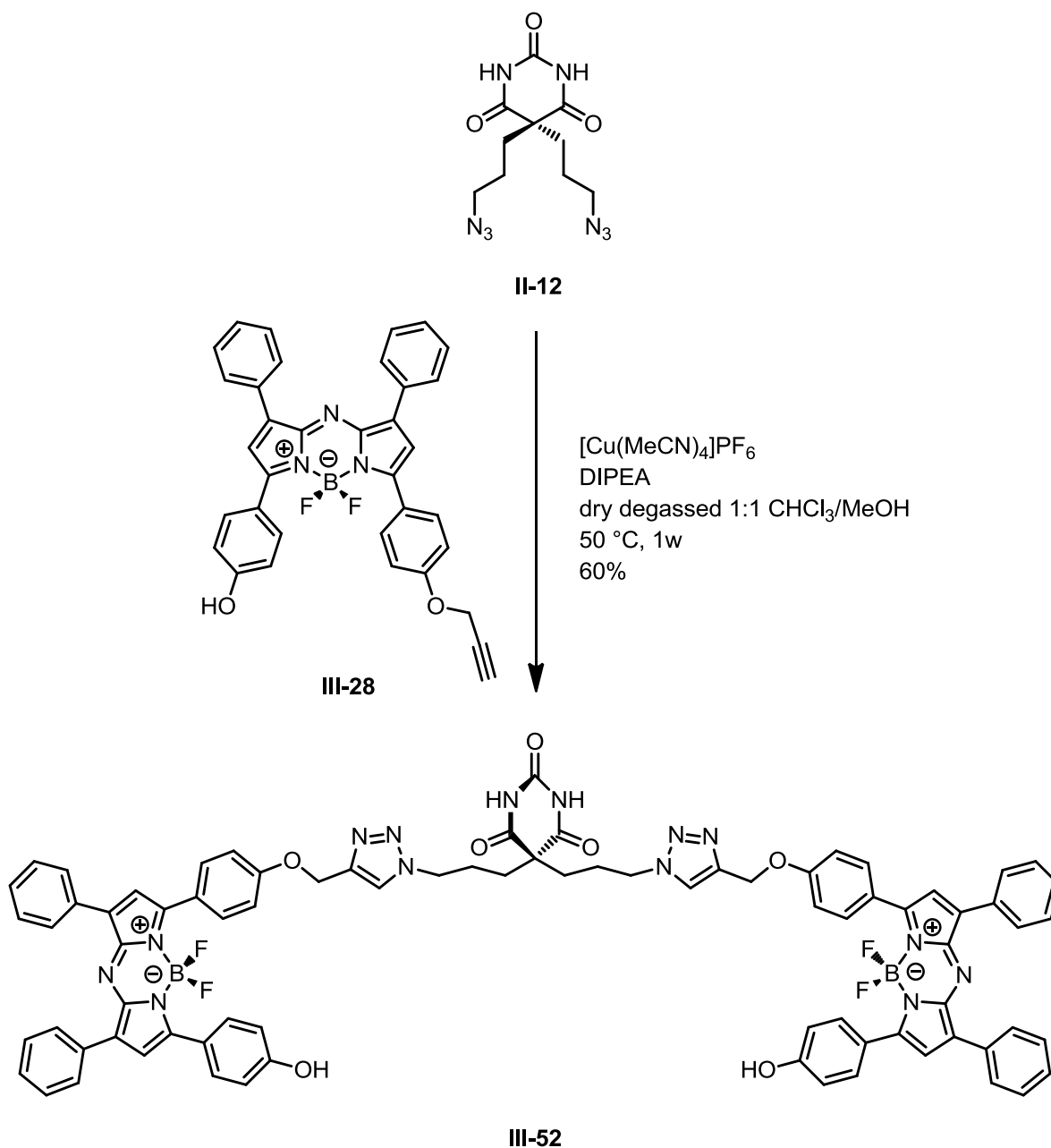


Figure 3.30 - Synthetic scheme of barbiturate-containing BF_2 -chelate azadipyrromethene thread **III-52**.

3.6.2 Characterization

The barbiturate-containing BF₂-chelate azadipyrromethene thread **III-52** was by ¹H-NMR.

High quality spectra for **III-52** cannot be obtained, due to the low solubility in every common deuterated solvents (chloroform-d, DMSO-d₆, acetone-d₆, THF-d₈, DMF-d₇, toluene-d₈, benzene-d₆ and acetonitrile-d₃).

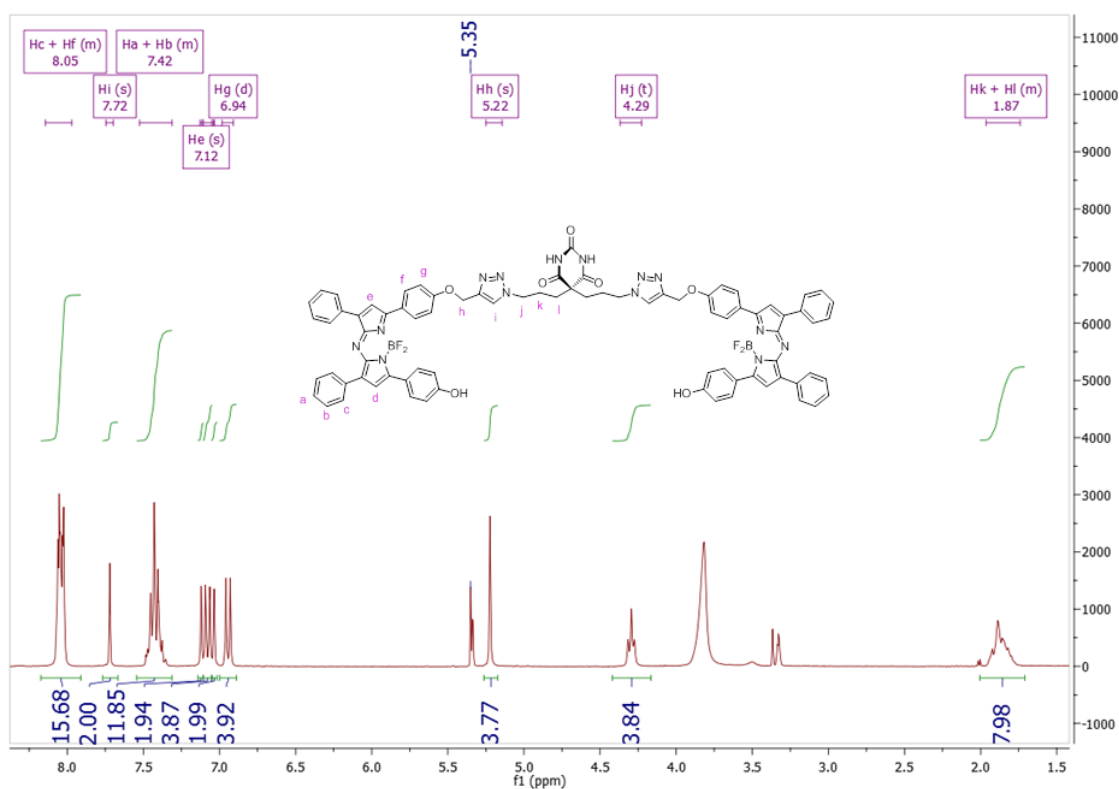


Figure 3.33 - ¹H NMR of barbiturate-containing BF₂-chelate azadipyrromethene thread **III-52** (300 MHz in dichloromethane-d₂ + 0.5% of methanol-d₄).

Using deuterated dichloromethane and adding few drops of deuterated methanol, a good ¹H NMR spectrum was obtained (Figure 3.33).

Triazole peaks at δ 7.74 (s, 2H), alongside barbiturate alkyl chain peaks at δ 4.31 (t, J = 6.3 Hz, 4H) and δ 1.89 (m, 8H), proved the formation of thread **III-52**.

3.7 Conclusion and perspectives

Two unsymmetrical BF₂-chelate azadipyrromethenes **III-29** and **III-30** have been successfully synthesized and fully characterized, moreover improved synthetic procedures have been achieved for the classical stoppers, for the Si-Rhodamine and for the monoalkylation of the di-hydroxy azadipyrromethene BF₂-chelate.

It is noteworthy the key role of cesium fluoride as base in the monoalkylation step, although high purity of this reagent is required in order to obtain very high yields.

Improved procedures have been described for the silicon-rhodamine **III-34** and for the trityl stoppers **III-50** and **II-14**, leading to higher yields and higher purity molecules.

For the silicon-rhodamine longer reaction times were required, especially for the synthesis of the substituted benzophenone: the bulkiness of the substrate for the one-pot formation of two Si-C bonds and the low solubility of potassium permanganate in acetone are the probable reasons of the slowness of these reactions.

A deuterated version of the classical alkyne stopper **III-51** was synthesized in excellent yield and fully characterized by ¹H NMR, ¹³C NMR and HRMS. This stopper is a promising tool that will be involved in the construction of ²D-labeled molecular machines and in detailed dynamic NMR studies to better understand the hydrogen bonding interaction between the proton present on the triazole, which is a recurrent motif in mechanically interlocked molecules, and the pyridine moieties present on the cyclic Hamilton receptors.

A barbiturate-containing BF₂-chelate azadipyrromethene thread **III-52** has been also synthesized and partially characterized. This thread comprises both a barbiturate motif, which is complementary to the Hamilton receptor present on the tryarylamine-bearing macrocycle **II-50**, and two BF₂-chelate azadipyrromethenes that act like stoppers and give optic properties to the structure.

This photoactive structure is a building block that will be involved in the construction of functional mechanically interlocked molecules via a slipping approach.

4. Assembly of functional [2]rotaxanes

4.1 Introduction

Synthetic methodologies for the preparation of interlocked molecules, and in particular rotaxanes, has been fully developed in recent years. This provides a toolbox of methods that chemists can use to build a wide range of structures with tailored properties. In particular, [n]rotaxanes can be assembled adopting 4 main strategies, as mentioned in the Introduction (Figure 4.1).

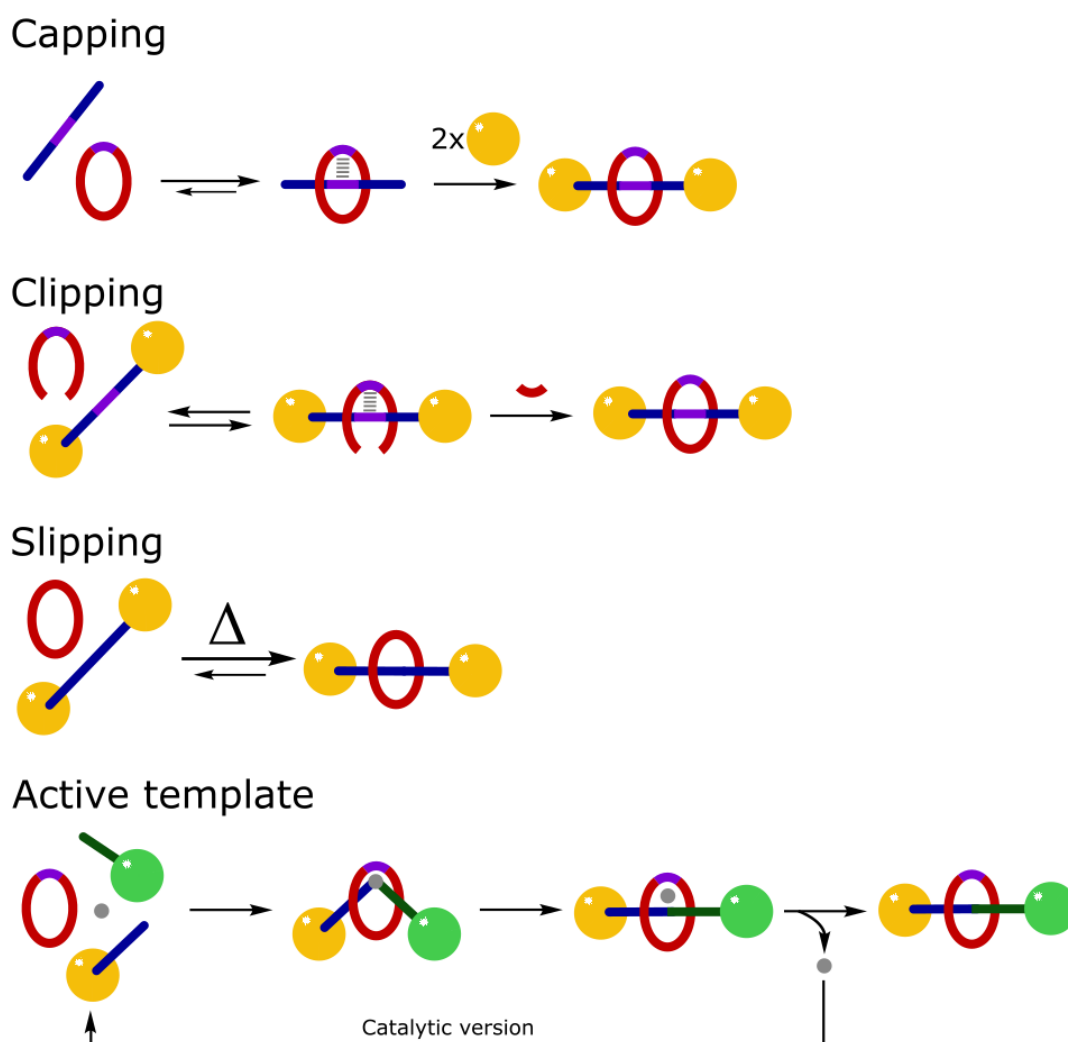


Figure 4.1 -Schematic representation of [n]rotaxane synthetic approaches.

4.1.1 Capping approach

The capping, or threading-followed-by-stoppering, method is based upon a thermodynamically driven template effect between macrocycle and unstoppered thread. Upon formation of covalent bonds with bulky stoppering units, the supramolecular complex is converted in the corresponding mechanically interlocked molecule: the rotaxane.²⁰⁶

Secondary alkyl-ammonium ions and dibenzo-24-crown-8-ether are among the most applied structural motifs for the construction of pseudorotaxanes (Figure 4.2).²⁰⁷

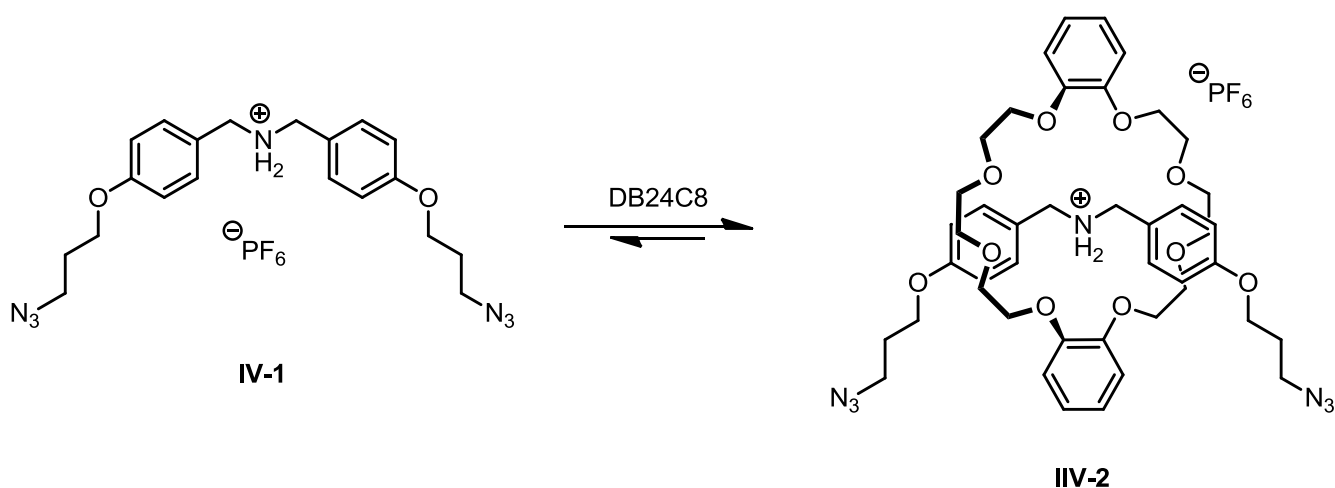


Figure 4.2 - Formation of secondary alkylammonium **IV-1**:crown ether pseudorotaxane.

Different types of covalent bond forming reactions have been exploited for the capture of pseudorotaxanes as rotaxanes.²⁰⁸

²⁰⁶ M. Gómez-López, J.A. Preece and J.F. Stoddart, *Nanotechnology*, **1996**, 7, 18.

²⁰⁷ A. Tron, H.-P. Jacquot, A. Ducrot, J.H.R. Tucker, M. Baroncini, A. Credi and N.D. McClenaghan, *Chem. Commun.*, **2015**, 51, 2810

²⁰⁸ a) N. Watanabe, T. Yagi, N. Kihara and T. Takata, *Chem. Comm.*, **2002**, 22, 2720.

b) K. Nakazono, S. Kuwata and T. Takata, *Tetrahedron Lett.*, **2008**, 49, 2397.

c) Y. Tachibana, N. Kihara, Y. Furusho and T. Takata, *Org. Lett.*, **2004**, 6, 4507.

d) Y. Tachibana, H. Kawasaki, N. Kihara, T. Takata, *J. Org. Chem.*, **2006**, 71, 5093.

e) C.J. Zhang, S. J. Li, J. Q. Zhang, K. L. Zhu, N. Li and F.H. Huang, *Org. Lett.*, **2007**, 9, 5553.

f) S.J. Rowan, S.J. Cantrill, J.F. Stoddart, A.J.P. White and D. J. Williams, *Org. Lett.*, **2000**, 2, 759.

g) A.M. Elizarov, S.H. Chiu, P.T. Glink and J.F. Stoddart, *Org. Lett.*, **2002**, 4, 679.

h) S.J. Rowan, S.J. Cantrill and J.F. Stoddart, *Org. Lett.*, **1999**, 1, 129.

In 2012, Stoddart and coworkers synthesized a naphthalene diimide [2]rotaxane **IV-3**, exploiting the self-assembly of the electron-rich dinaphtho-38-crown-10-ether (DN38C10) **IV-4** with the electron-deficient dipropargylnaphthalenediimide **IV-5**. The so formed pseudorotaxane were converted in the corresponding rotaxanes upon addition of azide-bearing stoppers **IV-6** (Figure 4.3).

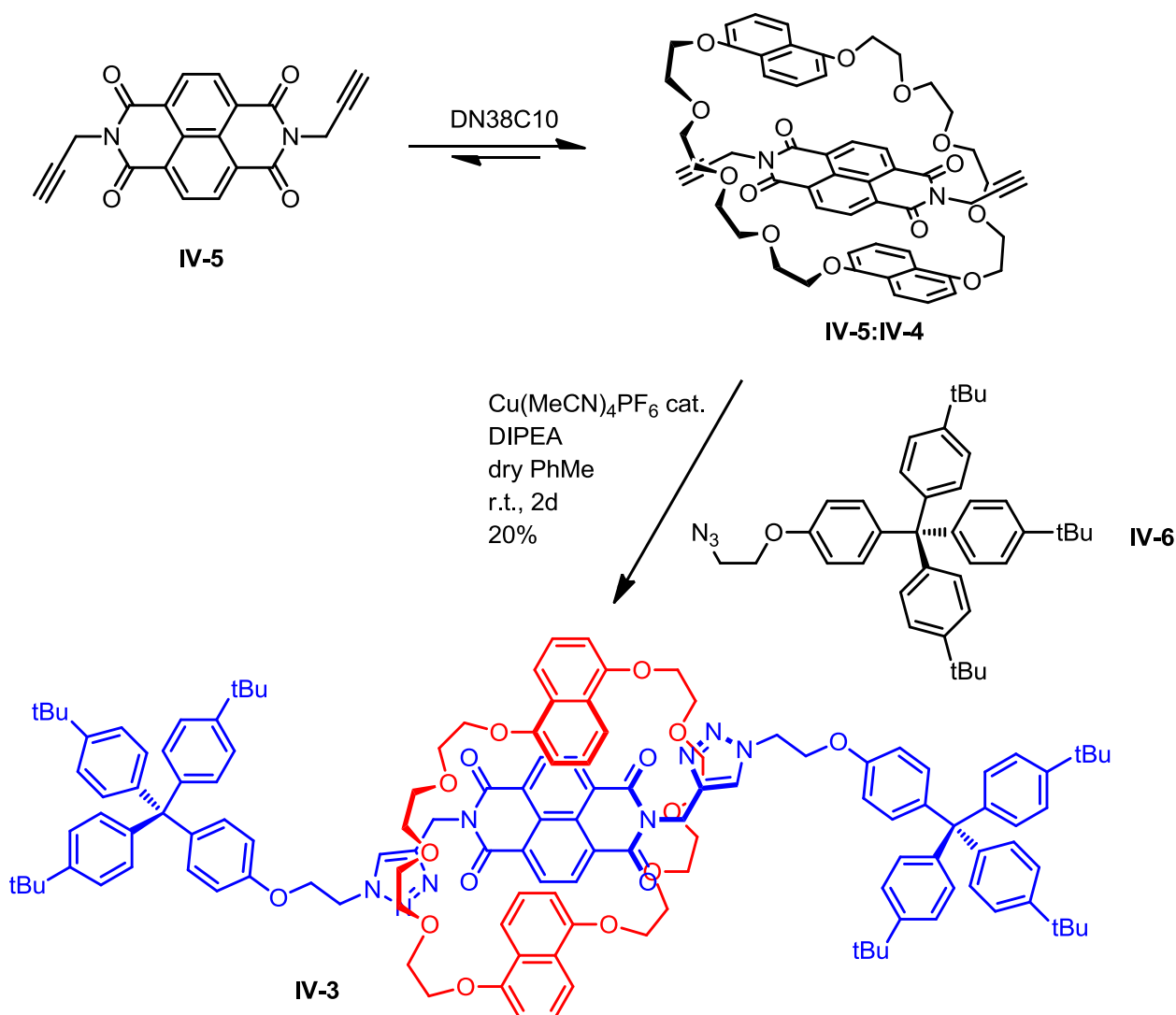


Figure 4.3 - Rotaxane formation via capping approach.

The azide-bearing bulky stopper units **IV-6** were covalently bonded to the pseudorotaxane **IV-5:IV-4** by a copper(I)-catalyzed azide-alkyne cycloaddition.²⁰⁹

²⁰⁹ H.-P. Jacquot de Rouville, J. Iehl, C.J. Bruns, P.L. McGrier, M. Frasconi, A.A. Sarjeant and J.F. Stoddart, *Org. Lett.*, **2012**, *14*, 5188.

4.1.2 Clipping approach

The clipping method consists in the macrocyclization of acyclic precursors around the template site of a thread which already has the stoppers.

In 2014 Berna and coworkers synthesized a [2]rotaxane **IV-7** via a five-component clipping approach using a preformed di(acylamino)pyridine-bearing thread **IV-8** as templating site and *p*-xylylenediamine **IV-9** and isophthaloyl chloride **IV-10** as benzyl amide-based macrocycle precursors (Figure 4.4).²¹⁰

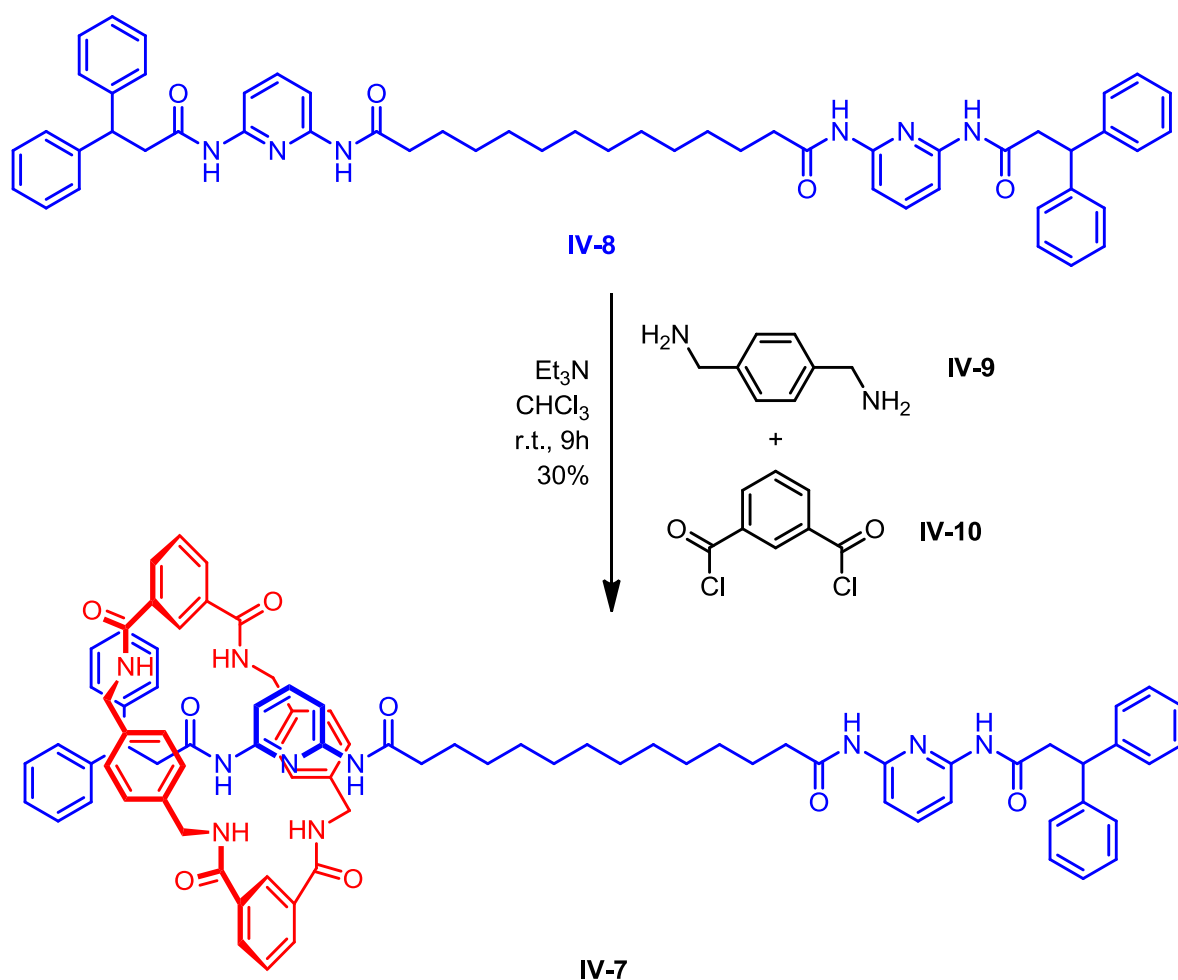


Figure 4.4 - Rotaxane formation via clipping approach.

²¹⁰ A. Martinez-Cuezva, J. Berna, R.-A. Orenes, A. Pastor and M. Alajarin, *Angew. Chem. Int. Ed.*, **2014**, 53, 6762.

4.1.3 Slipping approach

The slipping method consists in the self-assembly of a preformed macrocycle and a dumbbell-shaped preformed thread: the two components are mixed and heated in order to overcome the energy barrier related to the slipping-on of the macrocycle over the stoppers of the thread.

This method was first reported by Stoddart in 1993: a [2]rotaxane **IV-11** was obtained exploiting the complementarity between an electron-poor thread **IV-12** and an electron-rich macrocycle **IV-13** (Figure 4.5).²¹¹

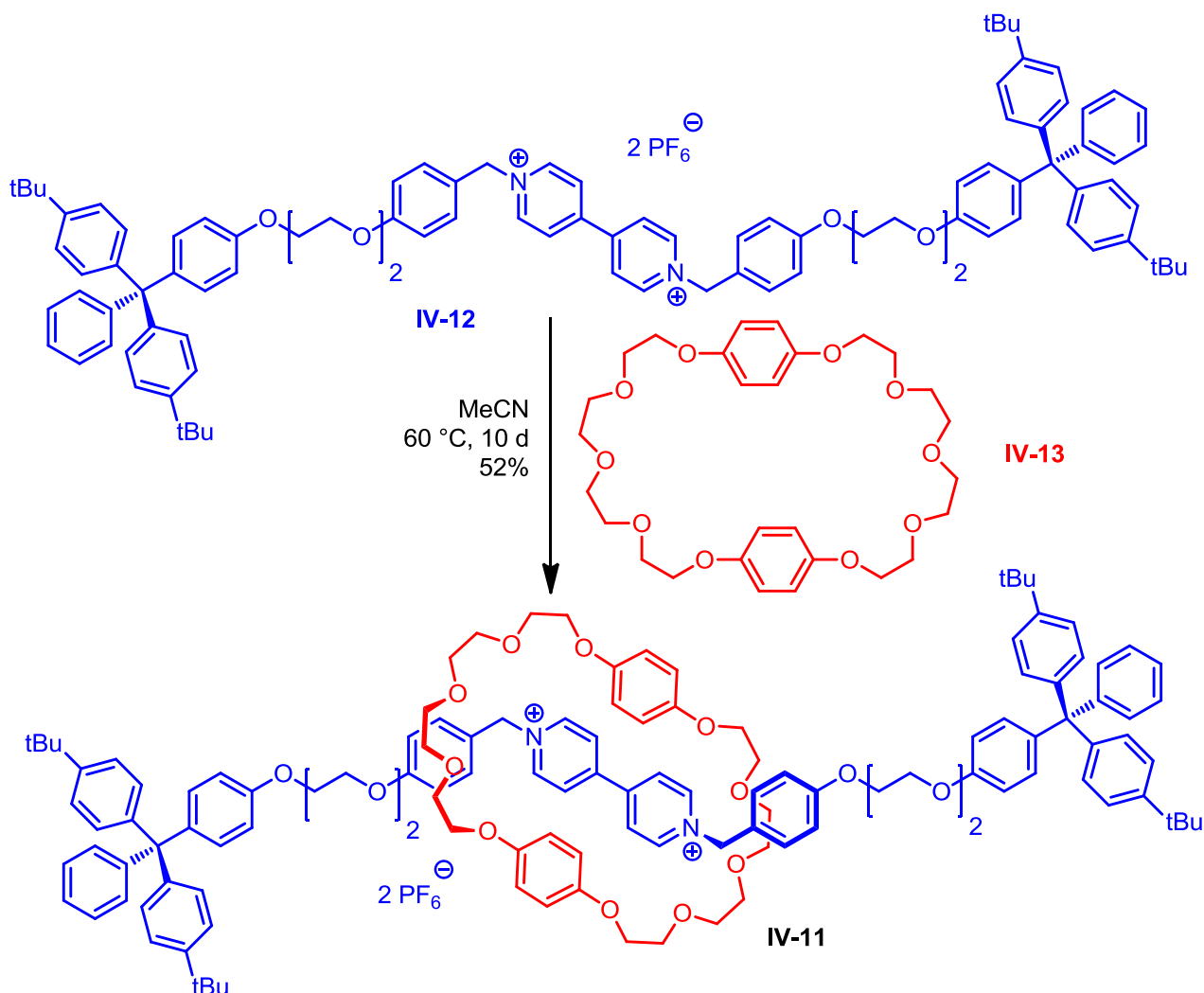


Figure 4.5 - Rotaxane formation by slipping approach.

²¹¹ P.R. Ashton, M. Bělohradský, D. Philp and J.F. Stoddart, *J. Chem. Soc., Chem. Commun.*, **1993**, 0, 1269.

4.1.4 Active metal-template approach

The active-template approach is the most recent method for the synthesis of interlocked molecules. Leigh and coworkers reported first this new methodology in 2006, showing the dual function of the metal ion: it acts as a template for entwining the ring and thread precursors and it also promote the covalent bond formation between the reactants providing the mechanically interlocked molecule. In the work, the rotaxane **IV-14** was obtained in 94% yield via a copper(I)-catalyzed terminal alkyne-azide cycloaddition (Figure 4.6).²¹²

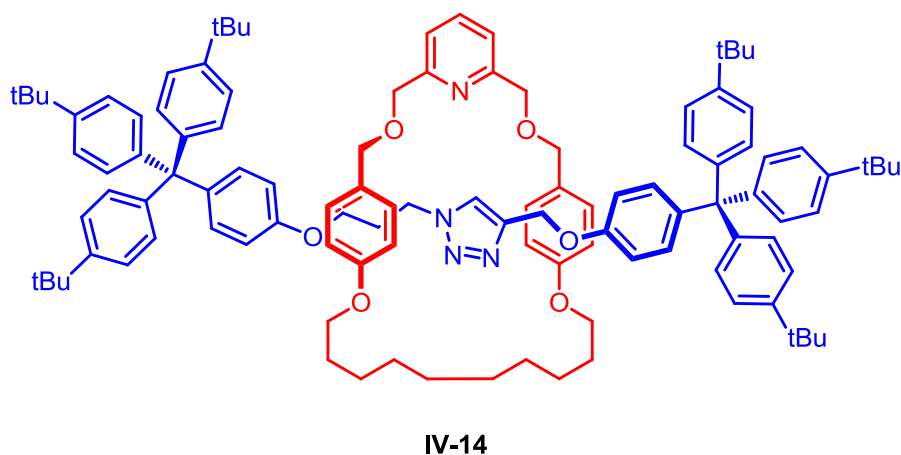


Figure 4.6 - Rotaxane **IV-14** synthesized by active template approach.

Since its' discover, other different metal-catalyzed reactions have been used in active-template - based method for the synthesis of rotaxanes, like Cadiot-Chodkiewicz heterocoupling, palladium-catalyzed oxidative Heck couplings and nickel- and copper-catalyzed alkyne homocouplings and heterocouplings.^{213, 214, 215, 216}

²¹² V. Aucagne, K.D. Hanni, D.A. Leigh, P.J. Lusby and D.B. Walker, *J. Am. Chem. Soc.*, **2006**, *128*, 2186.

²¹³ J. Berná, S.M. Goldup, A.L. Lee., D.A. Leigh, M.D. Symes, G. Teobaldi and F. Zerbetto, *Angew. Chem. Int. Ed.*, **2008**, *47*, 4392.

²¹⁴ J.D. Crowley, K.D. Hanni, A.L. Lee, D.A. Leigh, *J. Am. Chem. Soc.*, **2007**, *129*, 12092.

²¹⁵ J.D. Crowley, S.M. Goldup, N.D. Gowans, D.A. Leigh, V.E. Ronaldson and A.M.Z. Slawin, *J. Am. Chem. Soc.*, **2010**, *132*, 6243.

²¹⁶ H. Lahlali, K. Jobe, M. Watkinson and S.M. Goldup, *Angew. Chem. Int. Ed.*, **2011**, *50*, 4151.

4.1.5 Miscellaneous methods

Alongside the previously discussed four main synthetic approaches for the formation of [n]rotaxanes, other way have been studied.

In 2002 Watanabe and coworkers proposed a new methodology for the synthesis of [2]rotaxanes based on amide covalent bond formation.

The macrocyclic precursor **IV-15** bears a constrained succinate diester with the carbonyls outside the plane of the crown ether moiety. Upon addition of (9-anthrylmethyl)amine **IV-16**, a double aminolysis takes place and [2]rotaxane **IV-17** is formed (Figure 4.7).²¹⁷

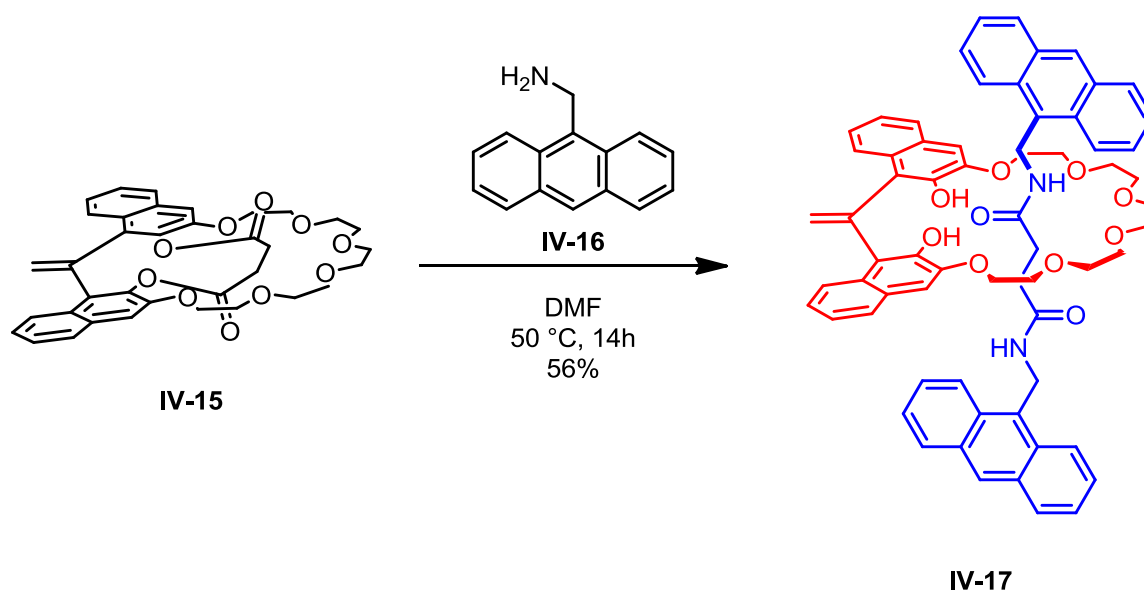


Figure 4.7 - Rotaxane formation by double aminolysis approach.

In 2004, Nagawa and coworkers reported the synthesis of chiral [2]rotaxanes adopting the same aminolysis-based method.²¹⁸

²¹⁷ K. Hiratani, J. Suga, Y. Nagawa, H. Houjou, H. Tokuhisa, M. Numata and K. Watanabe, *Tetrahedron Lett.*, **2002**, 43, 5747.

²¹⁸ N. Kameta, K. Hiratani and Y. Nagawa, *Chem. Comm.*, **2004**, 0, 466.

In 2004 Asakawa and coworkers reported the synthesis of [2]rotaxane **IV-18**, which was obtained by a new method they developed, the threading-followed-by-shrinking approach (Figure 4.8).

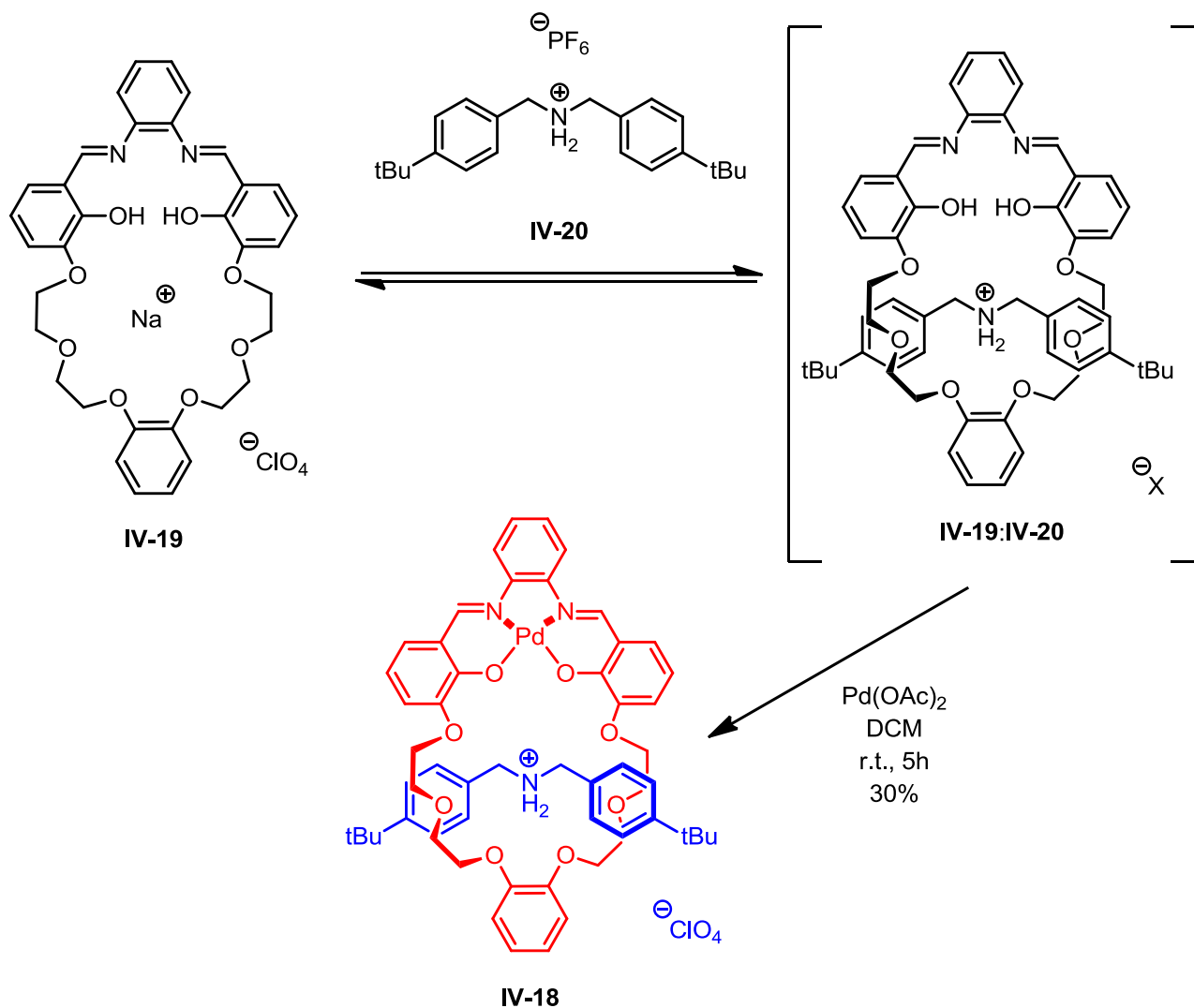


Figure 4.8 - Rotaxane synthesis by threading-followed-by-shrinking approach.

The dumbbell-shaped thread **IV-20** is first complexed with the macrocycle **IV-19** and then the pseudorotaxane is captured in the mechanically interlocked molecule upon shrinking the macrocycle cavity.²¹⁹

²¹⁹ I. Yoon, M. Narita, T. Shimizu and M. Asakawa, *J. Am. Chem. Soc.*, **2004**, *126*, 16740.

4.2 Development of functional [2]rotaxane by an active metal-template approach

4.2.1 Synthesis

A triarylamine-containing [2]rotaxane **IV-21** was designed and synthesized by a Glaser-type coupling in an active metal-template approach.

In 1869 Glaser reported the first oxidative homocoupling of terminal alkynes: the coupling was performed on phenylacetylene in order to form the corresponding 1,3-diphenyldiyne. This reaction was based on copper(I) salts, like copper(I) chloride or copper(I) bromide, aqueous ammonia was used as base and oxygen was used as oxidant.²²⁰

Coupling of terminal alkynes is a well-known reaction in the synthesis of mechanically interlocked molecules.²²¹

Commercially available copper(I) iodide and triarylamine macrocycle **II-50** were dissolved in a dry dichloromethane/acetonitrile mixture, 1:1 v/v, and stirred at room temperature for 1 hour.

Two equivalents of alkyne-bearing trityl stoppers **II-14**, iodine and anhydrous potassium carbonate were then added. The reaction mixture was stirred at 60 °C for 72 hours, then quenched upon addition of dilute aqueous potassium cyanide solution. Purification by column chromatography afforded the pure mechanically interlocked molecule **IV-21** in 36% yield (Figure 4.9).

The yield of rotaxane **IV-21** (36%) is considerably higher compared to the yield of its structural analogue (9%), previously reported in literature: this fact can be explained by the presence of the triarylamine unit which significantly enhances the solubility of the ring in chloroform, leading to a more homogeneous reaction mixture.²²²

²²⁰ C. Glaser, *Annalen der Chemie und Pharmacie*, **1869**, 154, 137.

²²¹ D.G. Hamilton, J.E. Davies, L. Prodi and J.K.M. Sanders, *Chem. Eur. J.*, **1998**, 4, 608.

²²² A. Tron, P.J. Thornton, B. Kauffmann, J.H.R. Tucker and N.D. McClenaghan, *Supramol. Chem.*, **2016**, 28, 733.

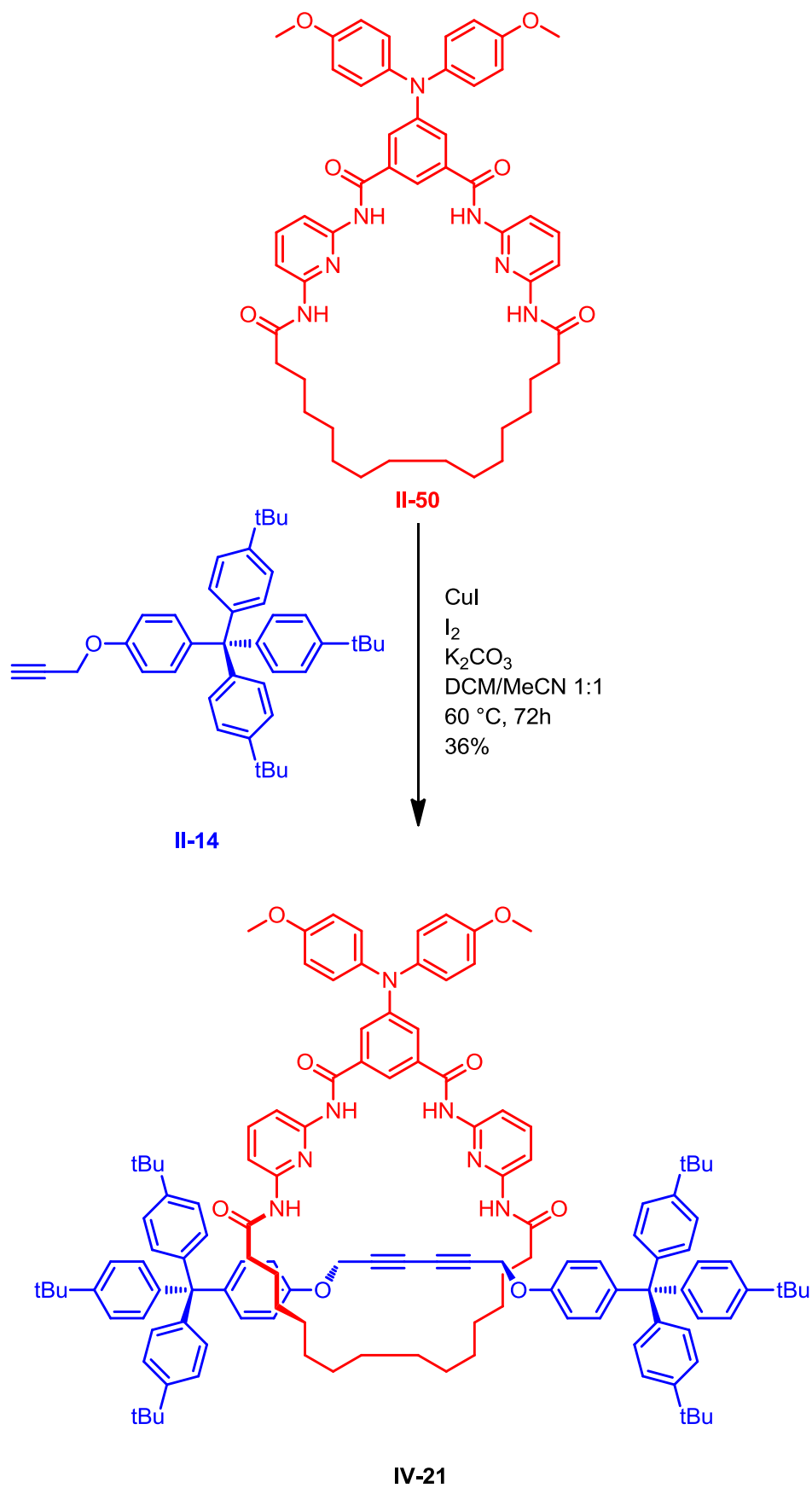


Figure 4.9 - Synthetic scheme of triarylamine-containing Glaser [2]rotaxane **IV-21**.

4.2.2 Characterization

Triarylamine-containing Glaser [2]rotaxane **IV-21** was fully characterized by ^1H -, ^{13}C -NMR and mass spectrometry. The [2]rotaxane **IV-21** is fully soluble in common deuterated chlorinated solvents. High quality NMR spectra were recorded for [2]rotaxane **IV-21** with no sign of degradation even a few days after the preparation of the sample (Figure 4.10).

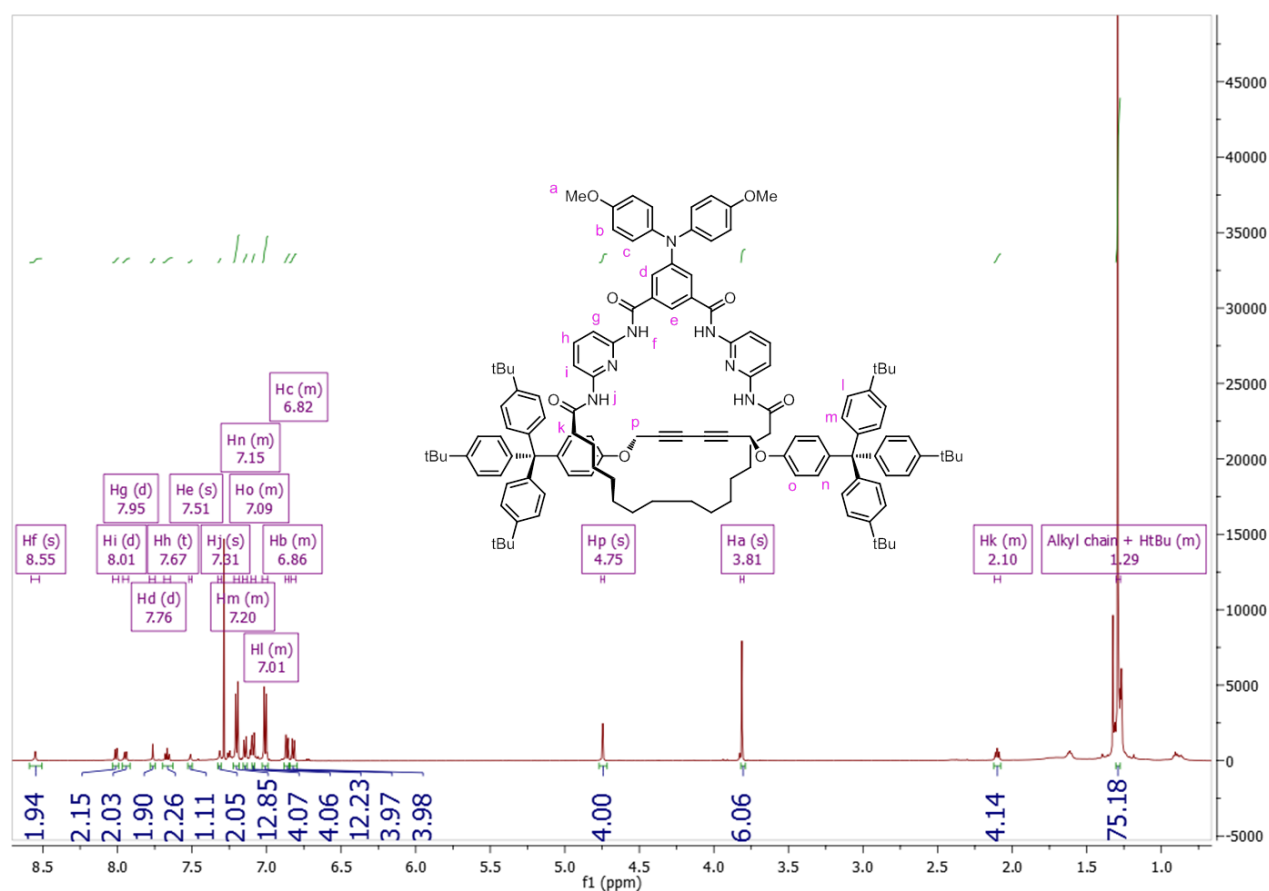


Figure 4.10 - ^1H -NMR of triarylamine-containing Glaser [2]rotaxane **IV-21** (600 MHz in CDCl_3).

In figure 4.10, peaks at δ 4.75 (s, 4H) and δ 3.81 (s, 6H) are the methylene groups of the dyine-containing thread and methoxy groups of the triarylamine-containing ring, respectively. The 2:3 ratio between those peaks proved the formation [2]rotaxane **IV-21**. Taking this observation in conjunction with all the other peaks, it could be assumed that the target rotaxane was obtained.

4.3 Development of functional [2]rotaxanes by a clipping approach

Two benzylic amide-based [2]rotaxanes **IV-22** and **IV-23** were synthesized by a five-component clipping reaction by using a dumbbell-shaped tetrabutylsuccinamide thread **IV-24** as template and *p*-xylylenediamine **IV-9** and 5-functionalized isophthaloyl chlorides **II-48** and **IV-25** as precursor of the benzylic amide macrocycles.

4.3.1 Synthesis

The succinamide thread **IV-24** was prepared according to a reported literature procedure.²²³

Commercially available succinyl chloride **IV-26** and 4 equivalents of dibutylamine in dry dichloromethane were stirred at room temperature. The reaction mixture was stirred overnight then it was quenched upon sequential addition of sodium hydroxide solution, dilute hydrochloric acid solution and water. The product was obtained in quantitative yield and no purification step was required.

We note in passing that the reaction can also be performed in gram-scale without any loss of purity and yield (Figure 4.11).

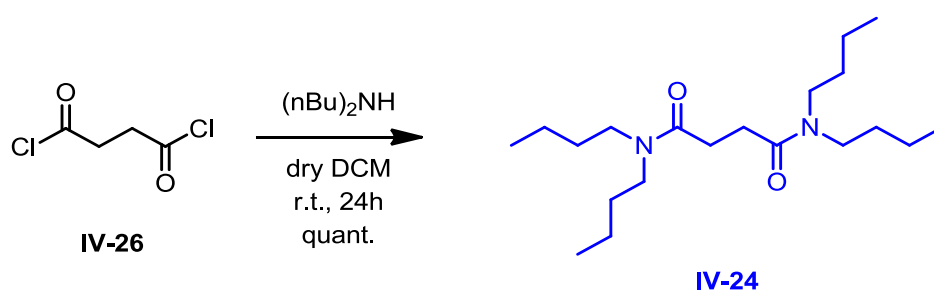


Figure 4.11 - Synthetic scheme of tetrabutylsuccinamide thread **IV-24**.

²²³ A. Martinez-Cuezva, L.V. Rodrigue, C. Navarro, F. Carro-Guillen, L. Buriol, C.P. Frizzo, M.A.P. Martins, M. Alajarin and J. Berna, *J. Org. Chem.*, **2015**, *80*, 10049.

A triarylamine-containing benzylic amide-based [2]rotaxane **IV-22** was obtained reacting commercially available *p*-xylylenediamine **IV-9** and 5-[bis(4-methoxyphenyl)amino]-isophthaloyl chloride **II-48**, which was obtained using the procedure reported in Chapter 2. A solution of diamine **IV-9** and a solution of freshly prepared 5-substituted isophthaloyl **II-48**, both in dry chloroform, were simultaneously added during 5 hours to a solution of tetrabutylsuccinamide thread **IV-24** and dry triethylamine in the same solvent under high dilution conditions. The product was purified by column chromatography (Figure 4.12).

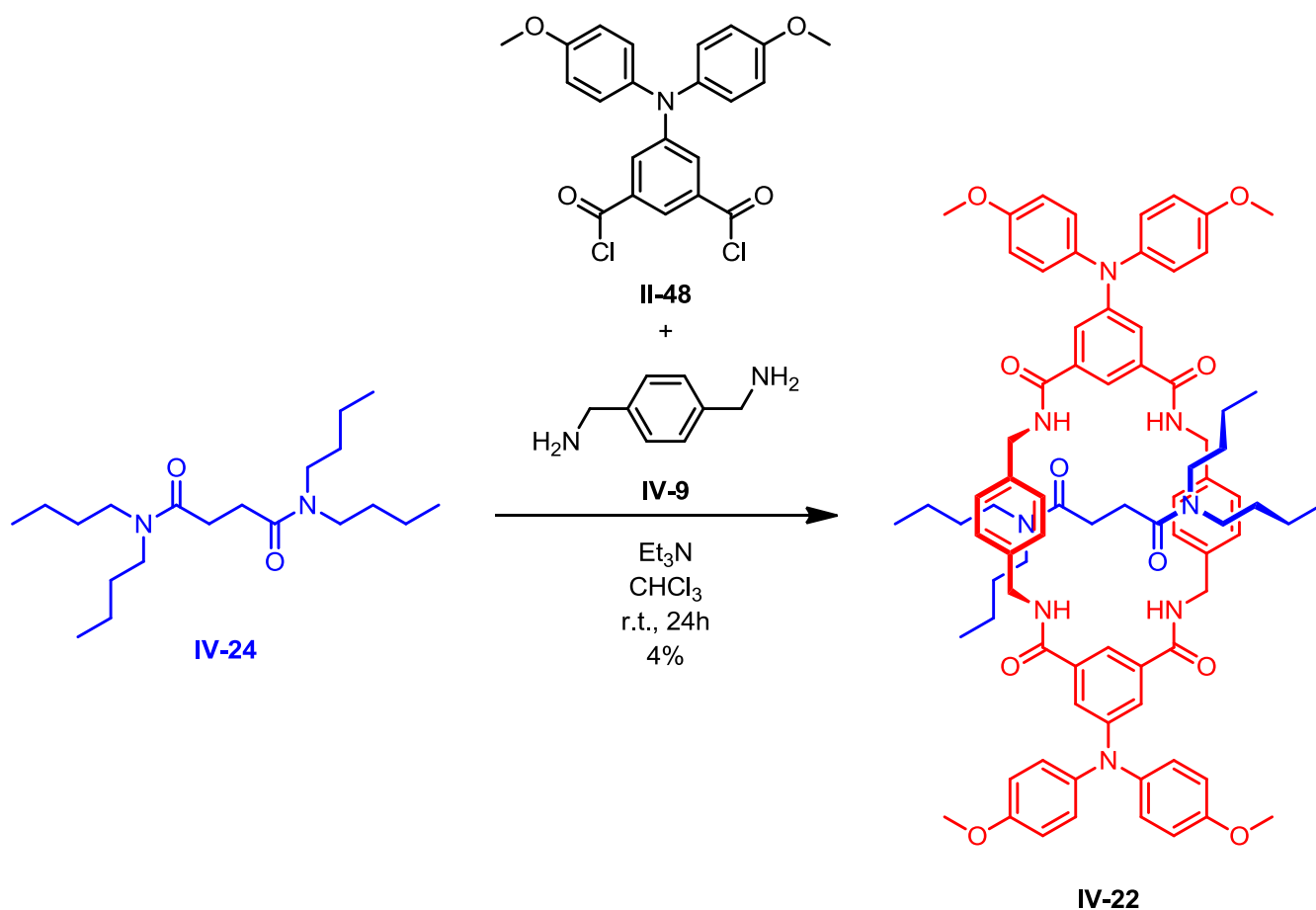


Figure 4.12 - Synthetic scheme of triarylamine-clipped [2]rotaxane **IV-22**.

The same clipping approach was also used to develop a ferrocene-containing [2]rotaxane **IV-23**.

5-Ferrocenylisophthaloyl chloride **IV-25** was prepared in three steps following a previously reported literature procedure.²²⁴

Dimethyl 5-aminoisophthalate **II-40** was first treated with sodium nitrite in 6M HCl at 0 °C, it was stirred for 30 minutes at the same temperature and then freshly prepared ferrocenium sulfate, obtained by treating ferrocene with concentrated sulfuric acid, and copper powder were added and the reaction was stirred overnight. Ascorbic acid was added in order to quench the reaction and the mixture was extracted with dichloromethane. Dimethyl 5-ferrocenylisophthalate **IV-27** was purified by column chromatography followed by recrystallization in ethanol and obtained as orange cotton-like needles in 19% yield. The ferrocene-containing isophthalate then was hydrolysed by stirring at room temperature overnight in a 1:1 ethanol/6M potassium hydroxide aqueous solution and then the 5-ferrocenylisophthalic acid **IV-28** was recovered by acidification with citric acid, filtration and subsequent recrystallization in EtOH. The product was obtained in quantitative yield as cotton-like crystals.

The 5-ferrocenylisophthalic acid **IV-28** was then treated with oxalyl chloride and a catalytic amount of dimethylformamide in dry dichloromethane.

The 5-ferrocenylisophthaloyl chloride **IV-25** was obtained in quantitative yield as blood red oil and used in the next step without further purification (Figure 4.13).

²²⁴ N.H. Evans, H. Rahman, A.V. Leontiev, N.D. Greenham, G.A. Orłowski, Q. Zeng, R.M.J. Jacobs, C.J. Serpell, N.L. Kilah, J.J. Davis and P.D. Beer, *Chem. Sci.*, **2012**, 3, 1080.

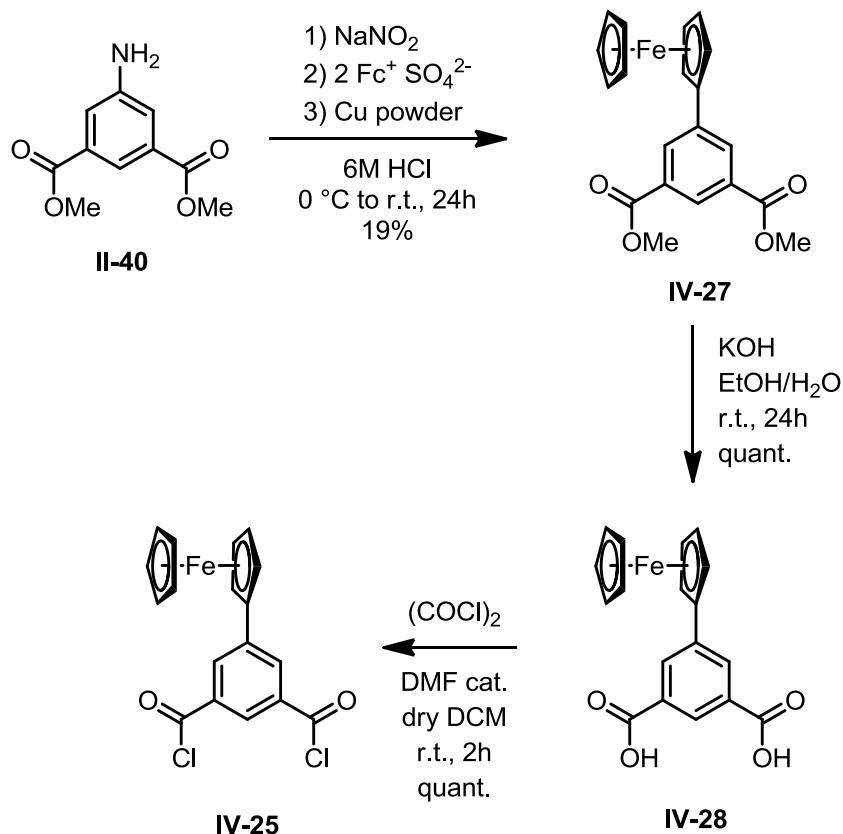


Figure 4.13 - Synthetic scheme of 5-ferrocenylisophthaloyl chloride **IV-25**.

A ferrocene-containing benzyl amide-based [2]rotaxane was obtained reacting commercially available *p*-xylylenediamine **IV-9** and 5-ferrocenylisophthaloyl chloride **IV-25**.

A solution of *p*-xylylenediamine **IV-9** and a solution of freshly prepared dichloride, both in dry tetrahydrofuran, were simultaneously added during 5 hours to a solution of tetrabutylsuccinamide thread **IV-24** and dry triethylamine in the same solvent under high dilution conditions. The product was purified by column chromatography and obtained in 41% yield (Figure 4.14).

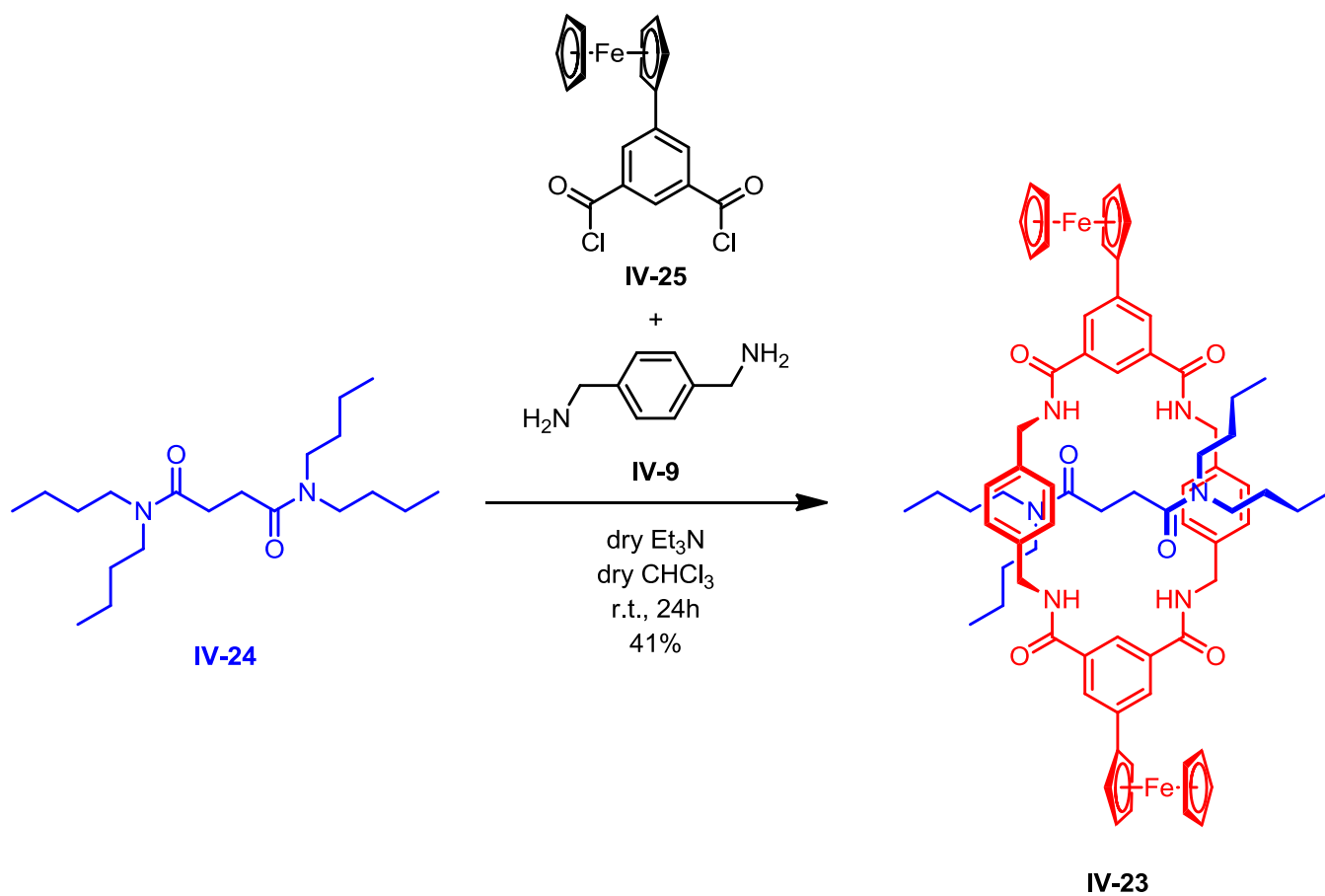


Figure 4.14 - Synthetic scheme of ferrocene-containing clipped [2]rotaxane **IV-23**.

4.3.2 Characterization

4.3.2.1 NMR studies and mass spectrometry

The two benzylic amide-based clipped [2]rotaxanes, **IV-22** and **IV-23**, was fully characterized by ^1H -, ^{13}C -NMR and mass spectrometry.

The triarylamine-containing benzylic amide-based clipped [2]rotaxane **IV-22** is fully soluble in most common deuterated solvents. High quality NMR spectra were recorded for [2]rotaxane **IV-22** with no sign of degradation even a few days after the preparation of the sample (Figure 4.15 and 4.16).

The ferrocene-containing benzylic amide-based clipped [2]rotaxane **IV-23** is fully soluble in common deuterated chlorinated solvents, while fast degradation of the sample occurred when deuterated dimethylsulfoxide was used.

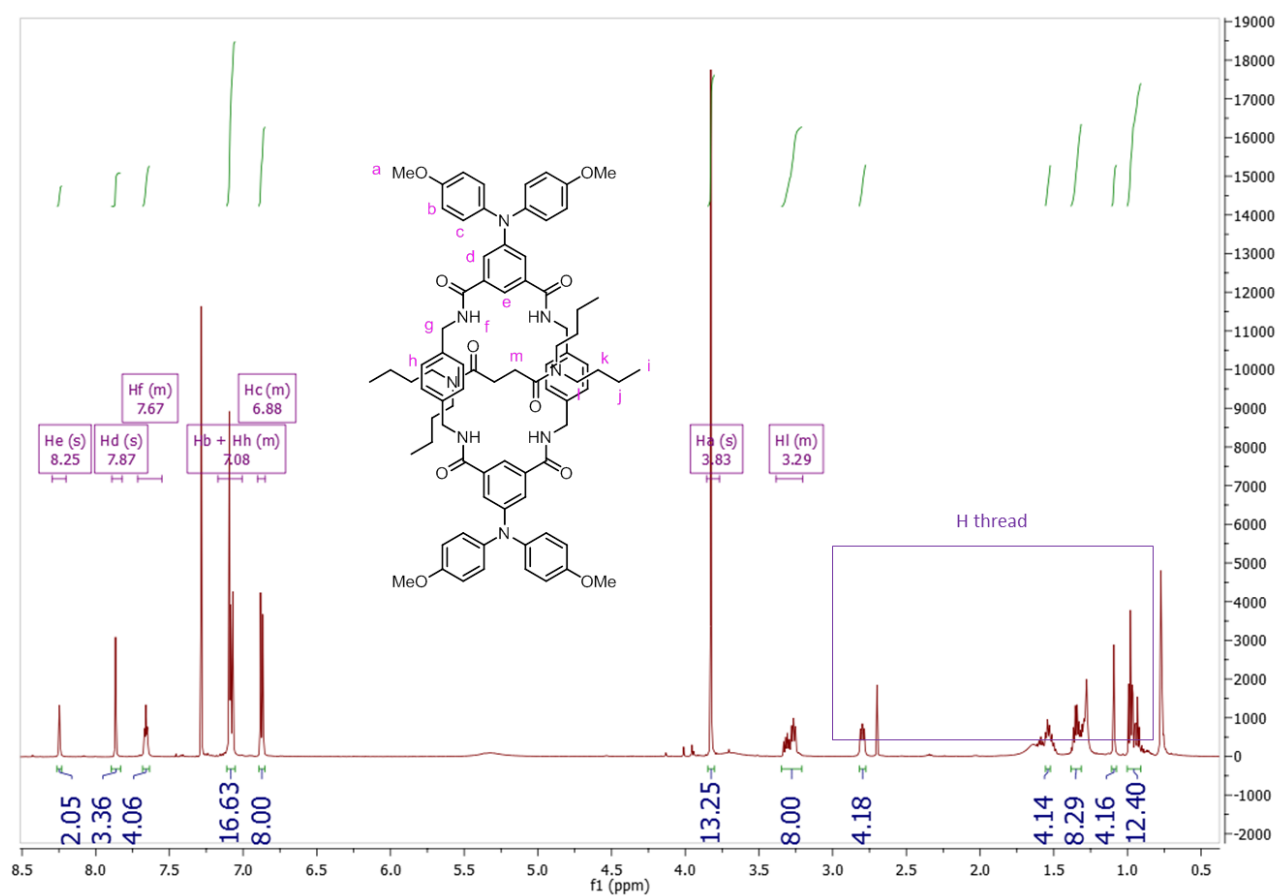


Figure 4.15 - ^1H -NMR of triarylamine-containing clipped [2]rotaxane **IV-22** (600 MHz in CDCl_3).

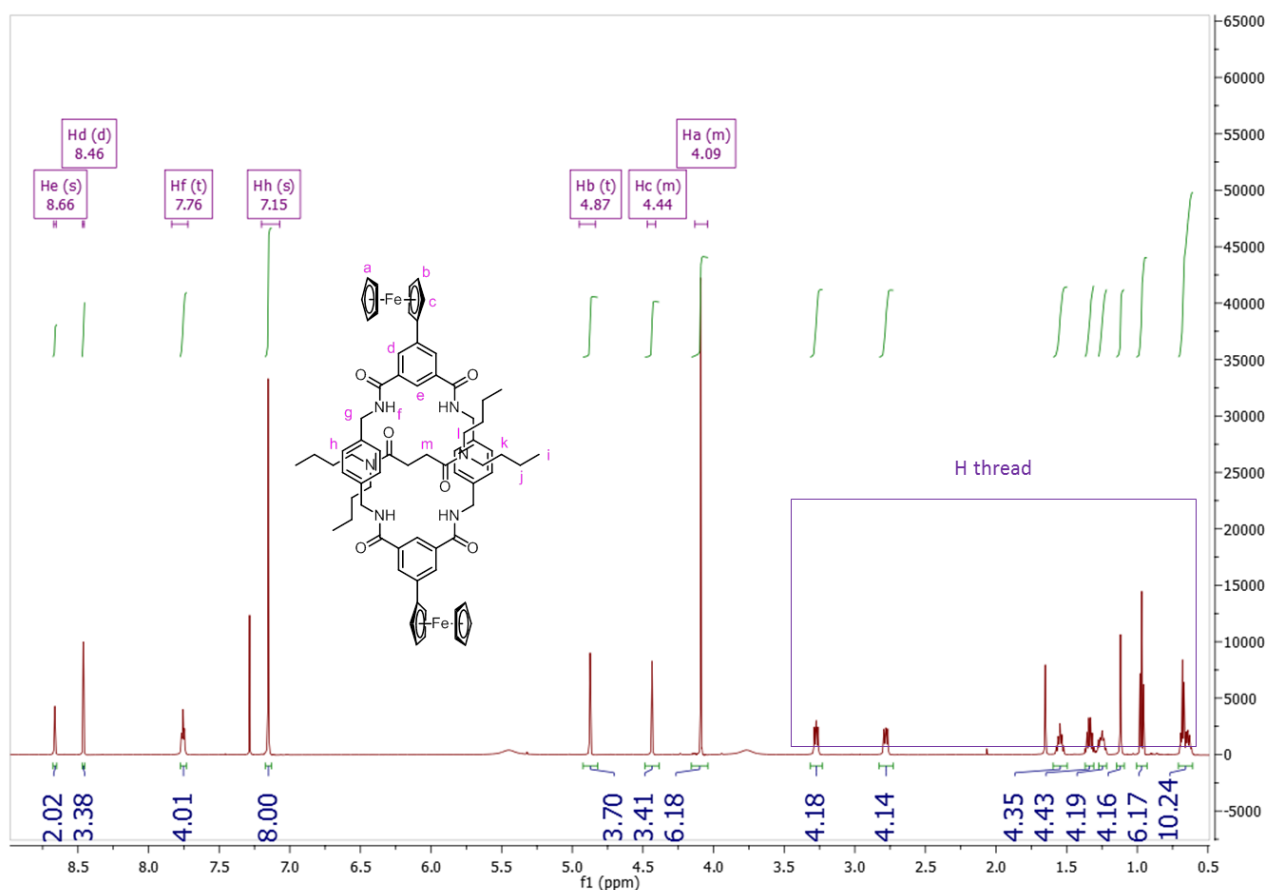


Figure 4.16 - $^1\text{H-NMR}$ of ferrocene-containing clipped [2]rotaxane **IV-23** (600 MHz in CDCl_3).

In figure 4.15, peaks at δ 8.25 (s, 2H) and δ 7.87 (m, 4H) are the aromatic proton of the isophthalic core, while peak at δ 3.83 (s, 12H) are the methoxy groups of triarylamine core. Comparing their integral values with the integrals of the thread (40H in total), it can be assumed that the isolated molecule was the triarylamine-containing clipped [2]rotaxane **IV-22**.

In figure 4.16, peaks at δ 8.66 (s, 2H) and δ 8.46 (m, 4H) are the aromatic proton of the isophthalic core. Their ratio with the peaks of the thread (40H in total) proved the formation of the ferrocene-containing clipped [2]rotaxane **IV-23**. Those observation are consistent with all the other data ($^{13}\text{C-NMR}$, HRMS and X-ray crystal structures).

4.3.2.2 Electrochemistry studies

Ferrocene-containing clipped [2]rotaxane **IV-23** was studied by cyclic voltammetry (CV) using a three electrode cell, with a glassy carbon working electrode, silver wire counter electrode and silver/silver chloride reference electrode.

The sample was dissolved in the minimal amount of dry dichloromethane, sonicated for 5 minutes then diluted in acetonitrile, tetrabutylammonium hexafluorophosphate (TBAPF₆) was used as supporting electrolyte (Figure 4.17).

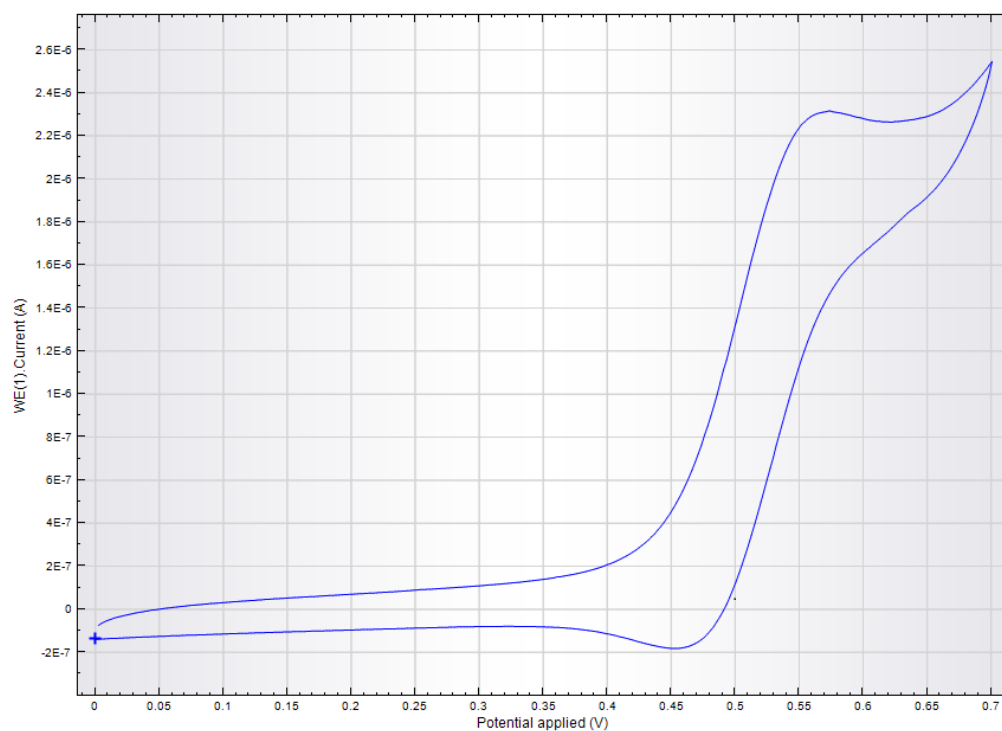


Figure 4.17 - Cyclic voltammogram of **IV-23**, in a solution of 10^{-2} M TBAPF₆ in dry degassed acetonitrile at scan rate = 200 mVs^{-1} .

From data analysis, ferrocene-containing clipped [2]rotaxane **IV-23** was seen to undergo a redox transition at $E_{1/2} = 0.51 \text{ V}$, where $E_{1/2} = (E_p^a + E_p^c) / 2$.

4.3.2.3 X-ray structural determination

Single crystals of suitable quality for X-ray structural determination were obtained for both triarylamine- and ferrocene-containing clipped [2]rotaxanes **IV-22** and **IV-23**.

Crystals of **IV-22** were grown by slow diffusion of pentane in a concentrated solution of sample in chloroform, while crystals of **IV-23** were grown by slow evaporation of a solution of sample in dichloromethane.

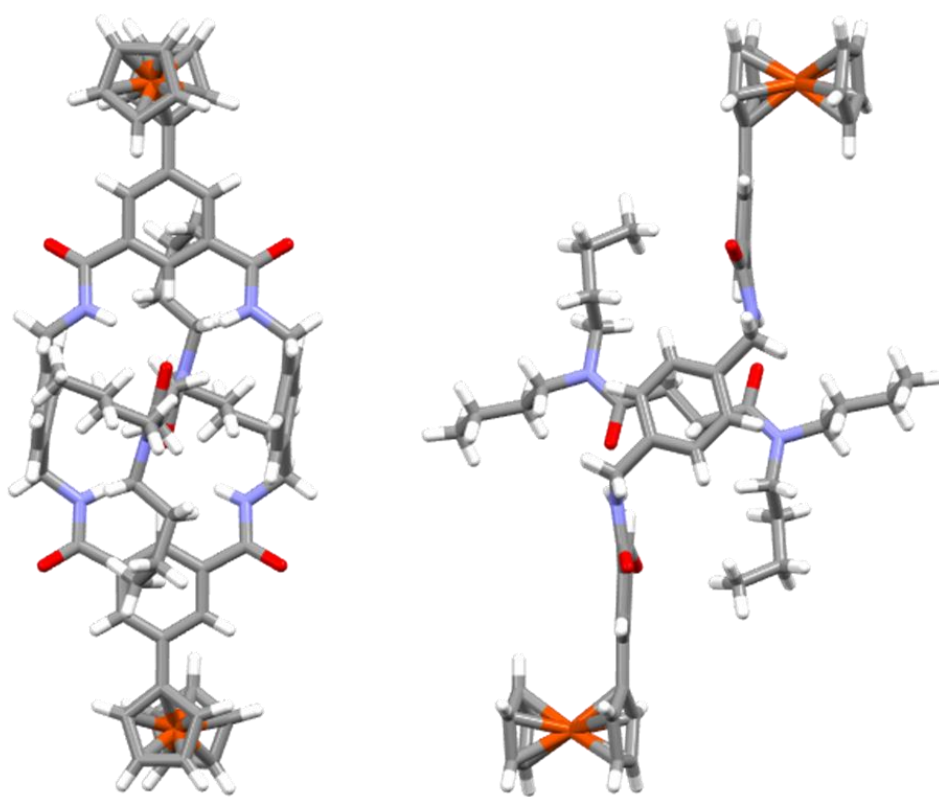


Figure 4.18 - Crystal structure of ferrocene-containing benzylic amide-based clipped [2]rotaxane **IV-23**, front view (left) and side view (right).

The ferrocene-containing benzylic amide-based macrocycle adopts a chair-like conformation with both isophthalamide groups forming bifurcated hydrogen bonds (2.224 and 2.279 Å for each interaction couples) with the thread carbonyls. The cyclopentadienyl ring of ferrocene is almost coplanar with the isophthalic ring, having a torsion angle of 167.21° (Figure 4.18).

Table 4.1 - Crystal data of ferrocene-containing benzylic amide-based clipped [2]rotaxanes **IV-23**.

Compound	IV-23
Empirical formula	C ₃₀ H ₃₀ FeN ₄ O ₆
Formula weight	598.43
Temperature/K	293(2)
Radiation type	CuK α
Crystal system	Triclinic
Space group	P-1
a/Å	9.5366(5)
b/Å	11.6279(7)
c/Å	14.9396(9)
α /deg	99.002(5)
β /deg	108.001(5)
γ /deg	90.007(4)
V/Å ³	1554.09(16)
Abs. coeff. (mm ⁻¹)	4.277
F(000)	624
Resolution (Å)	0.811
Index ranges	-10 ≤ h ≤ 9, -12 ≤ k ≤ 12, -15 ≤ l ≤ 15
No. of collected reflections	14633
Data/restraints/parameters	3928/0/391

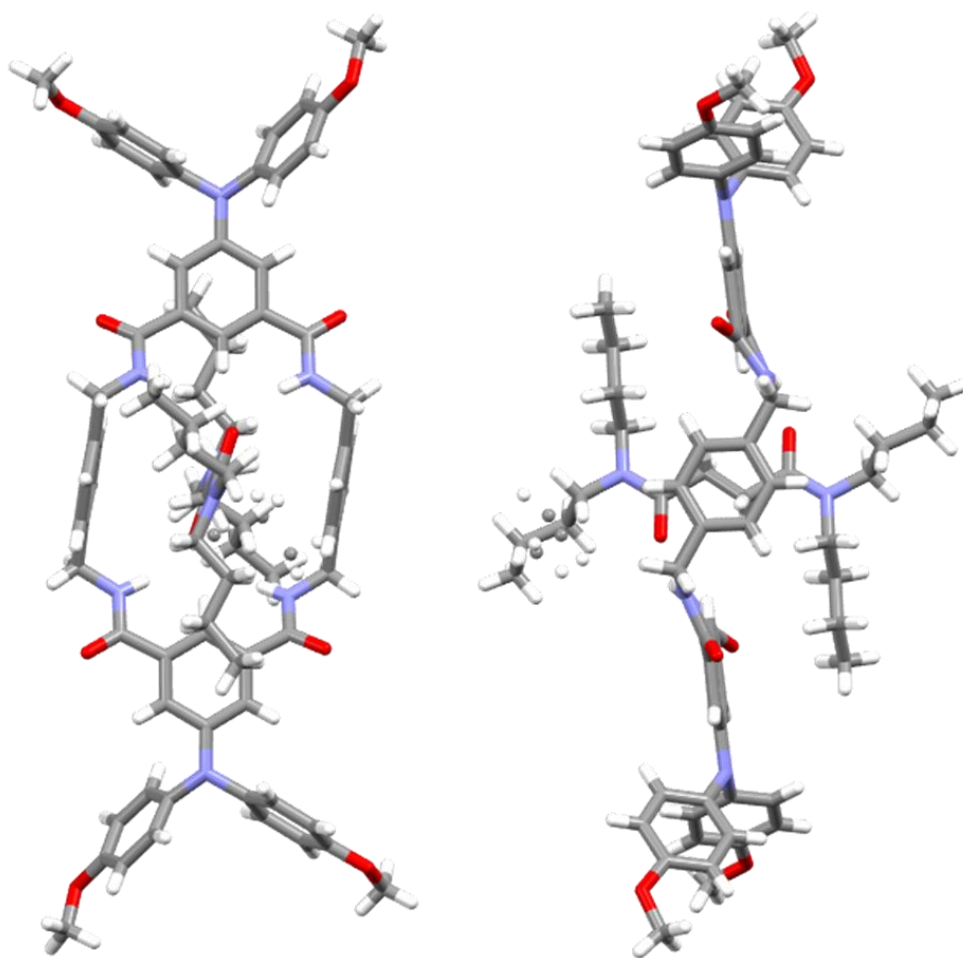


Figure 4.19 - Crystal structure of triarylamine-containing benzylic amide-based clipped [2]rotaxane **IV-22**, front view (left) and side view (right).

The triarylamine-containing benzylic amide-based macrocycle adopts a chair-like conformation with both isophthalamide groups forming bifurcated hydrogen bonds (2.192 and 2.533 Å for each interaction couples) with the thread carbonyls. The triarylamine core presents C-N bonds length of 1.399, 1.438 and 1.446 Å and C-N-C angles of 113.55°, 118.71° and 120.72° (Figure 4.19).

Table 4.2 - Crystal data of triarylamine-containing benzylic amide-based clipped [2]-rotaxanes **IV-**

22.

Compound	IV-22
Empirical formula	C ₄₀ H ₄₇ N ₄ O ₅
Formula weight	663.81
Temperature/K	293(2)
Radiation type	CuK α
Crystal system	Triclinic
Space group	P-1
a/Å	9.9368(4)
b/Å	12.4037(5)
c/Å	15.9957(6)
α /deg	78.603(3)
β /deg	76.799(3)
γ /deg	74.097(3)
V/Å ³	1826.66(13)
Abs. coeff. (mm ⁻¹)	0.639
F(000)	710
Resolution (Å)	0.811
Index ranges	-11 \leq h \leq 12, -14 \leq k \leq 15, -19 \leq l \leq 19
No. of collected reflections	25358
Data/restraints/parameters	6836/27/484

4.4 Conclusion and perspectives

Three novel [2]rotaxanes **IV-21**, **IV-22** and **IV-23** have been successfully synthesized and fully characterized by ^1H -, ^{13}C -NMR and mass spectrometry.

An active metal-template reaction Glaser coupling reaction was employed for the synthesis of triarylamine-bearing [2]rotaxane **IV-21**, while triarylamine-bearing [2]rotaxane **IV-22** and ferrocene-bearing [2]rotaxane **IV-23** were obtained by a second complementary “clipping”-type approach to rotaxane formation.

In this methodology, the electroactive rings, one integrating two ferrocene units while the other comprised two triarylamine units, were directly formed encircling the tetrabutylsuccinamide-based thread via a template-assisted five-component clipping reaction.

From electrochemistry studies, ferrocene-containing benzyl amide-based clipped [2]-rotaxane **IV-23** was seen to undergo a redox transition.

X-ray crystal structures which were obtained for both benzyl amide-based [2]rotaxanes **IV-22** and **IV-23**, proved the interlocked nature of the assemblies.

5. General conclusion and perspectives

Having straightforward and reproducible synthetic procedures is fundamental for the development of solid methodologies for the construction of mechanically interlocked molecules. This thesis reported the synthesis of electroactive macrocycles, NIR components and [2]rotaxanes, along with several improved procedures for the synthesis of versatile building blocks.

In chapter 2, the synthesis of three novel hydrogen-bonding 31- and 35-member Hamilton-type cyclic receptors (**II-28**, **II-29** and **II-50**), all comprising a bis(2,6-diamidopyridine) motif and an electroactive group, namely ferrocene or triarylamine, has been described and characterized by ¹H- and ¹³C-NMR spectroscopy and mass spectrometry. The dimethyl 5-[bis(4-methoxyphenyl)amino]-isophthalate **II-43** was a key intermediate for the synthesis of macrocycle **II-50** and it was achieved by a copper-catalyzed Goldberg-like reaction between 4-iodoanisole and dimethyl 5-aminoisophthalate using tetraethyl orthosilicate (TEOS) as solvent. This particular reaction conditions allowed to obtain the desired intermediate **II-43** in good yield, while other palladium- or copper-catalyzed coupling reactions were unsuccessful, mainly leading to complex mixture of degradation products. The main advantages of the use of TEOS as solvent are the dehydrating nature of this compound, which avoids the hydrolysis of ester groups during the reaction, and the extremely easy workup of the mixture: the solvent itself is fully converted in silicon dioxide upon addition of aqueous ammonium fluoride and the crude is recovered by addition of ethyl acetate and filtration. Moreover the reaction involves cheap and commercially available reactants and it can be easily performed on the gram-scale.

Host-guest interactions between macrocycle **II-50** and a complementary 5,5'-diethylbarbituric acid **II-4** as model guest were also studied by electronic absorption and ¹H-NMR spectroscopic titrations: the experimental binding constant ($K_{\text{ass}} = 70000 \text{ M}^{-1}$ in deuterated dichloromethane) is

much higher than the structural analogue where a central *tert*-butyl phenyl is present instead of the triarylamine moiety ($K_{\text{ass}} = 23500 \text{ M}^{-1}$ in deuterated chloroform). Host-guest interactions with the same model guest **II-4** were also studied for both the ferrocene-containing Hamilton-type macrocycle **II-28** and **II-29**: the determined binding constants ($K_{\text{ass}} = 742 \text{ M}^{-1}$ for 31-member ring **II-28** and $K_{\text{ass}} = 1011 \text{ M}^{-1}$ for 35-member ring **II-29** in deuterated chloroform, respectively) were found to be higher than the previously reported acyclic version **II-25** ($K_{\text{ass}} = 575 \text{ M}^{-1}$ in deuterated chloroform). This feature can be explained by the macrocyclic nature of the receptors **II-28** and **II-29**: the presence of the alkyl chains reduces the degrees of freedom of the molecules and the loss of entropy leads to an higher rigidity of the structures with a consequent enhancement of the binding constants. Macrocycles **II-28**, **II-29** and **II-50** were also studied by cyclic voltammetry and reversible oxidations have been observed for all of them. Crystallographic structural analysis of macrocycles **II-29** and **II-50** have been fundamental for the elucidation of the structures: **II-29** showed a crescent-shaped structure and twisting of H-bonding groups out of the plane of the binding cavity, damping its use in the construction of interpenetrating molecular architectures, while macrocycle **II-50** showed a very well-defined cavity with all the H-bonding groups in the plane of the binding cavity. The presence of the isophthalic linkage between the 2,6-diamidopyridines was found to be fundamental for the construction of a rigid and efficient receptor for barbiturate motifs, making the macrocycle **II-50** a very promising candidate for the construction of mechanically interlocked molecules.

In chapter 3, a detailed synthetic procedure for the synthesis of BF_2 -chelate of monopropargylated tetraaryl azadipyrromethene has been reported **III-28**, which is an important intermediate for the development of NIR chromophore-bearing building blocks of novel photoactive biocompatible mechanically interlocked molecules. Adapting a previously reported procedure, the di-hydroxy tetraaryl azadipyrromethene BF_2 -chelate **III-27** has been successfully monofunctionalized using propargyl bromide as alkylating agent in presence of cesium fluoride as base in dry DMSO. This

protocol allowed the full conversion of the starting material **III-27** only after 30 minutes, affording the desired product **III-28** in very good yield (90 %) and only traces of the di-alkylated product. This straightforward synthetic methodology allowed the synthesis of two unsymmetrical BF₂-chelate tetraaryl azadipyromethenes **III-29** and **III-30**, comprising a methoxy- and a *tert*-butylcarboxy-group, respectively, and a propargyloxy group, which were characterized by ¹H- and ¹³C-NMR spectroscopy and mass spectrometry. A novel barbiturate-containing BF₂-chelate azadipyromethene thread **III-52** has been synthesized in order to test the possibility to assemble [2]rotaxanes by a slipping approach. Improved synthesis for trityl stopper precursor **III-42**, azide stopper **III-50** and alkyne stopper **II-14** have been reported, showing that higher yield and higher purity for the precursor **III-42** can be obtained adopting the synthetic route that passes through the chloride intermediate **III-41**. A deuterium-labeled alkyne trityl stopper **III-51** has also been designed and synthesized: it was obtained in quantitative yield from alkyne stopper **II-14**, treating it with sodium hydride and quenching the reaction with deuterated methanol. The deuterium-bearing alkyne stopper **III-51** will be a useful tool for the development of deuterium-labeled mechanically interlocked molecules in the perspective to study the gliding of the ring along the thread in rotaxane-based supramolecular assemblies by dynamic NMR techniques.

In chapter 4, three new [2]rotaxanes **IV-21**, **IV-22** and **IV-23**, comprising electroactive groups, namely ferrocene or triarylamine, have been synthesized and fully characterized by ¹H- and ¹³C-NMR spectroscopy and mass spectrometry. The [2]rotaxane **IV-21** was obtained via an active metal-template approach by a copper-catalyzed Glaser reaction: copper ion was coordinated by the pyridine groups of macrocycle **II-50** and the coupling reaction between two alkyne trityl stoppers **II-14** took place inside the cavity of the ring, affording the diyne-bearing thread and the consequent mechanically interlocked molecule. An important aspect is that the [2]rotaxane **IV-21** was obtained in 36% yield, which is 4-fold higher than the structural analogue where a central *tert*-butyl phenyl is present in the place of the triarylamine moiety (9% yield): this increase in the yield can be

explained by the fact that the triarylamine group enhance the solubility of the macrocycle in the organic solvents.

The [2]rotaxanes **IV-22** and **IV-23** were obtained via a five component template-assisted clipping reactions. Dumbbell-shaped tetrabutylsuccinamide thread **IV-24** was synthesized in one step from commercially available succinyl chloride dibutylamine and employed as templating agent. Both the [2]rotaxanes **IV-22** and **IV-23** were synthesized reacting *p*-xylylenediamine with 5-[bis(4-methoxyphenyl)amino]-isophthaloyl chloride **II-48** and 5-ferrocenylisophthaloyl chloride **IV-25**, respectively, in presence of the thread and triethylamine as base under high dilution conditions.

The synthesis was particularly efficient for the ferrocene-containing [2]rotaxane **IV-23**, which was obtained in 41% yield, higher than other [2]rotaxanes obtained with the same thread, without using an excess of macrocycle precursors. A reversible oxidation was observed for [2]rotaxane **IV-23** by cyclic voltammetry and X-ray crystal structures for both the [2]rotaxanes **IV-22** and **IV-23** were obtained, proving the interlocked nature of the supramolecular assemblies.

In summary, the goal of this thesis was the synthesis and characterization of electroactive macrocycles and multifunctional NIR building blocks, and the application of those components in the construction of functional [2]rotaxanes has been shown. Improvement on the synthesis of versatile building blocks, alongside with electroactive macrocyclic molecules and NIR “clickable” components has also been reported. This thesis intends to be a solid starting point that can lead towards the construction of photoactive and electroactive mechanically interlocked molecules.

6. Experimental part

6.1 Solvents

Solvents of technical grade were distilled and dried prior to utilization. All manipulations were performed under a nitrogen atmosphere using standard techniques. Toluene was distilled over sodium, acetonitrile and dichloromethane were distilled over calcium hydride, THF was distilled over sodium/benzophenone and chloroform ExtraDry 99.9%, dimethylformamide ExtraDry 99.8% (DMF), dimethylsulfoxide ExtraDry 99.8% (DMSO), tetraethyl orthosilicate ExtraDry 99.9%, absolute ethanol (99.8%), anhydrous methanol (99.8%) were purchased from Sigma Aldrich and stored over molecular sieves. Deuterated solvents for NMR analysis were bought from Sigma-Aldrich. Deionized water was obtained by purification over an ion exchange column and a membrane filter of 0.45 μm (Micron separation, Inc.).

6.2 Thin layer chromatography and column chromatography

Thin layer chromatography was performed on silica gel 60 F254 sheets on aluminum produced by Merck. Spots on the TLC plate were observed under UV lamp (254 nm / 365 nm), while an appropriate staining agent, KMnO_4 solution, was employed for non-absorbing compounds.

Column chromatography for the separation of organic compounds was performed using silica gel from Merck with a particle size of 40 - 63 μm (230 - 400 mesh).

6.3 Nuclear magnetic resonance spectroscopy (NMR)

^1H and ^{13}C -NMR spectra were recorded at 600, 400, and 300 MHz at 295 K on a Bruker Avance 160 300 (^1H : 300 MHz, ^{13}C : 75 MHz), Avance II 400 (^1H : 400 MHz, ^{13}C : 100 MHz), and an Avance III 600 (^1H : 600 MHz, ^{13}C : 150 MHz) spectrometer. Chemical shifts are reported in ppm

(δ) and are referenced to the NMR solvent residual peaks (CD_2Cl_2 , CDCl_3 , Tetrahydrofuran- d^8 , CD_3OD , CD_3CN , $(\text{CD}_3)_2\text{SO}$) residual peak. Abbreviations used are s = singlet, d = doublet, t = triplet, q = quartet, dd = doublet of doublets, dt = doublet of triplets, td = triplet of doublets and m = multiplet. The coupling constants (J) are reported in Hertz (Hz).

6.4 Mass spectrometry

Mass spectrometry was performed by the “Centre d’Etude Structurale et d’Analyse des Molecules Organique” (CESAMO) at the University of Bordeaux, on a QStar Elite mass spectrometer (Applied Biosystems). ESI-QTOF mass spectra (including all HRMS) were performed on an instrument equipped with an ESI source and spectra were recorded in the positive mode. The electrospray needle was maintained at 5000 V and operated at room temperature. Samples were introduced by injection through a 20 μL sample loop into a 4500 $\mu\text{L}/\text{min}$ flow of methanol from the LC pump. ESI-MS experiments were performed on an ion trap spectrometer equipped with an electrospray ion source (ESI) and spectra were recorded in the positive mode. Field desorption (FD) spectra were recorded on a TOF mass spectrometer using an FD emitter with an emitter voltage of 10 kV. One to two microliters solution of the compound is deposited on a 13 μm emitter wire.

6.5 Electrochemistry

The glassy carbon working electrodes was polished in a figure of eight fashion using 1, 0.3 and 0.05 gamma alumina on a microcloth pad (Buehler, UK) (for 3,3 and 5 mins respectively). The electrodes were then sonicated in 1:1 ethanol/water for 5 mins before being finally washed in stream of dry tetrahydrofuran for 1 min.

The counter electrode was a silver wire which was cleaned by annealing with a Bunsen burner before quenching with dry tetrahydrofuran and was then used immediately. A Ag/AgCl reference electrode, stored in 3M KCl, and washed thoroughly in a stream of dry tetrahydrofuran water for 1

min before use was used initially before changing to a Ag wire pseudo reference electrode, heat annealed with a Bunsen burner and quenched with dry DCM. Both were used immediately after washing.

The supporting electrolytes were a solution of 0.1M TBAPF₆ or TBABF₄ and 1mM ferrocene (to act as an internal reference) dissolved in dry tetrahydrofuran and degassed with argon for 15 mins. All the macrocycles were dissolved in a 1mg/mL solution. This solution was subsequently sonicated for 10 mins.

6.6 Titrations

Titrations monitored by UV-visible: A solution (2.5 mL) of host (2.5×10^{-5} M, DCM) was introduced in a quartz cuvette at 20°C. Increasing aliquots (20 μ L) of guest stock solution (5 mM, DCM) were successively added until the final total volume reached 2.8 ml at maximum. The titration data (absorbance versus guest concentration) were fitted using the nonlinear curve-fitting procedure with a (1:1) binding equation using Letagrop program.²²⁵

Titrations monitored by ¹H-NMR: A solution (100 μ L) of host (5 mM, CDCl₃) was introduced in each NMR tube (12-13 experiments). Increasing aliquots of guest stock solution (0.2 M, CDCl₃) were added and the total volume (500 μ L) was adjusted with CDCl₃. The titration data (chemical shift versus guest equivalents) were fitted using the nonlinear curve-fitting procedure with a (1:1) binding equation.²²⁶

²²⁵ (a) L. G. Sillen and B. Warnquist, *Ark. Kemi.*, **1968**, *31*, 315.

b) L. G. Sillen and B. Warnquist, *Ark. Kemi.*, **1968**, *31*, 377.

c) J. Havel, Haltafalspefo program, Masaryk University, Brno, Maravia, Czech Republic.

²²⁶ P. Thordarson, *Chem. Soc. Rev.* **2011**, *40*, 1305

6.7 UV-Vis and Fluorescence

Electronic absorption spectra were measured on a Varian UV-Vis-NIR spectrophotometer Cary 5000 or Cary 100. The wavelengths observed ranged from 200 – 800 nm. Sample solutions were measured in matched quartz cells with a pathlength of 10 mm. Before each measurement a baseline of pure solvent was recorded, which was subtracted from the measured spectra. Fluorescence emission spectra were measured on a HORIBA Jobin-Yvon Fluorolog-3 equipped with a xenon lamp (450 W), with Hamamatsu R2658P and R928P photomultiplier (PMT) detection. Quartz cells of 10 mm length were employed for study of optically dilute samples with fluorescence emission being measured at a right angle with respect to the excitation beam. Time-correlated single photon counting was performed with a monochromatic pulsed light source (nanoLED 370 nm and 456 nm; 1.2 ns FWHM) on a Fluorolog-3 spectrofluorometer.

6.8 Single X-ray crystallographic information

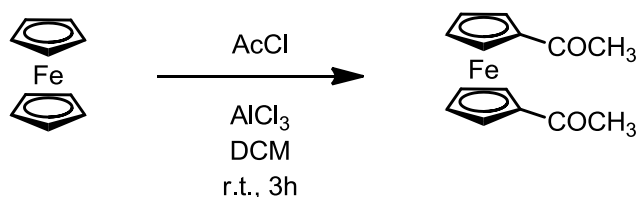
Crystals of compound **II-28**, **II-29**, **II-50**, **IV-22** and **IV-23** were mounted on a short glass fibre attached to a tapered copper pin. A full hemisphere of data were collected on a Brüker Nonius Kappa diffractometer fitted with a CCD based detector using $\text{CuK}\alpha$ radiation. The structures were solved by direct methods, completed by subsequent Fourier syntheses and refined with full-matrix least-squares methods against $|F^2|$ data. All non-hydrogen atoms were refined anisotropically. All hydrogen atoms were treated as idealized contributions.

6.9 Synthesis

Ferrocene, acetyl chloride, aluminum chloride, sodium hypochlorite, oxalyl chloride, 1,16-hexadecanedioic acid, 1,20-eicosadecanedioic acid, 4'-hydroxyacetophenone, benzaldehyde, diethylamine, nitromethane, ammonium acetate, boron trifluoride etherate complex, propargyl bromide (80% wt solution in toluene), potassium carbonate, cesium fluoride, methyl iodide, *tert*-

butyl bromoacetate, *p-tert*-butylbromobenzene, methyl *p-tert*-butylbenzoate, iodine, magnesium, dimethyl 5-aminoisophthalate, sodium nitrite, potassium iodide, 5-hydroxyisophthalic acid, triflic anhydride, 4-iodoanisole, cesium carbonate, copper(I) iodide, 3-bromopropan-1-ol, sodium azide, 4-toluenesulfonyl chloride, sodium iodide, diethyl malonate, urea, tetrakis(acetonitrile)copper(I) hexafluorophosphate, sodium hydride, 3-bromo-N,N-dimethylaniline, formaldehyde (37% wt in H₂O), *sec*-BuLi (1.3 M solution in cyclohexane/n-hexane 98:2 v/v), dimethyldichlorosilane, potassium permanganate, *tert*-BuLi (1.9 M solution in pentane), were purchased from the Sigma Aldrich, TCI Europe, Alfa Aesar, Fluorochem and Acros Chemicals and they were used as received. N,N-diisopropylethylamine and triethylamine were distilled over potassium hydroxide, 2,6-diaminopyridine was recrystallized from hot chloroform, phenol was recrystallized from hot toluene.

1,1'-Diacetyl ferrocene **II-22**

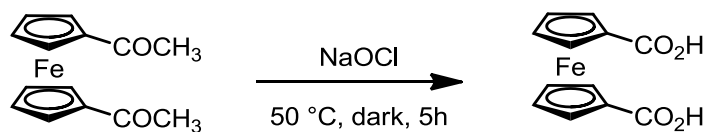


A solution of ferrocene **II-17** (5.58 g, 30 mmol) in DCM (30 mL) was added dropwise to a solution of acetyl chloride (6.42 mL, 90 mmol) and aluminum chloride (12 g, 90 mmol) in dry DCM (30 mL). The mixture was stirred at room temperature for 3 hours, then it was carefully poured into ice water (150 mL), filtered through neutral alumina and washed with chloroform until the red coloration disappeared. The biphasic mixture was extracted with chloroform (2 × 100 mL). The organic layer was washed with brine (150 mL), dried over Na₂SO₄ and the solvent was removed under vacuum. Purification by recrystallization (cyclohexane, 600 mL) afforded the **II-22** as red crystals (5.9 g, 73% yield).

¹H NMR (300 MHz, CDCl₃) δ 4.72 (s, 4H), 4.52 (s, 4H), 2.37 (s, 6H).

Analysis is in agreement with literature data (*Organometallics*, **2013**, 32, 5899).

1,1' - Ferrocenedicarboxylic acid **II-23**

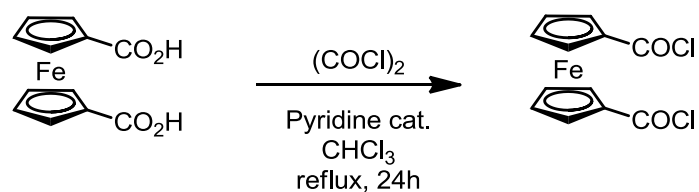


1,1'-Diacetylferrocene **II-22** (5.4 g, 20 mmol) was suspended in sodium hypochlorite solution (140 mL) and stirred in the dark at 50 °C. Three other portions of sodium hypochlorite solution (70 mL) were then added after 1.5, 2 and 3 hours. After the last addition, the mixture was stirred for another 2h in the dark at the same temperature. The resulting mixture was filtered hot, the red residue was redissolved in 2M sodium hydroxide (200 mL), sodium metabisulfite (10 g) was added and the clear orange solution was acidified with conc HCl until pH<1, an orange precipitate was obtained. Purification by recrystallization (acetic acid, 100 mL) afforded **II-23** as shiny red crystals (1.62 g, 30% yield).

¹H NMR (300 MHz, DMSO-d₆) δ 12.29 (br, s, 2H), 4.69 (s, 4H), 4.45 (s, 4H).

Analysis is in agreement with literature data (*Organometallics*, **2013**, 32, 5899).

1,1' - Ferrocenedicarboxyl chloride **II-24**

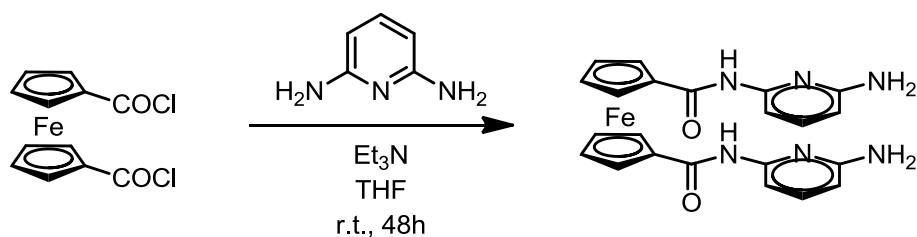


1,1'-Ferrocenedicarboxylic acid **II-23** (3.5 g, 12.8 mmol) was suspended in chloroform (13 mL), then pyridine (0.05 mL, 0.091 mmol) and oxalyl chloride (3.9 mL, 5.82 mmol) were added. The mixture was stirred at room temperature overnight, then the solvent and the volatiles were removed under vacuum. Purification by recrystallization (*n*-heptane, 100 mL) afforded **II-24** as dark red crystals (3.78 g, 95% yield).

¹H NMR (300 MHz, CDCl₃) δ 5.05 (s, 4H), 4.77 (s, 4H).

Analysis is in agreement with literature data (*Organometallics*, **2013**, 32, 5899).

Ferrocene-containing Hamilton-type acyclic receptor **II-25**

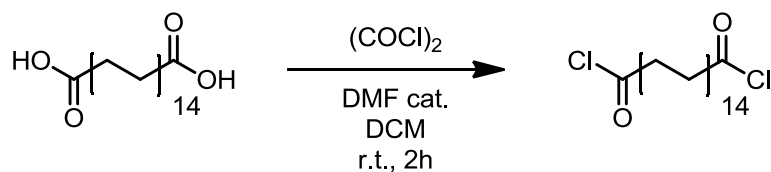


A solution of 1,1'-bis(chlorocarbonyl)ferrocene **II-24** (400 mg, 1.17 mmol) in dry DCM (30 mL) was added dropwise to a solution of 2,6-diaminopyridine (840 mg, 7.7 mmol) and triethylamine (0.39 mL, 2.77 mmol) in THF (30 mL) over 1h. The mixture was stirred at room temperature overnight, then the solution was washed with H₂O (2 × 100 mL) and brine (100 mL). The organic phase was dried over Na₂SO₄ and the solvent was removed. Purification by column chromatography (SiO₂, DCM:MeOH, 4:1, v/v) afforded **II-25** as orange solid (518 mg, 52% yield).

¹H NMR (300 MHz, CDCl₃) δ 8.15 (s, 2H), 7.56 (d, 2H), 7.41 (m, 2H), 6.22 (d, 2H), 4.83 (s, 4H), 4.48 (s, 4H).

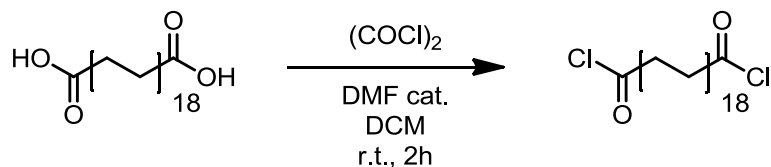
Analysis is in agreement with literature data (*Inorg. Chem.*, **1997**, 36, 2112).

1,16-Hexadecanedioyl dichloride II-26



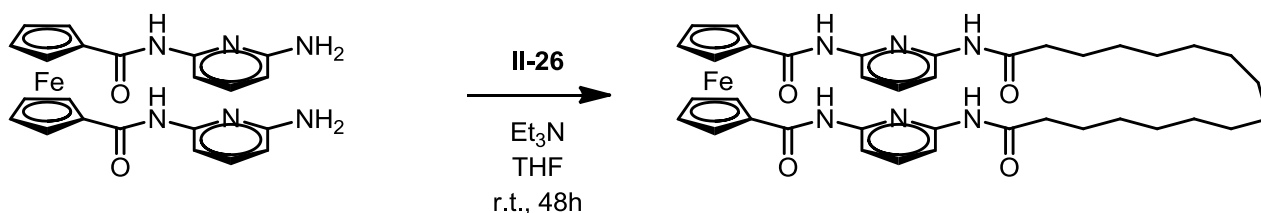
1,16-Hexanedioic acid (286 mg, 1 mmol) was suspended in DCM (10 mL), then oxalyl chloride (0.89 mL, 10.4 mmol) and DMF (2 drops) were added and stirred at room temperature overnight. The mixture was concentrated under reduced pressure to afford **II-26** as beige oil, which was used in the next step without further purification (323 mg, quantitative yield).

1,20-Eicosanedioyl dichloride II-27



1,20-Eicosanedioic acid (342 mg, 1 mmol) was suspended in DCM (10 mL), then oxalyl chloride (0.89 mL, 10.4 mmol) and DMF (2 drops) were added and stirred at room temperature overnight. The mixture was concentrated under reduced pressure to afford **II-27** as beige oil, which was used in the next step without further purification (379 mg, quantitative yield).

Ferrocene-containing Hamilton-type macrocycle **II-28**



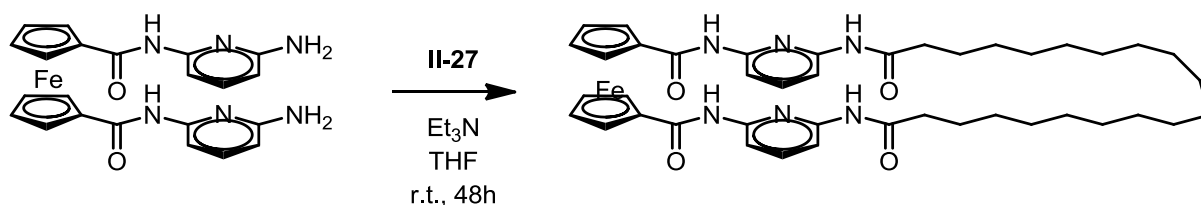
A solution of 1,1'-Bis[(((6-aminopyridyl)amino)carbonyl)]ferrocene **II-25** (456 mg, 1 mmol) and triethylamine (280 μ L, 2 mmol) in dry THF (100 mL) and a solution of 1,16-hexadecanedioyl dichloride **II-26** (323 mg, 1 mmol) in dry THF (100 mL) were added dropwise simultaneously to dry THF (50 mL) over 3 h. The mixture was stirred at room temperature for 4 days, then the solvent and the volatiles were removed under vacuum. The crude product was dissolved in chloroform (250 mL) and washed with a saturated solution of Na_2CO_3 (2×200 mL) and brine (200 mL). The organic phase was dried over MgSO_4 and the solvent was removed. Purification by column chromatography (SiO_2 , MeOH:DCM, 1:49, v/v) afforded **II-28** as an orange solid (179 mg, yield: 25%).

$^1\text{H NMR}$ (600 MHz, Acetic Acid - d_4): δ 7.96 - 7.66 (m, 6H), 5.19 - 5.16 (m, 4H), 4.70 - 4.68 (m, 4H), 2.52 (t, $J = 7.5$ Hz, 4H), 1.83 - 1.68 (m, 4H), 1.52 - 1.34 (m, 20H).

$^{13}\text{C NMR}$ (600 MHz, Acetic Acid - d_4): δ 174.1, 169.2, 148.6, 148.2, 142.6, 109.9, 76.1, 73.3, 70.5, 36.6, 28.4, 28.3, 28.2, 28, 27.7, 27.5, 24.6.

HRMS (ESI) calcd for $\text{C}_{38}\text{H}_{46}\text{N}_6\text{O}_4\text{NaFe}$ [$\text{M}+\text{Na}$] $^+$ $m/z = 729.2822$, found $m/z = 729.2836$.

Ferrocene-containing Hamilton-type macrocycle **II-29**



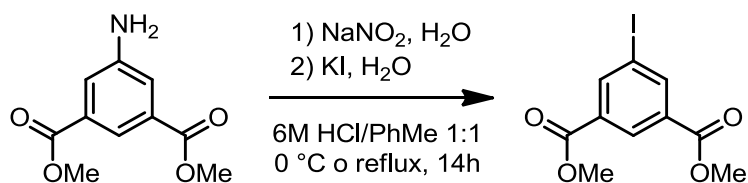
A solution of 1,1'-Bis[[(6-aminopyridyl)amino]carbonyl]ferrocene **II-25** (456 mg, 1 mmol) and triethylamine (280 μ L, 2 mmol) in dry THF (100 mL) and a solution of 1,20-eicosanedioyl dichloride **II-27** (379 mg, 1 mmol) in dry THF (100 mL) were added dropwise simultaneously to dry THF (50 mL) over 3 h. The mixture was stirred at room temperature for 4 days, then the solvent and the volatiles were removed under vacuum. The crude product was dissolved in chloroform (250 mL) and washed with a saturated solution of Na₂CO₃ (2 \times 200 mL) and brine (200 mL). The organic phase was dried over MgSO₄ and the solvent was removed. Purification by column chromatography (SiO₂, DCM:MeOH, 49:1, v/v) afforded **II-29** as an orange solid (225 mg, 29% yield).

¹H NMR (600 MHz, Acetic Acid - d₄): δ 7.84 - 7.68 (m, 6H), 5.17 (s, 4H), 4.69 (s, 4H), 2.52 (t, J = 6.8 Hz, 4H), 1.80 - 1.70 (m, 4H), 1.48 - 1.33 (m, 28H).

¹³C NMR (600 MHz, Acetic Acid - d₄): δ 174.1, 169.1, 148.5, 148.2, 142.6, 109.8, 76.2, 73.1, 70.6, 36.7, 28.8, 28.7, 28.5, 28.3, 28.1, 27.8, 27.7, 24.8.

HRMS (ESI) calcd for C₄₂H₅₄N₆O₄NaFe [M+Na]⁺ m/z = 785.3448, found m/z = 785.3459.

Dimethyl 5-iodoisophthalate **II-41**

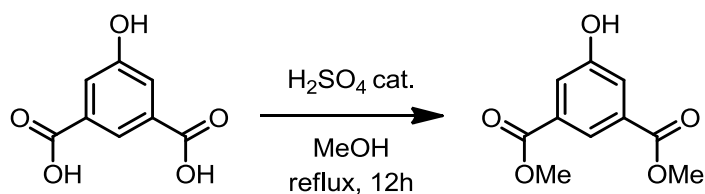


Dimethyl 5-aminoisophthalate **II-40** (26.15 g, 125 mmol) was suspended in conc. HCl (50 mL) and H₂O (50 mL), and cooled to 0° C. A solution of sodium nitrite (9 g, 125 mmol) in H₂O (150 mL) was then added dropwise at 0° C, then the reaction was stirred at the same temperature for 15 minutes. Toluene (200 mL) and a solution of potassium iodide (42 g, 250 mmol) in H₂O (100 mL) slowly added to the suspension. Following the addition, the suspension was stirred overnight at room temperature and afterwards heated for 1 h under reflux. The reaction mixture was cooled at room temperature, then the organic layer was separated, washed with H₂O (2 × 200 mL) and brine (100 mL). The organic phase was dried over Na₂SO₄ and the solvent was removed. Purification by recrystallization (methanol, 500 mL) afforded **II-41** as pale yellow crystals (35 g, 88% yield).

¹H NMR (300 MHz, acetone – d₆) δ 8.75 (s, 1H), 8.26 (s, 2H), 3.85 (s, 6H).

Analysis is in agreement with literature data (*Chem. Eur. J.*, **1999**, 5, 345).

Dimethyl 5-hydroxyisophthalate **II-45**

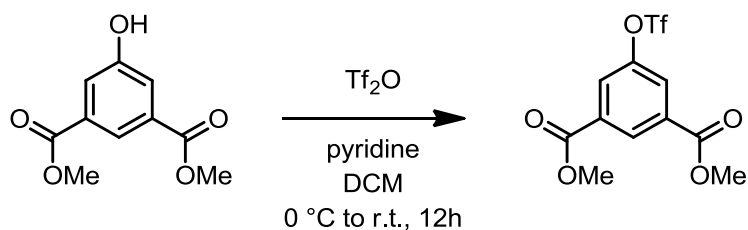


5-Hydroxyisophthalic acid (9.11 g, 50 mmol) was suspended in methanol (300 mL) at room temperature, then sulfuric acid (0.2 mL) was added and stirred at reflux overnight. After cooling to room temperature, the pale yellow solution was poured into ice H_2O (900 mL) and stirred vigorously for 1 hour. The white precipitate was filtered and washed with H_2O (500 mL). Purification by recrystallization (methanol, 200 mL) afforded **II-45** as white cotton-like crystals (10.5 g, quantitative yield).

$^1\text{H NMR}$ (300 MHz, acetone – d_6) δ 7.94 (s, 1H), 7.56 (m, 2H), 3.86 (s, 6H).

Analysis is in agreement with literature data (*J. Am. Chem. Soc.*, **2017**, 139, 335).

Dimethyl 5-[(trifluoromethylsulfonyl)oxy]isophthalate **II-46**

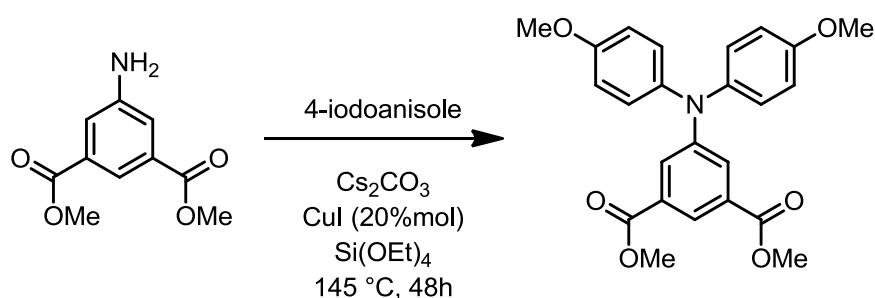


Dimethyl 5-hydroxyisophthalate **II-45** (2.1 g, 10 mmol) was suspended in dry DCM (10 mL) and cooled to 0°C . Pyridine was added (1.2 mL, 15 mmol), then triflic anhydride (2.5 mL, 15 mmol) was added dropwise at 0°C . The reaction mixture was stirred at room temperature overnight, then the organic layer was separated, washed with H_2O ($2 \times 200\text{ mL}$) and brine (100 mL). The organic phase was dried over Na_2SO_4 and the solvent was removed. Purification by recrystallization (hexane, 5 mL) afforded **II-46** as colorless crystals (3.3 g, 95% yield).

$^1\text{H NMR}$ (300 MHz, CDCl_3) δ 8.27 (s, 1H), 8.25 (m, 2H), 3.89 (s, 6H).

Analysis is in agreement with literature data (*Tetrahedron Lett.*, **2001**, 42, 547).

Dimethyl 5-(*N,N*-Bis(4-methoxyphenyl)amino)isophthalate **II-43**

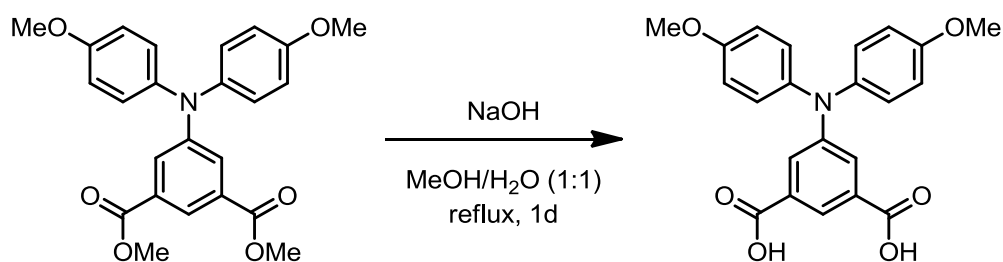


Dimethyl 5-aminoisophthalate **II-40** (4.18 g, 20 mmol), 4-iodoanisole (14.04 g, 60 mmol), cesium carbonate (13.04 g, 40 mmol) and copper(I) iodide (760 mg, 4 mmol) were suspended in dry degassed tetraethyl orthosilicate (100 mL) and stirred at 150 °C for 48 hours. The reaction mixture was cooled and diluted with AcOEt (100 mL) and EtOH (200 mL). NH₄F on silica gel (100 g) was added and the resulting slurry was stirred at room temperature for 5 hours. The mixture was filtered and the solvent was removed under reduced pressure. Purification by column chromatography (SiO₂, Pet.Ether/AcOEt 9:1 v/v), followed by recrystallization (EtOH, 5 mL) afforded the desired product **II-43** as yellow crystals (5.4 g, 65% yield).

¹H NMR (300 MHz, CDCl₃) δ 8.11 (s, 1H), 7.16 (d, , *J* = 8.8 Hz, 4H), 7.69 (s, 2H), 6.97 (d, *J* = 8.8 Hz, 4H), 3.89 (s, 6H), 3.81 (s, 6H).

Analysis is in agreement with literature data (*J. Org. Chem.* **2007**, 72, 4974).

5-(*N,N*-Bis(4-methoxyphenyl)amino)isophthalic acid **II-47**

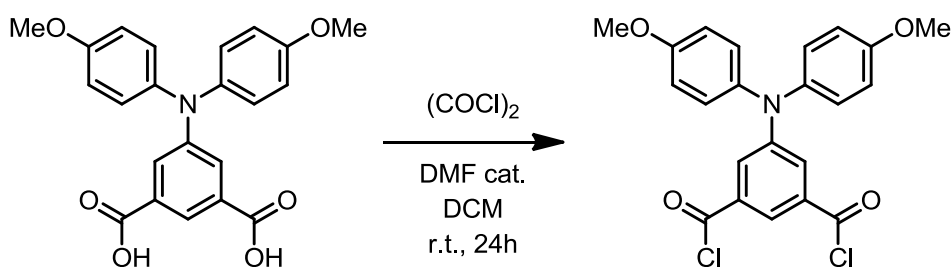


Dimethyl 5-(*N,N*-Bis(4-methoxyphenyl)amino)isophthalate **II-43** (2.34 g, 5.21 mmol) and sodium hydroxide (834 mg, 20.8 mmol) were suspended in a solution of methanol/water 9:1 (60 mL) and stirred at reflux overnight. The reaction mixture was cooled at room temperature, the organic solvent removed and the residue diluted with H₂O (50 mL). The clear yellow solution was acidified with conc.HCl until a yellow precipitate was obtained. The crude product was filtered and washed with H₂O (100 mL). Purification by recrystallization (EtOH, 10 mL) **II-47** as yellow crystals (1.78 g, 87% yield).

¹H NMR (300 MHz, DMSO-d₆) δ 8.11 (s, 1H), 7.16 (d, 4H, J=8.8 Hz), 7.69 (s, 2H), 6.97 (d, 2H, J=8.8 Hz), 3.81 (s, 6H).

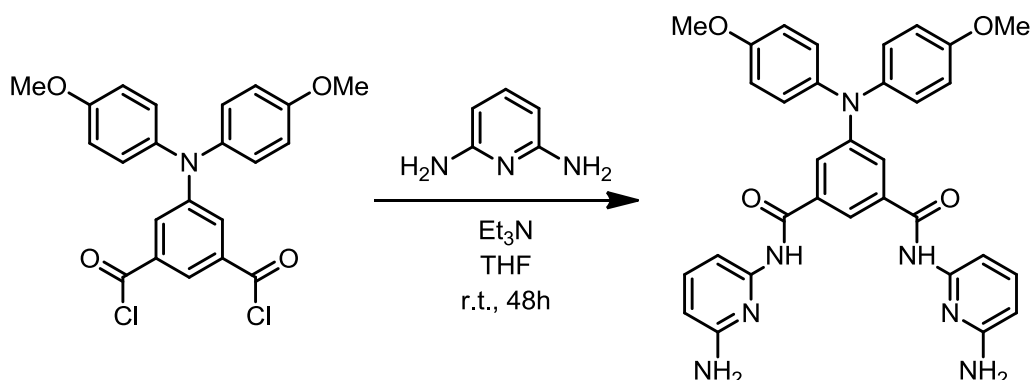
Analysis is in agreement with literature data (*J. Org. Chem.*, **2007**, 72, 4974).

5-(*N,N*-Bis(4-methoxyphenyl)amino)isophthalyl dichloride **II-48**



5-(*N,N*-Bis(4-methoxyphenyl)amino)isophthalic acid **II-47** (680 mg, 1.73 mmol) was suspended in DCM (10 mL), then oxalyl chloride (0.89 mL, 10.4 mmol) and a catalytic amount of DMF (2 drops) were added and stirred at room temperature overnight. The mixture was concentrated under reduced pressure to afford **II-48** as red oil, which was used in the next step without further purification (744 mg, quantitative yield).

N,N'*-Bis-(6-aminopyridin-2-yl)-5-(*N,N*-Bis(4-methoxyphenyl)amino)isophthalamide **II-49*



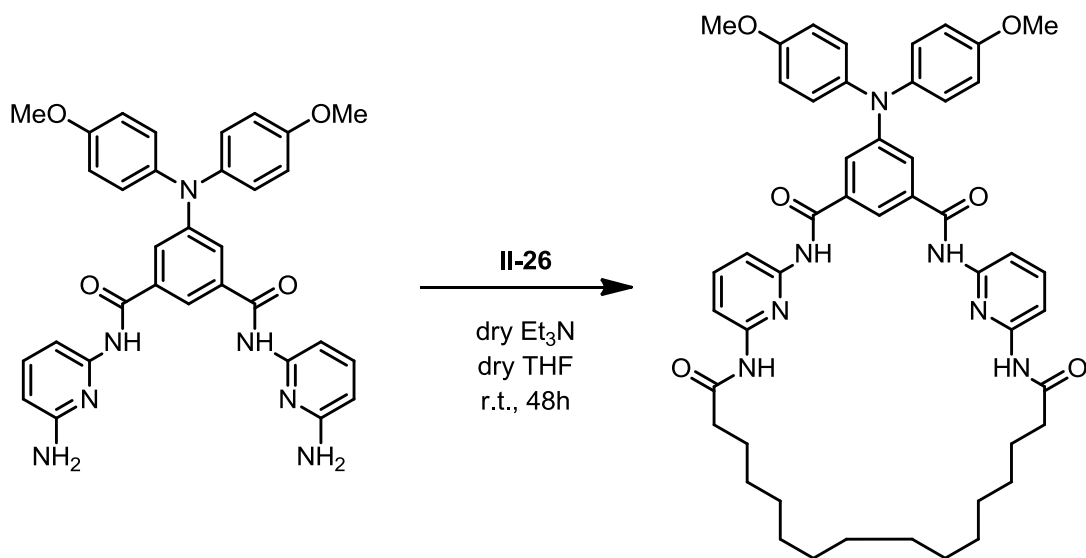
A solution of 5-(*N,N*-Bis(4-methoxyphenyl)amino)isophthalyl dichloride **II-48** (744 mg, 1.73 mmol) in dry THF (20 mL) was added dropwise to a solution of 2,6-diaminopyridine (1.13 g, 10.4 mmol) and dry triethylamine (0.53 mL, 3.81 mmol) in dry THF (10 mL) over 1h. The mixture was stirred at room temperature for 2 days, then the solvent and the volatiles were removed under vacuum. The crude product was dissolved in DCM (100 mL) and washed with a saturated solution of NaHCO_3 (2×100 mL) and brine (100 mL). The organic phase was dried over Na_2SO_4 and the solvent was removed. Purification by column chromatography (SiO_2 , DCM: MeOH, 49:1, v/v) afforded **II-49** as a yellow solid (518 mg, 52% yield).

^1H NMR (300 MHz, CDCl_3) δ 8.66 (s, 6H), 7.61 (s, 1H), 7.54 (d, $J = 7.8$ Hz, 6H), 7.45 (d, $J = 1.4$ Hz, 6H), 7.35 (t, $J = 8.0$ Hz, 6H), 6.97 – 6.86 (m, 4H), 6.78 – 6.67 (m, 4H), 6.15 (d, $J = 7.6$ Hz, 2H), 3.68 (s, 6H).

^{13}C NMR (76 MHz, CDCl_3) δ 165.02, 157.09, 156.67, 150.05, 149.77, 140.17, 139.48, 135.89, 127.15, 120.84, 115.65, 115.14, 104.74, 103.63, 55.43.

HRMS (ESI) calcd for $\text{C}_{32}\text{H}_{30}\text{N}_7\text{O}_4$ $[\text{M}+\text{H}]^+$ $m/z = 576.2353$, found $m/z = 576.2365$.

Triarylamine-containing Hamilton-type macrocycle **II-50**



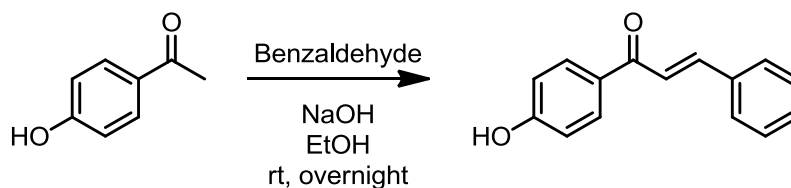
A solution of dichloride **II-26** (86.2 mg, 0.44 mmol) in dry THF (40 mL) and a solution of acyclic receptor **II-49** (255 mg, 0.44 mmol) and dry Et₃N (0.14 mL, 0.97 mmol) in dry THF (40 mL) were added simultaneously to dry THF (30 mL) over 48 hours. The mixture was stirred at room temperature for 2 days, then the solvent and the volatiles were removed under vacuum. The crude was dissolved in DCM (100 mL) and washed with a saturated solution of NaHCO₃ (2 × 100 mL) and brine (100 mL). The organic phase was dried over Na₂SO₄ and the solvent was removed. Purification by column chromatography (SiO₂, DCM:MeOH, 99:1, v/v) afforded **II-50** as a yellow solid (170 mg, 46% yield).

¹H NMR (600 MHz, CDCl₃) δ 8.20 (s, 2H), 8.06 - 7.98 (m, 4H), 7.77 (t, J = 8.1 Hz, 2H), 7.69 (d, J = 1.2 Hz, 2H), 7.62 (s, 2H), 7.32 (s, 1H), 7.14 - 7.08 (m, 4H), 6.92 - 6.86 (m, 4H), 3.82 (s, 6H), 2.41 (t, J = 7.5 Hz, 4H), 1.84 - 1.71 (m, 4H), 1.44 - 1.25 (m, 20H).

¹³C NMR (101 MHz, CDCl₃) δ 171.80, 165.10, 157.02, 150.71, 149.72, 149.40, 140.85, 138.99, 135.39, 127.44, 121.24, 115.21, 112.10, 109.93, 109.62, 55.44, 37.84, 28.68, 25.32.

HRMS (ESI) calcd for C₄₈H₅₅N₇O₆Na [M+Na]⁺ m/z = 848.4106, found m/z = 848.4112.

4'-Hydroxychalcone **III-24**

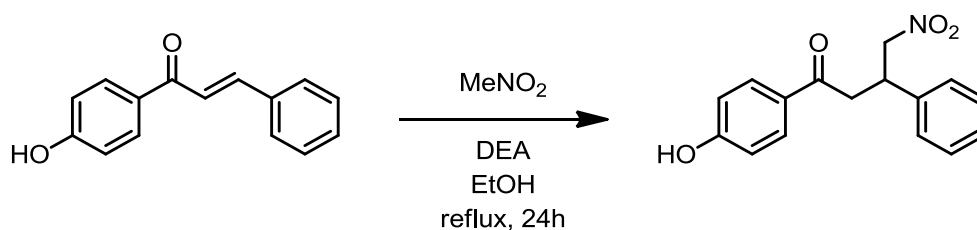


4'-Hydroxyacetophenone **III-23** (13.6 g, 100 mmol) and benzaldehyde (10.13 mL, 100 mmol) were dissolved in EtOH (200 mL), then 2M sodium hydroxide solution (200 mmol) was added. The reaction mixture was stirred at room temperature overnight, then it was diluted in distilled water (2 L) and concentrated hydrochloric acid until pH=0, where precipitation of a pale fluffy solid occurred. The heterogeneous mixture was stirred for 1 hour, then the crude was recovered by filtration and washed with distilled water (500 mL). Purification by recrystallization (EtOH, 200 mL) afforded **III-24** as yellow needles (21.3 g, 95% yield).

¹H NMR (300 MHz, acetone-d₆): δ = 7.99–8.04 (m, 2H), 7.77–7.84 (m, 1H), 7.60–7.68, (m, 2H), 7.5–7.58 (m, 1H), 7.39–7.45(m, 3H), 6.9–6.97 (m, 2H).

Analysis is in agreement with literature data (*Analyst*, **2015**,140, 4576).

1-4-Hydroxyphenyl-4-nitro-3-phenylbutan-1-one **III-25**

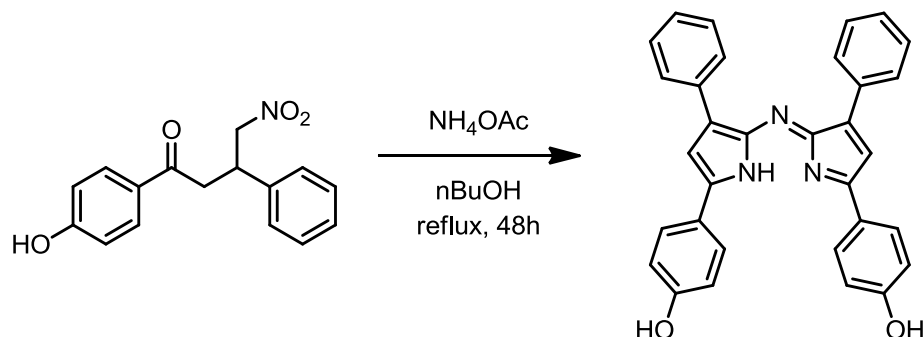


4'-Hydroxychalcone **III-24** (10 g, 44.6 mmol) was suspended in EtOH (70 mL), then diethylamine (23 mL, 223 mmol) and nitromethane (24 mL, 447 mmol) were added and the reaction mixture was stirred at reflux overnight. The reaction mixture was cooled at room temperature and concentrated under reduced pressure. The residue was partitioned between 4M HCl (100 mL) and AcOEt (100mL), the organic layer was separated, washed with brine (100 mL), dried over Na₂SO₄ and the solvent was removed under reduced pressure. Purification by trituration (cyclohexane/Et₂O, 9:1 v/v, 50 mL) afforded **III-25** as a beige powder (11.6 g, 91% yield).

¹H NMR (300 MHz, CDCl₃): δ 7.86 (d, *J* = 8.5 Hz, 2H), 7.35-7.26 (m, 5H), 6.85 (d, *J* = 8.5, 2H), 5.44 (s, 1H), 4.86-4.80 (m, 1H), 4.64-4.71 (m, 1H), 4.25-4.16 (m, 1H), 3.46-.31(m, 2H).

Analysis is in agreement with literature data (*Org. Lett.*, **2009**, *11*, 5386).

[5-(4-Hydroxyphenyl)-3-phenyl-1H-pyrrol-2-yl]-[5-(4-hydroxyphenyl)-3-phenylpyrrol-2-ylidene]amine **III-26**

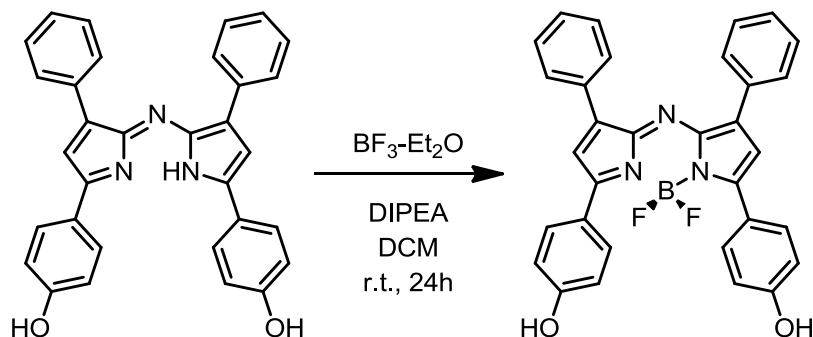


Ammonium acetate (61.5 g, 800 mmol) and 1-(4-hydroxyphenyl)-4-nitro-3-phenylbutan-1-one **III-25** (5.7 g, 20 mmol) were suspended in n-butanol (200 mL). The mixture was stirred at reflux for 48h, then cooled at room temperature, concentrated under reduced pressure and kept in the fridge overnight. The mixture was filtered and the solid washed with cold EtOH (50 mL) and n-pentane (200 mL). **III-26** was obtained as dark blue powder (2.3 g, 24% yield).

$^1\text{H NMR}$ (300 MHz, MeOD-d_4): δ 7.99 (d, $J = 6.6$ Hz, 4H), 7.79 (d, $J = 8.7$ Hz, 4H), 7.36-7.29 (m, 6H), 7.20 (s, 2H), 6.92 (d, $J = 8.7$ Hz, 4H).

Analysis is in agreement with literature data (*Org. Lett.*, **2009**, *11*, 5386).

BF₂ Chelate of [5-(4-hydroxyphenyl)-3-phenyl-1H-pyrrol-2-yl]-[5-(4-hydroxyphenyl)-3-phenylpyrrol-2-ylidene]amine **III-27**

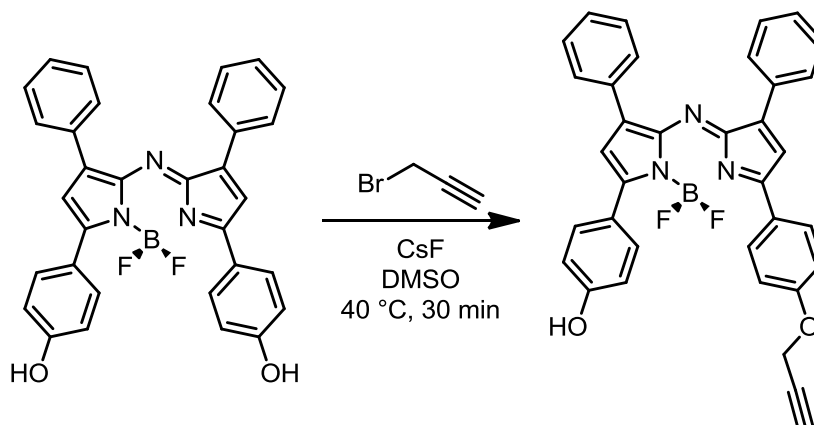


[5-(4-Hydroxyphenyl)-3-phenyl-1H-pyrrol-2-yl]-[5-(4-hydroxyphenyl)-3-phenylpyrrol-2-ylidene]amine **III-26** (1.5 g, 3.1 mmol) and N,N-diisopropylethylamine (5.4 mL, 31 mmol) were dissolved in DCM (150 mL), then boron trifluoride etherate complex (5.5 mL, 43.5 mmol) was added. The solution was stirred at room temperature overnight, then the mixture was diluted with AcOEt (300 mL) and washed with brine (300 mL). The organic phase was dried over Na₂SO₄ and the solvent was removed. Purification by column chromatography (SiO₂, DCM/AcOEt 4:1 v/v) afforded **III-27** as a red metallic solid (1.58 g, 90% yield).

¹H NMR (300 MHz, MeOD-d₄): δ 8.08-8.05 (m, 8H), 7.40-7.30 (m, 6H), 7.20 (s, 2H), 6.9-6.88 (m, 4H).

Analysis is in agreement with literature data (*Org. Lett.*, **2009**, *11*, 5386–5389).

BF₂ Chelate of 4-{4-phenyl-5-[3-phenyl-5-(4-prop-2-ynoxyphenyl)-pyrrol-2-ylideneamino]-1H-pyrrol-2-yl}phenol **III-28**

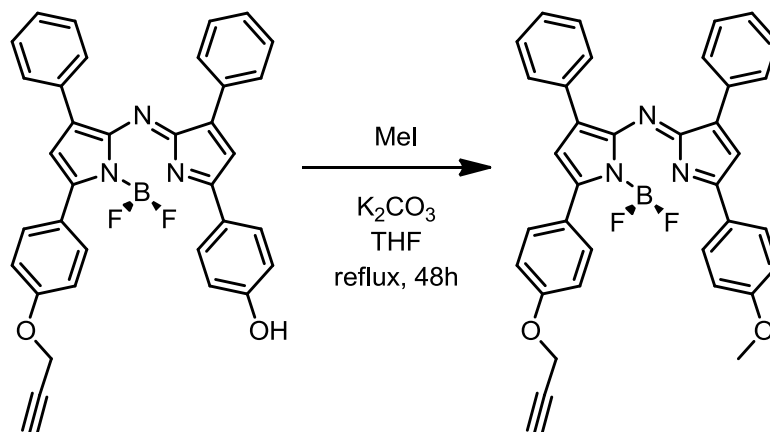


[5-(4-Hydroxyphenyl)-3-phenyl-1H-pyrrol-2-yl]-[5-(4-hydroxyphenyl)-3-phenylpyrrol-2-ylidene]amine BF₂-chelate **III-27** (1.06 g, 2 mmol) and caesium fluoride (53 mg, 2.2 mmol) were dissolved in DMSO (25 mL), then propargyl bromide (80% wt in PhMe, 0.4 mL, 2.2 mmol) was added. The solution was stirred at 40 °C for 30 minutes, then the mixture was cooled in an ice bath to 0°C, a saturated solution of NH₄Cl (30 mL) was added and the product extracted with ethyl acetate (2 × 30 mL). The combined organic layers were washed with brine, dried over anhydrous Na₂SO₄, filtered and concentrated under reduced pressure. Purification by column chromatography (SiO₂, DCM 100% to DCM/ethyl acetate 9:1, v/v) afforded **III-28** as a red metallic solid (1.58 g, 90% yield).

¹H NMR (300 MHz, CDCl₃) δ 8.18 – 7.99 (m, 8H), 7.56 – 7.41 (m, 6H), 7.12 (d, *J* = 9.0 Hz, 2H), 7.06 (s, 2H), 6.93 (d, *J* = 8.8 Hz, 2H), 4.79 (d, *J* = 2.4 Hz, 2H), 2.60 (t, *J* = 2.4 Hz, 1H).

Analysis is in agreement with literature data (*Org. Lett.*, **2009**, *11*, 5386–5389).

BF₂ chelate of [5-(4-methoxyphenyl)-3-phenyl-1H-pyrrol-2-yl]-[5-(4-propargyloxyphenyl)-3-phenylpyrrol-2-ylidene]amine **III-29**



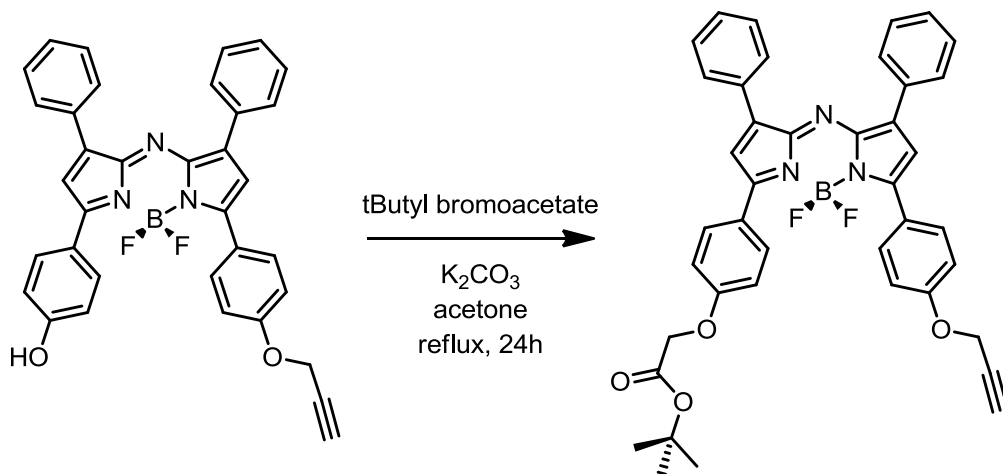
BF₂ Chelate of 4-{4-phenyl-5-[3-phenyl-5-(4-prop-2-ynyloxyphenyl)-pyrrol-2-ylideneamino]-1H-pyrrol-2-yl}phenol **III-28** (100 mg, 0.17 mmol) and potassium carbonate (536 mg, 3.8 mmol) were dissolved in dry THF (10 mL), then methyl iodide was added (0.25 mL). The solution was stirred at reflux for 2 days, then the mixture was poured into 1M aqueous sodium hydroxide solution (100 mL) and extracted with DCM (2 × 50 mL) and washed with brine (100 mL). The organic layer was dried over Na₂SO₄, filtered and the solvent removed. Purification by column chromatography (SiO₂, DCM) afforded **III-29** as a red metallic solid (56 mg, 57% yield).

¹H NMR (600 MHz, CDCl₃) δ 8.15 – 8.07 (m, 8H), 7.52 – 7.41 (m, 6H), 7.13 – 7.10 (m, 2H), 7.08 (s, 1H), 7.06 – 7.03 (m, 3H), 4.80 (d, *J* = 2.4 Hz, 2H), 3.92 (s, 3H), 2.60 (t, *J* = 2.4 Hz, 1H).

¹³C NMR (151 MHz, CDCl₃) δ 163.45, 161.10, 160.07, 159.04, 146.93, 146.59, 144.92, 144.43, 133.91, 133.80, 133.09, 132.88, 130.69, 130.66, 130.59, 129.95, 126.46, 125.42, 120.23, 119.92, 116.41, 115.68, 79.44, 77.43, 57.25, 56.83.

HRMS (ESI) calcd for C₃₆H₂₆BN₃O₂F₂Na [M+Na]⁺ *m/z* = 604.1978, found *m/z* = 604.1963.

BF₂ chelate of [5-(4-methoxyphenyl)-3-phenyl-1H-pyrrol-2-yl]-[5-(4-propargyloxyphenyl)-3-phenylpyrrol-2-ylidene]amine III-30



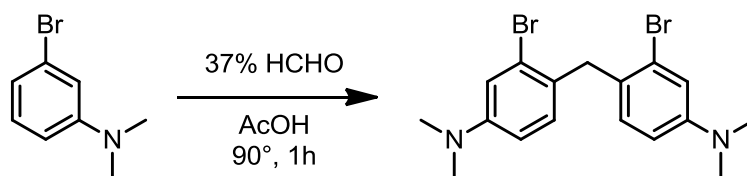
BF₂ Chelate of 4-{4-phenyl-5-[3-phenyl-5-(4-prop-2-ynyloxyphenyl)-pyrrol-2-ylideneamino]-1H-pyrrol-2-yl}phenol **III-28** (113 mg, 0.2 mmol) and potassium carbonate (138 mg, 1 mmol) were dissolved in acetone (10 mL), then *tert*-butylbromoacetate (0.05 mL, 0.3 mmol). The solution was stirred at reflux overnight, then the mixture was cooled, the solvent was removed and the crude was redissolved in DCM (25 mL). The organic layer was washed with water (50 mL) and brine (50 mL), dried over Na₂SO₄, filtered the solvent removed. Purification by column chromatography (SiO₂, DCM) afforded **III-30** as a red metallic solid (95 mg, 70% yield).

¹H NMR (600 MHz, CDCl₃) δ 8.17 - 8.04 (m, 8H), 7.52 - 7.39 (m, 6H), 7.11 (d, *J* = 8.9 Hz, 4H), 7.06 (s, 2H), 7.03 (d, *J* = 8.9 Hz, 4H), 4.79 (d, *J* = 2.3 Hz, 2H), 4.62 (s, 2H), 2.60 (t, *J* = 2.3 Hz, 1H), 1.53 (s, 9H).

¹³C NMR (151 MHz, CDCl₃) δ 167.54, 160.21, 159.84, 158.20, 158.10, 145.42, 143.43, 143.38, 132.44, 131.64, 131.62, 131.59, 129.32, 128.59, 124.96, 118.73, 115.06, 114.85, 82.75, 78.04, 76.10, 65.67, 55.89, 28.08.

HRMS (ESI) calcd for C₄₁H₃₄BN₃O₄F₂Na [M+Na]⁺ *m/z* = 704.2502, found *m/z* = 704.2492.

4,4'-methylenebis(3-bromo-N,N-dimethylaniline) **III-36**



3-Bromo-N,N-dimethylaniline **III-35** (6 g, 30 mmol) was dissolved in acetic acid (60 ml), then 37% aqueous formaldehyde solution (11.1 ml, 150 mmol) was added and the reaction mixture was stirred at 90 °C for 1 hour. After cooling, acetic acid was evaporated, then saturated aqueous sodium bicarbonate solution (100 mL) was added carefully. The aqueous layer was extracted with AcOEt (3 × 100 mL), and the combined organic phase was washed with water (100 mL) and brine (100 mL), dried over Na₂SO₄, filtered and the solvent removed. Purification by column chromatography (SiO₂, *n*-hexane/AcOEt 19:1 to 9:1, v/v) afforded **III-36** as a pink crystalline solid (5.4 g, 88% yield).

¹H NMR (300 MHz, CDCl₃): δ 6.94 (d, 2H, *J* = 2.7 Hz), 6.85 (d, 2H, *J* = 8.6 Hz), 6.59 (dd, 2H, *J* = 8.6, 2.6 Hz), 4.00 (s, 2H), 2.92 (s, 12H).

Analysis is in agreement with literature data (*Nat. Chem.*, **2013**, 5, 132).

2,7-Bis(dimethylamino)-9,9-dimethyl-9-silaanthracen-10(9H)-one III-38

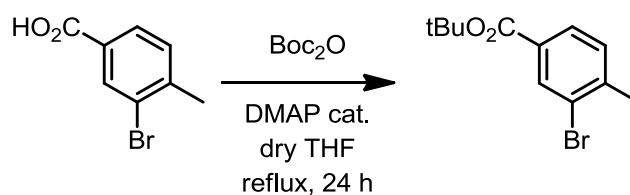


4,4'-Methylenebis(3-bromo-N,N-dimethylaniline) **III-36** (4.12 g 10 mmol) was dissolved in dry THF (100 ml) and stirred at -80 °C. *sec*-BuLi (1.3 M solution in cyclohexane/*n*-hexane 98:2 v/v, 20 mL, 26 mmol) was slowly added for 30 min to the solution and stirred for further 15 min at the same temperature. Dichlorodimethylsilane (1.8 mL, 15 mmol) was added to the reaction mixture and stirred at room temperature overnight. 1M HCl aqueous solution (100 mL) was added carefully to neutralize the solution, and solvent was evaporated. The resulting aqueous solution was extracted with ethyl acetate (3 × 50 mL), and the organic phase was washed with saturated aqueous sodium bicarbonate solution (100 mL), water (100 mL) and brine (100 mL), dried over Na₂SO₄, filtered and the solvent removed. The crude **III-37** was dissolved in degassed acetone (30 mL) at 0 °C, then KMnO₄ powder (9.48 g, 60 mmol) was added portionwise over 1 hour, and the reaction mixture was stirred for 5 hours at the same temperature. The purple suspension was filtered through a Celite pad and washed with chloroform (100 mL). The yellow filtrate was dried over MgSO₄, filtered and the solvent removed. Purification by column chromatography (SiO₂, petroleum ether/ethyl acetate 3:1, v/v), followed by reprecipitation (*n*-hexane) afforded the desired product **III-38** as a yellow crystalline solid (1.62 g, 50% yield over two steps)

¹H NMR (300 MHz, CDCl₃) δ 8.44 (d, 2H, *J* = 8.9 Hz), 6.87 (dd, 2H, *J* = 9.0 Hz, 2.4 Hz), 6.83 (d, 2H, *J* = 2.4 Hz), 3.12 (s, 12H), 0.51 (s, 6H).

Analysis is in agreement with literature data (*Nat. Chem.*, **2013**, 5, 132).

tert*-Butyl 3-bromo-4-methylbenzoate **III-40*

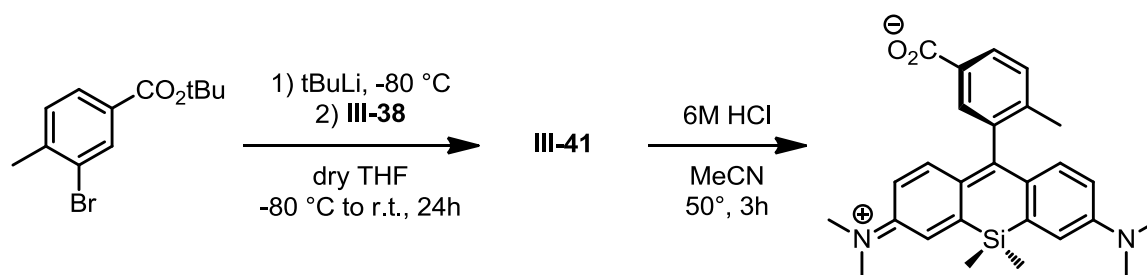


3-Bromo-4-methylbenzoic acid **III-39** (2.15 g, 10 mmol), (Boc)₂O (5.45 g, 25 mmol) and DMAP (122 mg, 1 mmol) were dissolved in dry THF (20 ml) and refluxed overnight. After cooling to room temperature and evaporation of the solvent, the residue was redissolved in diethyl ether (50 ml) and washed with saturated aqueous sodium bicarbonate solution (50 mL), water (50 mL) and brine (50 mL). The organic layer was dried over Na₂SO₄, filtered and the solvent removed. Purification by column chromatography (SiO₂, petroleum ether/ethyl acetate 95:5, v/v) afforded **III-40** as a colourless oil (2.63 g, 97% yield).

¹H NMR (300 MHz, CDCl₃) δ 8.44 (d, 2H, *J* = 8.9 Hz), 6.87 (dd, 2H, *J* = 9.0 Hz, 2.4 Hz), 6.83 (d, 2H, *J* = 2.4 Hz), 3.12 (s, 12H), 0.51 (s, 6H).

Analysis is in agreement with literature data (*Nat. Chem.*, **2013**, 5, 132).

Carboxyl-methyl silicon rhodamine **III-34**



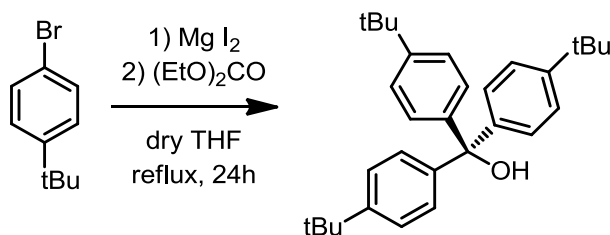
Ester **III-40** (542 mg, 2 mmol) was dissolved in dry THF (10 ml) and cooled at -80 °C. *tert*-BuLi (1.9 M in pentane, 2 mL, 3.8 mmol) was slowly added dropwise and the solution was stirred at the same temperature for 15 min. Ketone **III-38** (162 mg, 0.5 mmol) in dry THF (10 ml) was then added dropwise at -80 °C and the solution was let warming to room temperature overnight. 0.1 M aqueous hydrochloric acid was added to the reaction mixture and the resulting intense blue solution was poured into saturated aqueous sodium bicarbonate solution and extracted with DCM (3 × 100 mL). The organic layer was dried over MgSO₄, filtered and the solvent removed.

Crude **III-41** was dissolved in MeCN (15 ml), then 6M aqueous hydrochloric acid (50 ml) was added and stirred at 50 °C for 3 hours. After cooling to room temperature, the solution was poured into 0.1 M aqueous sodium hydroxide solution (200 mL) and extracted with DCM (4 × 100 mL). The organic layer was dried over MgSO₄, filtered and the solvent removed. Purification by column chromatography (DCM/MeOH 9:1, v/v) afforded **III-34** as a blue solid (177 g, 80% yield over two steps).

¹H NMR (300 MHz, MeOD-d₄) δ 8.12 (d, *J* = 7.3 Hz, 1H), 7.77 (s, 1H), 7.49 (d, *J* = 7.6 Hz, 1H), 7.39 (s, 2H), 7.07 (d, *J* = 9.5 Hz, 2H), 6.78 (d, *J* = 9.6 Hz, 2H), 3.37 (s, 12H), 2.10 (s, 3H), 0.65 (s, 3H), 0.63 (s, 3H).

Analysis is in agreement with literature data (*Nat. Chem.*, **2013**, 5, 132).

Tri-(4-*tert*-butylphenyl)methanol **III-44**

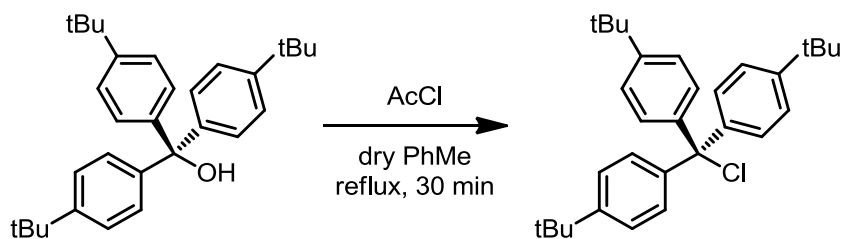


1-Bromo-4-*tert*-butylbenzene **III-43** (62 mL, 330 mmol) in THF (200 mL) was added dropwise to a suspension of magnesium turnings (9.7 g, 400 mmol) and iodine (few crystals) in THF (200 mL). The mixture was stirred at reflux for 1 h. Then diethyl carbonate (12.1 mL, 100 mmol) in THF (50 mL) was added dropwise to the mixture over 1 hour. The mixture was stirred at reflux overnight, then a saturated aqueous ammonium chloride solution (500 mL) was added and the reaction mixture was extracted with diethyl ether (2 × 200 mL). The organic layer was washed with brine (500 mL), dried over Na₂SO₄, filtered and the solvent was removed. Purification by recrystallization (*n*-hexane, 500 mL) afforded tri-(4-*tert*-butylphenyl)methanol **III-44** as a white crystalline powder (36.4 g, 85% yield).

¹H NMR (300 MHz, CDCl₃) δ 7.31 (d, *J* = 8.5 Hz, 6H), 7.19 (d, *J* = 8.5 Hz, 6H), 1.31 (s, 27H).

Analysis is in agreement with literature data (*Angew. Chem. Int. Ed.*, **2014**, 53, 9860).

Tri-(4-*tert*-butylphenyl)methyl chloride **III-45**

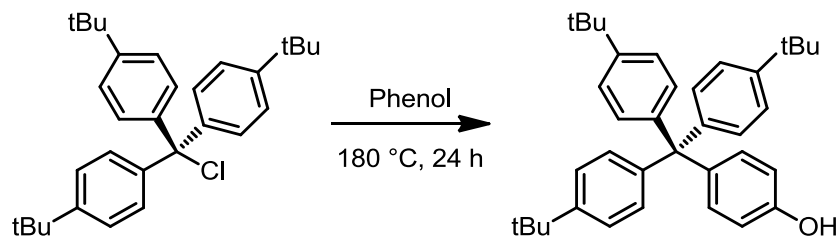


Tri-(4-*tert*-butylphenyl)methanol **III-44** (42.8 g, 100 mmol) was dissolved in dry toluene (100 mL), then acetyl chloride (17.8 mL, 250 mmol) was added. The reaction mixture was heated under reflux for 30 min. After the solution was allowed to cool down to ambient temperature, *n*-hexane (200 mL) was added and the flask was left at 4 °C overnight. The resulting precipitate was filtered and washed with pentane (500 mL). Tri-(4-*tert*-butylphenyl)methyl chloride **III-45** was obtained as a white crystalline powder (44.7 g, quantitative yield).

$^1\text{H NMR}$ (300 MHz, CDCl_3) δ 7.31 (d, $J = 8.5$ Hz, 6H), 7.19 (d, $J = 8.5$ Hz, 6H), 1.31 (s, 27H).

Analysis is in agreement with literature data (*Angew. Chem. Int. Ed.*, **2014**, 53, 9860).

4-[Tris-(4-*tert*-butyl-phenyl)-methyl]phenol **III-42**

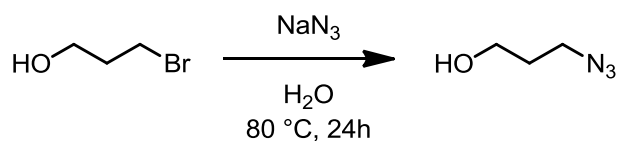


Tri-(4-*tert*-butylphenyl)methyl chloride **III-45** (13.4 g, 30 mmol) and freshly recrystallized phenol (56.4 g, 600 mmol) were charged in a 250 mL flask. The mixture was stirred at 180 °C overnight, then toluene (200 mL) was added while cooling and washed with a 2M aqueous sodium hydroxide solution (3 × 100 mL) and brine (2 × 100 mL). The organic phase was dried over Na₂SO₄ and the solvent was removed. Purification by boiling the crude residue in n-hexane (500 mL) afforded 4-[tris-(4-*tert*-butyl-phenyl)-methyl]phenol **III-42** as a beige solid (11.3 g, 75% yield).

¹H NMR (300 MHz, CDCl₃) δ 7.31 (d, *J* = 8.5 Hz, 6H), 7.19 (d, *J* = 8.5 Hz, 6H), 7.1 (d, *J* = 8.6 Hz, 6H), 6.84 (d, *J* = 8.9 Hz, 2H), 1.35 (s, 27H)

Analysis is in agreement with literature data (*J. Org. Chem.*, **1993**, 58, 3748).

3-Azidopropan-1-ol **III-47**

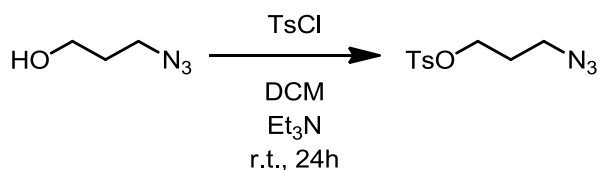


3-Bromopropan-1-ol **III-46** (27.8 mL, 200 mmol) was suspended in water (400 mL), then sodium azide (19.5 g, 300 mmol) was added. The reaction mixture was stirred at 80 °C overnight, then it was cooled and then extracted with AcOEt (5 × 100 mL). The combined organic layers were washed with brine (500 mL), and dried with MgSO₄. Solvent removal afforded the desired product **III-47** as a slightly yellow oil (20.2 g, quantitative yield).

¹H NMR (300 MHz, CDCl₃): δ 3.69 (t, *J* = 6.3 Hz, 2H), 3.41 (t, *J* = 6.6 Hz, 2H), 1.79 (qu, *J* = 6.6 Hz, 2H).

Analysis is in agreement with literature data (*Org. Lett.*, **2014**, *16*, 1358).

3-Azidopropyl-4-methylbenzenesulfonate **III-48**



3-Azidopropanol **III-47** (10.1 g, 100 mmol) and Et₃N (27.8 mL, 200 mmol) were dissolved in DCM (200 mL), then tosyl chloride (20.9 g, 110 mmol) was added. The reaction mixture was stirred at room temperature overnight, the crude was isolated upon quenched with water (200 mL), followed by extraction with DCM (4 × 100 mL). The organic layer was separated and dried over MgSO₄. Purification by column chromatography (SiO₂, petroleum ether/DCM 9:1, v/v) afforded 3-azidopropyl-4-methylbenzenesulfonate **III-48** as a slightly yellow oil (23 g, 90% yield).

¹H NMR (300 MHz, CDCl₃): δ 7.82 (d, *J* = 8.3 Hz, 2H), 7.39 (d, *J* = 8.3 Hz, 2H), 4.12 (t, *J* = 5.9 Hz, 2H), 3.46 (t, *J* = 6.5 Hz, 2H), 2.48 (s, 3H), 1.98 – 1.79 (m, 2H).

Analysis is in agreement with literature data (*Org. Lett.*, **2014**, *16*, 1358).

1-Azido-3-iodopropane **III-49**

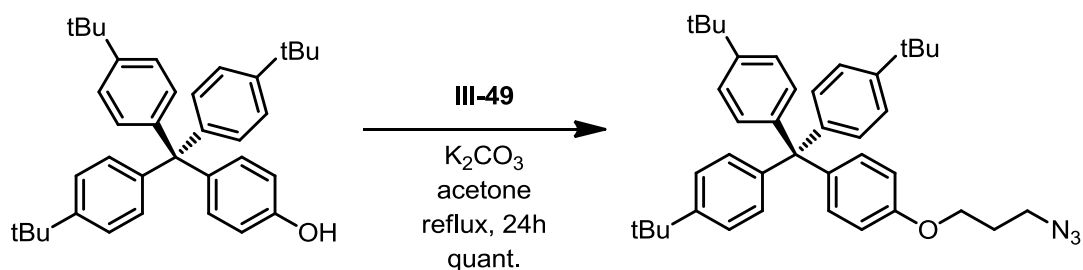


3-Azidopropyl-4-methylbenzenesulfonate **III-48** (5.1 g, 20 mmol) was dissolved in acetone (100 mL), then sodium iodide (3.3 g, 22 mmol) was added. The reaction mixture was stirred at reflux overnight. The white suspension was filtered, washed with acetone (50 mL) and the solvent was removed. The crude was redissolved in diethyl ether (100 mL) was added and the organic layer was washed with water (3 × 100 mL). The organic layer was dried with MgSO₄ and the solvent was removed. The 1-azido-3-iodopropane **III-49** was obtained as slightly yellow oil (4.2 g, quantitative yield) and used immediately in the next step due to its instability.

¹H NMR (300 MHz, CDCl₃): δ 3.46 (t, *J* = 6.3 Hz, 2H), 3.27 (t, *J* = 6.6 Hz, 2H), 2.06 (m, 2H).

Analysis is in agreement with literature data (*Org. Lett.*, **2014**, *16*, 1358).

Azide trityl stopper **III-50**

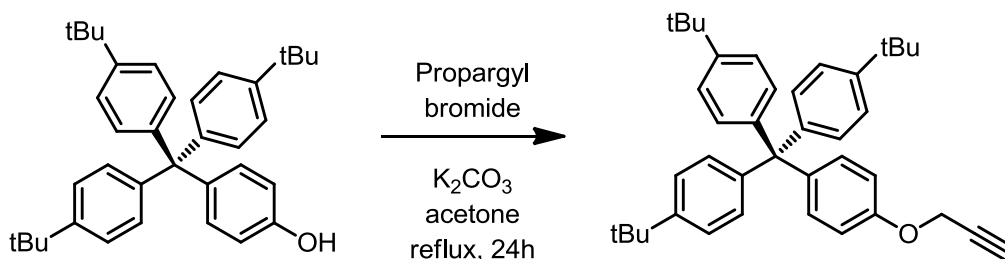


4-[tris-(4-tert-butyl-phenyl)-methyl]phenol **III-42** (5 g, 10 mmol) was dissolved in acetone (50 mL), then anhydrous potassium carbonate (2.76 g, 20 mmol) and 1-azido-3-iodopropane **III-49** (2.5 g, 12 mmol) were added. The suspension was stirred at reflux overnight, then the solvent was removed, water (100 mL) was added and extracted with DCM (4 × 50 mL). The organic phase was dried over Na_2SO_4 and the solvent was removed. Purification by column chromatography (SiO_2 , petroleum ether/DCM 7:3 v/v) afforded the azide trityl stopper **III-50** as a white solid (5.8 g, quantitative yield).

1H NMR (300 MHz $CDCl_3$): δ 7.30 (d, $J = 8.6$ Hz, 6H); 7.09 (d, $J = 8.9$ Hz, 2H); 7.07 (d, $J = 8.6$ Hz, 6H); 6.76 (d, $J = 8.9$ Hz, 2H); 4.02 (d, $J = 6.0$ Hz, 2H); 3.51 (d, $J = 6.7$ Hz, 2H); 2.05 (m, 2H); 1.30 (s, 27H).

Analysis is in agreement with literature data. (*J. Am. Chem. Soc.* **2006**, 128, 2186.)

Alkyne trityl stopper II-14

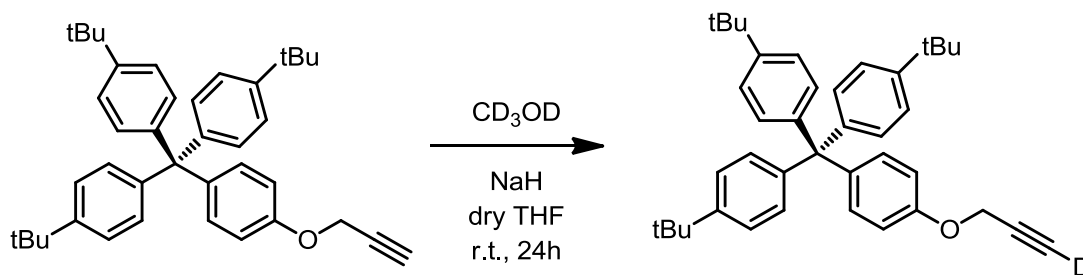


4-[tris-(4-tert-butyl-phenyl)-methyl]phenol **III-42** (5 g, 10 mmol) was dissolved in acetone (50 mL), then anhydrous potassium carbonate (2.76 g, 20 mmol) and propargyl bromide (80% wt in PhMe, 12 mmol) were added. The suspension was stirred at reflux overnight, then the solvent was removed, water (100 mL) was added and extracted with DCM (4 × 50 mL). The organic phase was dried over Na₂SO₄ and the solvent was removed. Purification by recrystallization (CHCl₃/MeCN 95:5 v/v, 100 mL) afforded the alkyne trityl stopper **II-14** as a white solid (4.7 g, 90% yield).

¹H NMR (300 MHz CDCl₃): δ 7.23 (d, *J* = 8.6 Hz, 6H), 7.11 (d, *J* = 8.9 Hz, 2H), 7.07 (d, *J* = 8.6 Hz, 6H), 6.84 (d, *J* = 8.9 Hz, 2H), 4.66 (d, *J* = 2.4 Hz, 2H), 2.51 (t, *J* = 2.4 Hz, 1H), 1.30 (s, 27H).

Analysis is in agreement with literature data (*J. Am. Chem. Soc.*, **2006**, *128*, 2186).

Deuterated alkyne trityl stopper **III-51**



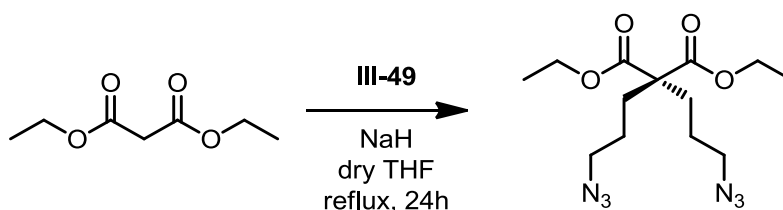
Alkyne trityl stopper **II-14** (542 mg, 1 mmol) was dissolved in dry THF (10 mL), then sodium hydride (24 mg, 1 mmol) was added and the reaction mixture was stirred at room temperature for 1 hour. Deuterated methanol (1.5 mL) was added dropwise and the reaction mixture was stirred at room temperature overnight. The solvent was removed, the crude was redissolved in DCM (10 mL) and the organic layer was washed with water (10 mL) and brine (10 mL), dried over MgSO₄, filtered and the solvent was removed. Deuterated alkyne trityl stopper **III-51** was obtained as beige solid (543 mg, quantitative yield).

¹H NMR (600 MHz, CDCl₃) δ 7.28 – 7.21 (m, 6H), 7.17 – 7.06 (m, 8H), 6.90 – 6.83 (m, 2H), 4.69 (s, 2H), 1.33 (s, 27H).

¹³C NMR (151 MHz, CDCl₃) δ 155.3, 148.8, 144.6, 140, 129.2, 127.8, 125.5, 114.8, 83.3, 74, 64.1, 56.9, 34.2, 31.3.

HRMS (ESI) calcd for C₄₀H₄₅DONa [M+Na]⁺ m/z = 566.3508, found m/z = 566.3504.

Diethyl 2,2-di-(1-azidopropyl)-malonate **III-54**

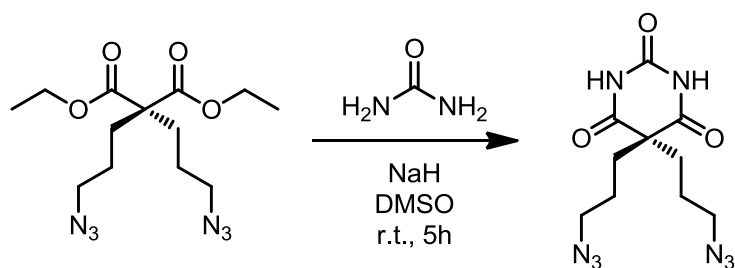


Sodium hydride (720 mg, 30 mmol) was suspended in dry THF (100 mL) and stirred for 10 min. The mixture was cooled at 0 °C, then diethyl malonate **III-53** (1.6 g, 10 mmol) was added and the reaction mixture was stirred at reflux for 1 hour. 1-Azido-3-iodopropane **III-49** (5.27 g, 25 mmol) was added and the reaction mixture was stirred at reflux overnight. The reaction was quenched by addition of saturated aqueous ammonium chloride solution (100 mL) and the crude was extracted with diethyl ether (4 × 50 mL). The organic layer was dried over MgSO₄, filtered and the solvent removed. Purification by column chromatography (SiO₂, petroleum ether/ethyl acetate, 9:1, v/v) afforded the desired product **III-54** as a colourless oil (2.8 g, 85% yield).

¹H NMR (CDCl₃, 300 MHz): δ 4.18 (q, *J* = 7.2 Hz, 4H), 3.28 (t, *J* = 6.6 Hz, 4H), 1.94 (m, 4H), 1.50 (m, 4H), 1.26 (t, *J* = 6.9 Hz, 6H).

Analysis is in agreement with literature data (*Org. Lett.*, **2014**, *16*, 1358).

5,5-Di(1-azido-propanyl) barbituric acid **II-12**

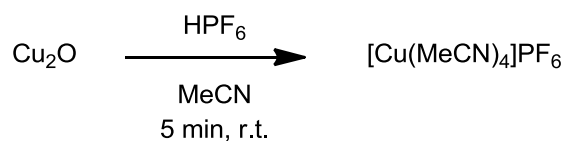


Sodium hydride (1.92 g, 80 mmol) was suspended in DMSO (50 mL) at room temperature, then urea (12 g, 200 mmol) was slowly added. The mixture was stirred at the same temperature for 1 hour, then a solution of **III-54** (6.52 g, 20 mmol) in DMSO (10 mL) was added dropwise and the resulting mixture was stirred at room temperature for 5 hours. The reaction mixture was quenched upon addition of saturated NH_4Cl solution (600 mL), stirred for 30 min and extracted with ethyl acetate (5×100 mL). The organic layer was washed with brine (200 mL), dried over Na_2SO_4 and the solvent was removed under reduced pressure. Purification by column chromatography (SiO_2 , petroleum ether/ethyl acetate 1:1), followed by reprecipitation (*n*-hexane) afforded the desired product **II-12** as white crystalline solid (2.9 g, 50% yield).

$^1\text{H NMR}$ (CDCl_3 , 300 MHz): δ 8.41 (s, 2H), 3.28 (t, $J = 6.0$ Hz, 4H), 2.07 (m, 4H), 1.53 (m, 4H).

Analysis is in agreement with literature data (*Org. Lett.*, **2014**, *16*, 1358).

Tetrakis(acetonitrile)copper(I) hexafluorophosphate

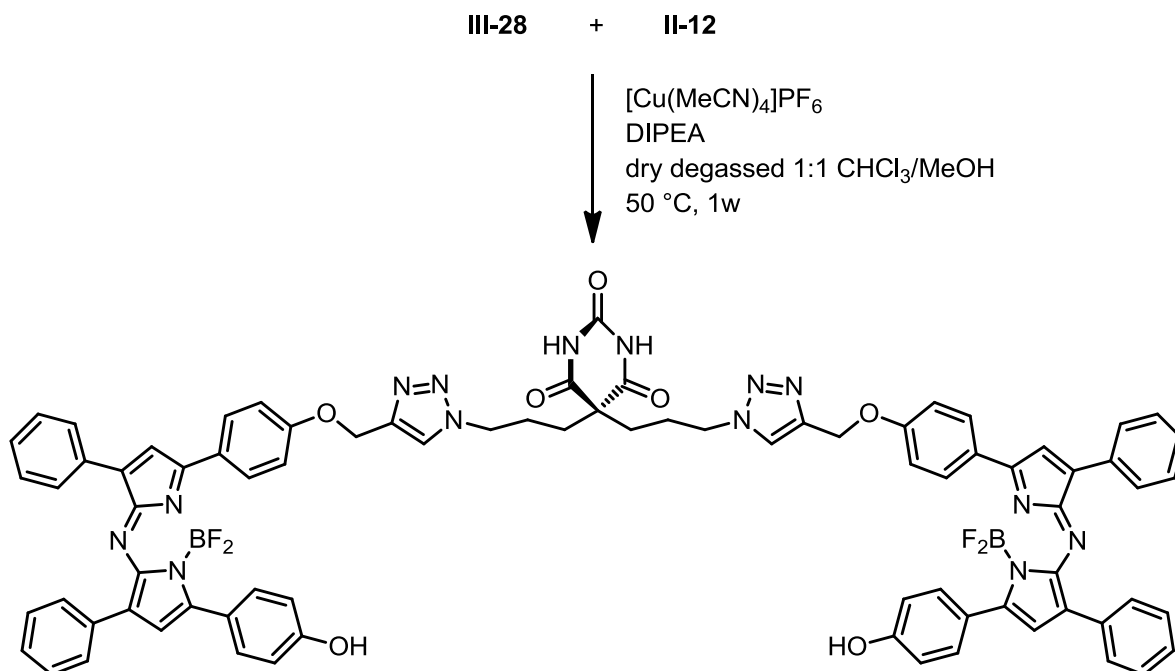


Hexafluorophosphoric acid (60% in water, 10 mL, 113 mmol) was added dropwise to a suspension of copper(I) oxide (4 g, 28 mmol) in acetonitrile (80 mL) at room temperature. The solution was stirred for 5 minutes at room temperature, then filtered hot (the reaction is strongly exothermic) through Celite and the filtrate was cooled at -20 °C overnight. The white precipitate was filtered, washed with Et₂O (100 mL) and redissolved in MeCN (100 mL). The pale blue solution was refluxed for 5 minutes, cooled at room temperature then Et₂O (100 mL) was added and the resulting mixture was cooled at -20 °C overnight. The pure tetrakis(acetonitrile)copper(I) hexafluorophosphate was recovered by filtration as white crystalline powder (10 g, 96% yield).

Elem. analysis calcd for C₈H₁₂N₄PF₆Cu: C, 25.78; H, 3.25; Cu, 17.05; F, 30.58; N, 15.03; P, 8.31, found: C, 25.8; H, 3.3; Cu, 16.8; F, 31.1; N, 15.1; P, 8.1

Analysis is in agreement with literature data (*Inorganic Syntheses*, **1979**, 19, 90).

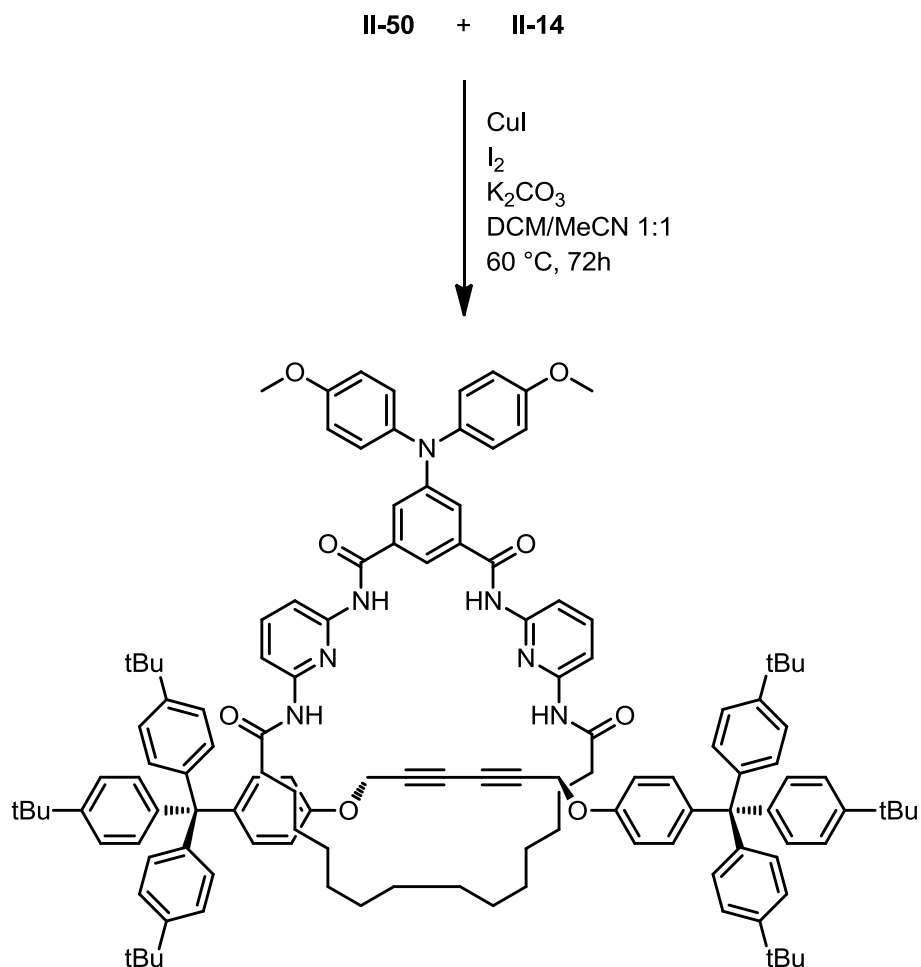
Barbiturate-containing BF₂-chelate azadipyrromethene thread **III-52**



Barbiturate **II-12** (29.4 mg, 0.1 mmol) and BF₂-chelate monopropargylated azadipyrromethene **III-28** (124 mg, 0.22 mmol) were dissolved in a dry degassed 1:1, v/v, chloroform/methanol mixture (2 mL) and stirred at room temperature for 1 hour. Tetrakis(acetonitrile)copper(I) hexafluorophosphate (82 mg, 0.22 mmol) and DIPEA (0.07 mL, 0.44 mmol) were then added and the reaction mixture was stirred at 50 °C for 1 week. The crude was isolated upon addition of 1M aqueous potassium cyanide solution (2 mL) and extraction with ethyl acetate (5 × 1 mL). The organic layer was dried over MgSO₄, filtered and the solvent was removed. Purification by column chromatography (SiO₂, DCM/MeOH, 95:5, v/v) afforded **III-52** as a dark green solid (85 mg, 60% yield).

¹H NMR (300 MHz, CD₂Cl₂) δ 8.14 – 7.98 (m, 16H), 7.74 (s, 2H), 7.52 – 7.36 (m, 12H), 7.13 (d, *J* = 8.2 Hz, 4H), 7.07 (d, *J* = 8.5 Hz, 4H), 6.96 (d, *J* = 8.8 Hz, 4H), 4.31 (t, *J* = 6.3 Hz, 4H). 1.98 – 1.73 (m, 8H).

Triarylamine-containing Glaser [2]rotaxane **IV-21**



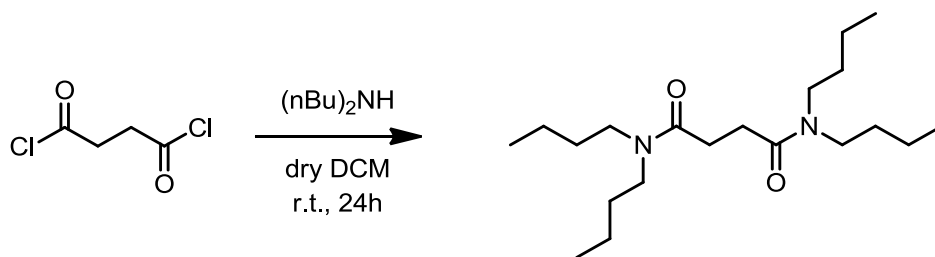
Macrocycle **II-50** (82.6 mg, 0.1 mmol) and copper (I) iodide (19 mg, 0.1 mmol) were dissolved in 1:1, v/v dichloromethane/acetonitrile mixture (1 mL) and stirred at room temperature for 1 hour. Iodine (253 mg, 1 mmol), potassium carbonate (138 mg, 1 mmol) and alkyne stopper **II-14** (109 mg, 0.2 mmol) were added and the reaction mixture was stirred at 60 °C for 72 hours. Then the reaction mixture was cooled to room temperature and the solvent was removed. The crude was redissolved in DCM (5 mL) and the organic layer was washed with 1M aqueous solution of potassium cyanide (5 mL), water (5 mL) and brine (5 mL). The solution was dried over MgSO₄, filtered and the solvent removed. Purification by column chromatography (SiO₂, petroleum ether/ethyl acetate, 9:1, v/v) afforded **IV-21** as yellow solid (68 mg, 36% yield).

¹H NMR (600 MHz, CDCl₃) δ 8.55 (s, 2H), 8.01 (d, *J* = 8.1 Hz, 2H), 7.95 (d, *J* = 8.1 Hz, 2H), 7.76 (d, *J* = 1.2 Hz, 2H), 7.67 (t, *J* = 8.1 Hz, 2H), 7.51 (s, 1H), 7.31 (s, 2H), 7.22 – 7.18 (m, 8H), 7.16 – 7.13 (m, 3H), 7.03 – 6.99 (m, 8H), 6.88 – 6.85 (m, 4H), 6.84 – 6.80 (m, 4H), 4.75 (s, 3H), 3.81 (s, 6H), 2.15 – 1.83 (m, 4H), 1.31 – 1.26 (m, 72H).

¹³C NMR (151 MHz, CDCl₃) δ 171.53, 164.59, 156.89, 155.31, 150.73, 149.51, 149.43, 148.54, 143.69, 141.39, 140.74, 139.29, 135.36, 132.49, 130.71, 130.60, 127.35, 124.14, 124.04, 121.88, 115.21, 113.05, 109.57, 109.46, 75.22, 71.19, 63.05, 56.30, 55.46, 37.58, 34.29, 31.94, 31.38, 31.35, 29.71, 28.53, 28.45, 28.39, 28.37, 28.15, 25.01.

HRMS (FD) calcd for C₁₂₈H₁₄₅N₇O₈ [M]⁺ *m/z* = 1908.1154, found *m/z* = 1908.1185.

Tetrabutylsuccinamide thread IV-24

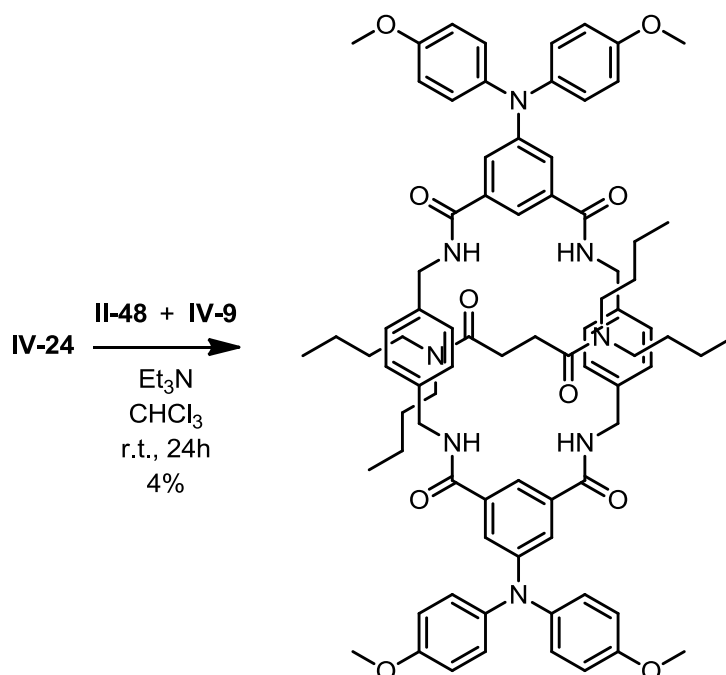


Succinyl chloride **IV-26** (1.55 g, 10 mmol) was dissolved in DCM (100 mL), then dibutylamine (5.2 g, 40 mmol) was added. The reaction mixture was stirred overnight then it was quenched upon sequential addition of 1M sodium hydroxide solution (100 mL), 1M hydrochloric acid solution (100 mL), water (100 mL) and brine (100 mL). The organic layer was dried over MgSO₄, filtered and the solvent removed. The tetrabutylsuccinamide thread **IV-24** was obtained as yellow oil (3.4 g, quantitative yield).

¹H NMR (CDCl₃, 300 MHz): δ 3.25-3.18 (m, 8H), 2.61 (s, 4H), 1.58-1.42 (m, 8H), 1.33-1.117 (m, 8H), 0.88 (t, *J* = 7.2 Hz, 6H), 0.84 (t, *J* = 7.2 Hz, 6H).

Analysis is in agreement with literature data (*J. Org. Chem.*, **2015**, *80*, 10049).

Triarylamine-containing benzylic amide-based [2]rotaxane **IV-22**



A solution of diamine **IV-9** (136 mg, 1 mmol) in chloroform (5 mL) and a solution of 5-substituted isophthaloyl **II-48** (430 mg, 1 mmol) in chloroform (5 mL) were simultaneously added during 5 hours to a solution of tetrabutylsuccinamide thread **IV-24** (42.5 mg, 0.125 mmol) and dry triethylamine (2 mL, 15 mmol) in chloroform (20 mL). The solution was stirred at room temperature overnight. The reaction mixture was filtered through Celite and the filtrate was washed with 1M hydrochloric acid solution (10 mL), saturated sodium bicarbonate solution (10 mL), water (10 mL) and brine (10 mL). The organic layer was dried over MgSO_4 , filtered and the solvent removed. Purification by column chromatography (SiO_2 , DCM/MeOH, 99:1, v/v) afforded **IV-22** as beige solid (6.4 mg, 4% yield).

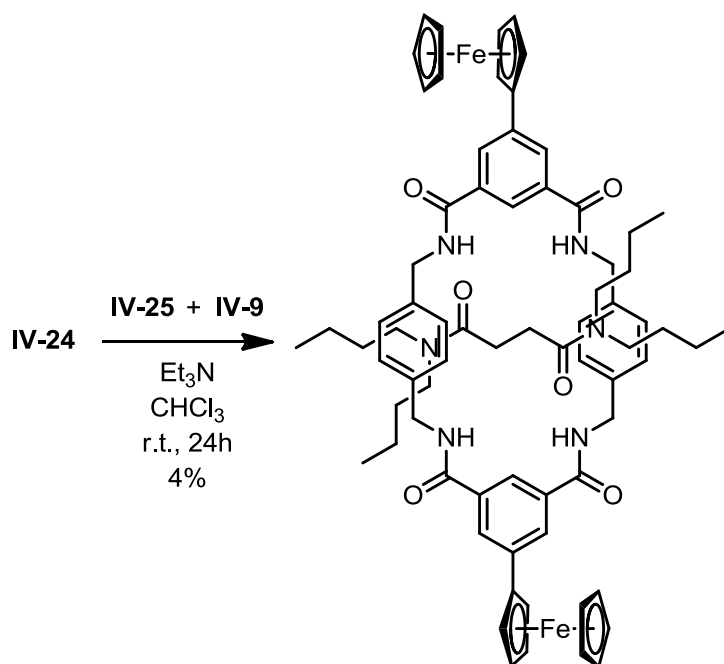
$^1\text{H NMR}$ (600 MHz, CDCl_3) δ 8.25 (s, 2H), 7.87 (s, 4H), 7.66 (t, $J = 5.8$ Hz, 4H), 7.13 – 7.02 (m, 16H), 6.88 (dd, $J = 7.2, 5.1$ Hz, 8H), 3.83 (s, 12H) 3.31 – 3.20 (m, 4H), 2.81 – 2.70 (m, 4H), 1.59 –

1.49 (m, 8H), 1.34 (dq, $J = 14.9, 7.4$ Hz, 4H), 1.25 (dt, $J = 15.4, 5.3$ Hz, 4H), 1.12 (s, 4H), 0.97 (t, $J = 7.3$ Hz, 12H).

^{13}C NMR (151 MHz, CDCl_3) δ 172.65, 165.51, 156.50, 150.26, 140.08, 138.67, 134.33, 128.89, 126.98, 122.50, 115.10, 113.61, 55.51, 48.20, 47.74, 46.56, 45.95, 43.18, 31.10, 30.80, 30.27, 29.97, 28.41, 28.15, 20.30, 20.26, 20.17, 19.83, 13.90, 13.87.

HRMS (ESI) calcd for $\text{C}_{80}\text{H}_{94}\text{N}_8\text{O}_{10}\text{Na}$ $[\text{M}+\text{Na}]^+$ $m/z = 1349.6985$, found $m/z = 1349.6928$.

Ferrocene-containing benzylic amide-based [2]rotaxane **IV-23**



A solution of diamine **IV-9** (272 mg, 2 mmol) in chloroform (15 mL) and a solution of 5-ferrocenylisophthaloyl chloride **IV-25** (402 mg, 1 mmol) in chloroform (15 mL) were simultaneously added during 5 hours to a solution of tetrabutylsuccinamide thread **IV-24** (85 mg, 0.25 mmol) and dry triethylamine (0.84 mL, 6 mmol) in chloroform (50 mL). The solution was stirred at room temperature overnight. The reaction mixture was filtered through Celite and the filtrate was washed with 1M hydrochloric acid solution (10 mL), saturated sodium bicarbonate solution (10 mL), water (10 mL) and brine (10 mL). The organic layer was dried over MgSO_4 , filtered and the solvent removed. Purification by column chromatography (SiO_2 , DCM/ethyl acetate, 9:1, v/v) afforded **IV-22** as beige solid (129 mg, 41% yield).

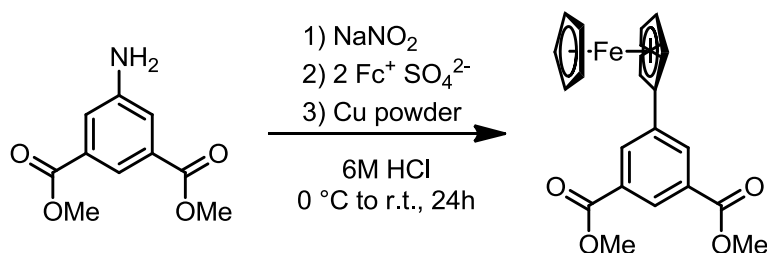
$^1\text{H NMR}$ (600 MHz, CDCl_3) δ 8.66 (s, 2H), 8.46 (d, $J = 1.3$ Hz, 4H), 7.76 (t, $J = 5.8$ Hz, 4H), 7.15 (s, 8H), 4.87 (t, $J = 1.8$ Hz, 4H), 4.44 (t, $J = 1.7$ Hz, 4H), 4.09 (s, 10H), 3.31 – 3.20 (m, 4H), 2.81 –

2.70 (m, 4H), 1.59 – 1.49 (m, 8H), 1.34 (dq, $J = 14.9, 7.4$ Hz, 4H), 1.25 (dt, $J = 15.4, 5.3$ Hz, 4H), 1.12 (s, 4H), 0.97 (t, $J = 7.3$ Hz, 12H).

^{13}C NMR (151 MHz, CDCl_3) δ 172.72, 165.46, 141.76, 138.71, 133.46, 129.25, 128.96, 119.70, 83.34, 66.89, 48.24, 46.63, 43.25, 30.79, 30.27, 28.15, 20.25, 19.83, 13.89, 13.77.

HRMS (FD) calcd for $\text{C}_{72}\text{H}_{84}\text{N}_6\text{O}_4\text{NFe}_2$ $[\text{M}]^+$ $m/z = 1240.5151$, found $m/z = 1240.5152$.

Dimethyl 5-ferrocenylisophthalate **IV-27**

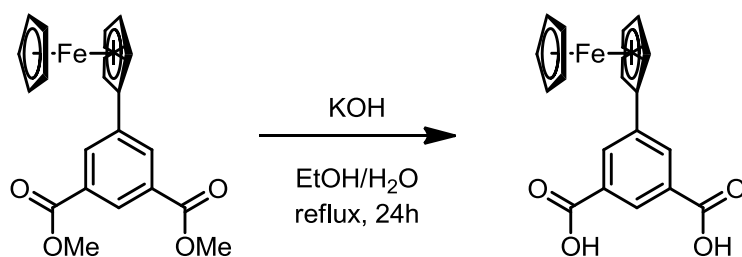


Ferrocene **II-17** (10 g, 54 mmol) was dissolved in conc. H₂SO₄ (150 mL), and stirred for 6 h. Meanwhile, dimethyl 5-aminoisophthalate **II-40** (3.7 g, 17.5 mmol) was suspended in conc. HCl (50 mL) and H₂O (50 mL), and cooled to 0°C. A solution of NaNO₂ (5 g, 72.5 mmol) in H₂O (10 mL) was then added dropwise at 0°C. This solution was then stirred at 0°C for 1 h, and then used immediately. The ferrocenium sulfate solution was added to ice H₂O (600 mL) and allowed to warm to room temperature. Copper powder (5 g, 78.5 mmol) was then added. This mixture was poured onto the diazonium ion solution, with the reaction mixture being stirred at 0°C for 30 min, then allowed to warm to room temperature and stirred for 24 hours. Excess ascorbic acid (30 g) was then added, followed by DCM (1 L). This mixture was filtered through Celite and washed thoroughly with DCM. The organic layer was washed with brine (5 × 100 mL), dried over MgSO₄ and the solvent removed. Purification by column chromatography (SiO₂, pentane/ethyl acetate 9:1, v/v) followed by recrystallization (EtOH, 5 mL) afforded **IV-27** as orange cotton-like needles (1.25 g, 19% yield).

¹H NMR (300 MHz, CDCl₃) δ 8.46 (t, *J* = 1.6 Hz, 1H), 8.27 (d, *J* = 1.6 Hz, 2H), 4.77 (t, *J* = 1.8 Hz, 2H), 4.40 (t, *J* = 1.9 Hz, 2H), 4.06 (s, 5H), 3.98 (s, 6H).

Analysis is in agreement with literature data (*Chem. Sci.*, **2012**, 3, 1080).

5-Ferrocenylisophthalic acid IV-28

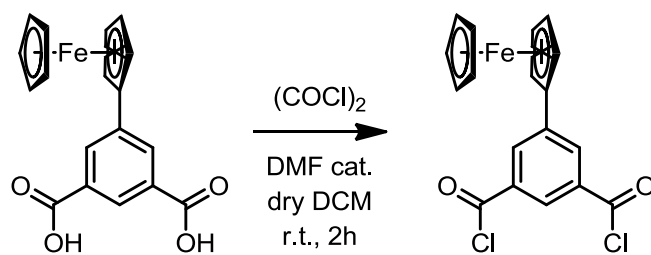


Dimethyl 5-ferrocenylisophthalate **IV-27** (980 mg, 2.6 mmol) was suspended in EtOH (100 mL), then potassium hydroxide (728 mg, 13 mmol) and water (10 mL) were added. The reaction mixture was stirred at reflux overnight, then cooled and the solvent removed. The crude was redissolved in water (100 mL) and 10% aqueous citric acid was added until precipitation occurred. The resulting orange precipitate was collected by filtration and washed with water (50 mL). Purification by recrystallization (EtOH, 10 mL) afforded **IV-28** as cotton-like crystals (949 mg, quantitative yield).

¹H NMR (300 MHz, DMSO-d₆) δ 8.46 (t, *J* = 1.6 Hz, 1H), 8.27 (d, *J* = 1.6 Hz, 2H), 4.77 (t, *J* = 1.8 Hz, 2H), 4.40 (t, *J* = 1.9 Hz, 2H), 4.06 (s, 5H).

Analysis is in agreement with literature data (*Chem. Sci.*, **2012**, 3, 1080).

5-Ferrocenylisophthaloyl chloride **IV-25**



5-Ferrocenylisophthalic acid **IV-28** (700 mg, 2 mmol) was suspended in dry DCM (20 mL), then oxalyl chloride (1.7 mL, 20 mmol) and dry DMF (a drop). The reaction mixture was stirred at room temperature overnight. The mixture was concentrated under reduced pressure to afford **IV-25** as blood red oil (804 mg, quantitative yield), which was used in the next step without further purification.

7. Annexes

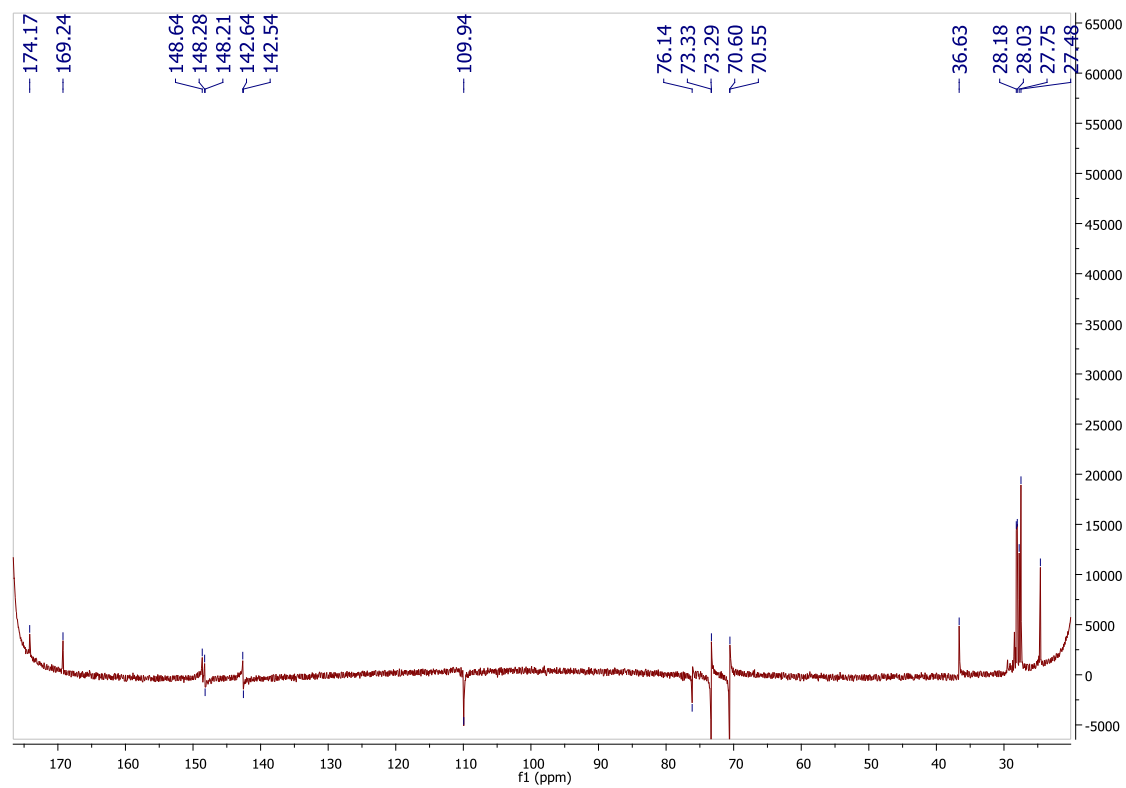


Figure 7.1 - ^{13}C -NMR of ferrocene Hamilton-type macrocycle **II-28** (600 MHz in AcOH-d_4).

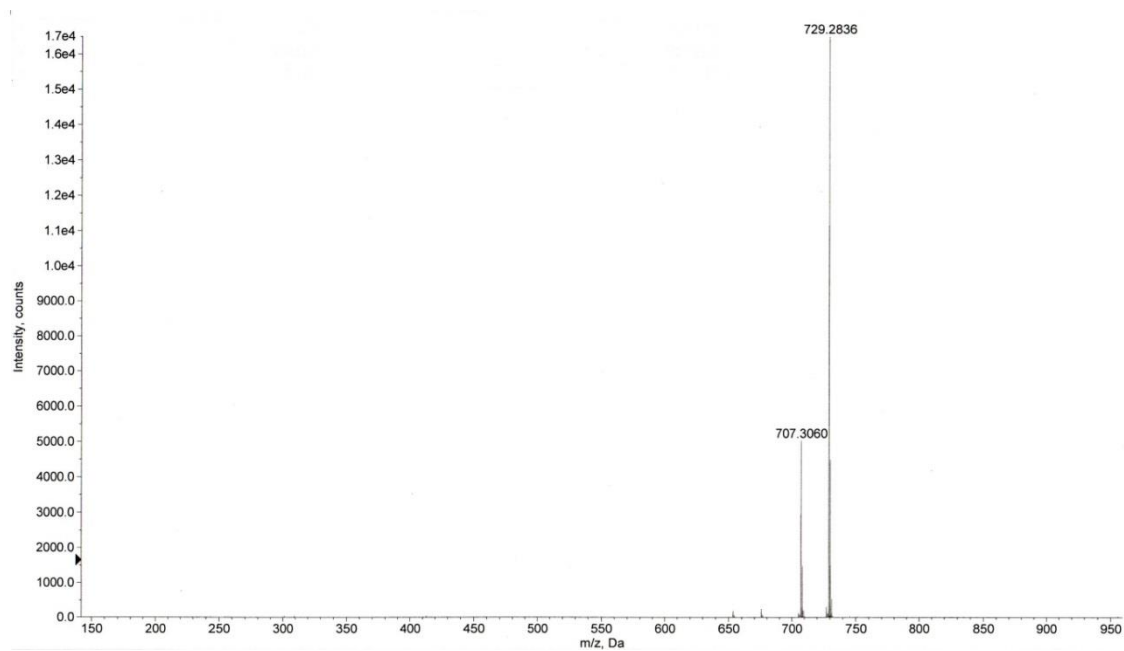


Figure 7.2 - Mass spectrum (ESI) of ferrocene Hamilton-type macrocycle **II-28**.

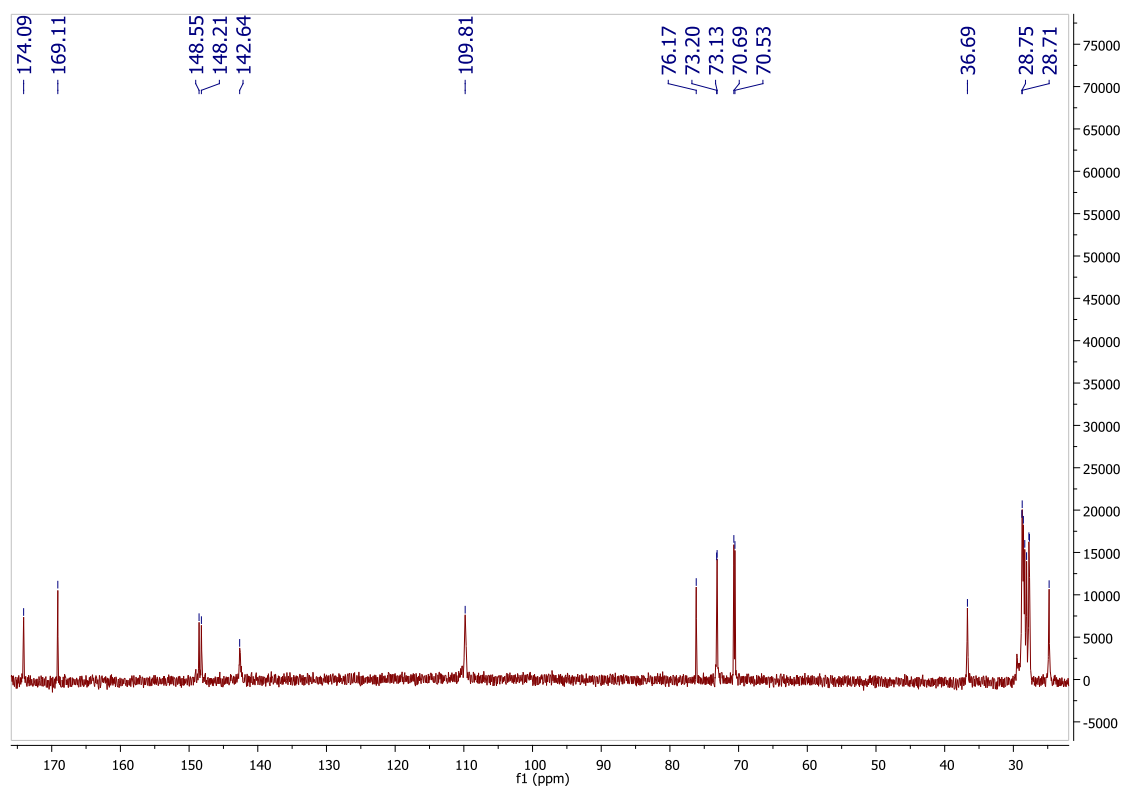


Figure 7.3 - ^{13}C - NMR of ferrocene Hamilton-type macrocycle **II-29** (600 MHz in AcOH-d_4).

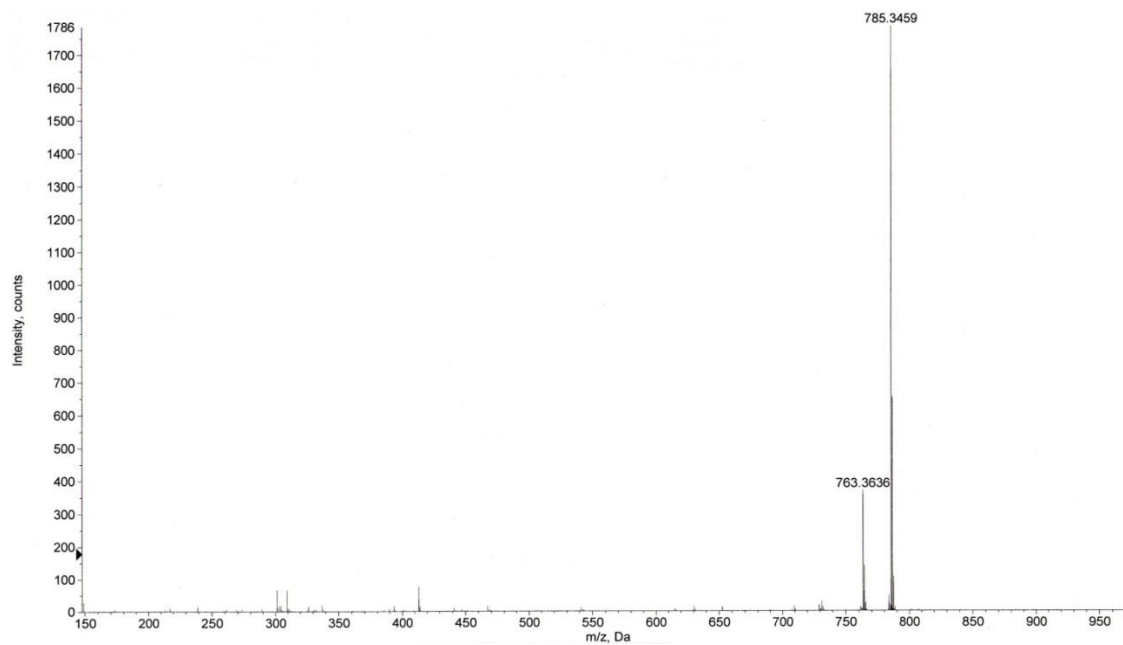


Figure 7.4 - Mass spectrum (ESI) of ferrocene Hamilton-type macrocycle **II-29**.

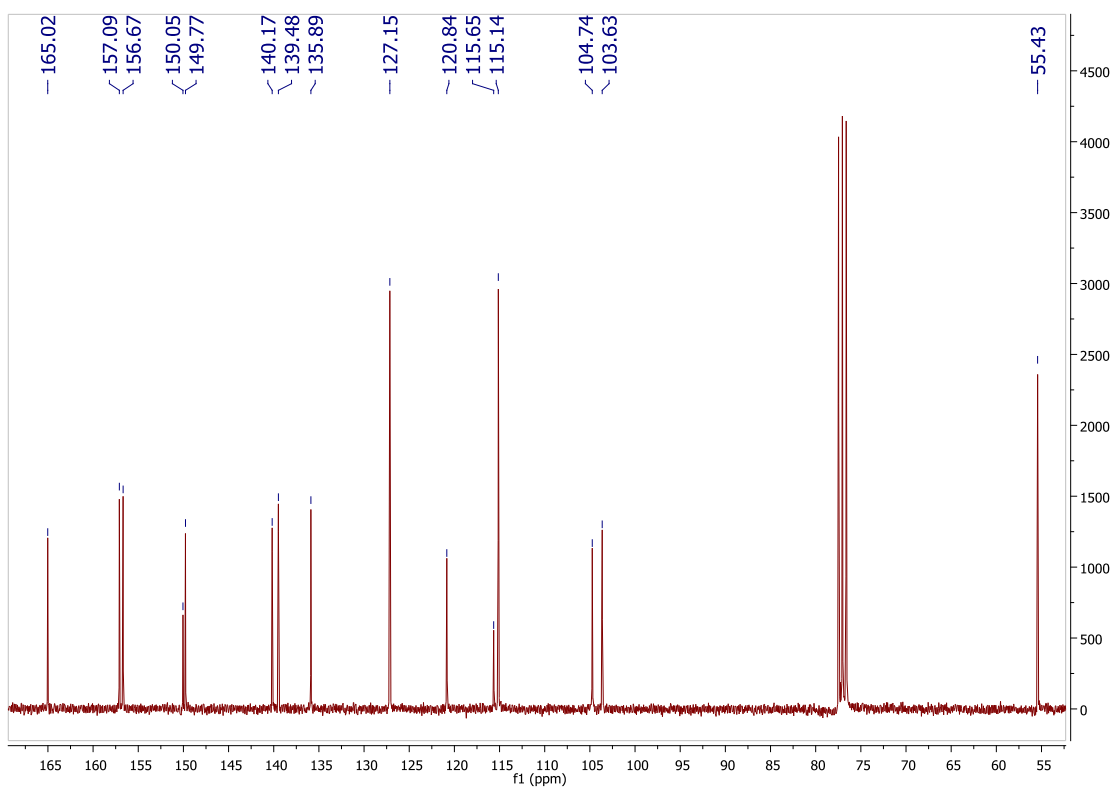


Figure 7.5 - ^{13}C -NMR of acyclic triarylamine Hamilton-type receptor **II-49** (600 MHz in CDCl_3).

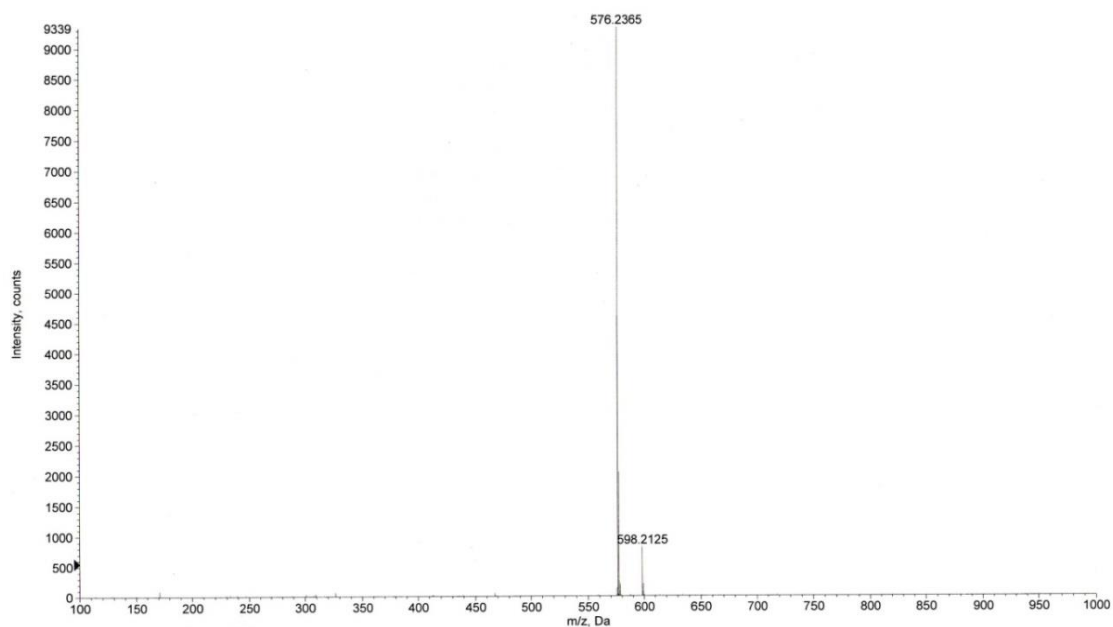


Figure 7.6 - Mass spectrum (ESI) of acyclic triarylamine Hamilton-type receptor **II-49**.

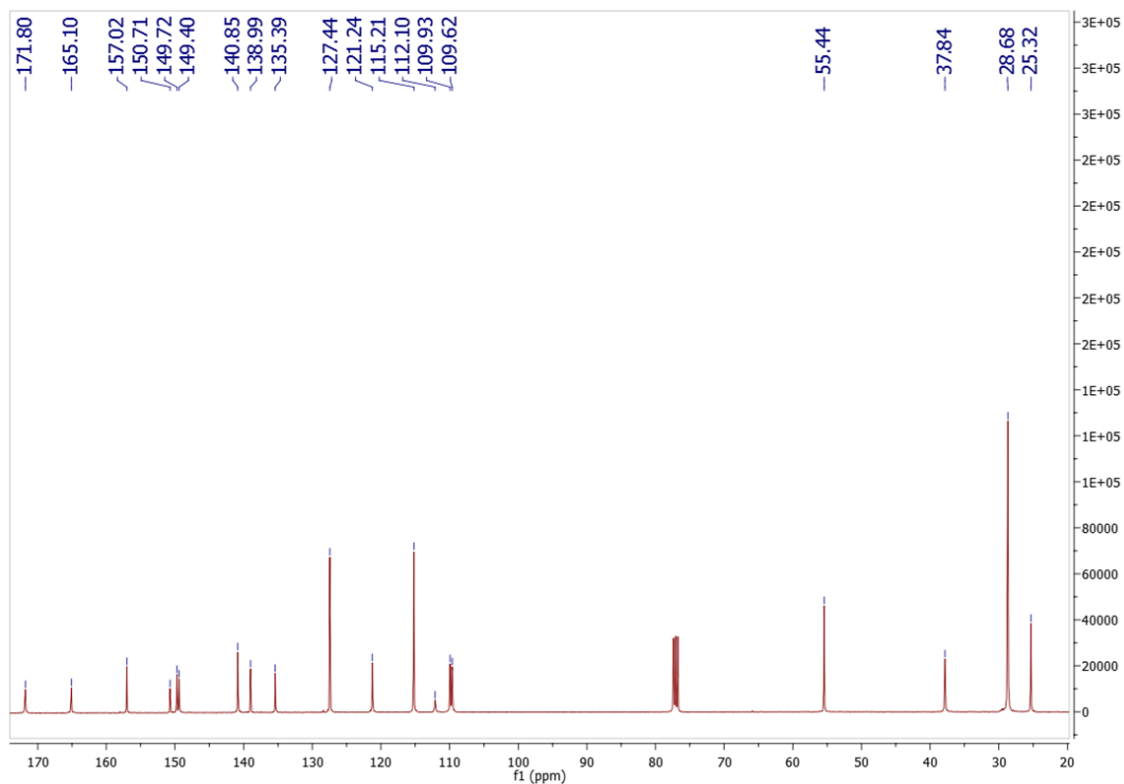


Figure 7.7 - ^{13}C NMR of cyclic triarylamine Hamilton-type receptor **II-50** (101 MHz in CDCl_3).

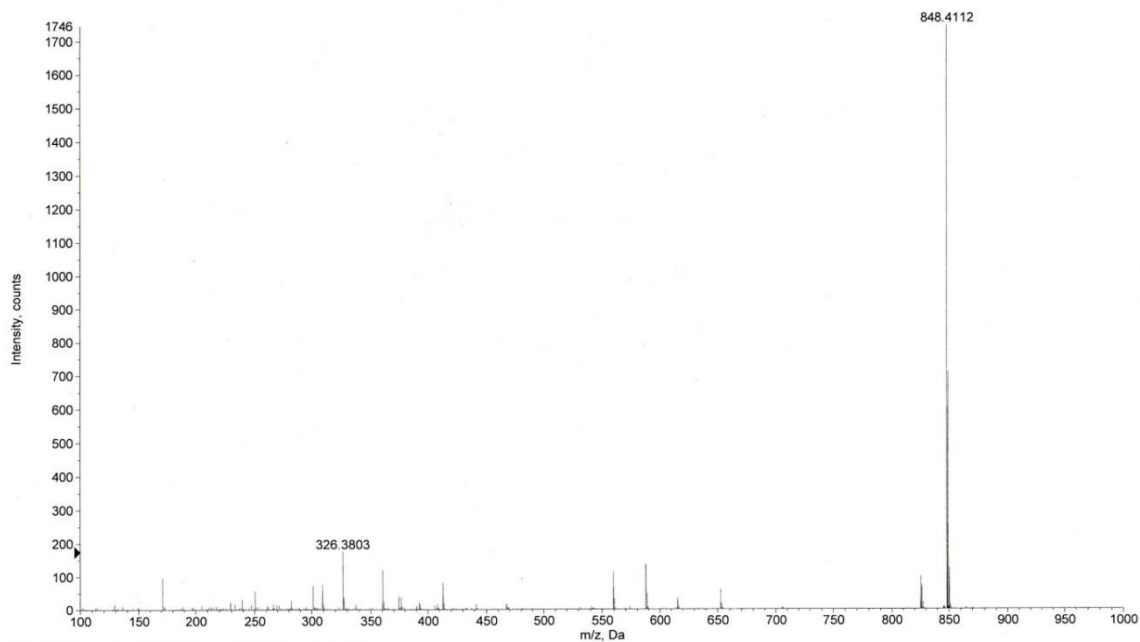


Figure 7.8 - Mass spectrum (ESI) of cyclic triarylamine Hamilton-type receptor **II-50**.

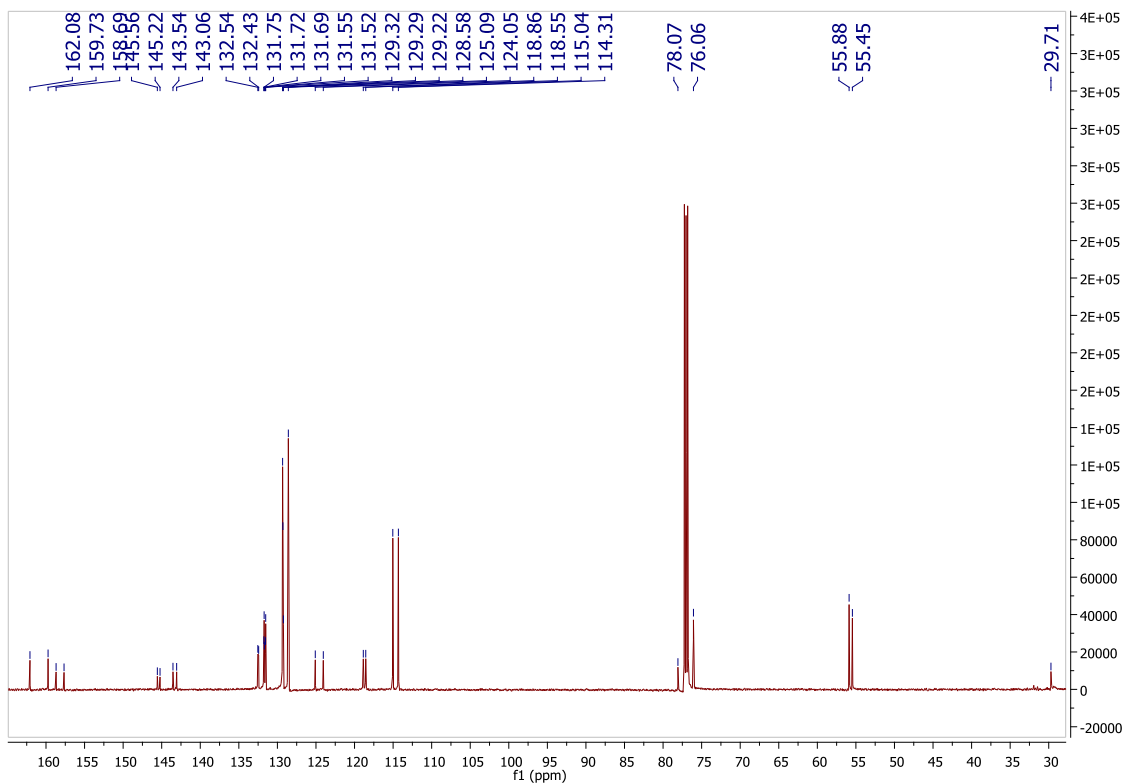


Figure 7.9 - ^{13}C -NMR of BF_2 - azadipyromethene **III-29** (600 MHz in CDCl_3).

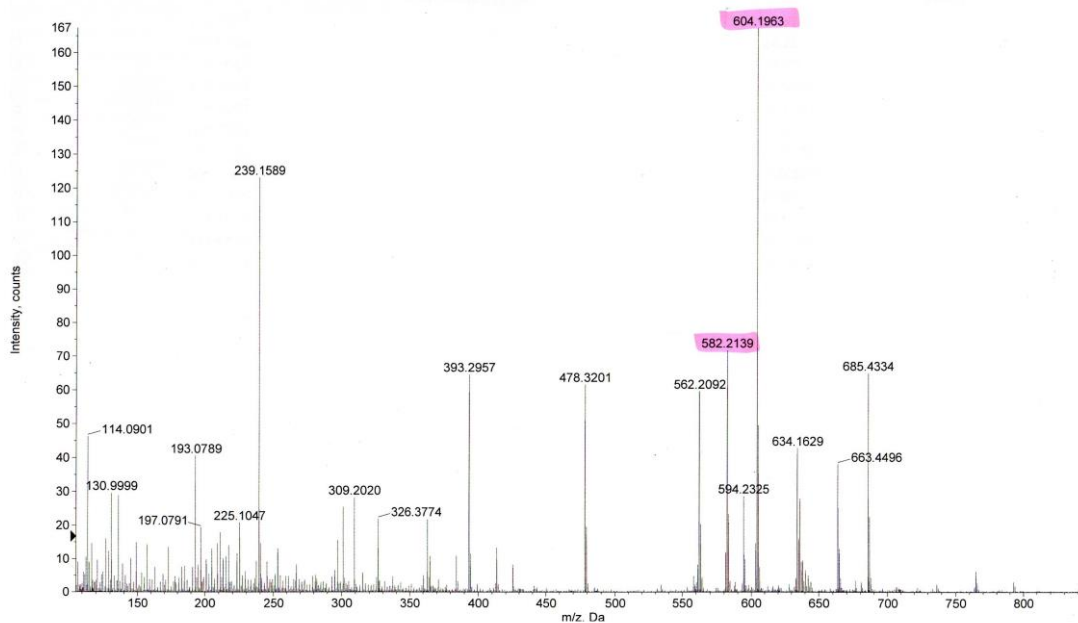


Figure 7.10 - Mass spectrum (ESI) of BF_2 - azadipyromethene **III-29**.

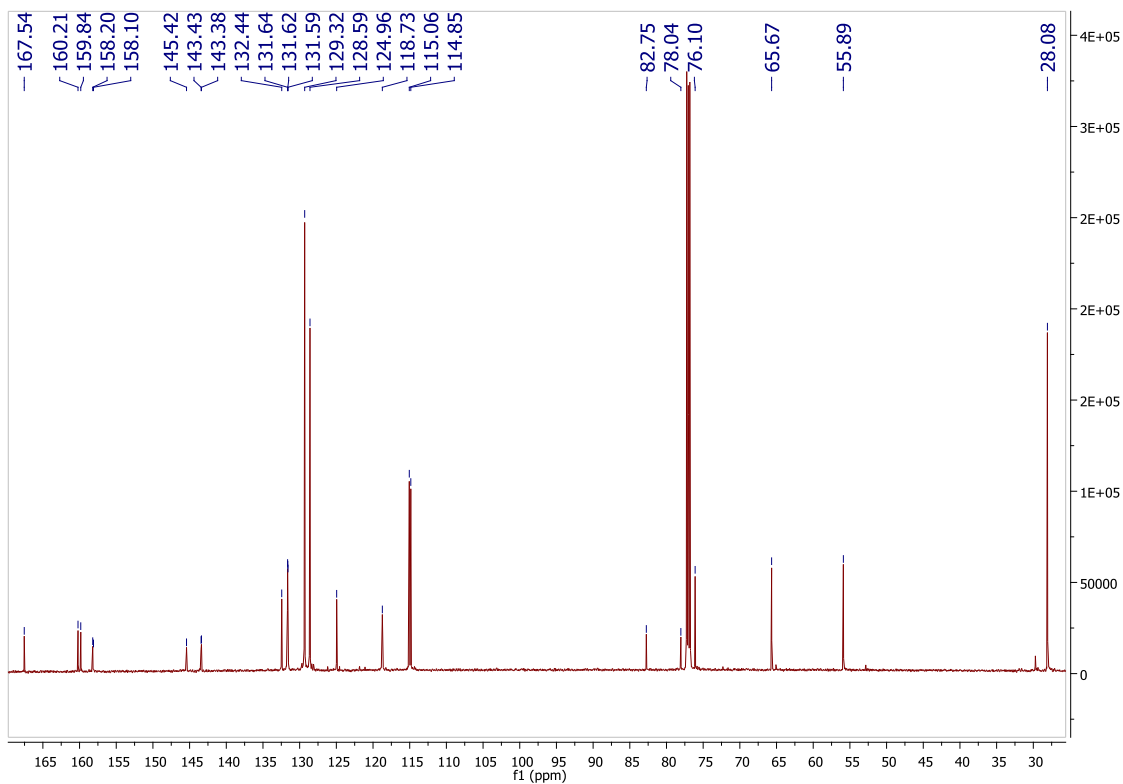


Figure 7.11 - ^{13}C -NMR of BF_2 - azadipyrromethene **III-30** (600 MHz in CDCl_3).

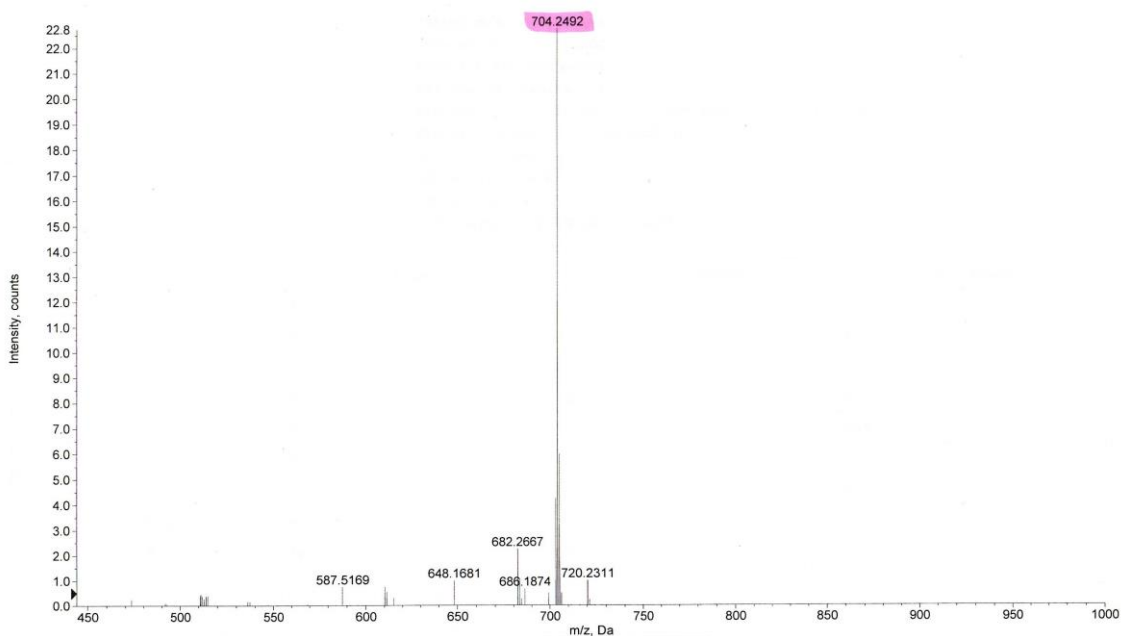


Figure 7.12 - Mass spectrum (ESI) of BF_2 - azadipyrromethene **III-30**.

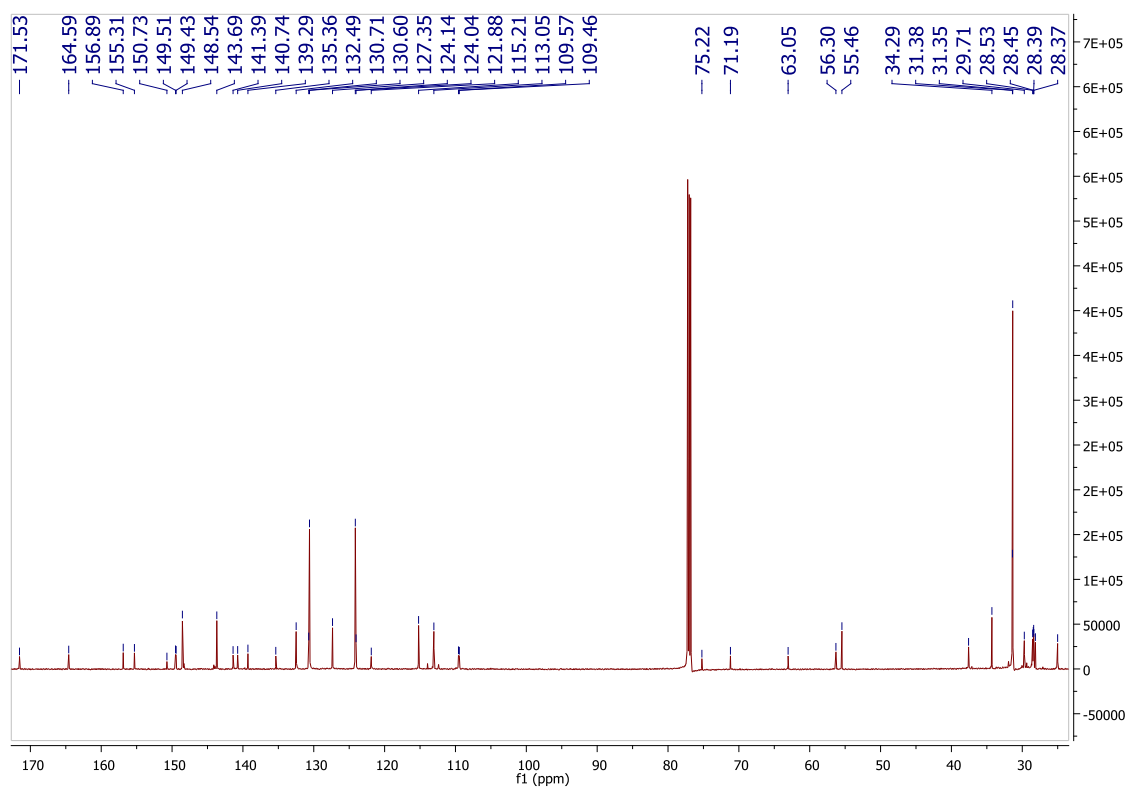


Figure 7.13 - ^{13}C -NMR of triarylamine-containing Glaser [2]rotaxane **IV-21** (600 MHz in CDCl_3).

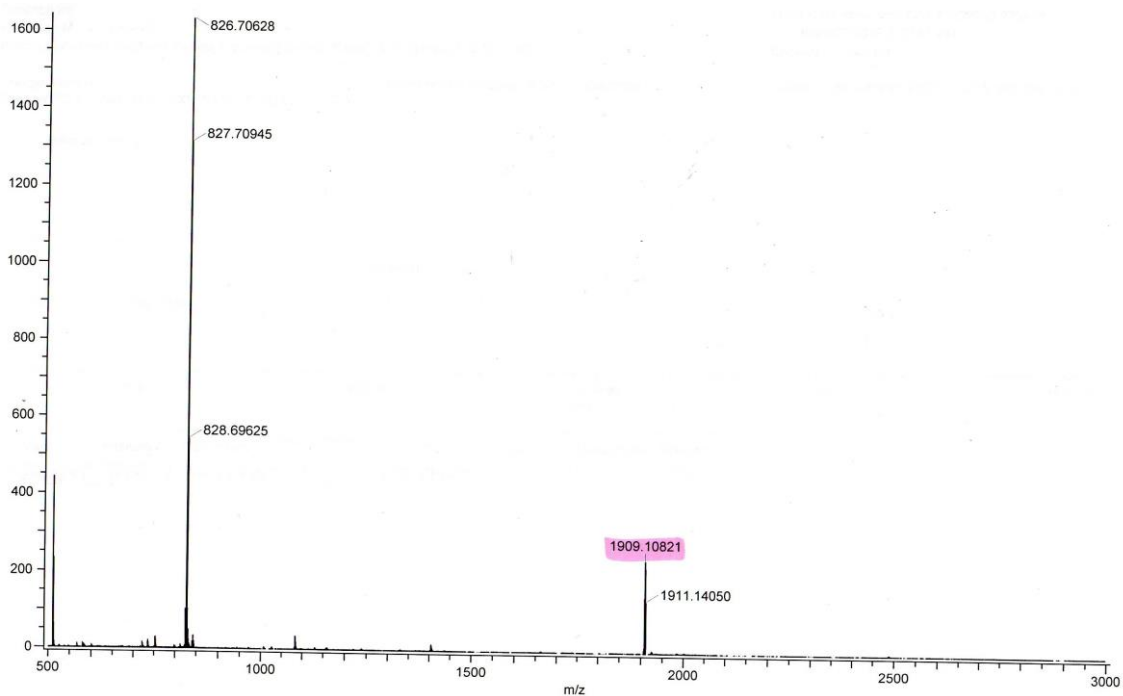


Figure 7.14 - Mass spectrum (FD) of triarylamine-containing Glaser [2]rotaxane **IV-21**.

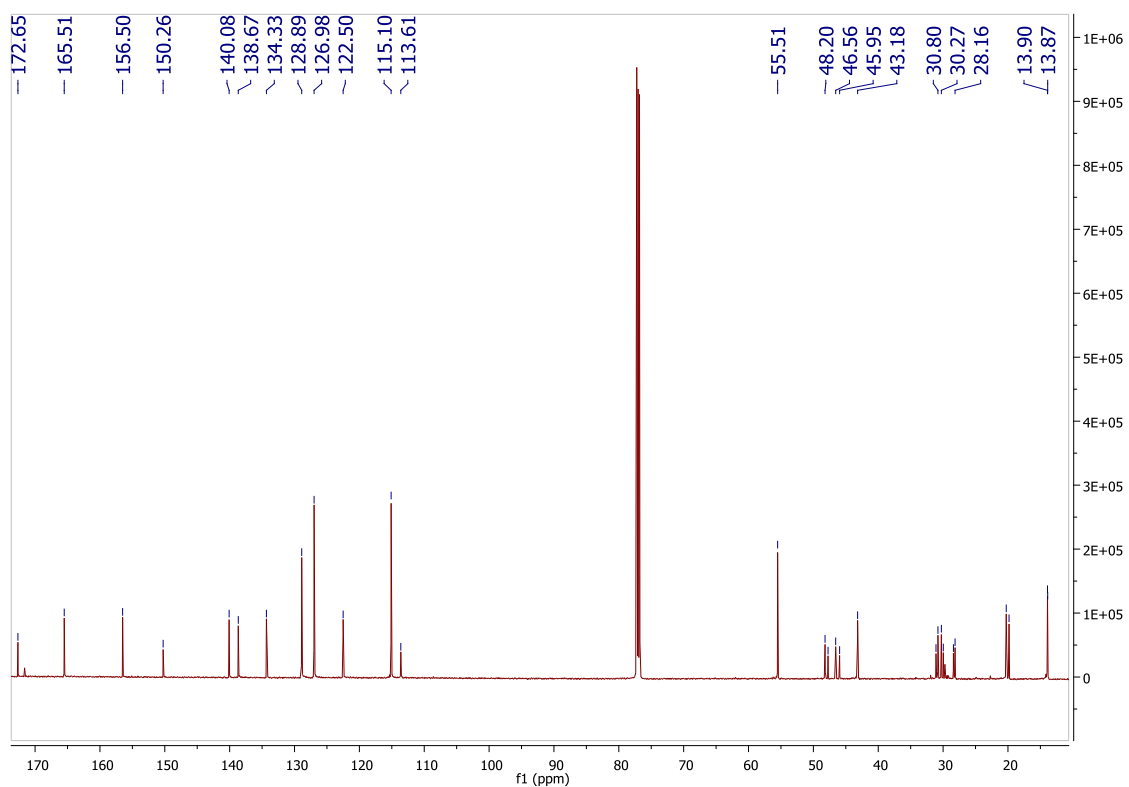


Figure 7.15 - ^{13}C -NMR of triarylamine-containing clipped [2]rotaxane **IV-22** (600 MHz in CDCl_3).

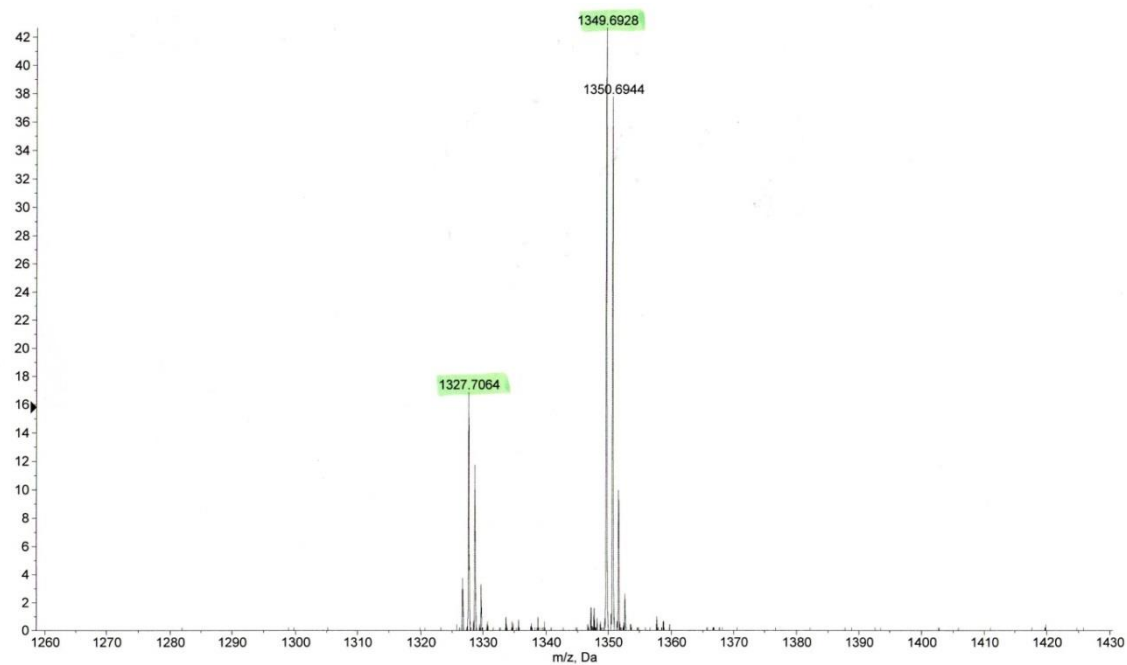


Figure 7.16 - Mass spectrum (ESI) of triarylamine-containing clipped [2]rotaxane **IV-22**.

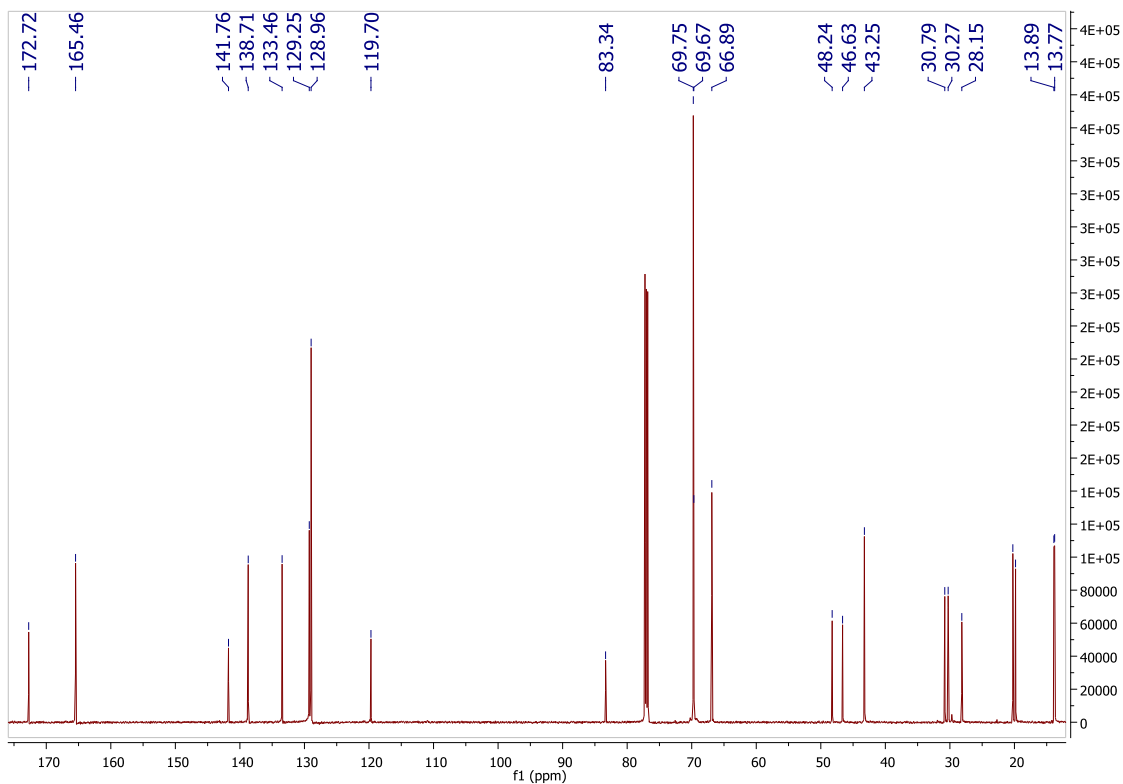


Figure 7.17 - ^{13}C -NMR of ferrocene-containing clipped [2]rotaxane **IV-23** (600 MHz in CDCl_3).

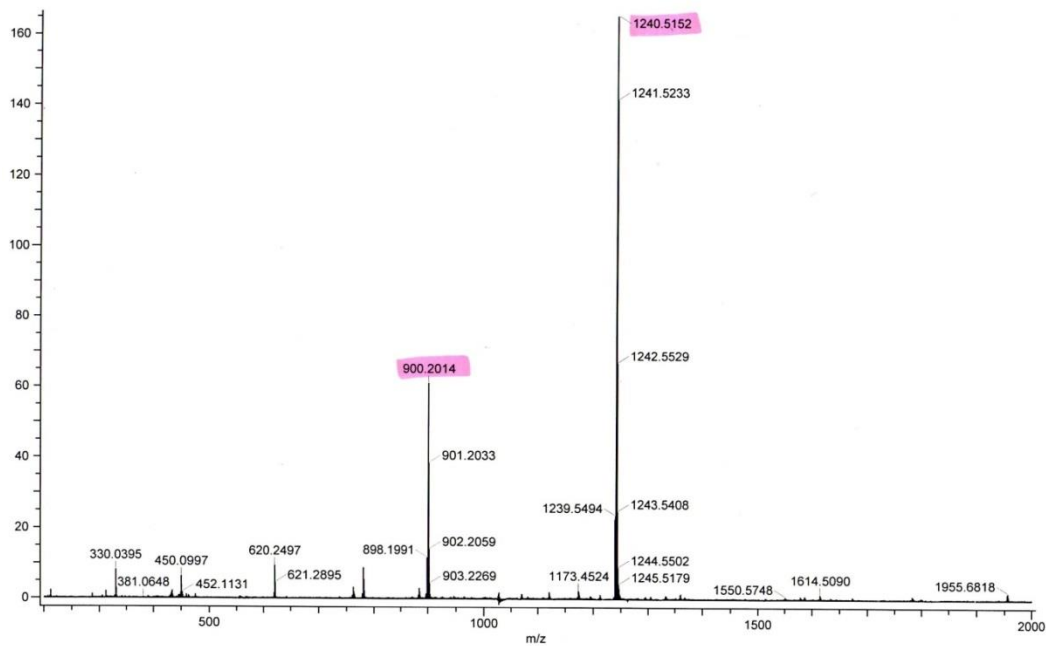


Figure 7.18 - Mass spectrum (FD) of ferrocene-containing clipped [2]rotaxane **IV-23**.

Synthèse de macrocycles et rotaxanes électroactifs : résumé de thèse

La chimie supramoléculaire est devenue un sujet central en chimie. Ce type de chimie repose sur la mobilisation de forces intermoléculaires, ou liaisons non covalentes, qui jouent un rôle fondamental dans les processus biologiques, tels que la réplication de l'ADN, le repliement des protéines, la communication neurale, la reconnaissance moléculaire et la formation de membranes et de cellules. Les chimistes organiques peuvent s'inspirer de la nature pour développer des systèmes biomimétiques artificiels basés sur les mêmes interactions intermoléculaires.

Au fil des ans, les architectures supramoléculaires sont devenues de plus en plus sophistiquées et des outils synthétiques efficaces sont nécessaires. Pour cette raison, la construction de molécules mécaniquement imbriquées est étroitement liée à la «chimie du clic». Sharpless a introduit ce concept pour la première fois en 2002 dans un domaine de synthèse organique qui a pour objectif principal l'étude et le développement de réactions chimiques simples et efficaces, qui doivent généralement être à haut rendement et hautement sélectives les conditions de réaction doivent être aussi douces que possible pour pouvoir être exécutées en présence d'une large gamme de groupes fonctionnels. Différentes réactions répondent à ces exigences et appartiennent à cette famille, comme la réaction thiolène, la réaction de Diels-Alder, la cycloaddition [4 + 1] entre isonitriles et tétrazines, la substitution nucléophile de petits cycles et la cycloaddition de 1,3-dipolaire azide-alcyne de Huisgen. La dernière réaction est le membre le plus célèbre de cette classe de réactions et sa version catalysée au cuivre (I) est omniprésente en chimie.

Au cours des trois dernières décennies, le développement de molécules à interverrouillage mécanique a toujours suscité un grand intérêt au sein de la communauté scientifique, comme le prouvent le prix Nobel de chimie de 1987 pour le développement de récepteurs biomimétiques artificiels et le prix Nobel de chimie de 2016 pour le développement de machines moléculaires. Ces structures comprennent des structures en rotaxane à anneau sur fil, formées par une molécule en

forme de tige (le fil) qui est enfilée dans une molécule macrocyclique. Le désenroulement des deux composants est empêché par la présence de groupes volumineux aux extrémités du fil qui sont plus larges que la cavité de la bague. La rupture d'une liaison covalente est nécessaire pour dissocier le filetage de la bague.

Au fil des années, de nombreuses architectures à base de rotaxane ont été développées, mais seul un faible pourcentage d'entre elles comprend des groupes fonctionnels. Des molécules photoactives à verrouillage mécanique sont présentes dans la littérature, mais seules quelques classes de chromophore UV-vis ont été exploitées et la plupart d'entre elles ont montré une faible photostabilité. Les chromophores proche infrarouge (NIR) sont une classe de chromophores photoactifs dans la région proche infrarouge (de 650 à 1350 nm). L'intérêt suscité par le chromophore NIR au cours des dernières années, en particulier pour son application biologique et médicale, en fait, dans cette région du spectre électromagnétique, les tissus biologiques sont transparents et aucun dommage aux processus biologiques ne se produit lors de l'irradiation.

En outre, grâce à leur extrême photostabilité et à leur facilité de fonctionnalisation, les chélates d'azadipyrométhène BF_2 ont également été utilisés dans le développement de chimiosenseurs, de polymères et de matériaux photoactifs, mais n'ont pas encore été exploités en tant que nouveaux blocs de construction chromophore NIR afin de développer des systèmes photoactifs molécules mécaniquement imbriquées.

Le but de cette thèse est la conception, la synthèse et la caractérisation de composants électroactifs et photoactifs pour le développement de nouvelles molécules fonctionnelles imbriquées mécaniquement.

Au chapitre 2, la synthèse de trois nouveaux récepteurs cycliques de type Hamilton à 31 et 35 chaînons liés par des liaisons hydrogène, comprenant tous un motif bis (2,6-diamidopyridine) et un groupe électroactif, à savoir le ferrocène ou la triarylamine, a été décrit et caractérisé par spectroscopie RMN ^1H et ^{13}C et spectrométrie de masse (Figure R1 et R2).

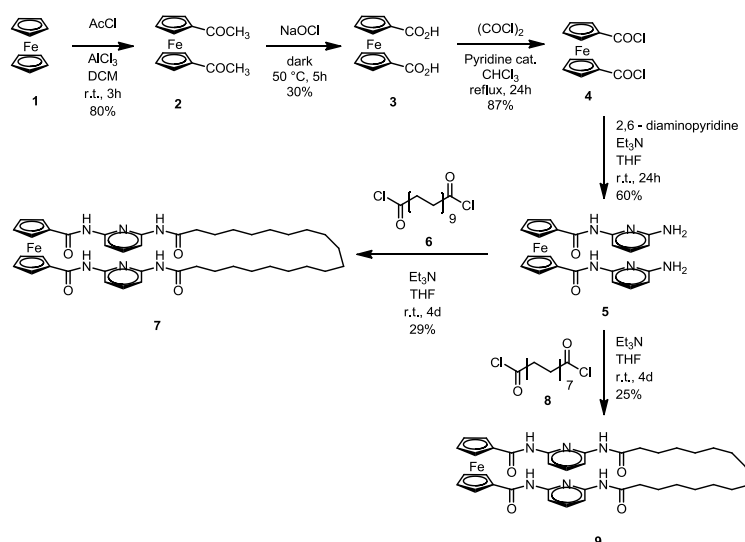


Figure R1 - Schéma de synthèse des récepteurs cycliques de type Hamilton contenant un motif ferrocène **7** et **9**.

Le 5-[bis (4-méthoxyphényl)amino]-isophtalate de diméthyle **11** était un intermédiaire clé pour la synthèse du macrocycle **15** et il a été obtenu par une réaction de type Goldberg catalysée au cuivre entre le 4-iodoanisole et le diméthyle 5-aminoisophtalate en utilisant le tétraéthyle orthosilicate (TEOS) comme solvant.

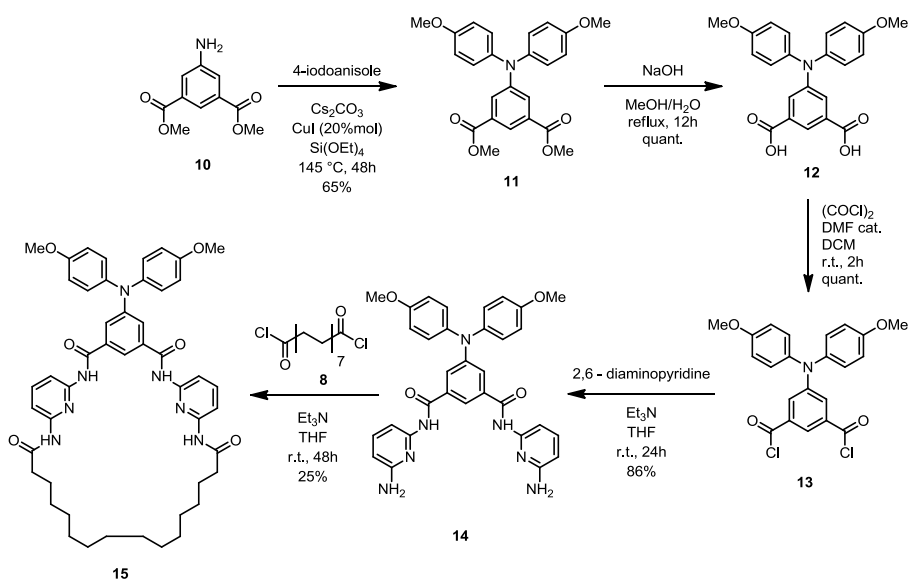


Figure R2 - Schéma de synthèse des récepteurs cycliques de type Hamilton contenant un motif triarylamine **15**.

Ces conditions réactionnelles particulières ont permis d'obtenir l'intermédiaire **11** souhaité avec un bon rendement, tandis que d'autres réactions de couplage catalysées par le palladium ou le cuivre ont été infructueuses, conduisant principalement à un mélange complexe de produits de dégradation. Les principaux avantages de l'utilisation du TEOS comme solvant sont le caractère déshydratant de ce composé, qui évite l'hydrolyse des groupes esters pendant la réaction, et le traitement extrêmement facile du mélange: le solvant lui-même est totalement converti en dioxyde de silicium lors de l'ajout de le fluorure d'ammonium aqueux et le brut est récupéré par addition d'acétate d'éthyle et filtration. De plus, la réaction implique des réactifs bon marché et disponibles dans le commerce et peut être facilement réalisée à l'échelle du gramme.

Les interactions hôte-invité entre le macrocycle **15** et un acide 5,5'-diéthylbarbiturique (barbital) complémentaire comme hôte modèle ont également été étudiées par absorption électronique et titrages spectroscopiques par RMN ^1H : la constante de liaison expérimentale ($K_{\text{ass}} = 70000 \text{ M}^{-1}$ dichlorométhane deutérié) est beaucoup plus élevée que l'analogue structural où un tert-butylphényle central est présent à la place de la fraction triarylamine ($K_{\text{ass}} = 23500 \text{ M}^{-1}$ dans le chloroforme deutérié). Les interactions hôte-invité avec le même invité modèle barbital ont également été étudiées pour les macrocycles **9** et **7** de type Hamilton contenant du ferrocène: les constantes de liaison déterminées ($K_{\text{ass}} = 742 \text{ M}^{-1}$ pour le macrocycle **9** à 31 chaînons et $K_{\text{ass}} = 1011 \text{ M}^{-1}$ pour le noyau **7** à 35 chaînons dans le chloroforme deutéré) se sont révélés supérieurs à la version acyclique **5** précédemment rapportée ($K_{\text{ass}} = 575 \text{ M}^{-1}$ dans le chloroforme deutéré). Cette particularité s'explique par la nature macrocyclique des récepteurs **9** et **7**: la présence des chaînes alkyles réduit les degrés de liberté des molécules et la perte d'entropie conduit à une plus grande rigidité des structures avec pour conséquence amélioration des constantes de liaison. Les macrocycles **7** et **15** ont également été étudiés par voltamétrie cyclique et des oxydations réversibles ont été observées pour chacun d'entre eux (Figure R3).

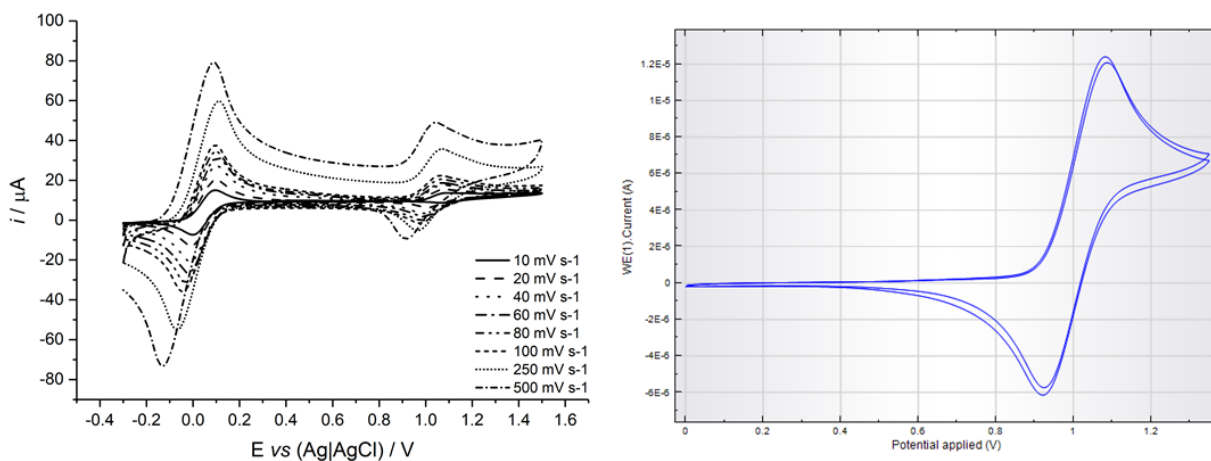


Figure R3 - Voltamogramme cycliques de DCMF 1:1 et de macrocycle **7**, enregistré à différentes vitesses de balayage, dans une solution de 10^{-1} M TBAPF₆ dans du DCM sec (gauche) et voltamogramme cyclique de macrocycle **15** dans une solution de 10^{-2} M TBAPF₆ dans du THF dégazé et sec à une vitesse de balayage = 100 mVs^{-1} (droite).

L'analyse cristallographique structurale des macrocycles **7** et **15** a été fondamentale pour l'élucidation des structures: le macrocycle **7** a montré une structure en forme de croissant et une torsion des groupes de liaisons H hors du plan de la cavité de liaison, ce qui en atténuait l'utilisation dans la construction d'architectures moléculaires interpénétrantes, alors que le macrocycle **15** présentait une cavité très bien définie avec tous les groupes de liaison H dans le plan de la cavité de liaison. La présence de la liaison isophtalique entre les 2,6-diamidopyridines s'est avérée fondamentale pour la construction d'un récepteur rigide et efficace pour les motifs barbituriques, faisant du macrocycle **15** un candidat très prometteur pour la construction de molécules à verrouillage mécanique (Figure R4).

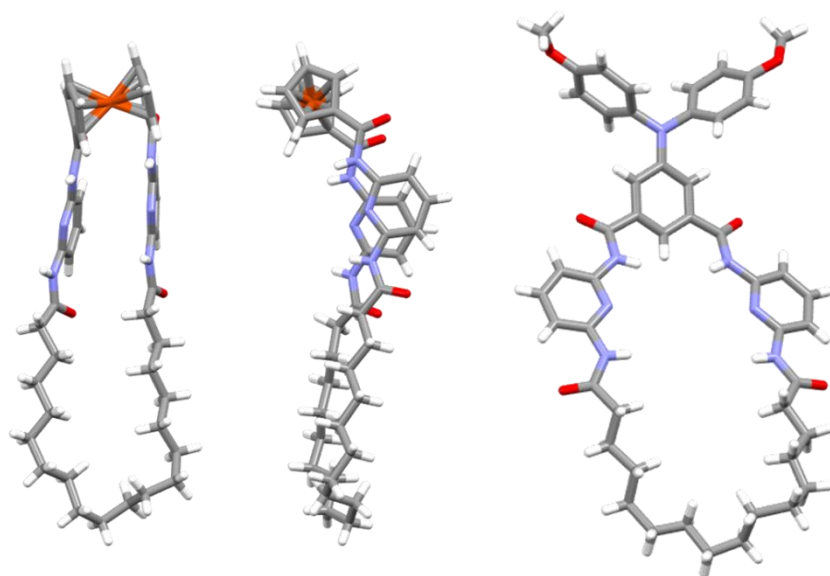


Figure R4 - Structures cristallines aux rayons X des macrocycles **7** et **15**.

Au chapitre 3, un procédé de synthèse détaillé pour la synthèse du BF_2 -chélate de tétraarylazadipyrrométhène monopropargylé a été décrit, qui constitue un intermédiaire important pour le développement de blocs constitutifs porteurs de chromophores NIR de nouvelles molécules photo-actives biocompatibles photoactives. En adaptant une procédure décrite précédemment, le dihydroxytétraarylazadipyrrométhène BF_2 -chélate **20** a été monofonctionnalisé avec succès en utilisant du bromure de propargyle comme agent alkylant en présence de fluorure de césium comme base dans du DMSO sec. Ce protocole permettait la conversion complète du produit de départ **20** seulement après 30 minutes, donnant le produit **21** avec un très bon rendement (Figure R5).

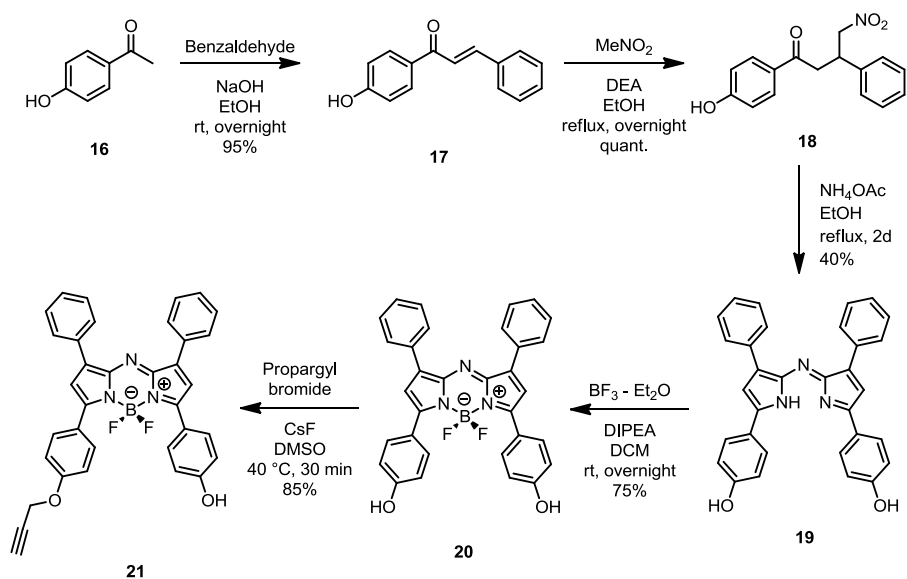


Figure 5 - Schéma de synthèse du tétraarylazadipyrrométhène monopropargylé BF₂-chélate **21**.

Cette méthodologie de synthèse simple a permis la synthèse de deux tétraarylazadipyrrométhène BF₂-chélates asymétriques **22** et **23**, comprenant un groupe méthoxy et un groupe tert-butylcarboxy, respectivement, et un groupe propargyloxy, qui ont été caractérisés par spectroscopie RMN ¹H et ¹³C et spectrométrie de masse (Figure R6).

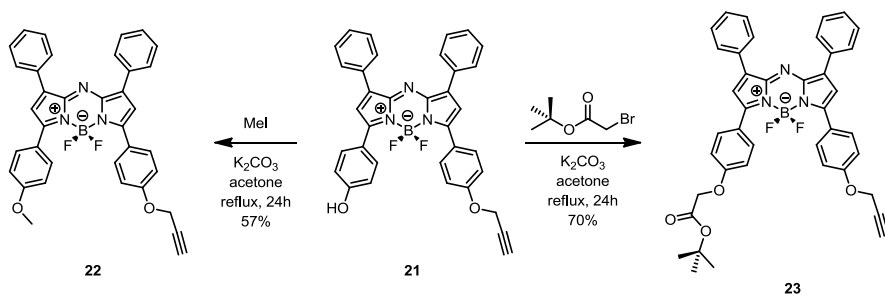


Figure R6 - Schéma de synthèse des deux tétraarylazadipyrrométhène BF₂-chélates asymétriques **22** et **23**.

Un nouveau fil d'azadipyrrométhène-chélate de BF₂ **25** contenant des barbiturates a été synthétisé afin de tester la possibilité d'assembler des [2]rotaxanes par une approche glissante (Figure R7).

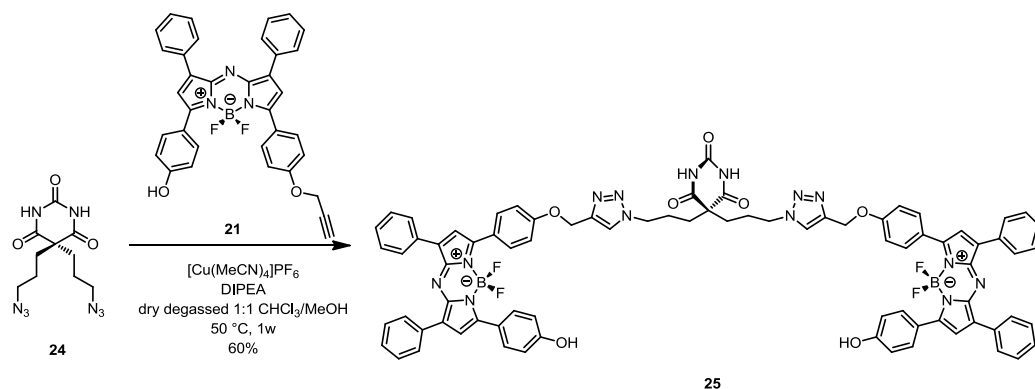


Figure R7 - Schéma de synthèse de fil d'azadipyrométhène-chélate de BF₂ **25**.

La synthèse améliorée du précurseur **29** a été rapportée, montrant que des rendements plus élevés et une plus grande pureté peuvent être obtenus en adoptant la voie de synthèse qui traverse le chlorure intermédiaire **28**. Un alkyne trityl stopper **31** marqué au deutérium a également été conçu et synthétisé: il a été obtenu avec un rendement quantitatif à partir de l'alkyne stopper **30**, en le traitant avec de l'hydruure de sodium et en arrêtant la réaction avec du méthanol deutérié (Figure R8).

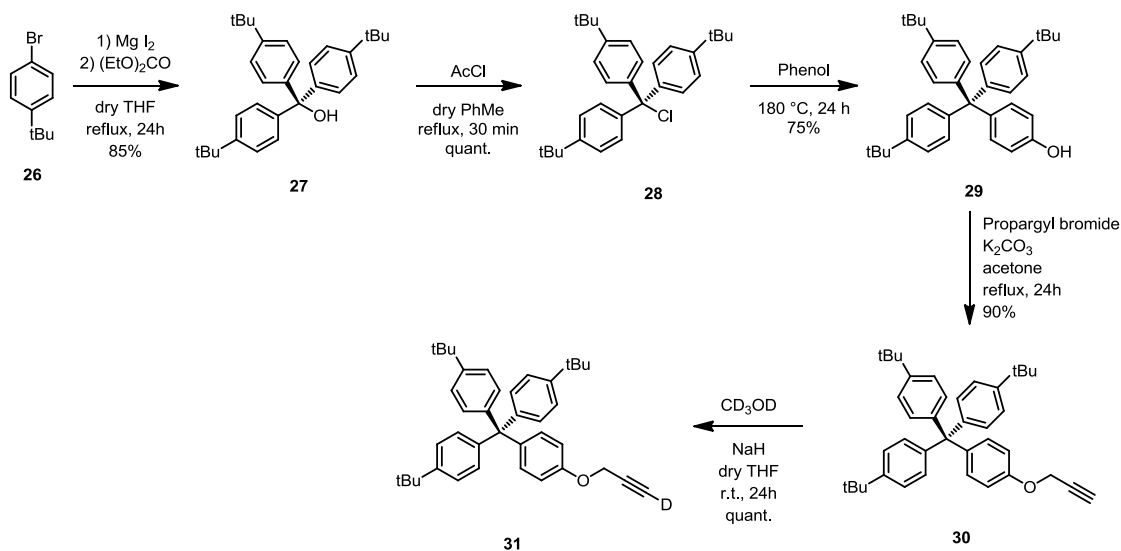


Figure R8 - Schéma de synthèse de alkyne trityl stopper marqué au deutérium **31**.

Le bouchon en alkyne **31**, porteur de deutérium, sera un outil utile pour le développement de molécules inter-verrouillées marquées au deutérium dans la perspective d'étudier le glissement de

l'anneau le long du fil dans des assemblages supramoléculaires à base de rotaxane par des techniques de RMN dynamique.

Au chapitre 4, trois nouveaux [2]rotaxanes **32**, **35** et **37**, comprenant des groupes électroactifs, à savoir le ferrocène ou la triarylamine, ont été synthétisés et entièrement caractérisés par spectroscopie RMN ^1H et ^{13}C et spectrométrie de masse.

Le [2]rotaxane **32** a été obtenu via une approche métal-matrice active par une réaction de Glaser catalysée par du cuivre: l'ion du cuivre a été coordonné par les groupes pyridine du macrocycle **15** et la réaction de couplage entre deux bloqueurs de trityle en alcyne **30** a eu lieu à l'intérieur de la cavité de l'anneau, donnant le filetage portant la diyne et la molécule consécutive à verrouillage mécanique (Figure R9).

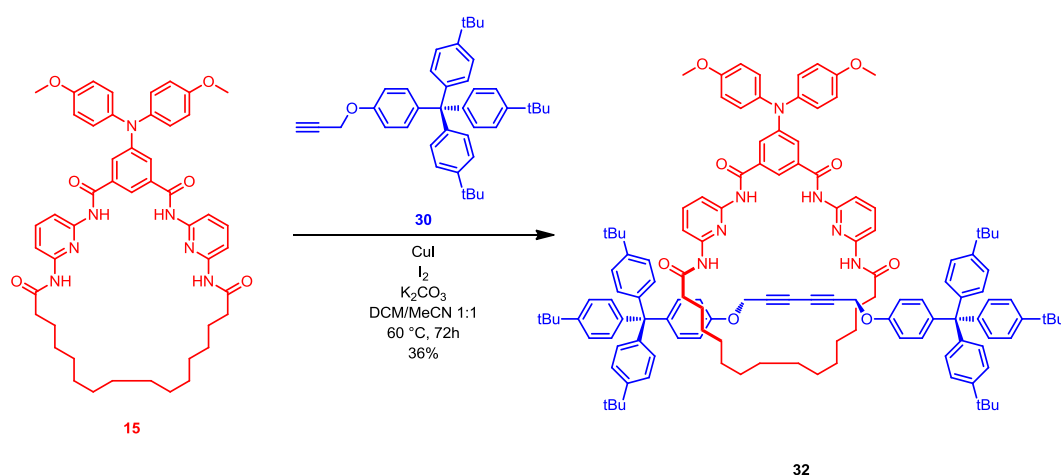


Figure R9 - Schéma de synthèse de [2]rotaxane **32** obtenu via une approche métal-matrice active.

Les [2]rotaxanes **35** et **37** ont été obtenus via une réaction d'écristage à cinq composants assistée par matrice. Le tétrabutylsuccinamide **33** a été synthétisé en une étape à partir de succinyl chlorure et dibutylamine, disponible dans le commerce, et a été utilisé comme fil. Les [2]rotaxanes **35** et **37** ont été synthétisés en faisant réagir la *p*-xylylènediamine **34** avec le chlorure de 5-[bis(4-méthoxyphényl)amino]-isophtaloyle **13** et le chlorure de 5-ferrocénylisophtaloyle **36**,

respectivement, en présence du fil **33** et de la triéthylamine comme base dans des conditions de forte dilution (Figure R10).

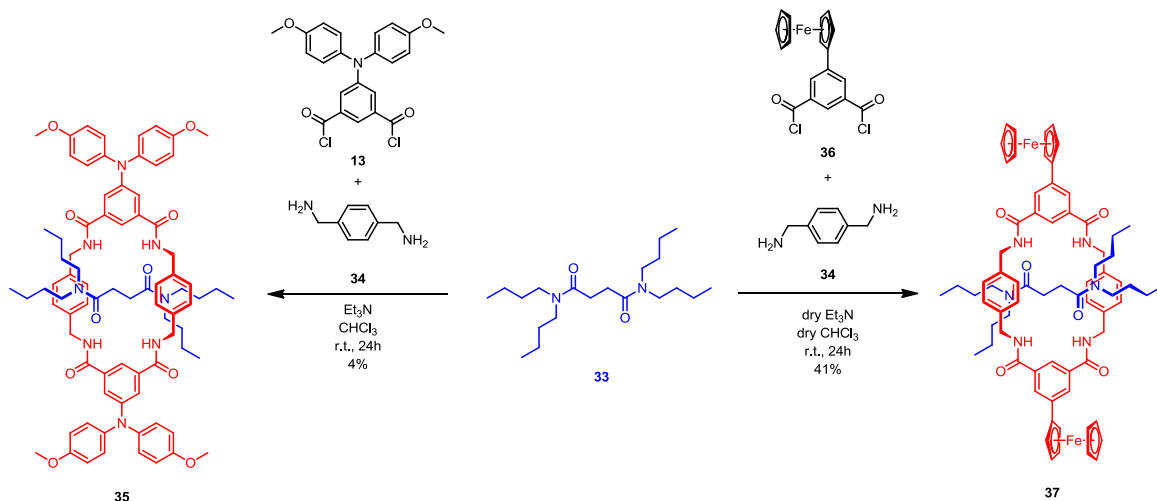


Figure R10 - Schéma de synthèse des [2]rotaxanes **35** et **37** obtenus par une fermeture de la molécule macrocyclique.

Des structures cristallines aux rayons X pour les [2]rotaxanes **35** et **37**, ce qui prouve le caractère imbriqué des assemblages supramoléculaires (Figure R11).

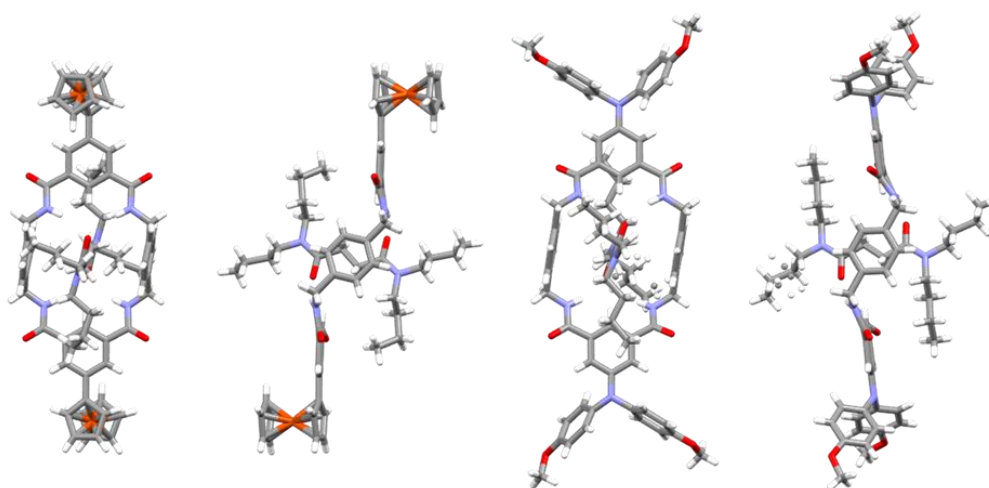


Figure R11 - Structures cristallines aux rayons X des [2]rotaxanes **35** et **37**.

En résumé, l'objectif de cette thèse était la synthèse et la caractérisation de macrocycles électroactifs et de blocs de construction NIR multifonctionnels, et l'application de ces composants à la construction de [2]rotaxanes fonctionnels a été montrée. Des améliorations de la synthèse de blocs de construction polyvalents, parallèlement aux molécules macrocycliques électroactives et aux composants «cliquables» NIR ont également été rapportées. Cette thèse se veut un point de départ solide pouvant mener à la construction de molécules photoactives et électroactives à verrouillage mécanique.

Titre : Synthèse de macrocycles et rotaxanes électroactifs

Résumé : Le développement d'architectures moléculaires enchevêtrées (rotaxanes) est un sujet d'actualité en chimie supramoléculaire. Cette thèse examine la synthèse multi-étape de sous-unités de rotaxanes, notamment de composants macrocycliques électroactifs, et leur assemblage dans des structures moléculaires imbriquées. De nouveaux cycles à 31 et 35 chaînons à liaison hydrogène comprenant un motif récepteur bis (2,6-diamidopyridine) et une unité électroactive, à savoir du ferrocène ou de la triphénylamine, ont été synthétisés. Ces macrocycles ont été analysés par voltampérométrie cyclique, analyse par diffraction des rayons X sur cristal unique, ainsi que par spectroscopie RMN et spectrométrie de masse. Les interactions hôte-invité avec un acide complémentaire 5,5'-diéthylbarbiturique (Barbital) en tant qu'invité modèle ont également été étudiées par titrage spectroscopique par absorption électronique et RMN ¹H. Les affinités de liaison étaient corrélées à la structure moléculaire. Des approches pour former des [2]rotaxanes, notamment en utilisant une réaction de matrice métallique active, où l'ion métallique joue le double rôle de matrice et de catalyseur, sont décrites. En particulier, les réactions de couplage de Huisgen ainsi que de Glaser catalysées au cuivre(I) ont été utilisées avec des bouchons de volumes variés. Dans une deuxième approche complémentaire de type "attache" de la formation de rotaxane, l'anneau électroactif a été formé directement entourant le composant de filetage servant de modèle. Cette méthodologie a permis d'obtenir deux [2] rotaxanes inédits via une réaction de "clipping" à cinq composants assistée par matrice, l'un des rotaxanes intégrant deux unités de ferrocène, tandis que l'autre comprenait deux unités de type triphénylamine. Les études de diffraction des rayons X sur cristal unique ont confirmé le caractère imbriqué des assemblages.

Mots clés : Synthèse organique, récepteurs de type Hamilton, macrocycles, ferrocène, chimie supramoléculaire.

Title: Synthesis of electroactive macrocycles and rotaxanes

Abstract : Development of interlocked molecular ring-on-thread architectures (rotaxanes) represents a central current topic in supramolecular chemistry. This thesis considers the multi-step synthesis of rotaxane subcomponents, notably electroactive macrocyclic components, and their assembly into interlocked molecular structures. Novel hydrogen-bonding 31- and 35-member rings comprising a bis(2,6-diamidopyridine) receptor motif and an electroactive unit, namely ferrocene or triphenylamine, were synthesized. These macrocycles were analyzed by cyclic voltammetry, single crystal X-ray diffraction analysis, as well as NMR spectroscopy and mass spectrometry. Host-guest interactions with a complementary 5,5'-diethylbarbituric acid (Barbital) as model guest were also studied by electronic absorption and ¹H-NMR spectroscopic titrations. Binding affinities were correlated to molecular structure. Approaches to form [2]rotaxanes, notably by employing an active metal template reaction, where the metal ion plays the dual role of template and catalyst, are described. In particular, the copper(I)-catalyzed Huisgen as well as Glaser coupling reactions were employed with a variety of bulky stopper groups. In a second complementary "clipping"-type approach to rotaxane formation, the electroactive ring was directly formed encircling the templating thread component. This methodology yielded two further novel [2]rotaxanes via a template-assisted five-component clipping reaction, one rotaxane integrating two ferrocene units while the other comprised two triphenylamine-like units. Single crystal X-ray diffraction studies confirmed the interlocked nature of the assemblies.

Keywords : Organic synthesis, Hamilton-type receptors, macrocycles, ferrocene, supramolecular chemistry.

Unité de recherche

Institut des Sciences Moléculaires, CNRS UMR 5255, Batiment A12, 251 cours de la Libération, 33405 Talence Cedex